Republic of Iraq
Ministry of Higher Education
and Scientific Research
University of Babylon
College of Science
Department of Physics

Study of Some Nuclear Structure Properties and Potential Energy for Even-Even Yb, Hf and W Nuclei in the Framework of Interacting Bosons Model

A Thesis
Submitted to the Council of College of Science, University of Babylon, in Partial Fulfillments of the Requirements for the Degree of Doctorate of Philosophy in Physics Sciences

By

Salar Hussein Ibrahem Mohamed

B.Sc. in Physics 2003
M.Sc. in Physics 2007

Supervised by

Prof. Dr.

Mohsin Kadhim Muttaleb Al-Janaby

2022 A.D. **1444 A.H.**

بِسْمِ اللَّهِ الرَّحْمَنِ الرَّحِيمِ

وَلَمَّا بَلَغَ أَشُدَّهُ وَاسْتَوَى آتَيْنَاهُ حُكْمًا وَعِلْمًا

وَكَذَلِكَ نَجْزِي الْمُحْسِنِينَ

صَدَقَ اللهُ العَظِيم

من سورة القصص الاية (١٤)

Dedications

To My parents who I knew the meaning of success by them, especially my mum who dreams at this moment.

To My husband… Who bore with me all the difficulties and stood with me and supported me step by step

To the source of my happiness in life … who their hearts with me…

My sister…

My sons …

My brothers …

My real friends…

To all who helped me and prayed for me.

Salar

Acknowledgments

First and foremost, I thank God for helping me to reach this stage, then I would like to thank my supervisor, Prof. Dr. Mohsin Kadhim Al-Janaby, for his supervision, his continuous follow-up, and his suggestions for the completion of this thesis.

I also extend my thanks to members of the Department of Physics, especially the head of the department Prof. Dr. Abdulazeez O. Mousa Al-Ogaili for his valuable observations and for what we learned from him throughout the study period and before, and I thank, the Dean of the College of Science and the staff of the College of Education for Pure Sciences at the University of Babylon for giving them the opportunity to complete the study.

I also thank Prof. Dr. Heiyam Najy, Dr. Rawaa Mezher, Dr. Ghaida Abdel Hafez and Dr. Mohammad Abdel Kadhim for helping me throughout the research period.

My thanks and gratitude to my teacher, Dr. Adnan Al-Araji, for what his words and encouragement had a good effect on me, may God bless them all and reward them the best.

Finally, I wish I could have a better word of thanks to express my feelings to my family: dear parents, my husband, my sister and my sons for their understanding, constant encouragement and support throughout this work, with apologies to them for any shortcomings I may have appeared to them.

Salar

Summary

The nuclear structure of series of even – even, Ytterbium ($^{160-178}$Yb), Hafnium ($^{166-180}$Hf) and Tungsten ($^{170-184}$W) isotopes are studied theoretically using the framework of the first interacting boson model IBM-1 and the second IMB-2.

The low lying positive party states, the energy levels, ratios between these levels, dynamic symmetries, reduced transition probability for electric quadruple B(E2), branching ratio, quadruple moment, magnetic dipole B(M1), monopole transition probability B(E0), mixing ratios δ(E2/M1), X(E0/E2), and the potential energy surfaces for these series of isotopes were studied in detail.

The surface potential energy is calculated and its contour diagrams are drawn using the (surfer) program, and the results are analyzed and discussed. Mixing symmetry states MSS of the levels are also calculated.

It was found that all the studied isotopes fall within the rotational region SU(3) and the unstable gamma region O(6), which is located on Casten's triangle.

The results are compared with the practical results and it was found that there is a good match is obtained between it.

The calculated potential energy surface for three isotopes series illustrates that nuclear shape is very sensitive to structural effects and it can change from nucleus to its adjacent in addition to shape alters with proton or neutron number.

List of Abbreviations	
Abb. Symbol	**Abb. Definition**
Yb	Ytterbium
Hf	Hafnium
W	Tungsten
IBM-1	The interacting boson model version one.
IBM-2	The interacting boson model version two.
IBFM	The interacting boson fermion model.
U(6)	The unitary group.
U(5)	Vibrational Limit.
SU(3)	Rotational Limit .
O(6)	γ-Unstable limit .
N_b	Total number of boson.
N_ρ	Total number of neutron bosons or proton bosons.
N_π	The number of proton boson.
N_ν	The number of neutron boson.
A	The mass number.
N	The neutron number.
Z	The atomic number.
E(5)	Critical point between U(5) and O(6).
X(5)	Critical point between U(5) and SU(3).
PES	Potential energy surface.
β	The deformation parameter.
γ	The angle of deviation from symmetry axes.

List of Abbreviations	
Abb. Symbol	**Abb. Definition**
$\hat{H}$	The Hamiltonian operator in IBM-1.
$d^{\dagger}, s^{\dagger}$	The creation operators for *d* and *s* bosons.
$\tilde{d}, \tilde{s}$	The annihilation operators for *d* and *s* bosons.
E_d	The energy of d- boson and in IBM-2 Hamiltonian is the energy difference between s and d boson.
a_0	The strength of the pairing interacting between the bosons.
a_1	The strength of the angular momentum interacting between the bosons.
a_2	The strength of the quadruple interacting between the bosons
a_3	The strength of the octupole interacting between the bosons
a_4	The strength of the hexadecapole interacting between the bosons
$\hat{p}$	The pairing operator.
$\hat{L}$	The angular momentum operator.
$\hat{Q}$	The quadruple operator.
χ	The quadruple structure parameter.
$\hat{T}_3$	The octoupole operator.
$\hat{T}_4$	The hexadecapole operator.
T^{E2}	The electric quadruple operator.
T^{M1}	The magnetic dipole operator.
E2SD = $\alpha_2 (e_b)$	The effective charge of s-d boson.
E2DD = β_2	The effective charge of d-d boson.
$g_L = g_b$	The gyromagnetic factor for boson
μ_L	The magnetic momentum.
α_{tot}	The total conversion coefficient.
α_L	The conversion coefficient for L shell.
E_γ	The transition energy.
E_V	The eigen value for dynamical symmetry.

List of Abbreviations	
Abb. Symbol	**Abb. Definition**
B(E2)	Reduced electric quadruple transition probability.
B(M1)	Reduced magnetic dipole transition probability.
B(E0)	Electric monopole transition.
R	The radius of nuclei.
$\delta(E2/M1)$	The mixing ratios of gamma transition between E2 and M1.
$\Delta(E2/M1)$	The reduced mixing ratio.
$\langle J_f \| T^{E2} \| J_i \rangle$	The reduced matrix element of E2 transition.
$\langle J_f \| T^{M1} \| J_i \rangle$	The reduced matrix element of M1 transition.
υ	The number of d-boson not paired to zero angular momentum called seniority.
Q_L	The electric quadruple moment. The branching ratios.
π	The parity
n_d	The number of d-boson.
n_Δ	The number of d-boson tripled coupled to zero angular momentum.
n_β	The number of d-boson paired to zero angular momentum.
L,M	The two quantum numbers which represent the angular momentum and components.
λ, μ	The two quantum numbers which represent the Casmir operator, represent cases SU(3).
K	The number of cases that have equal values of (λ, μ, L).
σ	The number of d-boson not pairwise coupled .
τ	The number of d-boson not pairwise coupled to zero angular momentum.
υ_Δ	The number of d-boson tripled coupled with zero angular momentum.

List of Abbreviations	
Abb. Symbol	**Abb. Definition**
R, R', R''	The branching ratio.
$\hat{H}_{\pi}$	The Hamiltonian operator bosons protons.
$\hat{H}_{\nu}$	The Hamiltonian operator bosons neutrons.
$\hat{H}_{\nu\pi}$	The Hamiltonian operator bosons protons and neutrons.
κ	Strength interaction between the quadruple – quadruple for proton and neutron.
χ_{ρ}	Quadrupole deformation parameter for proton and neutron.
$V_{\pi\pi}$, $V_{\nu\nu}$	The interaction between like boson.
$M_{\nu\pi}$	The Majorana term.
ξ_1 , ξ_2 , ξ_3	The Majorana parameters.
$\rho(E0)$	The matrix element of E0 transition.
e_{π}, e_{ν}	Effective charge for protons and neutrons respectively.
g_{π}, g_{ν}	The gyromagnetic factor for proton and neutron respectively.
$\tilde{\beta}_{0\nu}, \tilde{\beta}_{0\pi}$	deformation parameters for protons and neutrons respectively.
$NPBOS$	Neutron Proton Boson, software package.
$NPBEM$	Neutron Proton Boson Electromagnetic, software package.
E_B	Nucleus binding energy.
FLL, MSS	Full and mixed Symmetry States.
$\delta\langle r^2\rangle$	Isomer shift.
$\Delta\langle r^2\rangle$	Isotopes shift.

List of Tables

List of Tables

List of Figures

List of Figures

Contents

Contents

Contents

Contents

Chapter One

General Introduction

1.1. Introduction

Nuclear physics research is an important part of scientific research all over the world. Nuclear physicists study the structure and behavior of matter in all of its forms, from the primordial soup of quarks and gluons to the nuclear reactions that keep our world alive. Nuclear physics lacks a comprehensive theoretical framework that would allow for a basic study and explanation of all occurrences. Understanding the structure of nuclei is the aim of nuclear physics research [1].

The structure of the interaction results in numerous nucleons over an unknown number of separate forces, in theory. However, it is clear that overcoming the determination of the behavior of a dynamic system of this complexity or a fairly hefty core will take a significant amount of effort [2].

The strong, weak, and electromagnetic fundamental interactions play an important role in the atomic nucleus which is a highly multi-body quantum mechanical system composed of protons and neutrons. Therefore the study of the atomic nucleus has been important to clarify the origin of matter (or nuclear synthesis processes), tests of basic symmetries, and even the purpose of practical applications [3].

The spectroscopy of radiation emitted by nuclei, the pattern of nuclear stability and the results of nuclear reaction and have yield information that helps us to develop a picture of nuclear structure. But the situation for the nucleus is more complicated than the situation for the atom because there are two types of particles, neutrons and protons, backed close together, and there are two types

of forces: The short range strong nuclear force and the electrostatic force. This more complex state has caused slow progress in developing a satisfactory model, and no single nuclear model has been able to describe all nuclear phenomena [4].

The nucleus of an atom contains all the protons and neutrons while the electrons are all in the outer sphere conventionally, the number of protons and neutrons in the nucleus which must obviously be whole numbers are represented by the symbols Z and N respectively, follows that the charge on the nucleus is +Ze and that of the outer sphere is –Ze as the number of electrons must equal that of the protons to make the atom neutral as a whole it further follows that the entire mass of the atom is in the nucleus as the mass of an electron is negligible in comparison to that of the nucleon the common name for protons and neutrons as a result of this the density of the nucleus or the pure nuclear matter [5].

The most critical element in determining the predicted properties of a nucleus from a given effective interaction, are the general number of nucleons and the ratio of N/Z of neutrons to protons.

It is the extremes in these quantities, which define the limits of existence for the nuclear matter that will be opened up for study with radioactive beam accelerators [6].

1.2. The Nuclear Structure

The structure of the nucleus is the study of the properties of nuclei at low excitation energies, where single energy levels may be resolved, which is essential to physics. This means that quantum effects are often dominating, and nucleus states have a complex structure that is dependent on the intricate interrelationships of all the many nucleons involved [7].

Nuclei have a more complicated structure than atoms. The nucleus in an atom acts as a common center of attraction for the electrons, although inter electronic forces play a minor role and the coulomb forces are well understood. There is no center of attraction in nuclei; The nucleons are held together by their complicated mutual interactions.

In nuclear reactions, the behavior of nuclei in relation to other subatomic particles have been studied. From a quantum mechanics point of view, it is primarily a scattering problem. There are several marked differences from nuclear structure studies [8].

1.3. Shell Model

The basic assumption of the shell model is that despite the strong overall attraction between nucleons that provide the binding energy, the motion of each nucleon is practically independent of that of any other nucleon. If all inter nucleon couplings (called residual interactions) are ignored, the model called the "single- particle shell model". Each nucleon is then assumed to move in the same potential the potential is spherical in the simplest case [9]. The regularities of nuclear properties are apparent in the magic numbers. The magic nuclei being more tightly bound require more energy to be excited than non -magic nuclei. Shell model succeeded in explaining many nuclear properties of magic and neighboring nuclei [10].

1.4. The Liquid Drop Model

The liquid drop model was first presented by George Gamow, then elaborated by Nile Bohr and John Archibald. This model regards the nucleus as a drop of incompressible nuclear liquid which consists of the protons and neutrons that are bound together by the nuclear force. Though the model does not clarify all the characteristics of the nucleus, it can clarify the spherical shape

of the majority of nuclei in addition to its ability to foretell the energy that strongly held the nucleus [11].

The mathematical analysis comes up with an Equation capable of foretelling the energy that binds the nucleons by identifying the numbers of protons and neutrons in that nucleus. The Equation's terms correspond to the cohesive force that strongly binds the nucleons and the electrostatic mutual repulsion of the protons, a surface energy term, (an asymmetry term which is derived from the protons and neutrons that have independent momentum states) and a paring term (which is derived, in part, from the protons and neutrons that have independent quantum spin states). If one takes into account the total of the six types of energies, then the notion of an nucleus as a drop of incompressible liquid will justify the noticeable variation of the energy that binds the nucleus [12].

1.5. Nuclear Collective Motion

Collective motion in the nucleus is defined as the change in the density distribution of nuclear matter in time. Depending on this definition the Hamiltonian of nuclear rotation is determined using this approach, with moments of inertia that match experimental data well. The shape of the nucleus affects nuclear collective motion. The presence of a vibrating spectrum distinguishes a spherical nucleus. Closed-shell nuclei are characterized by this type of movement, where nuclear matter is a charged fluid with a smooth flow and surface vibrations resulting from the movement of nucleons from one region to another and this type of movement requires low energies.

The nuclear spectrum grows more convoluted as moving away from the largely closed shells. The collective model term is not explicit and clear term. In

many of the studies in the literature on the nuclear model, the term is utilized to denote any model that deals only with the collective conduct of nucleons [13].

Nuclide can have vibrational energy or rotational energy. In both states, the energies will be integer multiples of a phonon. According to the overall modeling of the nuclei structure, first, make certain assumptions about the nature of nuclei. Because it happens in spherical nuclei, compression mode can be considered a type of this vibrational motion, assuming that vibration occurs by changing the radius of the nucleus around a fixed value of the radius of the spherical nucleus [12].

1.6. Electric Quadrupole Moment

The nuclear electric quadrupole moment is a parameter that describes the effective shape of the ellipsoid of nuclear charge distribution. A non-zero quadrupole moment Q indicates that the charge distribution is not spherically symmetric. By convention, the value of Q is taken to be positive if the ellipsoid is prolate and negative if it is oblate.

The quantity Q_0 is the classical form of the calculation that represents the departure from spherical symmetry in the rest frame of the nucleus. The expression for Q is the quantum mechanical form that takes into account the nuclear spin I and the projection K in the z-direction [14].

One of the expectations of the shell model for the nucleus is that for closed shells the nuclear charge is spherically symmetric. If a nucleus is not spherically symmetric, it will have a non-zero electric quadrupole moment, so the measurement of the quadrupole moment is a test of the shell theory. Since the quadrupole moment depends upon the size and charge of the nucleus, a better comparison is obtained by normalizing for those factors, giving what is called a "reduced quadrupole moment". A plot of measured values shows that magic

numbers of neutrons or protons correlate with near-zero quadrupole moments [15].

1.7. Angular Momentum and Parity Selection Rules

In general, electric (charge) radiation or magnetic (current, magnetic moment) radiation can be classified into multipoles Eλ (electric) or Mλ (magnetic) of order 2λ, e.g., E1 for electric dipole, E2 for quadrupole, or E3 for octupole. In transitions where the change in angular momentum between the initial and final states makes several multipole radiations possible, usually, the lowest-order multipoles are overwhelmingly more likely and dominate the transition [16]. These considerations generate different sets of transition rules depending on the multipole order and type.

The expression *(* forbidden transitions) is often used, but this does not mean that these transitions cannot occur, only that they are electric-dipole forbidden. These transitions are perfectly possible; they merely occur at a lower rate. If the rate for an E1 transition is non-zero, the transition is said to be permitted; if it is zero, then M1, E2, etc. transitions can still produce radiation, albeit with much lower transition rates. These are the so-called "forbidden" transitions. The transition rate decreases by a factor of about 1000 from one multipole to the next one, so the lowest multipole transitions are most likely to occur. Semi-forbidden transitions (resulting in so-called intercombination lines) are electric dipole (E1) transitions for which the selection rule that the spin does not change is violated [17].

A selection rule, or transition rule, formally constrains the possible transitions of a system from one quantum state to another. Selection rules have been derived for electromagnetic transitions in molecules, atoms, atomic nuclei, and so on. The selection rules may differ according to the technique used to observe the transition. The selection rule also plays a role in chemical reactions,

where some are formally spin-forbidden reactions, that is, reactions where the spin state changes at least once from reactants to products [18].

1.8. Literature Survey

Many researchers and theses have studied the isotopes in different ways, the most important of them are the following:

In (2003), Zamfir, V. N. and Casten R. F. [19], have been discussed the theoretical description of new critical point symmetries for deformed spherical phase transitions and experimental evidence for the closely axially distorted shape in N = 90 isotopes. They discussed based on a microscopic perspective to identify potential new regions for critical point behavior, and this was demonstrated for the ^{162}Yb isotope.

In (2005), Subber, A. R. [20], had been studied monopolar transition in Hf isotopes. The structure and monopolar transitions of distorted neutron-rich Hf isotopes have been studied under the Interacting Boson Model (IBM-2). He calculated the energy levels for two isotopes ^{176,178} Hf, B(E2), B(E0), and X (E0/E2). He compared the numerical results obtained with the available experimental data, and he found a good attachment between them.

In (2006), Rath, A. K. *et al*. [21], had been used the deformed Hartree - Fock and angular momentum projection (PHF) technique. They tried to understand the intrinsic structure and the systematics in the lifetimes of K = 6^+ isomers in the Hafnium (Hf) isotopes (in $^{172\text{-}178}$Hf nuclei) and N = 104 for Ytterbium (Yb), Hf and Tungsten (W) isotones. The variation in the B(E2) values in the Hf isotopes, as well as N = 104 isotones are well reproduced. They calculated K-forbidden E2 transition probabilities from the isomer band heads to the 4^+ yrast states qualitatively and they could explain the variation of the lifetimes with N and Z.

In (2008), Sarriguren, P. *et al*. [22], had been studied the evolution of shapes with the number of nucleons in various chains of Ytterbium (Yb), Hafnium (Hf), Tungsten (W), Osmium (Os), and Platinum (Pt) isotopes from neutron number N=110 up to N=122. By analyzing potential energy curves as oblate-prolate phase shape transitions and results from various Skyrme and pairing forces are considered self-consistent axially symmetric Skyrme Hartree-Fock plus BCS calculations. Comparisons with results obtained with the Gogny interaction as well as with relativistic mean field calculations are presented. The role of the γ degree of freedom is also discussed.

In (2009), Robledo, L. M. *et al*. [23], had been studied, the evolution of the ground-state shape along the triaxial landscape of several isotopes of Yb, Hf, W, Os, and Pt is analyzed using the self-consistent Hartree-Fock-Bogoliubov approximation. Two well reputed interactions (Gogny D1S and Skyrme SLy4) have been used in the study in order to assess to which extent the results are independent of the details of the effective interaction. They found that a large number of even-even nuclei, with neutron numbers from N=110 up to N=122, has been considered, covering in this way a vast extension of the nuclear landscape where signatures of oblate-prolate shape transitions have already manifested both theoretically and experimentally.

In (2010), Usmanov, P. N., *et al*. [24], had been studied the structure of excited states and nonadiabatic effects manifested in the energies and probabilities of electromagnetic transitions in the context of a phenomenological model taking into account the Coriolis mixing of the low-lying states of positive parity in rotational bands. They calculated energies, the structure of wave functions of excited states, and the probabilities of E2 and M1 transitions. The calculated energies are in agreement with experimental data. The theoretical values of ratios and multipole-mixing coefficients δ(E2/M1) of transitions from the first and second β and γ vibrational bands are compared

with the available experimental data.They founed an accepted match between the available experimental data and the theoretical data.

In (2011), Nomura, K. *et al*. [25], had been studied the interacting boson model, Hamiltonian determined from Hartree-Fock-Bogoliubov calculations with the new microscopic Gogny energy density functional D1M, is applied to the spectroscopic analysis of neutron-rich Ytterbium (Yb), Hafnium (Hf).

In (2012), Sharrad, F. I. *et al*. [26], have been calculated energy levels, B(E2) values and potential energy surface for even-even $^{170\text{-}178}$Yb isotopes using the IBM-1 and compered these calculations with the experimental data and found that they wear in a good attachment and the nuclei in SU(3) limit.

In (2013), AL-Ammeer, M. A., and Hussein, M. A. [27], had been determined the most appropriate Hamiltonian that is needed for calculations of energy levels, quadrupole moment, and B(E2) values of $^{188,\ 190}$W nuclei using the interacting boson model (IBM-1). They compared results with the available experimental data, they found that it was in good agreement, the Tungsten ($^{188,\ 190}$W) isotopes have more O(6) properties. They calculated the energy levels at β band (k=2) which are not calculated experimentally.

In (2015), Okhunov, A. A. *et al.* [28], had been studied low-lying bands for many isotopes including $_{70}$Yb, $_{72}$Hf and $_{74}$W nuclei. They investigated the energy spectra of ground states, they found that the theoretical calculations are in good agreement with the experimental data these results refer to the high deformations in these isotopes and they belonged to SU(3) limit.

In (2016), Mahapatro, S. *et al.*[29], had been studied nuclear structure properties for various isotopes of Ytterbium (Yb), Hafnium (Hf), Tungsten (W), Osmium (Os), Platinum (Pt) and Mercury (Hg) in Z = 70-80 in the region starting from N = 80 to N = 170 within the formalism of relativistic mean field (RMF) theory. The pairing correlation is taken care of by using the BCS

approach. They compared the results with the finite range droplet model (FRDM) and experimental data and found that the calculated results are in good agreement, they also studied probable decay mechanisms of these elements.

In (2017), AL-Jubbori, M. A. [30], had been used the interacting boson and vector boson models, as well as the Bohr–Mottelson one, to describe the energy levels and electromagnetic transitions of the ^{178}Yb–^{186}Pt (N = 108) nuclei. He calculated the negative-parity and GSB bands, as will as calculated the reduced transition probabilities $B(E2)$. The obtained findings show a very well agreement with experimentally obtained results. He also used the intrinsic coherent state to obtain the potential energy surfaces. These results indicate that these nuclei have a rotational property SU(3).

In (2018), Kassiml, H. H. *et al.* [31], had been studied the even-even Hf isotopes for A=172-176 by using interacting boson model (IBM-1). The energy levels, B(E2) transition probabilities, electric quadrupole moment QL, and potential energy surface of those nuclei have been calculated. They found that the results were in good agreement with experimental results. By contour plots of the potential energy surfaces, they showed that the interested nuclei have rotational characters.

In (2020), Al-Jubbori, M. A., *et al.* [32], had been studied, the nuclear deformation of even–even rare-earth Er–Os isotopes with N = 102 has been calculated using a new empirical Equation and an interacting boson model (IBM-1). The potential energy surface, reduced transition probabilities B(E2) and the energy level have been calculated for these nuclei. The properties of gamma, beta and yrast bands have been also calculated and compared with the available experimental data. The results of both models have indicated the similarity or dissimilarity with the published experimental data. They have studied the ratio Eγ(I+2)/Eγ(I) versus the spin (I) to determine the character of

the ground-state band. From the outcome of their investigation, it is possible to conclude that the ^{170}Er, ^{172}Yb, ^{174}Hf and ^{176}W nuclei show a rotational SU(3) character and ^{178}Os show X(5) character. They found that the results of these calculations are in good agreement with the corresponding available experimental data.

In (2021), Hady, H. N. and Muttalb, M. K. [33], had been used the interacting boson models to perform a complete study of even-even $^{160\text{-}168}$Yb isotopes. They studied the low-lying positive parity states, reduced electric quadrupole transition probability, dynamic symmetries, quadruple momentum, and potential energy surface for these five isotopes were investigated. They found that the energy level sequences and energy ratios showed the gradual transition of the properties of these nuclei from the γ-unstable features to the rotational features, they found that by contour plot of the potential energy surface for the isotopes.

In (2022), Al-Jubbori, M. A., *et al*. [34], studied the nuclear structure of rare-earth of ^{172}Er, ^{174}Yb, ^{176}Hf, ^{178}W and ^{180}Os nuclei. They investigated the energy spectra of ground states, reduced electric quadrupole transition probability, dynamic symmetries and quadruple momentum, they found that the theoretical calculations are in good agreement with the experimental data, and these results refer to the high deformations in these isotopes.

In (2022), Zyriliou, A., *et al*. [35], studied the medium-to-heavy mass Ytterbium isotopes in the rare-earth mass region of some aspects of the nuclear structure in the even–even Yb isotopes. They investigated existing experimental data in by means of data systematics and new theoretical calculations with well-established models and studied, energy levels, deformation parameters, reduced transition probabilities B(E2) and transition quadrupole moments Q by

using the phenomenological model (IBM-1). An overall good agreement was found between available adopted data and theoretical predictions.

In this study, many values of the energy levels of the studied isotopes, which were not confirmed in practical calculations, were confirmed, and many values that were not calculated and indicated as showen in the chapter three, as well as the probability of electric, magnetic and zero transitions, and through all these tests it was found that most of the studied isotopes it located between the rotational limitation SU(3) and the unstable gamma O(6), but it tends greatly to the rotational limitation.

A comparison was also made between the groups of isotones and isobars, and the effect of increasing the number of neutrons with a constant mass number and an increase in the mass number with a constant number of protons

1.9. Aim of The Study

This study aims to explore the nuclear structure and potential energy for a chain of even-even nuclei Ytterebum ($^{160-178}$Yb), Hafnium ($^{166-180}$Hf) and Tungsten ($^{170-184}$W) isotopes and study the behavior of these isotopes by:

1. Investigating the energy levels of isotopes using two models: IBM-1 and IBM-2 by studying the energy ratios and branching ratios.
2. Calculating the reduced electric quadruple transitions probabilities B(E2), the reduced transitions probability for magnetic dipole B(M1) and δ(E2/M1) ratio and calculation of electric monopole transitions B(E0)and mixing ratio X(E0/E2).
3. The potential energy surface and the deformation for isotopes under study.
4. Studying the mixed symmetry states.

Chapter Two

Interacting Boson Model

2.1. Overview of The Interacting Boson Model (IBM)

The interacting boson model (IBM), suggested by Arima and Iachello in 1974, is a nuclear pattern precedent for the characterization of collective structures. It can fit out theoretical level energies and transition probability while including a harmonic ties from residual interactions. There are two essentially connotations on which the IBM is based: Firstly the low-lying collective states in even-even nuclei can be characterized by just valence nucleons, which take shape in interacting fermion pairs. Secondly the fermion pairs couple to form bosons, carrying the angular momentum (L) equal to (0) and (2) only, called (s) and (d) bosons. The energies ($\in_s$ and $\in_d$), and the interactions of the (s) and (d) bosons, predict low-lying agitation in the nucleus. There is one obtainable magnetic substates for the s-boson, specified by (2L + 1), and five obtainable magnetic substates for the d-boson, forming a 6-dimensional space characterized by the Group structure U(6) [36].

The spectroscopy of medium mass and heavy even-even nuclei are characterized by the occurrence of low-lying collective states. The study of the nuclear collective motion is one of the most interesting topics in nuclear physics. The basis for this was laid by Rainwater and Bohr and Mottelson [37].

2.2. The Interacting Boson Model-One (IBM-1)

The interacting boson model (IBM) is a model in nuclear physics in which nucleons (protons or neutrons) pair up, essentially acting as a single particle with boson properties, with an integral spin of 0, 2 or 4. It is sometimes known as the Interacting boson approximation (IBA) [38].

The IBM-1 model treats both types of nucleons the same and considers only pairs of nucleons coupled to total angular momentum 0 and 2, called respectively, s and d bosons, this model is restricted to nuclei with even numbers of protons and neutrons [39].

2.3. Hamiltonian of The IBM-1

The interaction of s-bosons and d-bosons in the IBM is used to explain the collective properties of even-even nuclei. In IBM characterizes a six-dimensional Hilbert space, and is given by linear combinations of the creation and annihilation operators: s, $s^{\dagger}$, d, and $d^{\dagger}$.

The allowed combinations are defined by the conservation of the finite number of bosons, *N* (1/2 the number of valence nucleons), as well as having up to only 2-body interactions. Therefore, terms must contain a creation and annihilation operator and terms involving three or more operators are not allowed.

IBM Hamiltonians have been used to suitable the experimental energy spectra and the electromagnetic transition probabilities, Casten Triangle can be used to classify the experimental spectra, which provides insight in terms of limiting symmetries as well as indicating phase transitions. One of the most general forms of the IBM-1 Hamiltonian is given by Equation (2.1) [40]:

$$\begin{aligned}\hat{H} &= E_s(s^{\dagger}.\tilde{s}) + E_d\left(d^{\dagger}.\tilde{d}\right) + \sum_{L=0,2,4}\frac{1}{2}(2L+1)^{\frac{1}{2}}C_L\left[\left[d^{\dagger}\times d^{\dagger}\right]^{(L)}\times\left[\tilde{d}\times\tilde{d}\right]^{(L)}\right]^{(0)}\\ &+\frac{1}{\sqrt{2}}\upsilon_2\left[\left[d^{\dagger}\times d^{\dagger}\right]^{(2)}\times\left[\tilde{d}\times\tilde{s}\right]^{(2)}+\left[d^{\dagger}\times s^{\dagger}\right]^{(2)}\times\left[\tilde{d}\times\tilde{d}\right]^{(2)}\right]^{(0)}\\ &+\frac{1}{2}\upsilon_0\left[\left[d^{\dagger}\times d^{\dagger}\right]^{(0)}\times\left[\tilde{s}\times\tilde{s}\right]^{(0)}+\left[s^{\dagger}\times s^{\dagger}\right]^{(0)}\times\left[\tilde{d}\times\tilde{d}\right]^{(0)}\right]^{(0)}\\ &+\frac{1}{2}u_0\left[\left[s^{\dagger}\times s^{\dagger}\right]^{(0)}\times\left[\tilde{s}\times\tilde{s}\right]^{(0)}\right]^{(0)}+u_2\left[\left[d^{\dagger}\times s^{\dagger}\right]^{(2)}\times\left[\tilde{d}\times\tilde{s}\right]^{(2)}\right]^{(0)}\end{aligned} \tag{2.1}$$

Where:

$(s^{\dagger}.\ \tilde{s})$ and $(d^{\dagger}.\tilde{d})$ are the creation and annihilation operators for (s) and (d) bosons, respectively [38].

Two terms of one body interactions (ε_s and ε_d) and seven terms of two-body interactions [C_L (L = 0,2,4), v_L (L = 0,2), u_L (L = 0, 2)] in this Hamiltonian, where the single-boson energies are (ε_s) and (ε_d), and the two-boson interactions had been described by,(C_L), (v_L), and (u_L) so on, it shows that for a fixed boson number (N), only one of the one-body term and five of the two body terms are independent, It can be seen, by noting (N = n_s + n_d). Yet, it is more common to write the Hamiltonian of the IBM-1 as a multipole expansion, grouped into different boson-boson interactions Equation (2.2) [41]:

$$\hat{H} = \varepsilon^{"}\hat{n}_d + a_0\widehat{P^{\dagger}}.\hat{P} + a_1\hat{L}.\hat{L} + a_2\hat{Q}.\hat{Q} + a_3\hat{T}_3.\hat{T}_3 + a_4\hat{T}_4.\hat{T}_4 \qquad (2.2)$$

The operators are defined by the following Equations:

$$\hat{n}_d = \left[d^{\dagger}.\tilde{d}\ \right]$$

$$\hat{P} = \frac{1}{2}\left(\tilde{d}\ .\tilde{d}\ \right) - \frac{1}{2}(\tilde{s}\ .\tilde{s}\ )$$

$$\hat{L} = \sqrt{10}\left[d^{\dagger} \times \tilde{d}\ \right]^{(1)} \qquad (2.3)$$

$$\hat{Q} = \left[d^{\dagger} \times \tilde{s} + s^{\dagger} \times \tilde{d}\ \right]^{(2)} + \chi\left[d^{\dagger} \times \tilde{d}\ \right]^{(2)}$$

$$\hat{T}_3 = \left[d^{\dagger} \times \tilde{d}\ \right]^{(3)}$$

$$\hat{T}_4 = \left[d^{\dagger} \times \tilde{d}\ \right]^{(4)}$$

where:

χ is the quadrupole structure parameter and take the values 0 and ± $\sqrt{7}/2$ [36].

ε = ε*d* –ε*s* is the boson energy

The ($\hat{n}_d$) operator gives the number of (*d*) bosons, $(\hat{P}\ )$ is the p

airing operator for the (*s*) and (*d*) bosons, $(\hat{L})$ is the angular momentum operator, $(\hat{Q})$ is the quadrupole operator, $(\hat{T_3})$ and $(\hat{T_4})$are the octupole and hexadecapole operators, respectively. The $(\hat{n}_d,\ \hat{L}, \hat{T}_3$ and $\hat{T}_4)$ operators have $(\Delta n_d = 0)$, while $(\hat{P}^\dagger.\ \hat{P})$ has $(\Delta n_d = 0, \pm 2)$ and $(\hat{Q}.\hat{Q}$)has $(\Delta n_d = 0, \pm 1, \pm 2)$. The parameters a_o, a_1, a_2, a_3 and a_4 designated the strength of the pairing, angular momentum, quadrupole, octoupole and hexadecapole interaction between the bosons.

The IBM Hamiltonian has exact solutions in three dynamical symmetry limits (U(5),O(6) and SU(3)), which are geometrically similar to the a harmonic vibrator, axial rotor and $\gamma-$unstable rotor, respectively. More generally, the Hamiltonian can be expressed in terms of an invariant operator of that chain of symmetries, and a shape phase transition between the dynamical symmetry limits results [42].

2.4. Electromagnetic Transitions in IBM-1

The construction of operators for the various nuclear structure observables of interest is again straightforward, given the fact that they must be built from the basic elements (s, $s^\dagger, d, d^\dagger$). Only the lowest-order contributions to these operators have been included. Electromagnetic transition rates had been characterized by IBM as well, besides agitation energy spectra. One has to specify the transition operators in conditions of the boson operators, in order to do so [43]. Another important attribute that can be deduced and calculated by using the IBM-1 is called the *reduced electric transition probability* B(E2).

The general form of the electromagnetic transition rates operators can be written as follows [36]:

$$\hat{T}_m^{(L)} = \alpha_2 \delta_{L_2} \left[d^\dagger \tilde{s} + s^\dagger \tilde{d}\right]_m^{(2)} + \beta_L \left[d^\dagger \tilde{d}\right]_m^{(L)} + \gamma_0 \delta_{L_0} \delta_{m_0} [s^\dagger \tilde{s}] \begin{matrix}(0)\\0\end{matrix} \qquad (2.4)$$

Where: L=0,1,2,3,4,…,; m=0,1,2,3,4,…, and $\alpha_L, \beta_L, \gamma_0$ represent free parameters, furthermore, Equation gives transition operator for transition (E0,M1,E2,M3,E4,…).

Therefore the electric quadrupole transition operators can be written as [36]:

$$\hat{T}_m^{(E2)} = \alpha_2 \left[d^\dagger \tilde{s} + s^\dagger \tilde{d} \right]_m^{(2)} + \beta_2 \left[d^\dagger \tilde{d} \right]_m^{(2)}. \quad (2.5)$$

The magnetic dipole transition operator can be defined in terms of nuclear gyromagnetic factor (g_β) units nuclear magneton (μ_N) and angular momentum [36]:

$$\hat{T}^{(M1)} = \sqrt{\frac{3}{4\pi}}\, g_\beta \hat{L} \quad (2.6)$$

Therefore the magnetic dipole transition operator for *d*- bosons is given in the following formula:

$$\hat{T}^{(M1)} = \beta_1 \left[d^\dagger \times \tilde{d} \right]_m^{(1)}. \quad (2.7)$$

From Equation (2.6) and (2.7) the nuclear gyromagnetic factor (g_β) can be defined as follow:

$$g_\beta = \frac{\beta_1}{\sqrt{10}} \sqrt{\frac{4\pi}{3}} \quad (2.8)$$

Generally, a nuclear geometric factor can be expressed by magnetic momentum (μ)

$$g_\beta = \frac{\mu_I}{I} \quad (2.9)$$

The general formula of the reduced transition probability for electric and magnetic transitions *B(EL), B(ML)* are known by the following expression [44].

$$B(L, I_i \rightarrow I_f) = \frac{1}{2I_i + 1} \mid < I_i || \hat{T}^L || I_f > \mid^2 \quad (2.10)$$

Where: $\mid < I_i || \hat{T}^L || I_f > \mid$ is the matrix element of (L2) transition.

2.5. Dynamical Symmetries in The IBM-1

The dynamic symmetries are utilized to resolve problems of the Eigen values in Hamiltonian operators. Bosons in the model of interacting bosons (IBM-1) have six-dimensional space because of they have six sub-levels like an outcome they could be characterized in the form of the unitary group which is illustrated by U(6), this could be resolved to three dynamical symmetries [36]. The three limits, or symmetries, of the IBM, are called the *U*(5), *SU*(3) and *O*(6) limits and correspond to the vibrational, rotational, and γ-unstable nuclear structures, respectively.

The first group, *U*(6) is represented by the quantum number, *N* (total number of bosons), and so all states in the *U*(6) group are degenerate. Each step of the group chain introduces a unique quantum number and breaks the degeneracy of the previous group, except for the (n_Δ) and (ν_Δ) terms. The degeneracy is broken until the *O*(3) group is reached.

The (n_Δ) and (ν_Δ) quantum numbers are labels to distinguish between degenerate states and are related to the number of boson triplets coupled to spin 0. Equation (2.11) can be formulated as follow [45]:

$$\hat{\mathrm{H}} = \sum_{i=1}^{N} \varepsilon_i + \sum_{i<j}^{N} V_{ij} \quad (2.11)$$

Where: (ε_i) is the energy of bosons and (N) represents the number of bosons and finally (V_{ij}) depicts the interaction effort between bosons.

2.5.1. The Vibrational SU(5) Limit

The vibrational limit clarifies by the sub-group U(5). The Hamiltonian function can be defined as follows.

$$\hat{\mathrm{H}}^{(I)} = \varepsilon\hat{n}_d + a_1\hat{L}.\hat{L} + a_3\hat{T}_3.\hat{T}_3 + a_4\hat{T}_4.\hat{T}_4 \quad (2.12)$$

Equation (2.12) obviously display the operators($\hat{P}$) and $\left(\hat{Q}\right)$ are ineffectual in this limit. The eigen value Equation for the Hamiltonian operator is given in the following formula [1]:

$$E = \varepsilon_{nd} + \frac{\alpha n_d}{2}(n_d - 1) + \beta(n_d - v)(n_d + v + 3) + \gamma[L(L+1)6n_d] \quad (2.13)$$

The quantum numbers which are shown in the eigen value Equation can be represented by degenerate chain U(5)

$$\left| \begin{array}{ccccc} U(6) \supset & U(5) \supset & O(5) \supset & O(3) \supset & O(2) \\ \downarrow & \downarrow & \downarrow & \downarrow & \downarrow \\ [N] & n_d & v, n_\Delta & L & M \end{array} \right\rangle \quad (2.14)$$

Where: N represents the total number of bosons, and n_d denotes the number of d -bosons and v is the seniority which calculates the number of d- bosons not pairwise coupled with (L=0). The (n_Δ) represents the number of d -bosons tripled coupled with (L=0), (L, M) is the two quantum numbers which represent the angular momentum and components. Even though the electric quadruple transition operator takes different forms depending on the type of the limit. In vibrational limit U(5), it achieves the selection rules ($n_d = 0, \pm 1$)[46]. A typical spectrum for the U(5) limit is shown in Figure (2.1). The reduced transition probabilities for electric quadruple are given according to the following formula [43]:

$$B(E2; L+2 \to L) = \frac{\alpha_2^2}{4}(L+2)\left(2N_\rho - L\right) \quad (2.15)$$

For the ground state

$$B(E2; 2_1^+ \to 0_1^+) = \alpha_2^2 N_\rho \quad (2.16)$$

The quadruple momentum can be written as follow [43]:

$$Q_L = \beta_2 \sqrt{\frac{16\pi}{5}} \sqrt{\frac{1}{14}} L \quad (2.17)$$

For 2_1^+ state

$$Q_{2_1^+} = \beta_2 \sqrt{\frac{16\pi}{5}} \sqrt{\frac{2}{7}} \tag{2.18}$$

The β_2 is :

$$\beta_2 = -\frac{0.7}{\sqrt{2}} \alpha_2 \tag{2.19}$$

The Equation below gives the branching ratio R, R' and R'' for U(5) limit [43]:

$$R = \frac{B(E2; 4_1^+ \to 2_1^+)}{B(E2; 2_1^+ \to 0_1^+)} = 2\frac{(N_\rho - 1)}{N} \leq 2 \tag{2.20}$$

$$R' = \frac{B(E2; 2_2^+ \to 2_1^+)}{B(E2; 2_1^+ \to 0_1^+)} = 2\frac{(N_\rho - 1)}{N} \leq 2 \tag{2.21}$$

$$R'' = \frac{B(E2; 0_2^+ \to 2_1^+)}{B(E2; 2_1^+ \to 0_1^+)} = 2\frac{(N_\rho - 1)}{N} \leq 2 \tag{2.22}$$

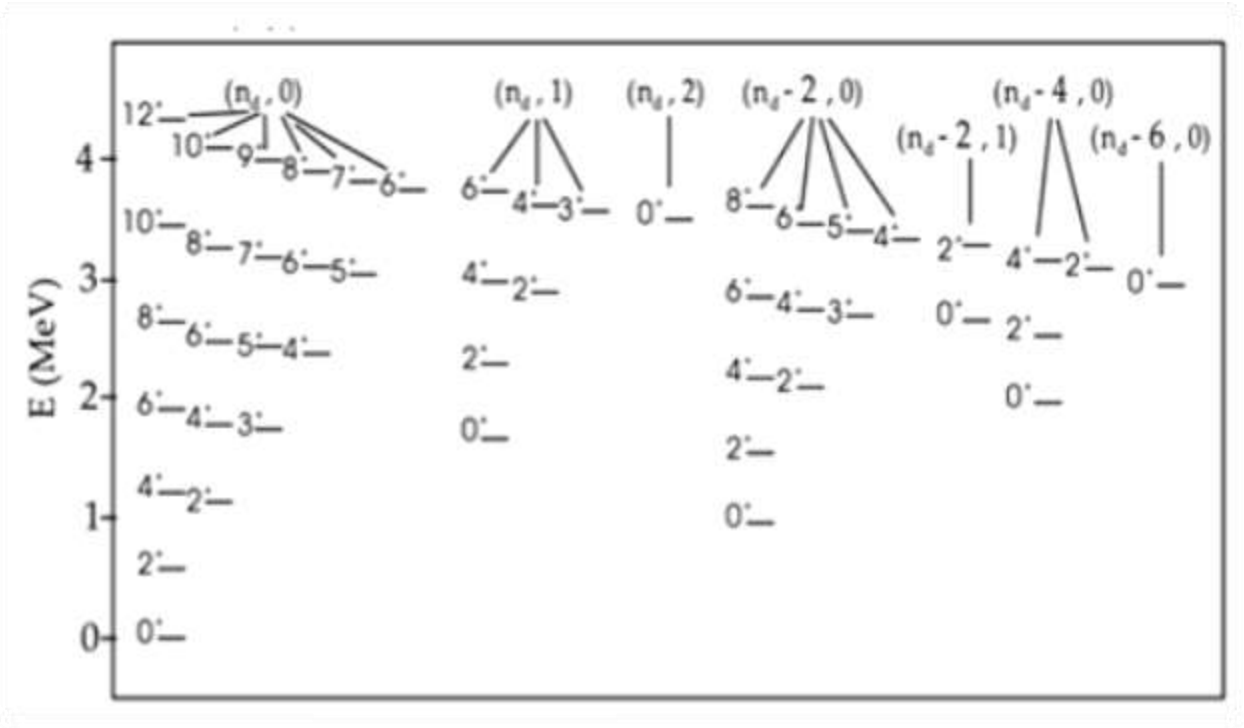

Figure (2.1) Typical spectrum and quantum numbers for U(5) symmetry when N=6 [1].

2.5.2. The Rotational SU(3) Limit

The Rotational limit is represented by the sub-group SU(3). The Hamiltonian function can be defined as follows [46]:

$$\hat{H}^{(II)} = a_1 \hat{L}.\hat{L} + a_2 \hat{Q}.\hat{Q} \tag{2.23}$$

The Equation (2.23) clearly shows that the operators ($\epsilon, \hat{P}, \hat{T}_3$ and $\hat{T}_4$) are ineffective in this limit, a typical spectrum for the SU(3) limit is shown in Figure (2.2). The Eigen value Equation is [1]:

$$E = K_2(\lambda^2 + \mu^2 + \lambda\mu + 3(\lambda + \mu)) + K_5 L(L+1) \tag{2.24}$$

The quantum numbers which are shown in the Eigen value Equation can be represented by degenerate chain SU(5).

$$\left| \begin{array}{cccccc} SU(6) \supset & SU(3) \supset & O(3) \supset & O(2) \\ \downarrow & \downarrow & \downarrow & \downarrow \\ [N] & (\lambda, \mu) \; K & L & M \end{array} \right\rangle \tag{2.25}$$

Where: $K_2 = \frac{a_2}{2}$ and $K_5 = a_1 - \frac{3a_2}{8}$ (2.26)

$$a_1 = \frac{E(2_1^+)}{6} + \frac{3}{8} a_2 \quad \text{and} \quad a_2 = -\frac{E(2_2^+) - E(2_1^+)}{3(2N-1)} \tag{2.27}$$

Where: the quantum numbers (λ, μ), represent cases SU(3) and (K) indicates the number of cases that have equal values of (λ, μ, L), the Equation below shows operator (E2) [46]:

$$T_m^{(E2)} = \alpha_2 \left[(d^\dagger \times \tilde{s} + s^\dagger \times \tilde{d})_m^{(2)} - \frac{\sqrt{7}}{2} (d^\dagger \times \tilde{d})_m^{(2)} \right] \tag{2.28}$$

Where: $\beta_2 = -\frac{\sqrt{7}}{2} \alpha_2$ (2.29)

The selection rules in this limit are :

$\Delta\lambda = 0, \Delta\mu = 0$

The value of *B(E2)* is given the following formula:

$$B(E2; L+2 \to L) = \alpha_2^2 \frac{3}{4} \frac{(L+2)(L+1)}{(2L+3)(2L+5)} \big(2N_\rho - L\big)\big(2N_\rho + L + 3\big) \tag{2.30}$$

For ground state:

$$B(E2; 2_1^+ \to 0_1^+) = \alpha_2^2 \frac{1}{5} N_\rho \big(2N_\rho + 3\big) \tag{2.31}$$

The electric quadrupole momentum for this limit is got form [46]:

$$Q_L = -\alpha_2 \sqrt{\frac{16\pi}{40}} \frac{L}{2L+3} (4N+3) \tag{2.32}$$

As $Q_{2_1^+}$ becomes ;

$$Q_{2_1^+} = -\alpha_2 \sqrt{\frac{16\pi}{40}} \frac{2}{7} (4N+3) \tag{2.33}$$

The branching ratios R, R' and R'' for SU(3) limit can be deduced from [46]:

$$R = \frac{B(E2; 4_1^+ \to 2_1^+)}{B(E2; 2_1^+ \to 0_1^+)} = \frac{10}{7} \frac{(N_\rho - 1)(2N_\rho + 5)}{N_\rho (2N_\rho + 3)} \leq \frac{10}{7} \tag{2.34}$$

$$R' = \frac{B(E2; 2_2^+ \to 2_1^+)}{B(E2; 2_1^+ \to 0_1^+)} = 0 \tag{2.35}$$

$$R'' = \frac{B(E2; 0_2^+ \to 2_1^+)}{B(E2; 2_1^+ \to 0_1^+)} = 0 \tag{2.36}$$

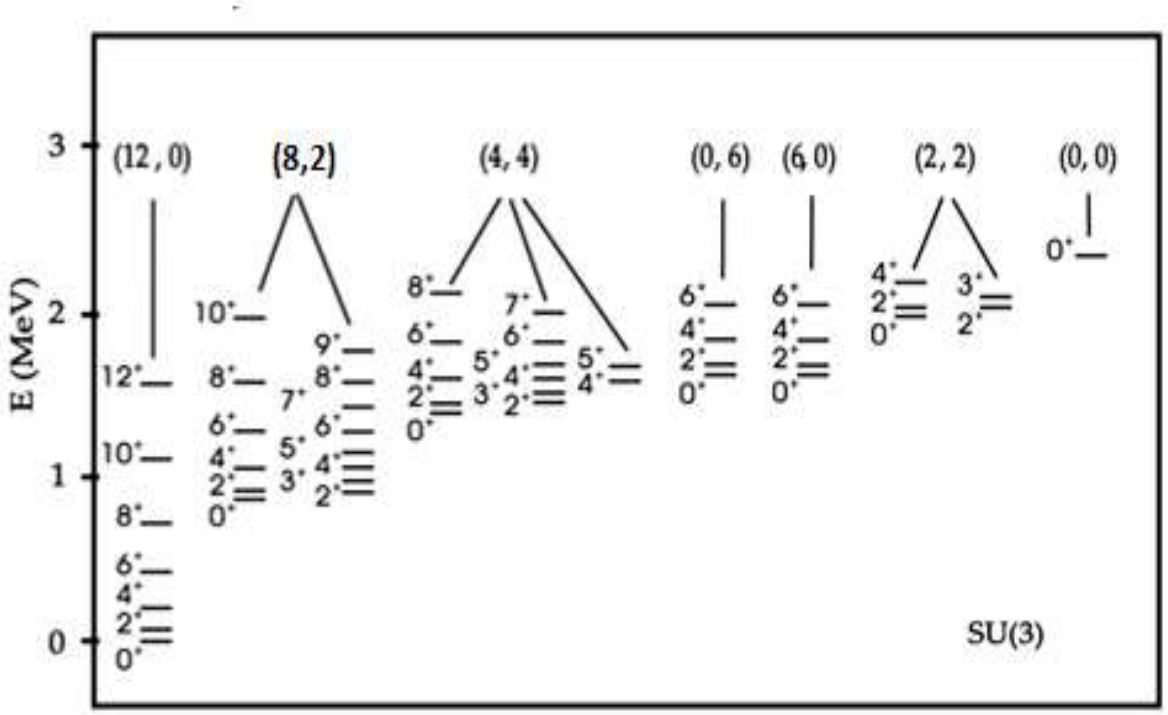

Figure (2.2) Typical spectrum and quantum numbers for SU(3) symmetry when N=6 [1].

When the IBM-1 model is utilized in the study of nuclei in the SU(3) limit, it gives a solution similar to that of the geometrical one by Bohr and Mottelson. The Q_{IBM} and the value gotten from the geometrical solution Q_{BM} are equivalent [1]:

$$Q_{BM}(L) = -eQ_0 \frac{L}{2L+3} \tag{2.37}$$

Where (Q_0) is the intrinsic quadrupole momentum and it is possible to find it after calculating the value of *B(E2)* [1]:

$$B(E2; L \to L-2) = \frac{5}{16\pi}\frac{3}{2}\frac{(L+2)}{(2L+3)}\frac{(L+1)}{(2L+5)} e^2 Q_0^2 (L \to L-2) \tag{2.38}$$

$$Q_0 = \sqrt{B(E2; L+2 \to L)\frac{32\pi(2L+3)(2L+5)}{15(L+2)(L+1)e^2}} \tag{2.39}$$

For state $(2_1^+ \to 0_1^+)$:

$$Q_0 = \sqrt{\frac{16\pi B(E2)}{e^2}} \tag{2.40}$$

2.5.3. ɣ-Unstable O(6)Limit

In regard to the IBM-1, the intruder band has been described in the *O*(6) symmetry limit with two additional proton bosons [7]. The *O*(6) group chain (III) and corresponds, geometrically, to the γ-soft deformed rotor. As can be seen in chain III the only difference between the *O*(6) and *U*(5) chains is the replacement of the *U*(5) subgroup with the *O*(6). The *O*(6) chain is defined by the quantum numbers (*N*, σ, τ , *v*, and *L*). Again, similar to the *U*(5) chain, the (v_Δ)term is necessary in transitioning from the *O*(5) to *O*(3) subgroups to uniquely identify the states.

The labels, (τ) and (v_Δ) used for the *O*(6) chain, are identical to the (*v*) and (n_Δ)quantum numbers in the *U*(5) scheme, while σ takes on the values (*N*, *N*-2,..., 0, or 1), and describes the generalized seniority, that is, the *s*-*d* boson seniority [38].

This limit is produced when the coupling interacting ($\hat{P}.\hat{P}$) is dominant between bosons on the energy of bosons (ε). The Hamiltonian operators in this case, are given by [46]:

$$\hat{\mathrm{H}}^{(III)} = a_0\hat{P}.\hat{P} + a_1\hat{L}.\hat{L} + a_3\hat{T}_3.\hat{T}_3 \qquad (2.41)$$

The eigenvalue Equation is [7]:

$$E = \frac{A}{4}\left(N_\rho - \sigma\right)\left(N_\rho + \sigma + 4\right) + \frac{B}{6}\tau(\tau+3) + CL(L+1) \qquad (2.42)$$

The quantum numbers shown in the eigenvalue Equation can be represented by degenerate chain SU(5)

$$\left|\begin{array}{ccccccc} SU(6) & \supset & O(6) & \supset & O(5) & \supset & O(3) \supset O(2) \\ \downarrow & & \downarrow & & \downarrow & & \downarrow \quad \downarrow \\ [N] & & \sigma & & \tau, v_\Delta & & L \quad M \end{array}\right\rangle \qquad (2.43)$$

σ, τ: is a quantum number which is given as follows:

$\sigma = N_\rho,\ N_\rho - 2, \ldots, 0 \text{ or } 1 \quad \text{for } \mathrm{N_\rho} = \text{even or } \mathrm{N_\rho} = \text{odd}$.

$\tau = 0, 1, \ldots, \sigma$.

Where: ($A = a_0/4,\ B = a_3/2$ and $C = a_1 - a_3/10$) which represent the conjugate eigenvalue and (v_Δ) represents the number of *d*- bosons tripled coupled with zero angular momentum. Figure (2.3) shows a typical spectrum to O(6) limit, the quadrupole transition operator($T_m^{(E2)}$) is [46]:

$$T_m^{(E2)} = \alpha_2 \left[d^\dagger \tilde{s} + s^\dagger \tilde{d} \right]_m^{(2)}. \tag{2.44}$$

where: ($\beta_2 = 0$), and the selection rules are ($\Delta\delta = 0, \Delta\tau = \pm 1$), the B(E2) value is given by

$$B(E2; L+2 \to L) = \alpha_2^2 \frac{(L+2)}{2(L+5)} \frac{1}{4} \left(2N_\rho - L\right)\left(2N_\rho + L + 8\right) \tag{2.45}$$

When L=0 is:

$$B(E2; 2_1^+ \to 0_1^+) = \alpha_2^2 \frac{1}{5} N_\rho \left(N_\rho + 4\right) \tag{2.46}$$

While when L=2 is:

$$B(E2; 4_1^+ \to 2_1^+) = \alpha_2^2 \frac{2}{7} \left(N_\rho - 1\right)\left(N_\rho + 5\right) \tag{2.47}$$

One concludes through selection rules that the value of quadrupole momentum is equal to zero: $Q_L = 0$.

The Equations below give the branching ratios R, R' and R'' for the O(6) limit [46]:

$$R = \frac{B(E2; 4_1^+ \to 2_1^+)}{B(E2; 2_1^+ \to 0_1^+)} = \frac{10}{7} \frac{(N_\rho - 1)(N_\rho + 5)}{N_\rho (N_\rho + 4)} < \frac{10}{7} \tag{2.48}$$

$$R' = \frac{B(E2; 2_2^+ \to 2_1^+)}{B(E2; 2_1^+ \to 0_1^+)} = \frac{10}{7} \frac{(N_\rho - 1)(N_\rho + 5)}{N_\rho (N_\rho + 4)} < \frac{10}{7} \tag{2.49}$$

$$R'' = \frac{B(E2; 0_2^+ \to 2_1^+)}{B(E2; 2_1^+ \to 0_1^+)} = 0 \tag{2.50}$$

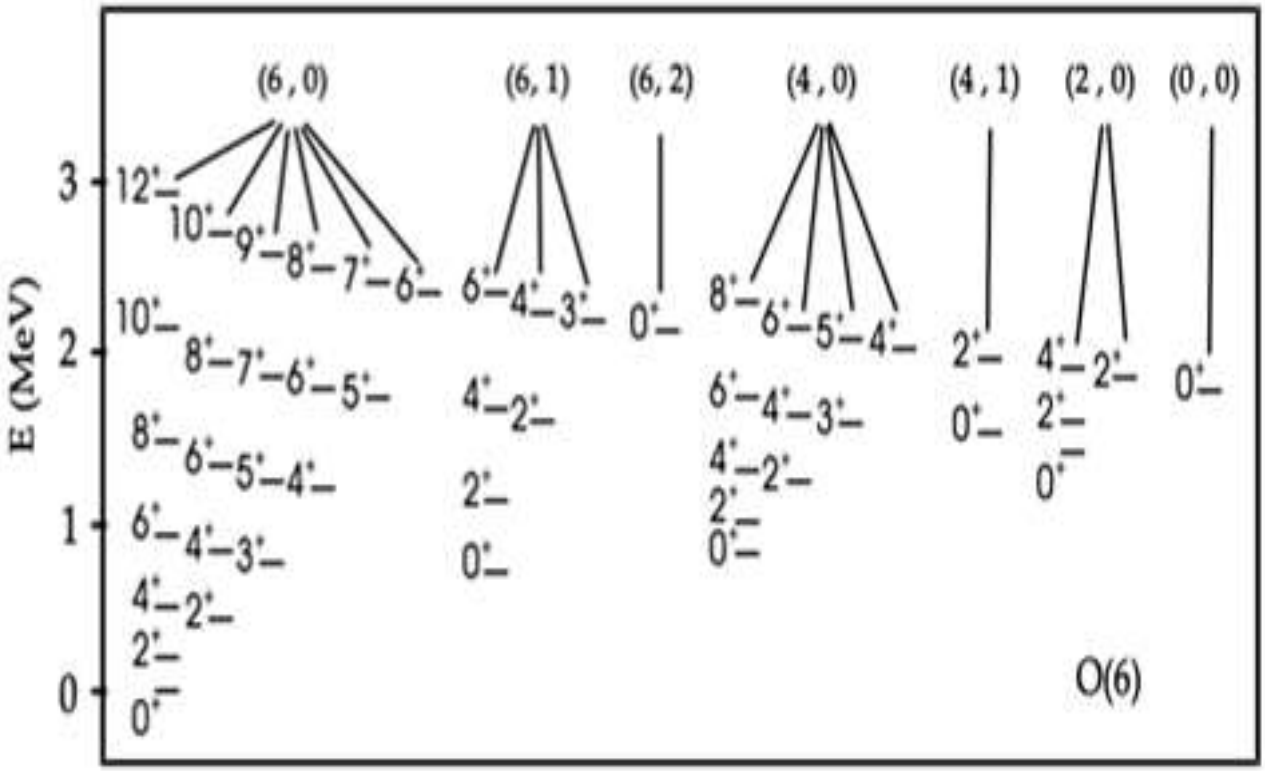

Figure (2.3) Typical spectrum and quantum numbers for O(6) symmetry when N=6 [1].

2.6. Transitions Regions in IBM-1

An important aspect of symmetry concepts is that pairs of symmetries act as benchmarks and, therefore, termini of transitional regions. Sequences of nuclei in such a phase transitional region can be very simply calculated, generally by a variation of a single parameter that specifies their location along the appropriate leg of the symmetry triangle. This parameter can usually be taken as the ratio of the coefficients in the Hamiltonian of the two symmetries occupying the vertices of the triangle at the termini of the transition leg.

The Casten triangle shows the three dynamical symmetries and the transitional areas and Figure (2.4) illustrates this.

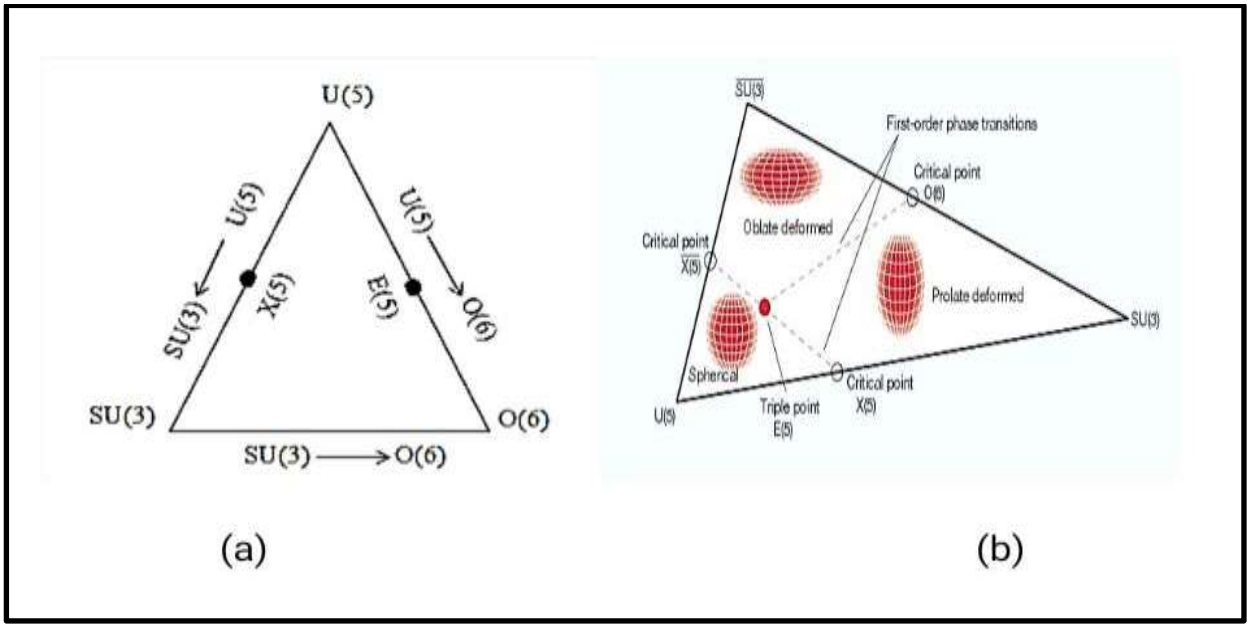

Figure (2.4) The Casten triangle [47].

In Figure (2.4)(a) each peak denotes a mathematical symmetry identical to one of the three forms displayed. Transition points and their related critical symmetries are specified, as are first-order phase transitions. Jolie *et al*. suggest that there is a nuclear triple point that marks the second-order transition between a spherical nuclear shape and a prolate or oblate distorted one. Figure (2.4)(b) shows the spherical and deformed region in the Casten triangle. The limits previously discussed give a set of analytical solutions that can be easily tested, as the number of the nuclei that can be characterized by these limits is so few because most of the nuclei have common properties between these limits called transition region, which can be divided into four classes:

2.6.1. Class A :$\mathbf{U(5) \rightarrow SU(3)}$

The nuclei have properties between vibrational and rotational limits in the transition region, and the Hamiltonian operator is given as follows [48]:

$$\hat{H}^{(I+II)} = \varepsilon + a_1 \hat{L}.\hat{L} + a_2 \hat{Q}.\hat{Q} \qquad (2.51)$$

The ratio (ε/a_2) determines the properties of nuclei in this region. Thus, when the ratio gets higher, the properties become closer to U(5) limit, but when the ratio gets lower, the properties become closer to SU(3) limit.

2.6.2. Class B : $\mathbf{SU(3) \rightarrow O(6)}$

The nuclei have properties between the rotational limit and γ_ unstable limit in the transition region and the Hamiltonian is [48]:

$$\hat{H}^{II+III} = a_0\hat{P}.\hat{P} + a_1\hat{L}.\hat{L} + a_2\hat{Q}.\hat{Q} \qquad (2.52)$$

The ratio (a_0/a_2) determines the properties of nuclei in this region. Thus, when the ratio gets higher, the properties become closer to O(6) limit, but when the ratio gets lower, the properties becomes closer to SU(3) limit.

2.6.3. Class C : $\mathbf{U(5) \rightarrow O(6)}$

The nuclei have properties between vibrational limit and γ- unstable limit in the transition region and the Hamiltonian is [49]:

$$\hat{H}^{(I+III)} = \varepsilon + a_0\hat{P}.\hat{P} + a_1\hat{L}.\hat{L} + a_3\hat{T}_3.\hat{T}_3 \qquad (2.53)$$

Properties of this limit depending on the ratio (ε/a_0).

2.6.4. Class D : $\mathbf{U(5) \rightarrow SU(3) \rightarrow O(6)}$

The nuclei of this class possess the common properties between three limits and the Hamiltonian operator is given as follows [49]:

$$\hat{H}^{(I+II+III)} = \varepsilon + a_0\hat{P}.\hat{P} + a_1\hat{L}.\hat{L} + a_2\hat{Q}.\hat{Q} + a_3\hat{T}_3.\hat{T}_3 + a_4\hat{T}_4.\hat{T}_4 \qquad (2.54)$$

In IBM, axial symmetric rotations and spherical vibrators are described schematically in the IBM by the analytical solvable dynamical symmetries SU(3) and O(6) with schematical describes γ – soft nuclei [50]. The unstable region γ –soft, from the ratio between $E^+_{0_2}/E^+_{2_1}$, $E^+_{4_1}/E^+_{2_1}$, $E^+_{6_1}/E^+_{2_1}$ and $E^+_{8_1}/E^+_{2_1}$ as in Table (2.1).

Table (2.1) Typical energy levels ratios.

Limit	$\frac{E_{0_2^+}}{E_{2_1^+}}$	$\frac{E_{4_1^+}}{E_{2_1^+}}$	$\frac{E_{6_1^+}}{E_{2_1^+}}$	$\frac{E_{8_1^+}}{E_{2_1^+}}$
U(5)	2	2	3	4
SU(3)	>>2	3.33	7	10
O(6)	4.5	2.5	4.5	7

2.7. Potential Energy Surface

The potential energy surface ($E(N,\beta,\gamma)$) gives a final shape to the nucleus that corresponds to the function of Hamiltonian, as shown in Equation (2.58) [50] :

$$E(N,\beta,\gamma) = \langle N,\beta,\gamma|H|N,\beta,\gamma\rangle / \langle N,\beta,\gamma|N,\beta,\gamma\rangle \quad (2.55)$$

The expectation value of the IBM-1 Hamiltonian with the coherent state ($|N,\beta,\gamma\rangle$) is used to create the IBM energy surface [38].

The state is a product of boson creation operators ($b_c^\dagger$), with

$$\left|N,\beta,\gamma\right\rangle = 1/\sqrt{N!}\left(b_c^\dagger\right)^N|0\rangle \quad (2.56)$$

$$b_c^\dagger = (1+\beta^2)^{-1/2}\left\{s^\dagger + \beta\left[\cos\gamma\left(d_0^\dagger\right) + \sqrt{1/2}\,\sin\gamma\left(d_2^\dagger + d_{-2}^\dagger\right)\right]\right\} \quad (2.57)$$

The energy surface, as a function of (β) and (γ), has been given by [38]:

$$V(N,\beta,\gamma) = \frac{N\varepsilon_d\beta^2}{(1+\beta^2)} + \frac{N(N+1)}{(1+\beta^2)^2}\,(a_1\beta^4 + a_2\beta^3\cos 3\gamma + a_3\,\beta^2 + a_4) \quad (2.58)$$

where: a_1's are related to the coefficients (C_L, ν_2, ν_0, u_2 and u_0) of Equation (2.1). (β) is a measure of the total deformation of the nucleus, when ($\beta = 0$) the shape is spherical, and be distorted when ($\beta \neq 0$) , and (γ) is the amount of deviation from the focus symmetry and correlates with the nucleus, if (γ = 0) the shape is prolate, and if (γ = 60) the shape becomes oblate [66]. The following Equations represented the potential energy surface for three dynamical symmetries:

$$E(N,\beta,\gamma) \propto \begin{cases} \text{U(5)}: & \varepsilon_d N\dfrac{\beta^2}{1+\beta^2} \quad (2.59) \\ \text{SU(3)}: & kN(N-1)\dfrac{\frac{3}{4}\beta^4 - \sqrt{2}\beta^3\cos 3\gamma + 1}{\left(1+\beta^2\right)^2} \quad (2.60) \\ \text{O(6)}: & k'N(N-1)\left(\dfrac{1-\beta^2}{1+\beta^2}\right)^2 \quad (2.61) \end{cases}$$

where ($k \propto a_2$ and $\acute{k} \propto a_0$) in Equation (2.2). The scheme of contour lines and coaxial Symmetries is shown in Figure (2.5).

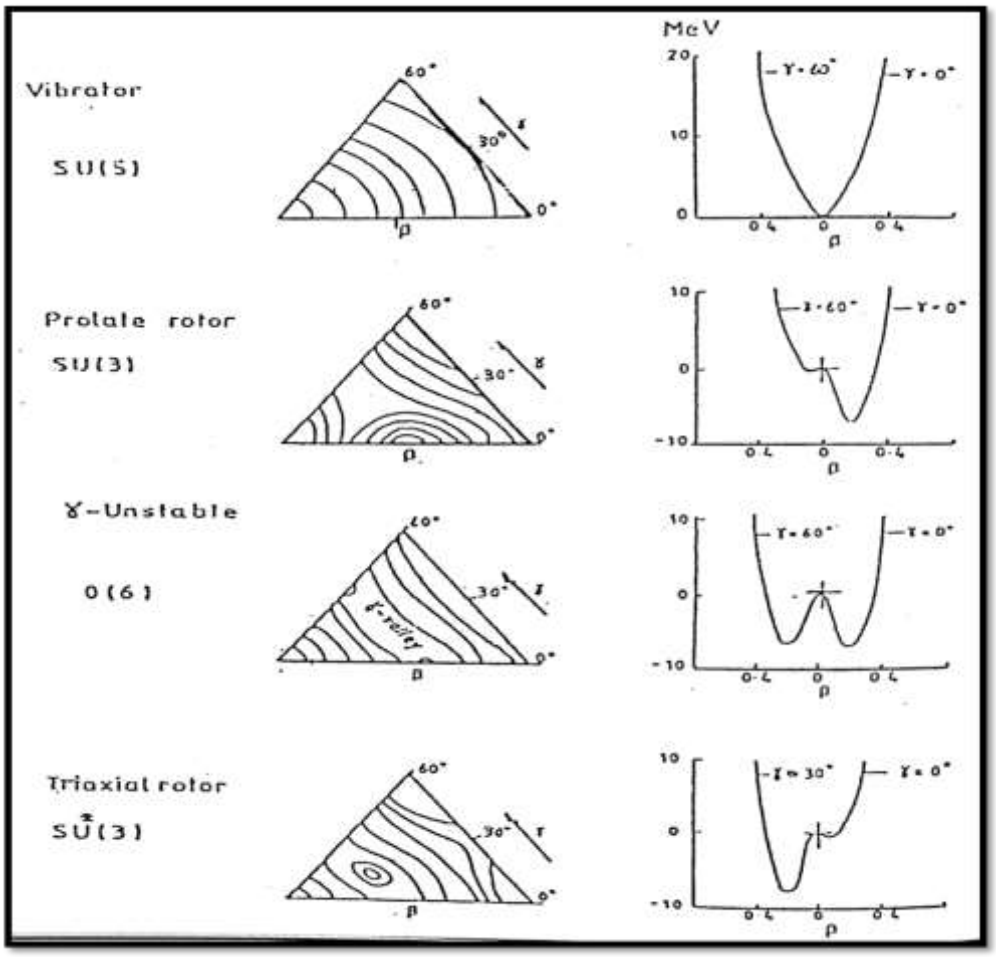

Figure (2.5) The ideal scheme of contour lines and coaxial symmetries [51].

2.8. The Interacting Boson Model-Two (IBM-2)

The second version of the interacting boson model (IBM-2), was introduced in 1978 as a modification of the first model (for neutrons, thus, it becomes possible to obtain some of the energy levels that could not be determined by IBM-1, these levels are called IBM-2), through introducing the concept of degrees of freedom. This made it possible to distinguish between wave function for protons and wave function mixed symmetry states (MSS). The mixing case between wave function for protons and wave function for neutrons can affect the site of energy level for the rest of the energy levels. As a result of this

modification, It becomes possible to calculate the magnetic transition and zero transition which were not possible to be calculated by the first model IBM-1 [46].

2.9. The Hamiltonian Operator In IBM-2

The pattern below is the general formula of the Hamiltonian operator in (IBM-2) model [52]:

$$\hat{H} = \hat{H}_{\pi} + \hat{H}_{\nu} + \hat{H}_{\pi\nu} \quad (2.62)$$

where:

$\hat{H}_{\pi}$ is the Hamiltonian operator bosons protons.

$\hat{H}_{\nu}$ is the Hamiltonian operator bosons neutrons.

$\hat{H}_{\pi\nu}$ is the Hamiltonian operator bosons protons and neutrons.

The Equation (2.62) can be rewritten in different formulas which introduce all parameters that are effective in the Hamiltonian operator [53]:

$$\hat{H} = \varepsilon_d(\hat{n}_{d\nu} + \hat{n}_{d\pi}) + \kappa\left(\hat{Q}_{\nu}.\hat{Q}_{\pi}\right) + V_{\nu\nu} + V_{\pi\pi} + M_{\nu\pi} \quad (2.63)$$

where: ε_d represents the energy difference between s and d boson, n_{ρ} represents the number of d bosons, where ρ goes along with π (proton) or ν (neutron) bosons, the second term refers to the quadrupole – quadrupole interaction between proton and neutron with strength κ, where the quadruple operator Q_{ρ} can be written as [53]:

$$Q_{\rho} = [\, d_{\rho}^{\dagger}s_{\rho} + s_{\rho}^{\dagger}d_{\rho}]^{(2)} + x_{\rho}[d_{\rho}^{\dagger}\, d_{\rho}]^{(2)} \quad (2.64)$$

Where:

χ_{ρ} is the quadrupole deformation parameter for proton and neutron, The $V_{\pi\pi}$ and $V_{\nu\nu}$, which refer to the interaction between like – boson, are sometimes present to improve the fit to experimental energy spectra and they are given by [54]:

$$V_{\rho\rho} = \frac{1}{2}\sum_{L=0,2,4} C_L^{\rho}([d_\rho^\dagger d_\rho^\dagger]^{(L)} \cdot [\tilde{d}_\rho \tilde{d}_\rho]) \quad (2.65)$$

The Majorana term $M_{\nu\pi}$ has the parameters of ξ_1 , ξ_2 and ξ_3 which can be expressed as;

$$M_{\nu\pi} = \frac{1}{2}\xi_2([\, s_\nu^\dagger d_\pi^\dagger - d_\nu^\dagger s_\pi^\dagger]^{(2)} \cdot [s_\nu d_\pi - d_\nu s_\pi\,]^{(2)}) -$$

$$\sum_{k=1,3} \xi_k([d_\nu^\dagger d_\pi^\dagger\,]^{(k)} \cdot [d_\nu d_\pi]^{(k)}) \quad (2.66)$$

The Majorana term has an essential role in studying the mixed symmetry states of some energy levels that are excited. The use of the Equation above demands the calculation of several parameters(χ_ν , $\varepsilon, \kappa, \chi_\pi$), which are all dependent on the numbers of protons and neutrons (N_π, N_V) sequentially. During the study, a set of isotopes will have (N_π) and (χ_π) of a fixed value. As there will be a change in the value of the parameters (χ_ν , ε, κ), the three limits that appeared in the (IBM-1) will reappear in (IBM-2) [54].

2.10. Electromagnetic Transitions in IBM-2

The electric quadropole (*E2*) transitions are one of the important factors within the collective nuclear structure. In IBM-2 model, the general linear *E2* operator is expressed as [55]:

$$T^{(l)} = T_\pi(l) + T_\nu(l) \quad (2.67)$$

$$T^{(E2)} = e_\pi Q_\pi + e_\nu Q_\nu \quad (2.68)$$

where Q_ν and Q_π are in the form of Equation (2.68), are the quadruple operator, the Equation (2.67) become as follows [56,57]:

$$T^{(E2)} = e_\pi[(d^\dagger s + s^\dagger d\ )_\pi^{(2)} + \chi_\pi(d^\dagger d)_\pi^{(2)}]^{(2)} + e_\nu[(d^\dagger s + s^\dagger d\ )_\pi^{(2)} + \chi_\pi(d^\dagger d)_\pi^{(2)}]^{(2)} \quad (2.69)$$

The e_π and e_ν are boson effective charges depending on the total boson number N and *E2* transition mainly depend on identifying proton and neutron bosons effective charges e_π and e_ν .

The reduced electric quadrupole transition rates between two states are given by [58, 59]:

$$B(E2: J_i^+ \to J_f^+) = \frac{1}{2J_i+1}\left|\left\langle J_f \parallel T^{(E2)} \parallel J_i \right\rangle\right|^2 \tag{2.70}$$

The relationship between (e_π, e_ν) and the reduced transition probability *B(E2)* for spherical, rotational and γ - Unstable limits are given in the forms [60]:

$$B(E2: 2_1^+ \to 0_1^+) = \frac{1}{N_\pi}(e_\pi N_\pi + e_\nu N_\nu) \qquad \text{for U(5)} \tag{2.71}$$

$$B(E2: 2_1^+ \to 0_1^+) = \frac{(2N+3)}{5N_\pi}(e_\pi N_\pi + e_\nu N_\nu) \quad \text{for SU(3)} \tag{2.72}$$

$$B(E2: 2_1^+ \to 0_1^+) = \frac{(N+4)}{5N_\pi}(e_\pi N_\pi + e_\nu N_\nu) \qquad \text{for O(6)} \tag{2.73}$$

The electric quadruple moment in IBM-2 can be written [61]:

$$Q = (\frac{16\pi}{5})^{\frac{1}{2}}\left[\frac{J(2J-1)}{(J+1)(2J+2)(2J+3)}\right]^{\frac{1}{2}}\left[B(E2: J_i \to J_f)\right]^{\frac{1}{2}} \tag{2.74}$$

The M1 transition operator up to the one-body term (L =1) is the *M1* operator obtained by letting $L=1$ in the single boson operator of the IBM-1 and can be written as [62]:

$$T^{(M1)} = \left[\frac{3}{4\pi}\right]^{1/2}(g_\pi L_\pi^{(1)} + g_\nu L_\nu^{(1)}) \tag{2.75}$$

where g_π, g_ν are the boson g-factors in units of μ_N and $L^{(1)} = \sqrt{10}(d^\dagger x\tilde{d})^{(1)}$. This operator can be written as[63, 64]:

$$T^{(M1)} = \left[\frac{3}{4\pi}\right]^{1/2}\left[1/2(g_\pi + g_\nu)(L_\pi^{(1)} + L_\nu^{(1)}) + 1/2(g_\pi - g_\nu)(L_\pi^{(1)} - L_\nu^{(1)})\right] \tag{2.76}$$

The first term on the right hand side, in the above Equation, is diagonal and therefore for M1 transitions the previous Equation may be written as [65]:

$$T^{(M1)} = 0.77\left[d^+\tilde{d})_\pi^{(1)} - (d^+\tilde{d})_\nu^{(1)}\right](g_\pi - g_\nu) \tag{2.77}$$

where: g_π, g_ν represent the gyromagnetic factor for proton and neutron respectively, the total g - factor is defined by Sambataro's Equation [66];

$$g = g_\pi \frac{N_\pi}{N_\pi + N_\nu} + g_\nu \frac{N_\nu}{N_\pi + N_\nu} \tag{2.78}$$

the reduced magnetic dipole transition rates between two states are given by [65]:

$$B(M1: J_i^+ \rightarrow J_f^+) = \frac{1}{2J_i + 1} \left| \left\langle J_f \parallel T^{M1} \parallel J_i \right\rangle \right|^2 \tag{2.79}$$

2.11. Mixing Ratios δ(E2/M1)

The study of multipole mixing ratios δ of γ-rays from excited nuclear states have been the subject of interest for many experimental and theoretical investigations. Theoretically, the multipole mixing ratios for *E2*, and *M1* mixed transition can be defined as the ratio of the electric quadrupole *E2* to magnetic dipole *M1* matrix elements for γ-transition from an initial state J_i to final state J_f.

The reduced *E2* and *M1* matrix elements were combined in the calculation of the mixing ratio δ(*E2/M1*) using the relation[67-69, 82, 84]:

$$\delta(E2/M1) = 0.835 E_\gamma (MeV).\Delta \tag{2.80}$$

where $\Delta = \frac{\left\langle J_f \parallel T^{E2} \parallel J_i \right\rangle}{\left\langle J_f \parallel T^{M1} \parallel J_i \right\rangle}$ *in* eb / μ_N (2.81)

2.12. Electric Monopole Ratio $X(E0/E2)$

Monopole transitions (*E0*) are caused by Coulomb interaction between nuclear protons and atomic shell electrons penetrating inside the nucleus (or electron-positron vacuum) [70, 71]. These transitions are known to be pure penetration effect, where the transition is caused by an electromagnetic interaction between the nuclear charge and the atomic electron penetrating the nucleus. An *E0* transition occurs between two states of the same spin and parity by transferring the energy and zero units of angular momentum. Thus *E0* has no competing gamma ray. These transitions are different from zero only in the case where the transition is accompanied by the nucleus surface change. For example in the nuclear models where the surface is assumed to be fixed *E0* transitions

are strictly forbidden. The monopole transition probability is related to the change in the root-mean-square charge radius of the nucleus between the initial and final states at the moment of quantum transition. The reduced nuclear matrix element of the *E0* transition is determined exclusively by the nuclear wave functions and thus an investigation of the monopole transitions gives significant information concerning the nuclear shape and details of nuclear [72].

Electric monopole transitions can occur not only in $0^+ \rightarrow 0^+$ transition but also, in competition with gamma multiple transition and depending on transition selection rules may compete in any $\Delta J = 0$ decay such as a $2^+ \rightarrow 2^+$ or any $J_i \rightarrow J_f$ states in the scheme. This transition in forbidden in the models which suggest in advance that the nucleus has a spherical shape. At transitions energies greater than $2m_oc^2$, monopole pair production is also possible[63]. The study of excited 0^+ in even-even nuclei can provide important facts on the nuclear structure in a given region of the nuclear chart, which in the case of isotopes is the rotational limit. A variety of the theoretical descriptions, for the existence of the first excited 0^+, have been suggested during the last four decays. The *E0* reduced transitions probability written as [73]:

$$B(E0;\ J_i \rightarrow J_f) = e^2 R^4 \rho^2(E0) \qquad J_i = J_f \tag{2.82}$$

where: e is the electronic effective charge, *R* is the nuclear radius and $\rho(E0)$ is the transition matrix element. However, there are only limited cases where $\rho(E0)$ can be measured directly [74].

The $T^{(E0)}$ operator may be found by setting $l = 0$ on the IBM-2 operator [75, 76]:

$$\rho_{if}(E0) = \frac{Z}{R_0^{\,2}} \sum \tilde{\beta}_{0\rho} \left\langle f \left| d^+_{\ \rho} x d_\rho \right| i \right\rangle \tag{2.83}$$

where: $R_o = 1.2A^{1/3}$ fm and $\rho(E0)$ is a dimensionless quantity. The two parameters $\tilde{\beta}_{0\pi}, \tilde{\beta}_{0\nu}$ in Equation (2.83) represent the deformation parameters

for (protons and neutrons) may be estimated by fitting an isotope shift [74], which is the difference in the square radius $\delta\langle r^2\rangle$ between neighboring isotopes in their ground state, whose definition can be stated as follows [77]:

i- The isomer shift is identified by manipulating the difference between the mean square radius $\langle r^2\rangle$ of an excited state and the ground state for any nucleus:

$$\delta\langle r^2\rangle = \langle e \mid r^2 \mid e\rangle - \langle 0 \mid r^2 \mid 0\rangle = \tilde{\beta}_{0\pi}\delta n_{d\pi} + \tilde{\beta}_{0\nu}\delta n_{d\nu} \qquad (2.84)$$

where:

$$\delta n_{d\rho} = \langle e \mid d_\rho^\dagger . \tilde{d}_\rho \mid e\rangle - \langle 0 \mid d_\rho^\dagger . \tilde{d}_\rho \mid 0\rangle \quad \rho = \pi, \nu \qquad (2.85)$$

ii- The isotopes shift is identified by manipulating the difference between two neighboring isotopes in the ground state [78]:

$$\Delta\langle r^2\rangle = \langle 0 \mid r^2 \mid 0_A\rangle - \langle 0 \mid r^2 \mid 0_{A-2}\rangle = \tilde{\beta}_{0\pi}\Delta n_{d\pi} + \tilde{\beta}_{0\nu}\Delta n_{d\nu} - \gamma_{0\nu} \qquad (2.86)$$

Where:

$\gamma_{0\nu}$ is the expected isotopes shift and $(\Delta n_{d\pi}, \Delta n_{d\nu})$ are defined as follows [79]:

$$\Delta n_{d\rho} = \langle 0 \mid d_\rho^\dagger . \tilde{d}_\rho \mid 0\rangle_{N_\nu} - \langle 0 \mid d_\rho^\dagger . \tilde{d}_\rho \mid 0\rangle_{N_{\nu+1}}. \qquad (2.87)$$

After identifying the reduced matrix element for zero transition, the $X(E0/E2)$ ratio can be calculated as follow [80]:

$$X\left(\frac{E0}{E2}\right) = \frac{B\left(E0\,; J_i \to J_f\right)}{B\left(E2\,; J_i \to J_{f'}\right)} \qquad (2.88)$$

where: $J_f = J_{f'}$ for $J_i = J_f \neq 0$, and $J_{f'} = 2$ for $J_i = J_f = 0$

This ratio is so essential as it mirrors to what extent the transition between *B(E2)* and *B(E0)* is strong [81].

2.13. Mixed Symmetry State (MSS)

Nuclear states that are particularly sensitive to the proton-neutron interaction in the valence shell are called mixed symmetry states [82, 83]. These

excitations in atomic nuclei are interesting collective structures of the nuclear many-body system. Their existence enables us to judge the capability of the corresponding phonon modes to act as building blocks of nuclear structure. Possible deviations from harmonic phonon coupling occur due to the structure of the underlying phonon modes and serve as a sensitive source of information on the formation of collectivity in the nuclear many-body system. The proton-neutron interaction in the nuclear valence shell has been known for a long time as the driving force for the evolution of the low-energy nuclear structure. Therefore, it is interesting to study those nuclear excitations that are most sensitive to the proton-neutron interaction in the valence shell. This class of states can occur in even-even nuclei spanning the mass range A = 50 to 240 [85-87]. They arise when the motions of the neutrons and protons which contribute to collective excitation are in a different phase. Any model which distinguishes between the two types of nucleons will naturally predict mixed symmetry states. These states have been observed in the three classes of collective nuclei, in vibrational, rotational and γ -soft nuclei, the lowest energy mixed-symmetry in vibrational nuclei is 2^+ and occurs at 2 MeV and in rotational nuclei is 1^+, the first experimental observation of such states was observed that of a 1^+ state, the so-called scissors mode, in deformed nuclei. A strong M1 excitation to a 1^+ state close to 3 MeV excitation energy, the scissor mode. The name refers to the geometrical picture of the neutron body oscillating against the proton body like cutting scissors [88].

A theoretical effort has been devoted to understanding this new type of collective excitation. Despite the considerable theoretical efforts relatively few nuclei that show MSS characteristics have been identified and in these, in general, only the lowest MSS state has been found. The importance of these states is emphasized by the comment of Arima and Iachello that ‘the location of collective states of mixed proton-neutron symmetry is one of the most

interesting open experimental problems in the study of collective features of nuclei [89].

Mixed symmetry states result from mixing one wave function of proton with a wave function of the neutron when the movements of the proton and neutrons are not in the quantum state [90].

Chapter Three

Calculations and Results

The interacting boson IBM-1 and IBM-2 models are used to describe some properties of the nuclear structure for three series even- even isotopes with series atomic number and heavy mass nuclei $^{160\text{-}178}$Yb, $^{166\text{-}180}$Hf and $^{170\text{-}184}$W isotopes, by studying the low-lying positive parity states, branching ratio, dynamic symmetries, reducing transition probabilities for electric quadrupole and magnetic dipole, quadrupole momentum, mixing ratios $\delta(E2\,/\,M1)$, $X(E0/E2)$ ratio and mixed symmetry states. The closed shell is adopted to be 82 and 126 in the calculation of the number of proton boson N_π and neutron boson N_ν for each nucleus. In calculations of the energy levels the software package (NBPOS) version of September 1983 is used by estimating a set of parameters described in the Hamiltonian operator. The program package (IBMT) and (NPBEM) are also used to calculate the reducing electromagnetic transition probabilities transitions in IBM-1 and IBM-2 respectively. (IBMP) is the program for giving potential energy surface in IBM-1 only. These parameters are treated as free parameters to get the best fit between theoretical values and experimental data. The calculations take into account the systematic state that must be met in these parameters depending on the nature of the increase or decrease of the neutron's number for each nucleus.

3.1 Ytterbium Isotopes (Yb)

Ytterbium is a soft, malleable and ductile chemical element that displays a bright silvery luster when pure. It is a rare-earth element, and it is readily dissolved by strong mineral acids. It reacts slowly with cold water and it oxidizes slowly in the air [91]. The isotopes of lanthanides are known to be very useful for nuclear, industrial and medical applications [92]. Ytterbium metal increases its electrical resistivity when subjected to high stresses. This property

is used in stress gauges to monitor ground deformations from earthquakes and explosions [93].

All isotopes under study ($^{160\text{-}178}$Yb) have Z=70, then 6 hole bosons the number of protons and neutrons lying between 50, 82 and 82,126 magic shells, respectively. The $^{160\text{-}174}$Yb isotopes have 90-104 neutrons, which mean (4-11) particle neutron bosons, while $^{176\text{-}178}$Yb isotopes have 106 and 108 neutrons which mean (10,9) hole neutron bosons with total bosons numbers equal to (10-17) respectively.

3.1.1 Energy Level Calculations

The software package IBM computer code for IBM-1 and neutron proton boson (NPBOS) code for IBM-2 have been used to calculate energy levels for $^{160\text{-}178}$Yb by estimating a set of parameters described in the Hamiltonian operator as it is shown in Equations (2.2) and (2.63) parameters estimated for the low-lying calculations of the excited energy levels for Ytterbium isotopes are given in Tables (3.1) and (3.2) the symbol (*) refers to hole boson, these parameters represented in Figures (3.1) and (3.2).

Table (3.1) Parameters used in the IBM-1 Hamiltonian for even-even $^{160\text{-}178}$Yb isotopes (in MeV).

Isotopes	N	Ɛ	a_0	a_1	a_2	a_3	a_4	χ
$^{160}_{70}Yb_{90}$	10	0	0.0182	0.0222	-0.0446	0	0	-0.221
$^{162}_{70}Yb_{92}$	11	0	0.0188	0.0119	-0.0394	0	0	-0.203
$^{164}_{70}Yb_{94}$	12	0	0.0462	0.00589	-0.0482	0	0	-0.135
$^{166}_{70}Yb_{96}$	13	0	0.0114	0.0104	-0.0199	0	0	-0.45
$^{168}_{70}Yb_{98}$	14	0	0.0098	0.00956	-0.0154	0	0	-0.63
$^{170}_{70}Yb_{100}$	15	0	0.0368	0.0226	-0.039	0	0	-0.168
$^{172}_{70}Yb_{102}$	16	0	0.0086	0.0074	-0.0142	0	0	-0.088
$^{174}_{70}Yb_{104}$	17	0	0.0098	0.0072	-0.0135	0	0	-0.062
$^{176}_{70}Yb_{106}$	16*	0	0.0117	0.0088	-0.0142	0	0	-0.106
$^{178}_{70}Yb_{108}$	15*	0	0.0116	0.0086	-0.0143	0	0	-0.084

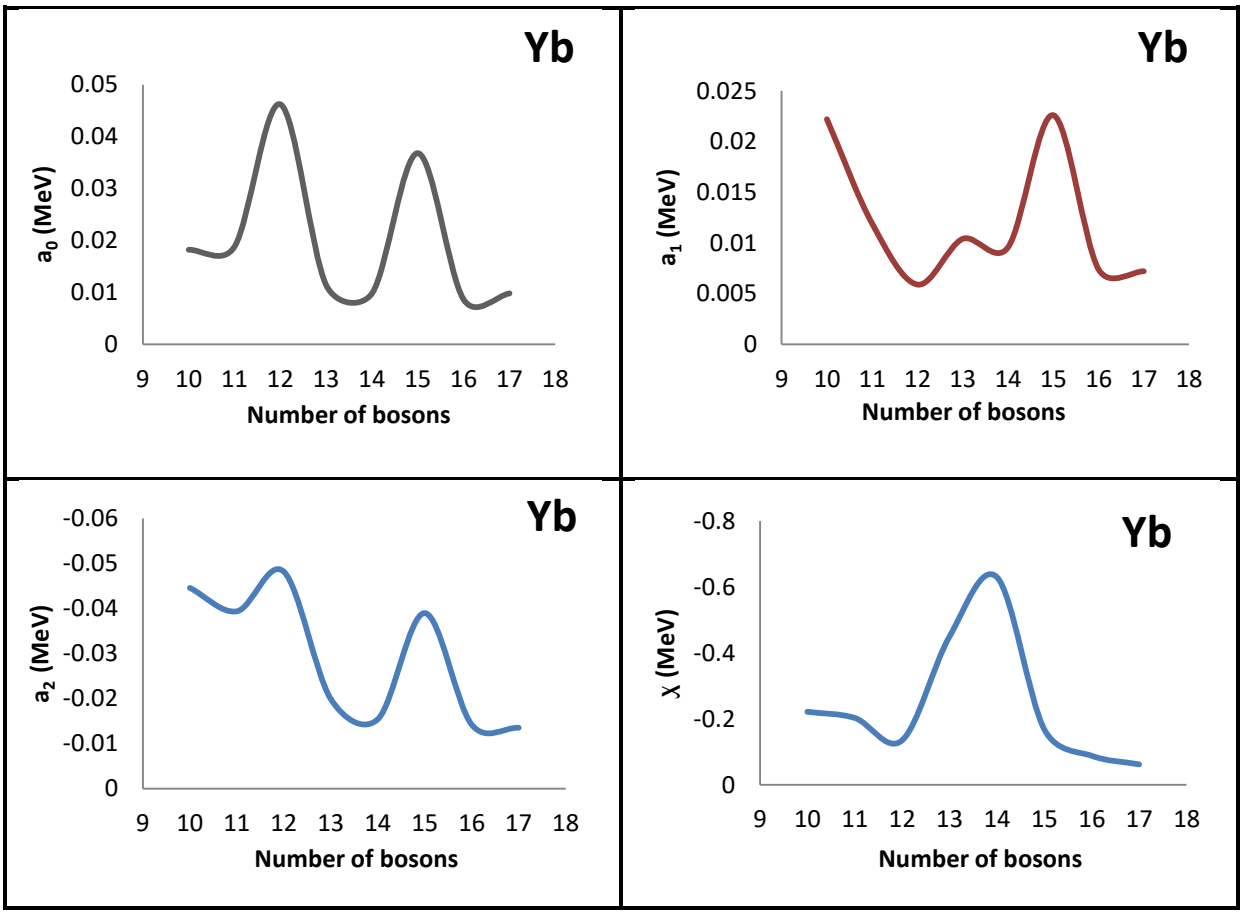

Figure (3.1) IBM-1 parameters (χ, a_0, a_1, a_2) for $^{160\text{-}178}$Yb isotopes as a function of the number of bosons.

Table (3.2) Parameters used in the IBM-2 Hamiltonian for even-even $^{160\text{-}178}$Yb isotopes (in MeV) except χ_ν and χ_π, without units, N_π=6.

Isotops	N_υ	Ɛ	Ƙ	X_υ	X_π	$\zeta_{1,3}$	ζ_2	C^L_υ			C^L_π		
$^{160}_{70}Yb_{90}$	4	0.62	-0.072	-1.11	-1.11	0.12	0.08	-0.16	0.48	0.18	0.17	0.15	0.062
$^{162}_{70}Yb_{92}$	5	0.55	-0.072	-1.11	-1.11	0.13	0.08	-0.15	0.6	0.17	0.16	0.14	0.05
$^{164}_{70}Yb_{94}$	6	0.462	-0.076	-1.112	-1.11	0.12	0.08	-0.14	0.9	0.16	0.15	0.13	0.04
$^{166}_{70}Yb_{96}$	7	0.435	-0.074	-1.113	-1.11	0.12	0.08	-0.15	0.64	0.17	0.14	0.12	0.02
$^{168}_{70}Yb_{98}$	8	0.34	-0.068	-1.113	-1.11	0.16	0.08	-0.13	0.8	0.13	0.12	0.8	0.005
$^{170}_{70}Yb_{100}$	9	0.31	-0.068	-1.113	-1.11	0.16	0.08	-0.12	0.8	0.12	0.11	0.07	0.004
$^{172}_{70}Yb_{102}$	10	0.21	-0.068	-1.114	-1.11	0.15	0.08	-0.11	0.9	0.13	0.12	0.06	0.003
$^{174}_{70}Yb_{104}$	11	0.19	-0.069	-1.114	-1.11	0.14	0.08	-0.1	1.1	0.12	0.14	0.05	0.002
$^{176}_{70}Yb_{106}$	10*	0.28	-0.068	-1.116	-1.11	0.14	0.08	-0.1	0.9	0.12	0.14	0.06	0.003
$^{178}_{70}Yb_{108}$	9*	0.31	-0.068	-1.115	-1.11	0.14	0.08	-0.1	0.9	0.13	0.15	0.07	0.003

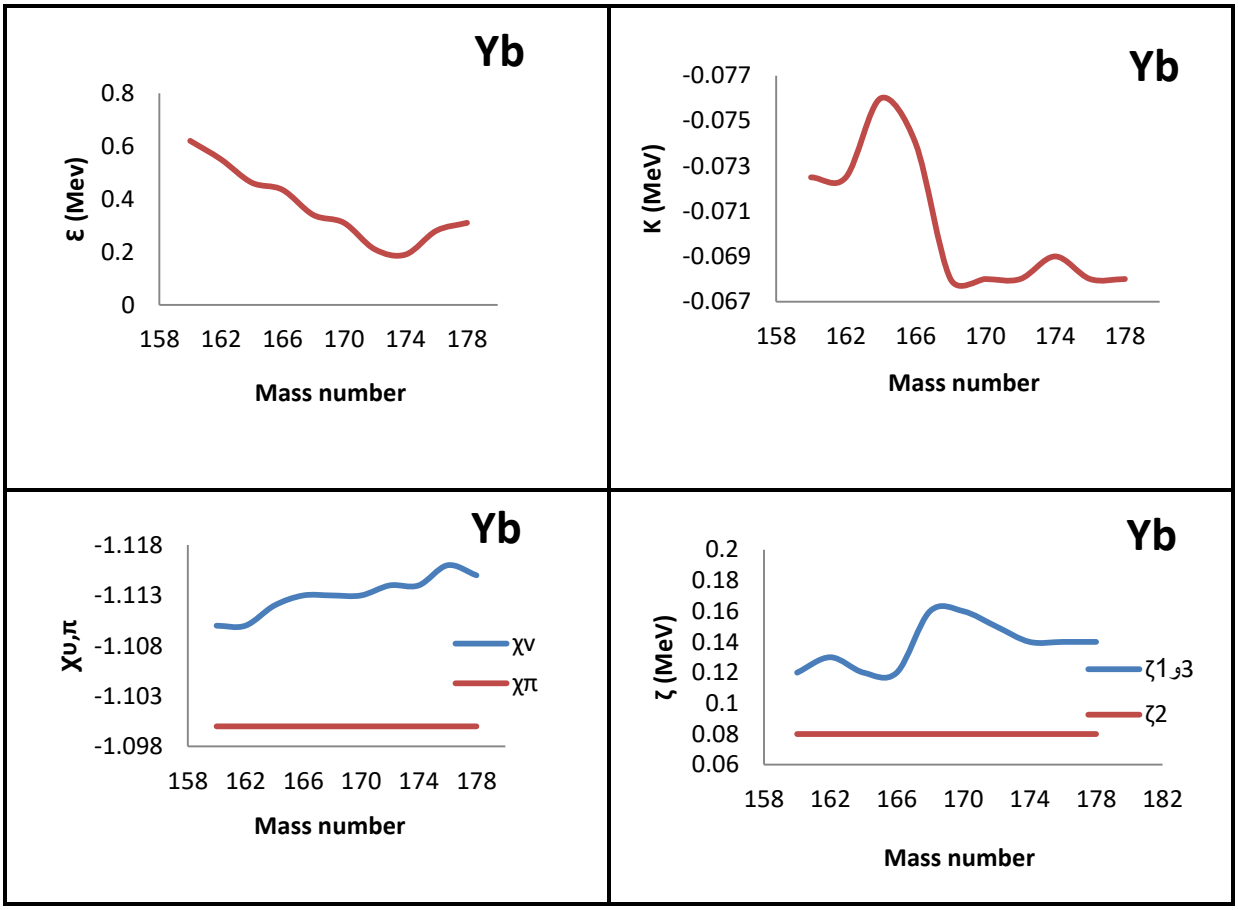

Figure (3.2) IBM-2 parameters (ε, κ, χ_π, χ_ν, ζ_2, $\zeta_{1,3}$) for $^{160\text{-}178}$Yb isotopes as a function of the mass number.

The calculated energy levels by IBM-1 and IBM-2 compared with the experimental data [94- 103] for $^{160\text{-}178}$Yb isotopes have been shown in Figures from (3.3) to (3.12).

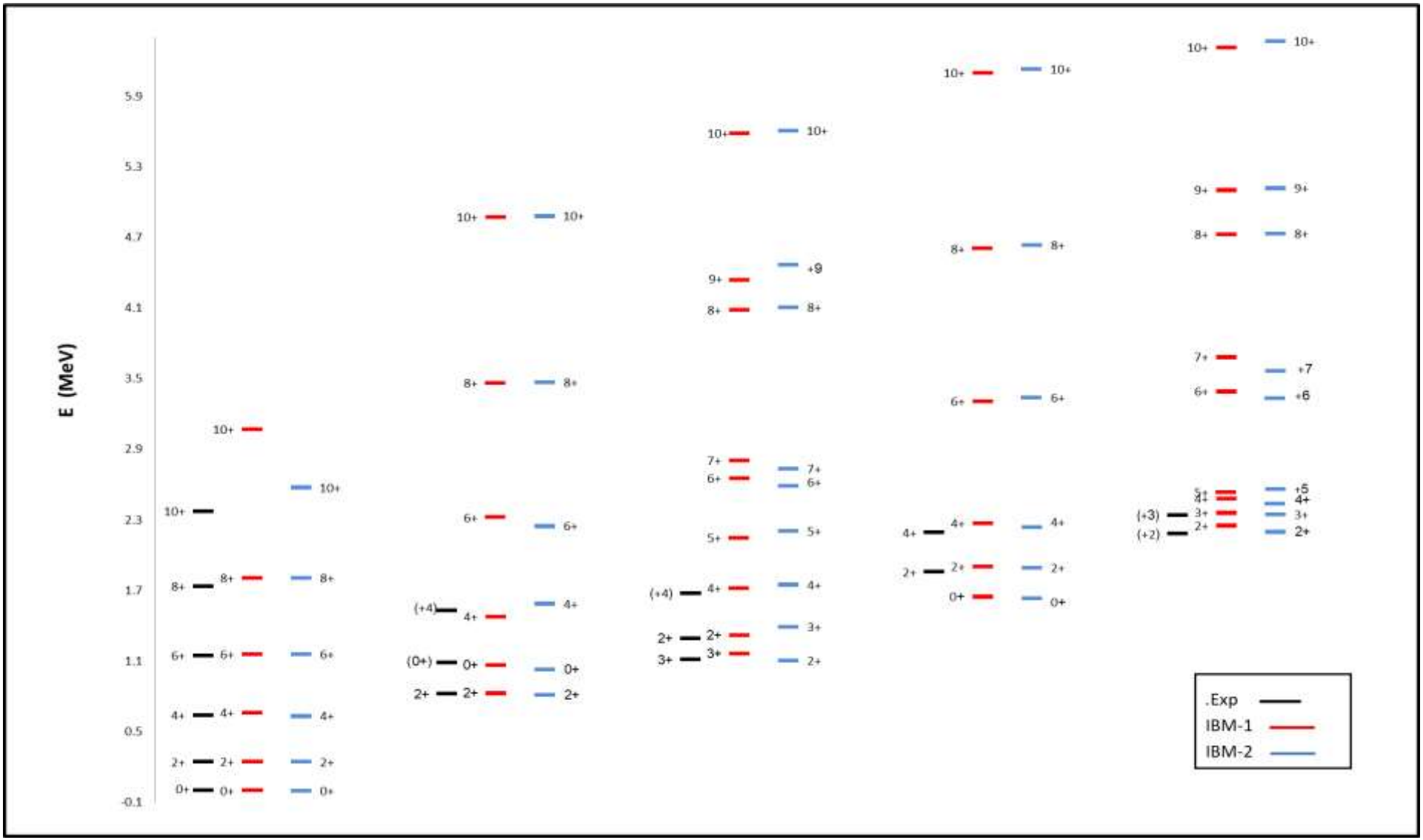

Figure (3.3) Energy levels for ^{160}Yb.

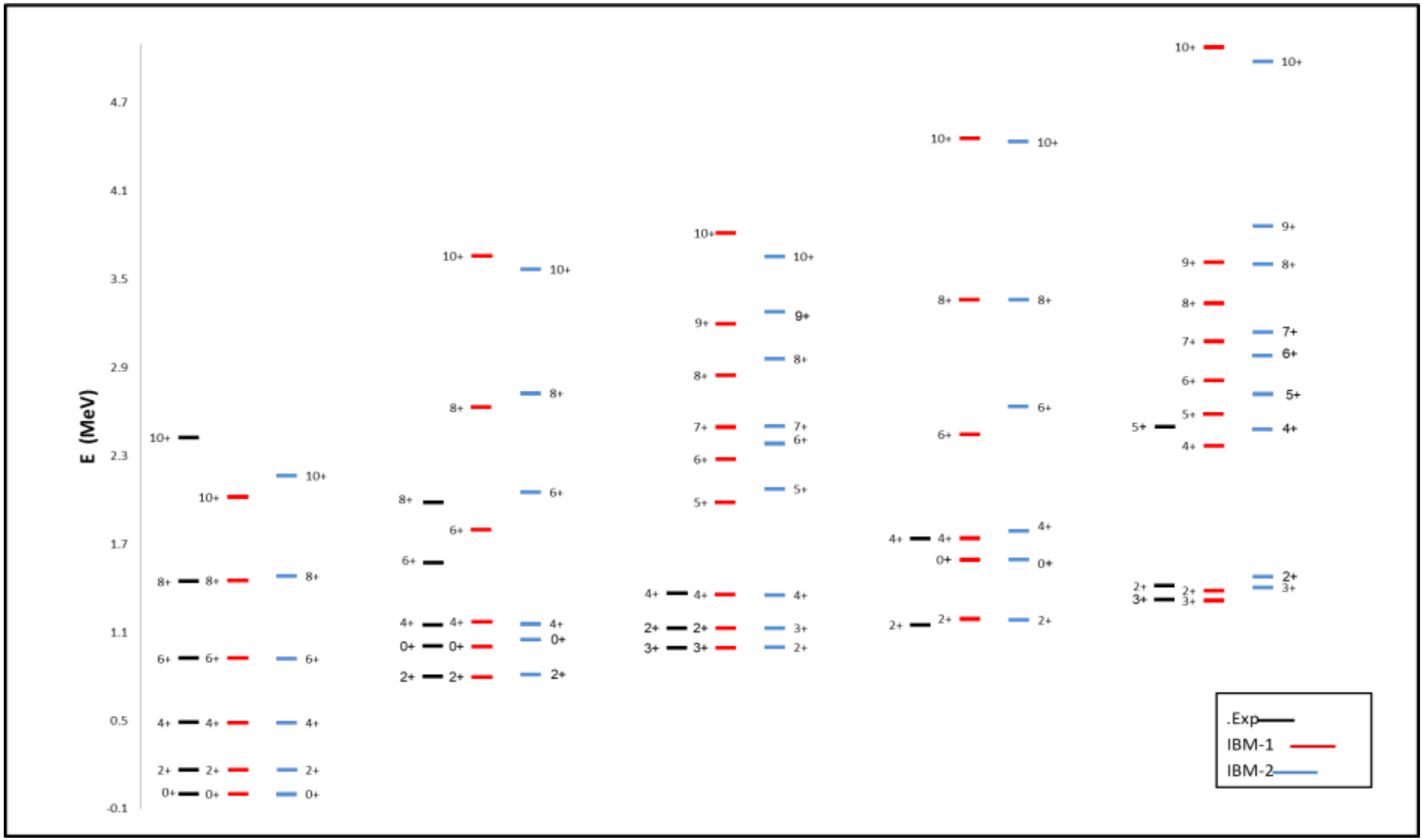

Figure (3.4) Energy levels for ^{162}Yb.

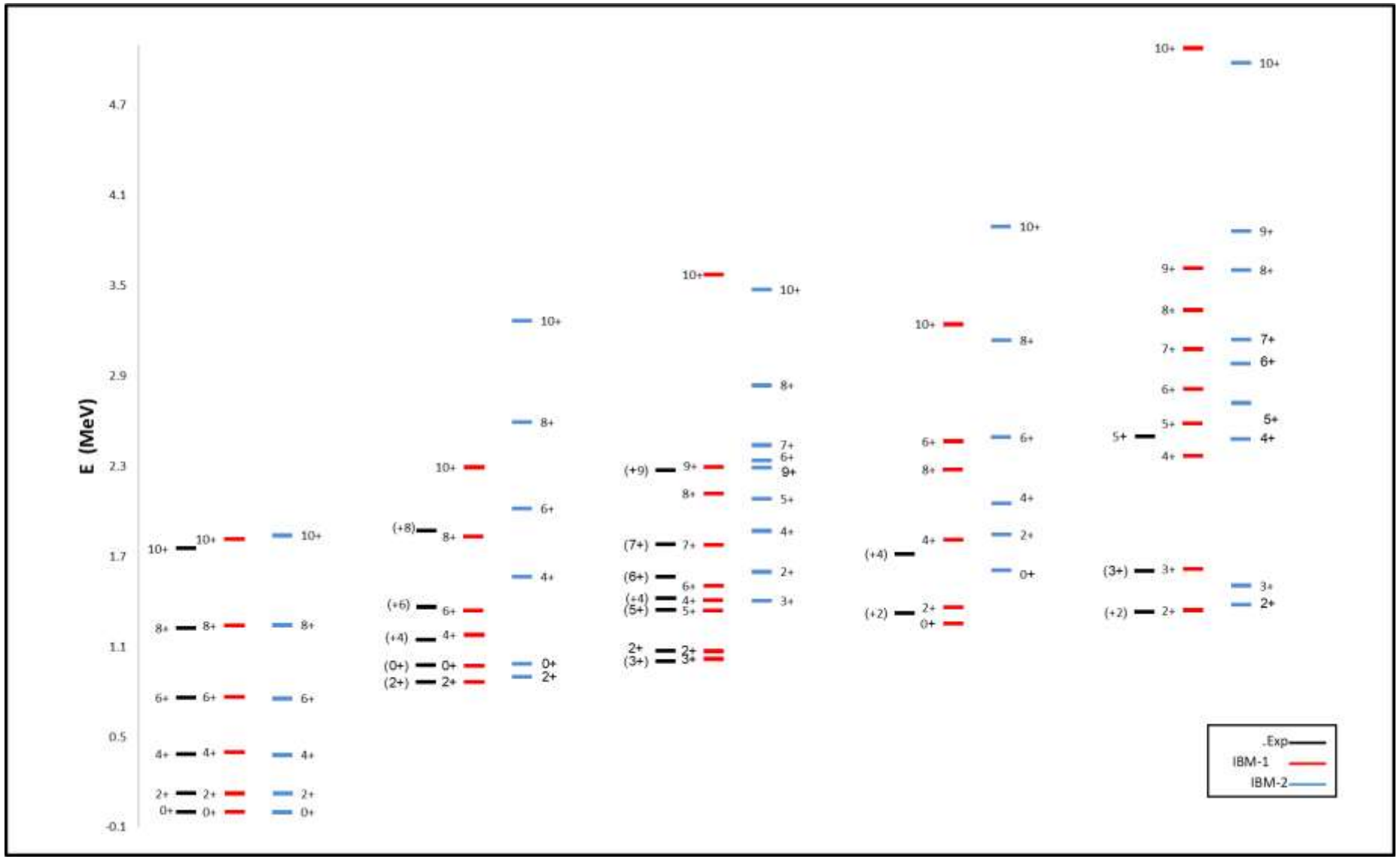

Figure (3.5) Energy levels for ^{164}Yb.

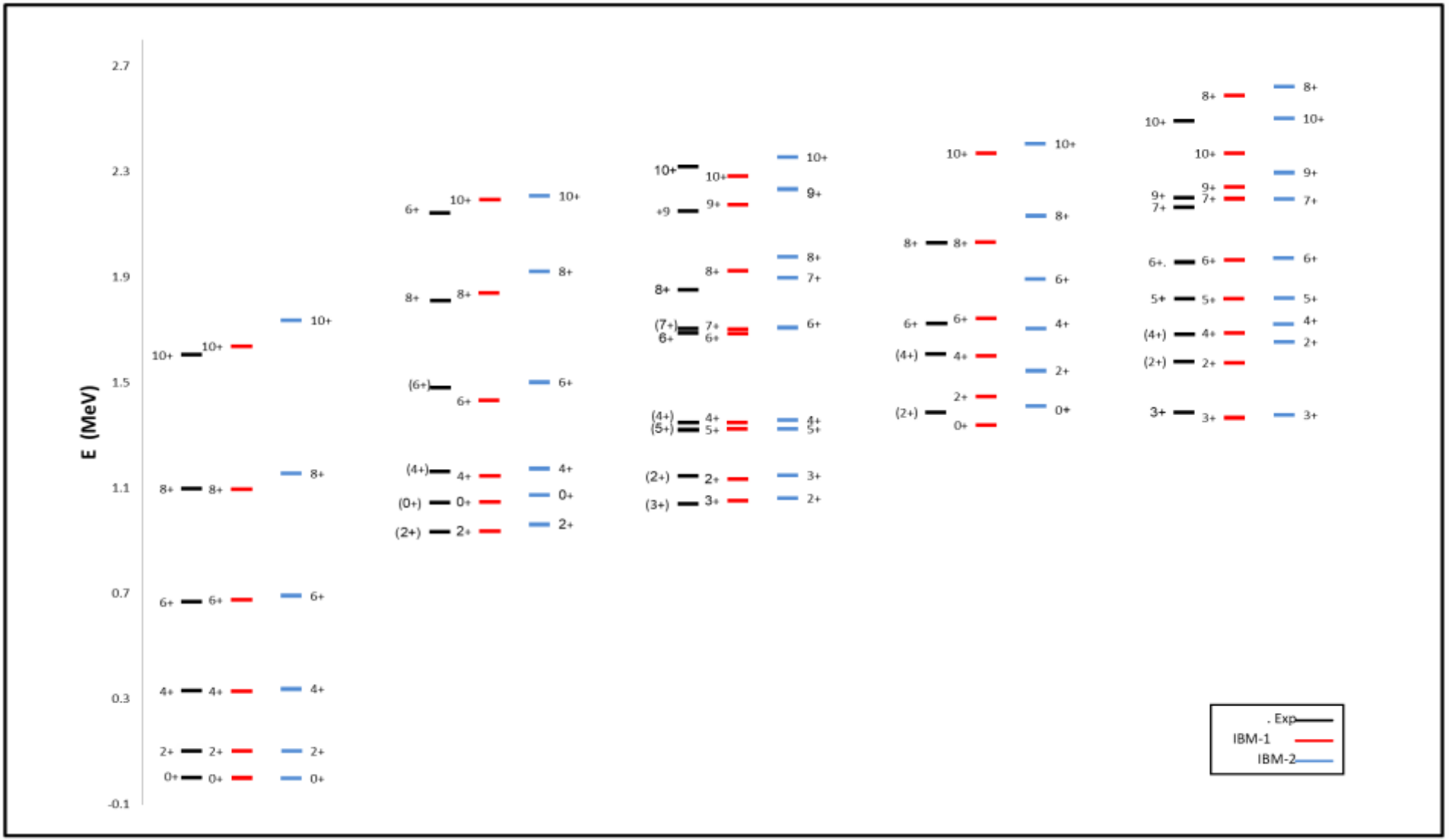

Figure (3.6) Energy levels for ^{166}Yb.

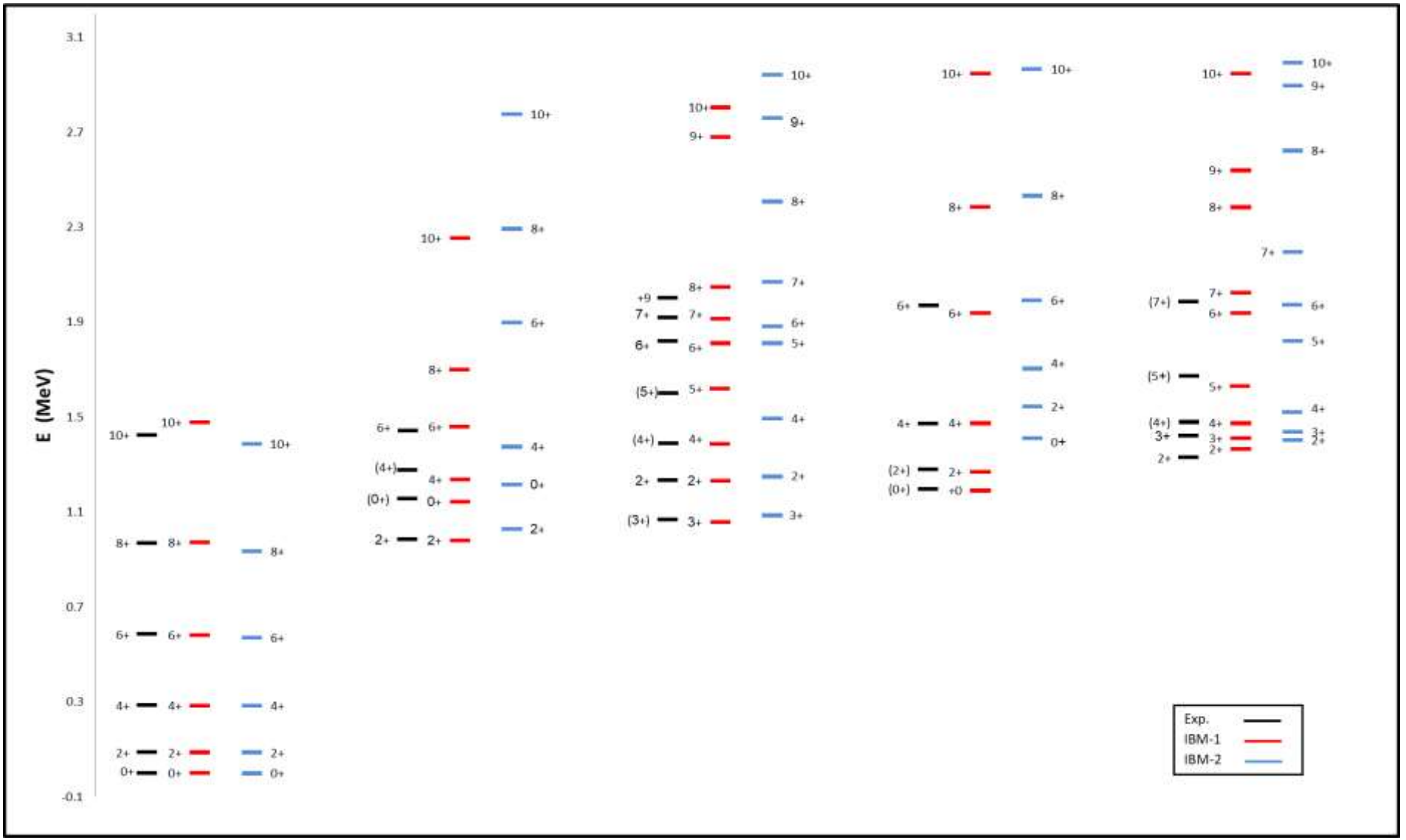

Figure (3.7) Energy levels for ^{168}Yb.

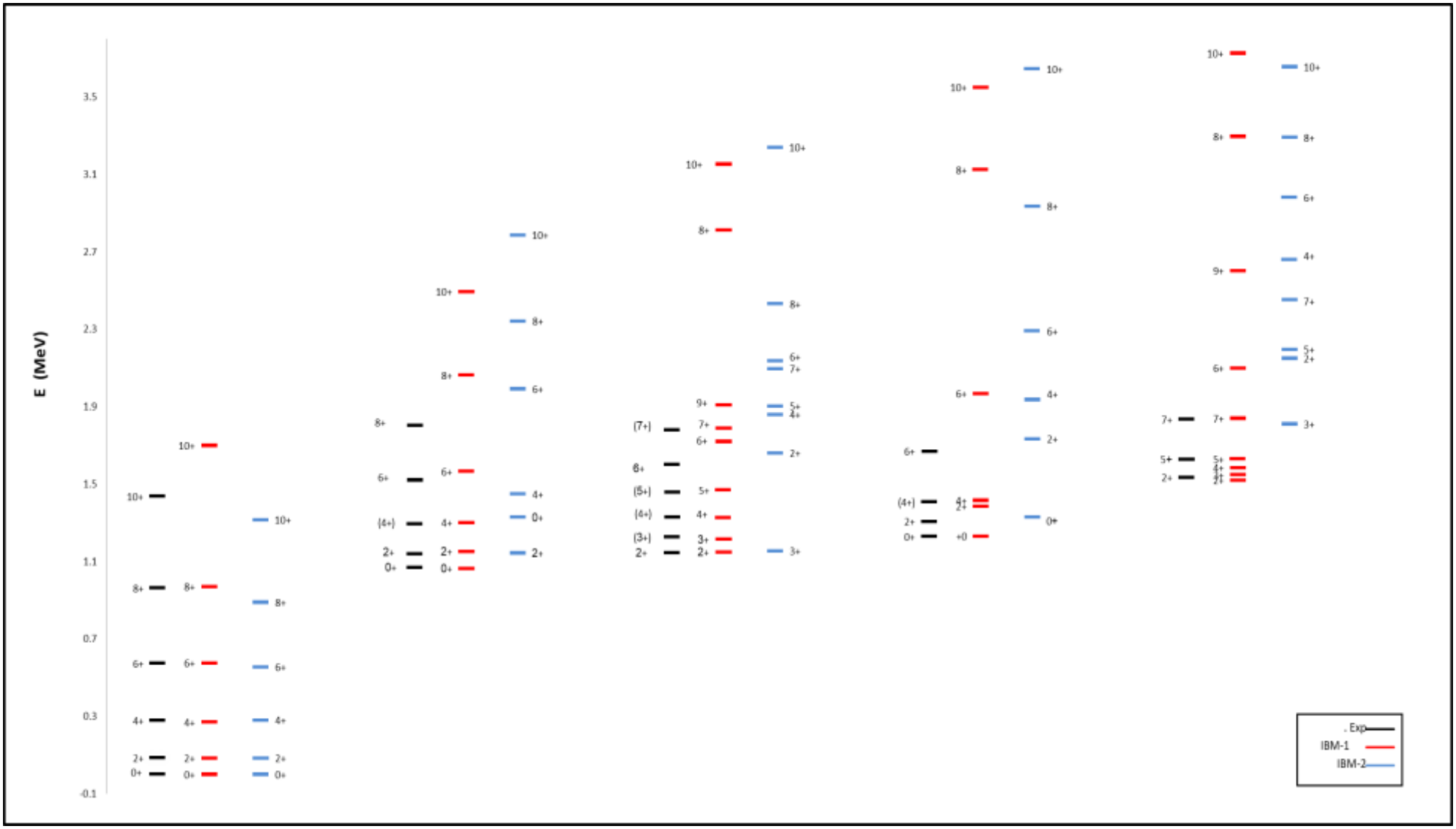

Figure (3.8) Energy levels for ^{170}Yb.

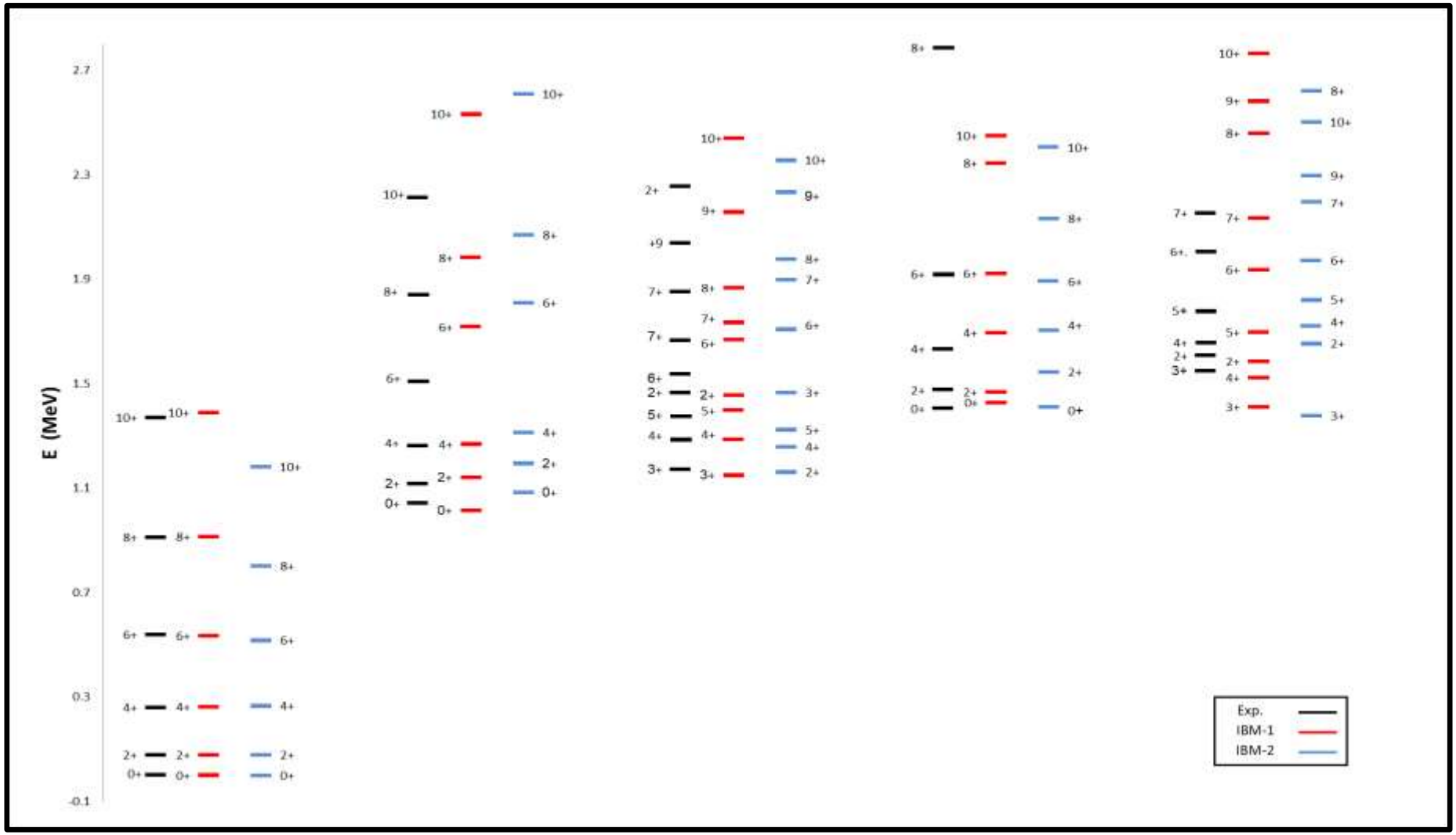

Figure (3.9) Energy levels for ^{172}Yb.

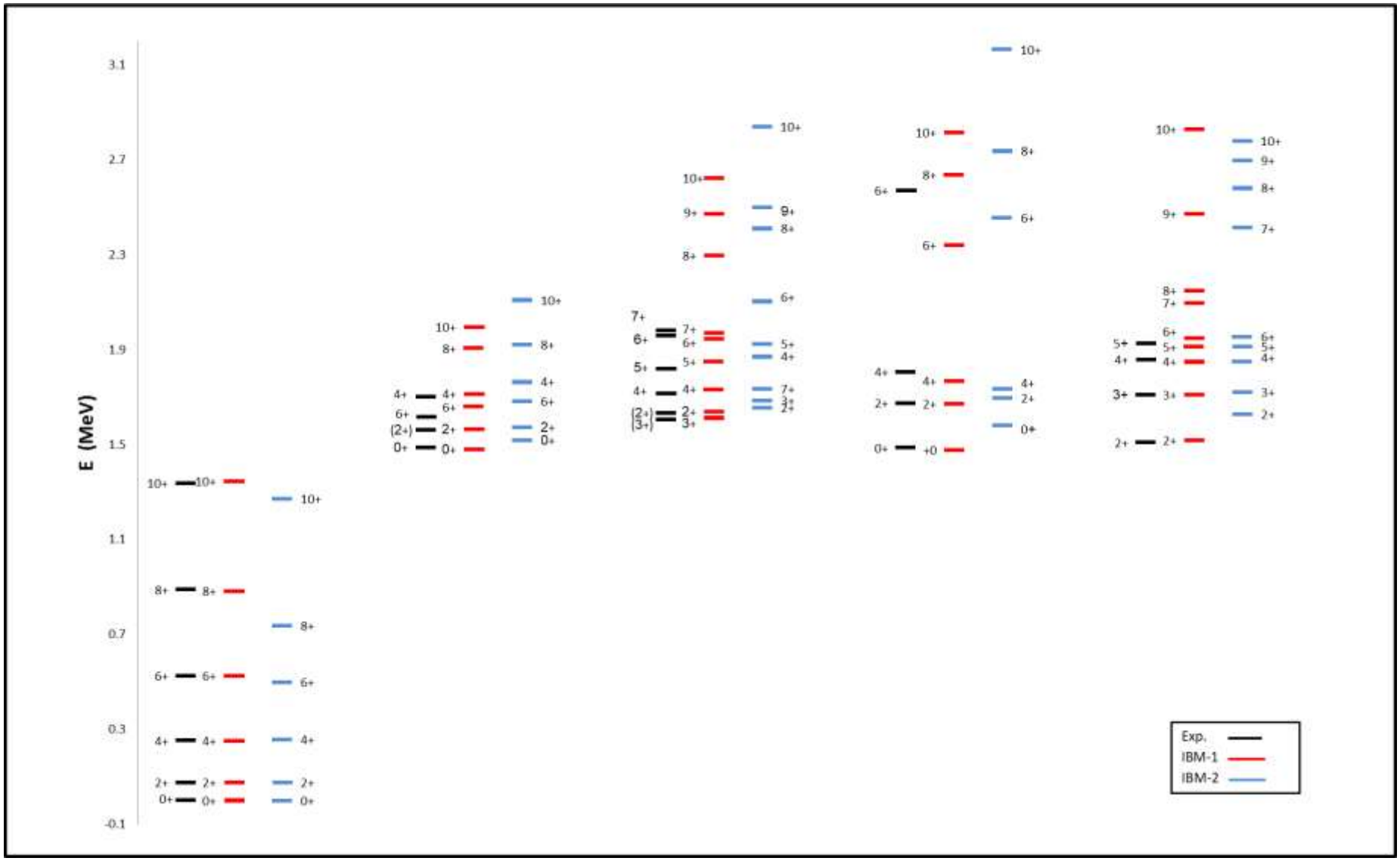

Figure (3.10) Energy levels for ^{174}Yb.

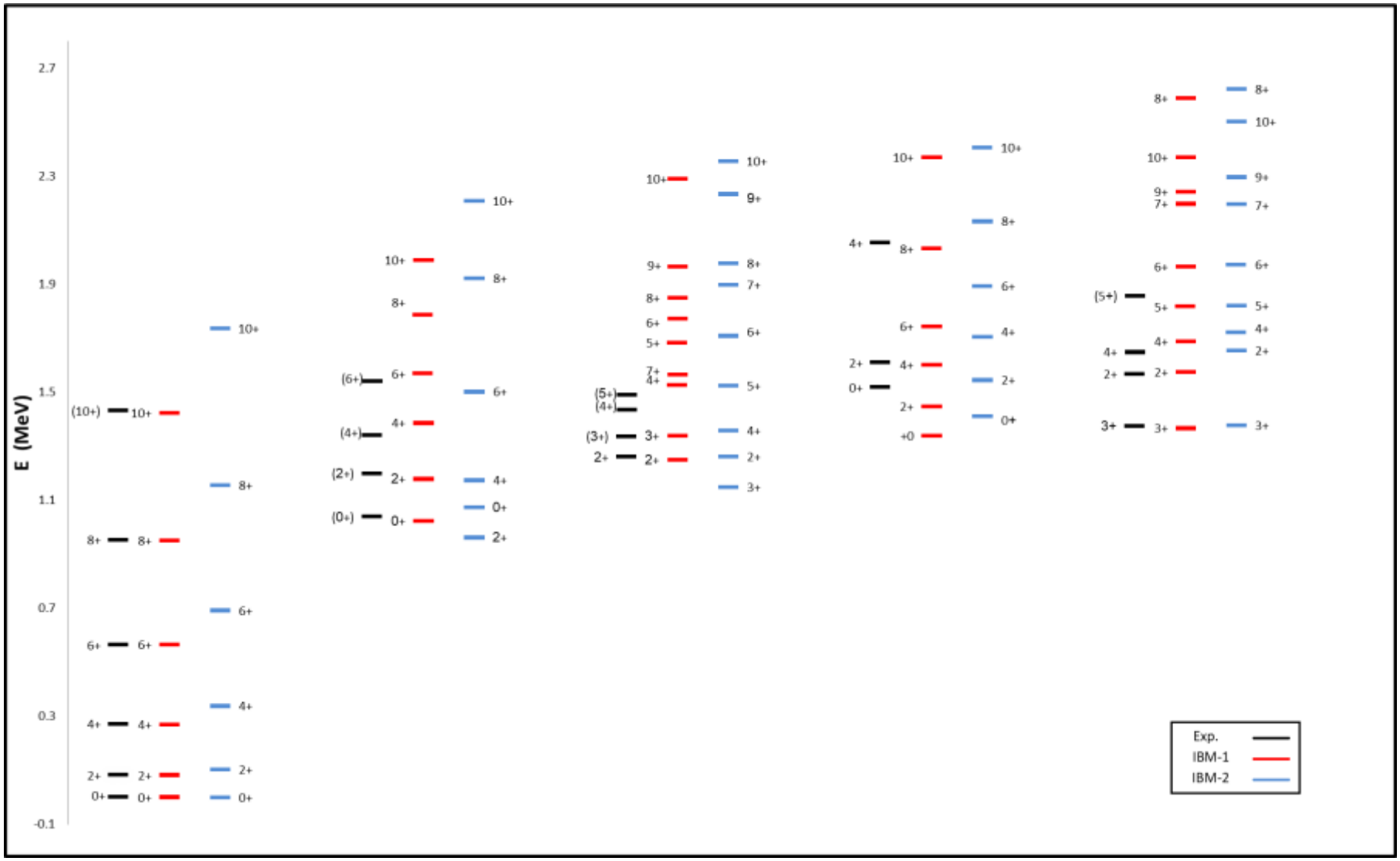

Figure (3.11) Energy levels for ^{176}Yb.

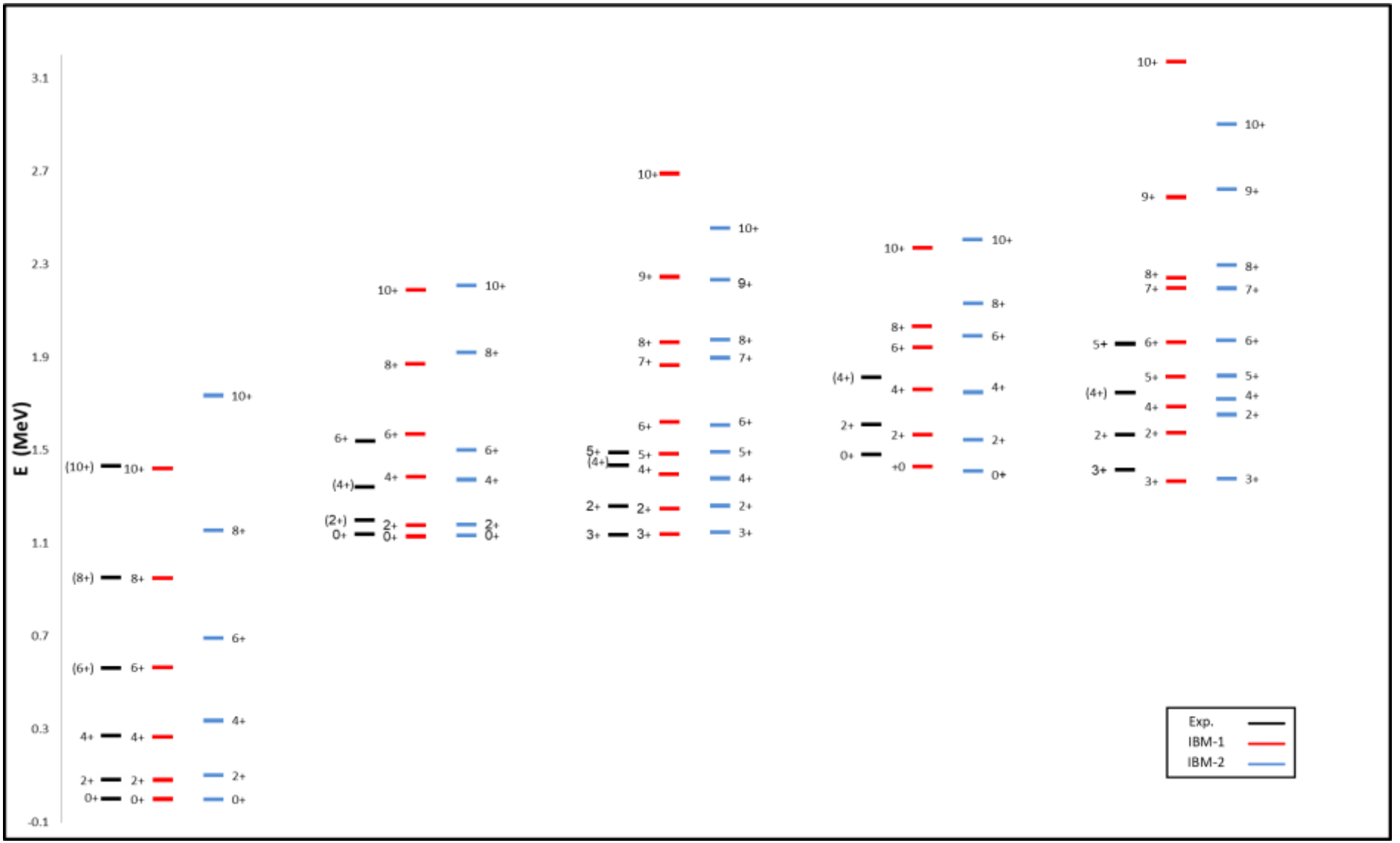

Figure (3.12) Energy levels for ^{178}Yb.

3.1.2 Energy Ratios

Calculating the energy ratios is one of the tests that are performed for each isotope to find out its position in the Casten triangle by comparing it with the ideal ratios in Table (2.1).

This calculation of dynamic symmetries by IBM-1, IBM-2 and experimental energy levels and after a comparison with the standard values for the energy ratios of ($E0_2^+/E2_1^+, E4_1^+/E2_1^+, E6_1^+/E2_1^+$ and $E8_1^+/E2_1^+$) ratios for all isotopes which in transitional region O(6)→ SU(3), that is clear in Figures (3.13) to (3.16). There is a good agreement between experimental data and the IBM-1 and IBM-2 results appear clearly in the Table and Figures below.

Table (3.3) Energy ratios for $^{160\text{-}178}$Yb isotopes.

Isotopes	Energy ratios											
	$E0_2^+/E2_1^+$			$E4_1^+/E2_1^+$			$E6_1^+/E2_1^+$			$E8_1^+/E2_1^+$		
	Exp. [94-103]	IBM-1	IBM-2	Exp. [94-103]	IBM-1	IBM-2	Exp. [94-103]	IBM-1	IBM-2	Exp. [94-103]	IBM-1	IBM-2
$^{160}_{70}Yb_{90}$	4.469	4.34	3.34	2.62	3.21	2.60	4.71	4.75	4.76	7.14	7.37	7.43
$^{162}_{70}Yb_{92}$	6.06	6.05	5.11	2.92	2.92	2.88	5.54	5.58	5.54	8.67	8.74	8.93
$^{164}_{70}Yb_{94}$	7.93	7.92	8.62	3.12	3.50	3.08	6.16	6.24	6.12	9.91	10.10	10.08
$^{166}_{70}Yb_{96}$	10.22	9.97	11.41	3.22	3.23	3.28	6.52	6.62	6.72	10.72	10.73	11.23
$^{168}_{70}Yb_{98}$	13.27	12.80	13.87	3.26	3.28	3.24	6.67	6.68	6.53	11.05	11.17	10.68
$^{170}_{70}Yb_{100}$	12.72	12.65	15.77	3.29	3.21	3.30	6.80	6.84	6.57	11.43	11.54	10.55
$^{172}_{70}Yb_{102}$	13.35	13.00	18.90	3.30	3.35	3.38	6.85	6.84	6.58	11.58	11.71	10.22
$^{174}_{70}Yb_{104}$	19.56	19.23	20.99	3.30	3.31	3.38	6.87	6.93	6.43	11.63	11.61	9.674
$^{176}_{70}Yb_{106}$	13.87	15.01	17.32	3.30	3.28	3.31	6.87	6.90	6.50	11.61	11.59	10.25
$^{178}_{70}Yb_{108}$	15.65	15.46	15.51	3.30	3.29	3.26	6.88	6.83	6.50	11.68	11.70	10.49

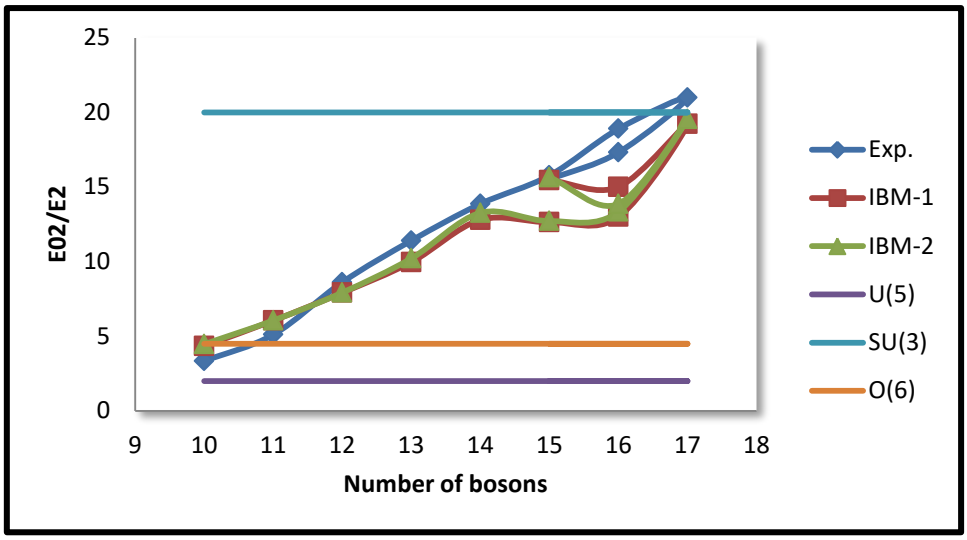

Figure (3.13) The experimental [94-103], theoretical and standard energy ratios ($E0_2^+/E2_1^+$), as a function of bosons numbers for even-even $^{160\text{-}178}$Yb isotopes.

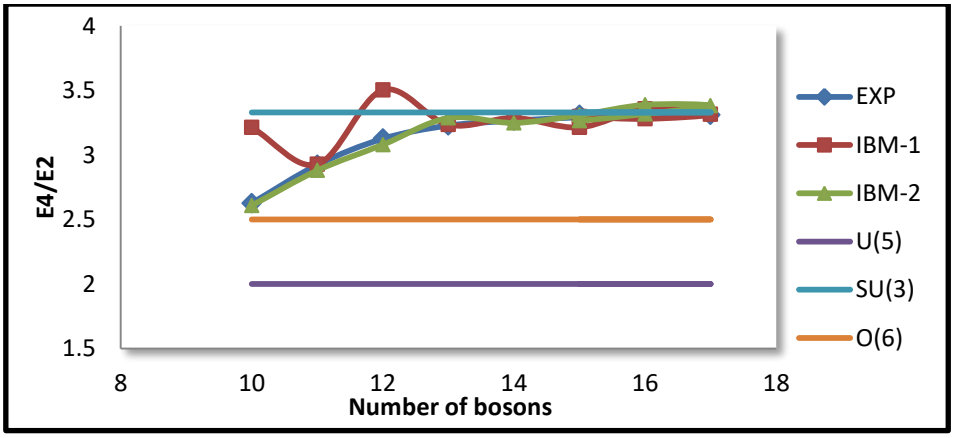

Figure (3.14) The experimental [94-103], theoretical and standard energy ratios ($E4_1^+/E2_1^+$), as a function of bosons numbers for even-even $^{160\text{-}178}$Yb isotopes.

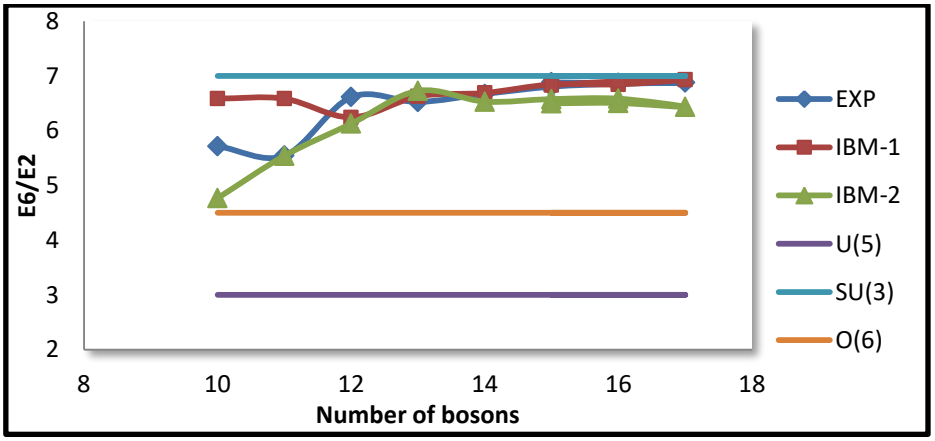

Figure (3.15) The experimental [94-103], theoretical and standard energy ratios ($E6_1^+/E2_1^+$), as a function of bosons numbers for even-even $^{160\text{-}178}$Yb isotopes.

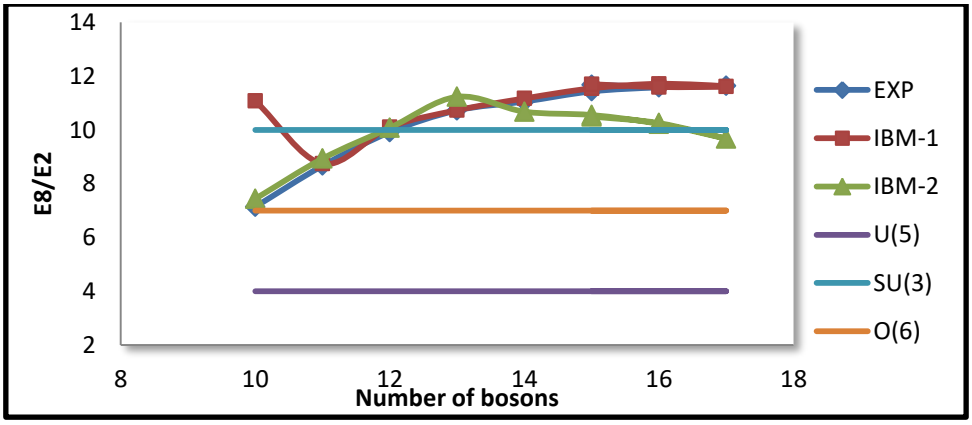

Figure (3.16) The experimental [94-103], theoretical and standard energy ratios ($E8_1^+/E2_1^+$), as a function of bosons numbers for even-even $^{160\text{-}178}$Yb isotopes.

3.1.3 Reduced Electric Quadruple Transitions Probability and Quadruple Momentum

The reduced electric quadrupole transition probability B(E2) is considered one of the most important properties of the nuclear structure, it can be found out the type of the dynamic symmetries for the nuclei through some transitions that occur between the energy levels for these nuclei.

In IBM-1 the reduced electric transition probability values for $^{160\text{-}178}$Yb isotopes can be calculated by calculating the values of effective charge e_b= E2SD and β_2 =E2DD from Equations (2.29) by using the experimental value of $B(E2;2_1^+ \rightarrow 0_1^+)$ [94-103], these values are presented in Table (3.4). In IBM-2 effective charge for neutron (e_ν) and for proton (e_π) must be calculated by using Equations (2.72) to find the reduced electric transition probability.

In this work, it found that the neutron's effective charge e_ν = 0.214(eb) and the proton's effective charge e_π = 0.052 (eb). The effective charges depend on the total bosons number N_ρ and the ratios between N_ν/N_π, these parameters are free and can take any value to fit the experimental data.

Table (3.4) The coefficients (E2SD, E2DD) for $^{160\text{-}178}$Yb.

Isotopes	Number of bosons	$B(E2;2_1^+ \to 0_1^+)$ ($e^2b^{2)}$ [94-103]	E2SD(eb)	E2DD(eb)
$^{160}_{70}Yb_{90}$	10	0.496	0.1037	-0.3068
$^{162}_{70}Yb_{92}$	11	0.69	0.119	-0.352
$^{164}_{70}Yb_{94}$	12	0.68	0.11	-0.327
$^{166}_{70}Yb_{96}$	13	1.028	0.1113	-0.329
$^{168}_{70}Yb_{98}$	14	1.146	0.0987	-0.292
$^{170}_{70}Yb_{100}$	15	1.094	0.107	-0.316
$^{172}_{70}Yb_{102}$	16	1.2	0.1135	-0.335
$^{174}_{70}Yb_{104}$	17	1.18	0.109	-0.322
$^{176}_{70}Yb_{106}$	16*	1.08	0.097	-0.286
$^{178}_{70}Yb_{108}$	15*	1.11	0.11	-0.314

Table (3.5) shows a comparison between B(E2) calculated by IBM-1, IBM-2 and experimental data. The values are acceptable in comparison and they have a good systematic.

Table (3.5) B(E2) values for $^{160\text{-}178}$Yb isotopes.

B(E2) (e^2b^2)									
Isotopes	^{160}Yb			^{162}Yb			^{164}Yb		
$J_i^+ \to J_f^+$	Exp.[94]	IBM-1	IBM-2	Exp.[95]	IBM-1	IBM-2	Exp.[96]	IBM-1	IBM-2
$2_1 \to 0_1$	0.496	0.496	0.497	0.69	0.698	0.636	0.68	0.69	0.68
$2_1 \to 0_2$	-----	0.006	0.038	-----	0.091	0.045	-----	0.041	0.025
$2_1 \to 2_2$	-----	0.195	0.207	-----	0.15	0.136	-----	0.008	0.004
$2_1 \to 2_3$	-----	0.001	0.001	-----	0.002	0.003	-----	0.030	0.088
$4_1 \to 2_1$	0.665	0.625	0.811	1.102	0.889	0.952	1.38	0.912	1.116
$2_2 \to 2_3$	-----	0.14	0.262	-----	0.419	0.427	-----	0.167	0.630
$2_2 \to 2_4$	-----	0.009	0.016	-----	0.007	0.006	-----	0.015	0.001
$2_4 \to 0_1$	-----	0.004	0.024	-----	0.009	0.016	-----	0.003	0.014
$4_3 \to 2_1$	-----	0.0012	0.725	-----	0.001	0.030	-----	0.021	0.026
$4_3 \to 2_3$	-----	0.055	0.056	-----	0.059	0.071	-----	0.022	0.045
$4_2 \to 2_2$	-----	0.302	2.454	-----	0.426	0.491	-----	0.107	0.599
$6_1 \to 4_1$	0.862	-----	0.930	1.002	-----	1.072	1.472	-----	1.227
$8_1 \to 6_1$	0.774	-----	0.981	1.312	-----	1.117	1.707	-----	1.254
$Q_{2_1^+}$ (eb)		0.82	0.631		2.160	0.863		2.420	1.085

B(E2) (e^2b^2)									
Isotopes	**^{166}Yb**			**^{168}Yb**			**^{170}Yb**		
$J_i^+ \rightarrow J_f^+$	**Exp.[97]**	**IBM-1**	**IBM-2**	**Exp.[98]**	**IBM-1**	**IBM-2**	**Exp.[99]**	**IBM-1**	**IBM-2**
$2_1 \rightarrow 0_1$	1.028	1.024	0.993	1.146	1.134	1.151	1.094	1.095	1.084
$2_1 \rightarrow 0_2$	-----	0.033	0.014	-----	0.033	0.013	-----	0.031	0.010
$2_1 \rightarrow 2_2$	-----	0.026	0.039	-----	0.026	0.014	-----	0.012	0.035
$2_1 \rightarrow 2_3$	-----	0.043	0.016	-----	0.043	0.015	-----	0.033	0.021
$4_1 \rightarrow 2_1$	1.474	1.382	1.282	-----	1.382	1.346	-----	1.475	1.431
$2_2 \rightarrow 2_3$	-----	0.008	0.664	-----	0.008	0.818	-----	0.726	0.712
$2_2 \rightarrow 2_4$	-----	0.018	0.001	-----	0.018	0.006	-----	0.012	0.024
$2_4 \rightarrow 0_1$	-----	0.008	0.012	-----	0.008	0.017	-----	0.003	0.023
$4_3 \rightarrow 2_1$	-----	0.004	0.018	-----	0.004	0.004	-----	0.002	0.001
$4_3 \rightarrow 2_3$	-----	0.023	0.015	-----	0.023	0.021	-----	0.015	0.020
$4_2 \rightarrow 2_2$	-----	0.853	0.843	-----	0.853	0.847	-----	0.907	0.911
$6_1 \rightarrow 4_1$	1.577	-----	1.387	-----	-----	1.456	-----	-----	1.545
$8_1 \rightarrow 6_1$	1.735	-----	1.409	-----	-----	1.483	-----	-----	1.578
$Q_{2_1^+}$ (eb)		2.793	1.279	-----	2.793	1.343	2.014	2.928	1.453
Isotopes	**B(E2) (e^2b^2)**								
	^{172}Yb			**^{174}Yb**			**^{176}Yb**		
$J_i^+ \rightarrow J_f^+$	**Exp. [100]**	**IBM-1**	**IBM-2**	**Exp. [101]**	**IBM-1**	**IBM-2**	**Exp. [102]**	**IBM-1**	**IBM-2**
$2_1 \rightarrow 0_1$	1.201	1.208	1.186	1.18	1.18	1.117	1.08	1.08	1.052
$2_1 \rightarrow 0_2$	-----	0.074	0.002	-----	0.103	0.007	-----	0.039	0.013
$2_1 \rightarrow 2_2$	-----	0.002	0.034	-----	0.036	0.055	-----	0.061	0.039
$2_1 \rightarrow 2_3$	-----	0.052	0.017	-----	0.057	0.002	-----	0.036	0.019
$4_1 \rightarrow 2_1$	-----	1.633	1.412	-----	1.606	1.559	-----	1.472	1.484
$2_2 \rightarrow 2_3$	-----	0.817	0.844	-----	0.414	0.305	-----	0.833	0.842
$2_2 \rightarrow 2_4$	-----	0.034	0.083	-----	0.225	0.653	-----	0.050	0.023
$2_4 \rightarrow 0_1$	-----	0.059	0.068	-----	0.058	0.040	-----	0.045	0.026
$4_3 \rightarrow 2_1$	-----	0.003	----	-----	0.071	----	-----	0.008	0.002
$4_3 \rightarrow 2_3$	-----	0.035	0.058	-----	0.043	0.042	-----	0.024	0.020
$4_2 \rightarrow 2_2$	-----	0.832	0.836	-----	0.590	0.652	-----	0.819	0.920
$6_1 \rightarrow 4_1$	1.819	-----	1.638	2.136	-----	1.681	1.746	-----	1.602
$8_1 \rightarrow 6_1$	2.273	-----	1.673	2.239	-----	1.723	1.758	-----	1.642
$Q_{2_1^+}$ (eb)		3.169	1.531		3.199	1.567		2.934	1.484

B(E2) (e^2b^2)			
Isotopes	**^{178}Yb**		
$J_i^+ \rightarrow J_f^+$	**Exp. [103]**	**IBM-1**	**IBM-2**
$2_1 \rightarrow 0_1$	1.11	1.11	1.093
$2_1 \rightarrow 0_2$	-----	0.069	0.012
$2_1 \rightarrow 2_2$	-----	0.018	0.047
$2_1 \rightarrow 2_3$	-----	0.047	0.014
$4_1 \rightarrow 2_1$	-----	1.505	1.405
$2_2 \rightarrow 2_3$	-----	0.907	0.906
$2_2 \rightarrow 2_4$	-----	0.030	0.011
$2_4 \rightarrow 0_1$	-----	0.053	0.021
$4_3 \rightarrow 2_1$	-----	0.003	0.005
$4_3 \rightarrow 2_3$	-----	0.033	0.023
$4_2 \rightarrow 2_2$	-----	0,214	0.867
$6_1 \rightarrow 4_1$	-----	-----	1.520
$8_1 \rightarrow 6_1$	-----	-----	1.554
$Q_{2_1^+}$ (eb)	-----	3.043	1.401

3.1.4 Branching Ratio

One of the important properties which can be calculated is the branching ratios, through which one can identify the position of the nuclei studied in the Casten triangle, and hence identify the dynamic symmetry for the nuclei by using the Equations (2.24)-(2.26), (2.38)-(2.40) and (2.52)-(2.54).

Table (3.6) shows the branching ratios for all studied Ytterbium isotopes. There is an acceptable agreement between theoretical calculation and available experimental values due to the strength of B(E2) values for each transition, which reflects the extent of deformation of these isotopes, which in turn affects the position of energy levels and finally affects the B(E2) values and branching ratios between them.

Table (3.6) Branching ratios for $^{160\text{-}178}$Yb isotopes.

Isotopes	Branching ratios								
	R			R′			R″		
	Exp. [94-103]	IBM-1	IBM-2	Exp.	IBM-1	IBM-2	Exp.	IBM-1	IBM-2
$^{160}_{70}Yb_{90}$	1.38	1.26	1.631	-----	0.208	0.416	-----	0.0026	0.015
$^{162}_{70}Yb_{92}$	1.55	1.306	1.491	-----	0.208	0.213	-----	0.0026	0.014
$^{164}_{70}Yb_{94}$	1.59	1.325	1.641	-----	0.061	0.005	-----	0.0121	0.0073
$^{166}_{70}Yb_{96}$	1.42	1.34	1.291	-----	0.080	0.039	-----	0.0064	0.0028
$^{168}_{70}Yb_{98}$	-----	1.35	1.169	-----	0.082	0.012	-----	0.0065	0.0022
$^{170}_{70}Yb_{100}$	-----	1.347	1.32	-----	0.047	0.0322	-----	0.0057	0.0018
$^{172}_{70}Yb_{102}$	1.41	1.351	1.190	-----	0.012	0.028	-----	0.0122	0.0003
$^{174}_{70}Yb_{104}$	1.39	1.358	1.395	-----	0.002	0.049	-----	0.0122	0.0012
$^{176}_{70}Yb_{106}$	1.47	1.352	1.410	-----	0.031	0.037	-----	0.0072	0.0024
$^{178}_{70}Yb_{108}$	-----	1.350	1.285	-----	0.011	0.043	-----	0.0123	0.0021

3.1.5 Reduced Transitions Probability for Magnetic Dipole and Mixing Ratio

In order to calculate B(M1) transition probability, one should estimate the effective $g-$factors for proton g_π and neutron g_ν by Equations (2.78). In Ytterbium isotopes the g- factor values are g_π= 0.422 (μ_N) and g_ν= 0.477 (μ_N). Equations (2.79) were used to calculate the B(M1) transition probabilities as it is shown in Table (3.7). The calculated values for B(M1) are acceptable to some extent as compared with the available experiments values, where some of the B(M1) values are small compared to the values of the quadrupole transition probabilities because the wavelength of the gamma ray transitions is greater than it is in the magnetic transitions according to the following relationship [34].

$$\lambda\,(ML) \;=\; 0.3\,A^{-2/3}\;\lambda(EL) \qquad (3.1)$$

Where:

$\lambda\ (ML)$: the wavelength of the gamma-ray in magnetic transitions, $\lambda(EL)$: the wavelength of the gamma ray in electec transitions, A: mass number.

This Equation shows that the B(M1) transition probability is less than B(E2) transition probability, the results gotten are confirmed this. The calculation values for these isotopes and mixing ratio δ(E2/M1) have been compared with the available experiments data as shown in Table (3.7).

Table (3.7) The B(M1) transition and mixing ratio for $^{160\text{-}178}$Yb isotopes.

Isotopes	**^{160}Yb**				**^{162}Yb**			
	B(M1) (e^2b^2)		**δ(E2/M1)**		**B(M1) (e^2b^2)**		**δ(E2/M1)**	
$J_i^+ \rightarrow J_f^+$	**Exp.**	**IBM-2**	**Exp.**	**IBM-2**	**Exp.**	**IBM-2**	**Exp.**	**IBM-2**
$2_1 \rightarrow 2_2$		1.19×10^{-3}		1.04×10^{-6}		7.41×10^{-7}		8.21×10^{-6}
$2_1 \rightarrow 2_3$	4.36×10^{-3}	1.31×10^{-3}		3.27×10^{-5}		6.67×10^{-6}		2.99×10^{-3}
$2_2 \rightarrow 2_3$		4.74×10^{-4}		2.34×10^{-6}	1.56×10^{-3}	6.55×10^{-7}		1.75×10^{-6}
$2_2 \rightarrow 2_4$		2.42×10^{-3}		2.12×10^{-2}		1.07×10^{-6}		4.691×10^{-3}
$3_1 \rightarrow 2_1$		2.25×10^{-5}		5.68×10^{-4}		3.59×10^{-6}		7.15×10^{-6}
$3_1 \rightarrow 2_2$		8.05×10^{-6}		2.27×10^{-5}		3.02×10^{-5}		4.63×10^{-6}
$4_1 \rightarrow 3_1$		4.73×10^{-2}		8.86×10^{-5}		3.46×10^{-6}		4.51×10^{-5}
$5_1 \rightarrow 4_1$		4.61×10^{-2}		1.99×10^{-3}		6.3×10^{-5}		6.69×10^{-5}
$5_1 \rightarrow 4_2$		6.79×10^{-5}		7.66×10^{-4}		3.59×10^{-6}		6.69×10^{-5}
Isotopes	**^{164}Yb**				**^{166}Yb**			
	B(M1) (e^2b^2)		**δ(E2/M1)**		**B(M1) (e^2b^2)**		**δ(E2/M1)**	
$J_i^+ \rightarrow J_f^+$	**Exp.**	**IBM-2**	**Exp.**	**IBM-2**	**Exp.**	**IBM-2**	**Exp.**	**IBM-2**
$2_1 \rightarrow 2_2$		1.62×10^{-6}		5.34×10^{-4}		3.52×10^{-6}		8.33×10^{-5}
$2_1 \rightarrow 2_3$		1.9×10^{-6}		2.86×10^{-5}		8.33×10^{-7}		5.01×10^{-5}
$2_2 \rightarrow 2_3$		2.04×10^{-6}		3.24×10^{-6}		7.59×10^{-8}		1.03×10^{-7}
$2_2 \rightarrow 2_4$		5.09×10^{-6}		2.88×10^{-2}		4.02×10^{-5}		1.22×10^{-3}
$3_1 \rightarrow 2_1$		2.34×10^{-6}		6.67×10^{-5}		6.48×10^{-5}		1.52×10^{-4}
$3_1 \rightarrow 2_2$		7.15×10^{-6}		1.58×10^{-3}		1.63×10^{-3}		6.31×10^{-3}
$4_1 \rightarrow 3_1$		4.63×10^{-6}		3.58×10^{-6}	8.32×10^{-3}	4.08×10^{-3}		3.05×10^{-6}
$5_1 \rightarrow 4_1$		4.51×10^{-5}		1.89×10^{-3}	3.31×10^{-3}	1.98×10^{-3}		2.18×10^{-3}
$5_1 \rightarrow 4_2$		6.69×10^{-5}		1.78×10^{-6}		2.58×10^{-6}		8.84×10^{-7}

Isotopes	^{168}Yb				^{170}Yb			
	B(M1) (e^2b^2)		δ(E2/M1)		B(M1) (e^2b^2)		δ(E2/M1)	
$J_i^+ \rightarrow J_f^+$	Exp.	IBM-2	Exp.	IBM-2	Exp.	IBM-2	Exp.	IBM-2
$2_1 \rightarrow 2_2$		4.27×10^{-3}		1.81×10^{-4}		3.59×10^{-2}		6.67×10^{-5}
$2_1 \rightarrow 2_3$		4.34×10^{-3}		3.52×10^{-4}		3.02×10^{-3}		3.77×10^{-5}
$2_2 \rightarrow 2_3$		1.62×10^{-2}		8.69×10^{-6}		3.46×10^{-4}		3.58×10^{-6}
$2_2 \rightarrow 2_4$		5.32×10^{-5}		6.01×10^{-4}		6.23×10^{-5}		8.98×10^{-4}
$3_1 \rightarrow 2_1$		2.64×10^{-5}		3.58×10^{-6}		1.54×10^{-4}		3.59×10^{-6}
$3_1 \rightarrow 2_2$		8.12×10^{-4}		3.59×10^{-6}		6.11×10^{-3}		3.02×10^{-5}
$4_1 \rightarrow 3_1$	5.85×10^{-3}	3.97×10^{-4}		3.02×10^{-5}		3.05×10^{-4}		3.46×10^{-6}
$5_1 \rightarrow 4_1$		4.21×10^{-4}		3.46×10^{-6}	8.70×10^{-3}	2.68×10^{-4}		6.37×10^{-5}
$5_1 \rightarrow 4_2$		6.79×10^{-5}		6.32×10^{-5}	1.01×10^{-2}	8.82×10^{-3}		8.34×10^{-4}
Isotopes	^{172}Yb				^{174}Yb			
	B(M1) (e^2b^2)		δ(E2/M1)		B(M1) (e^2b^2)		δ(E2/M1)	
$J_i^+ \rightarrow J_f^+$	Exp.	IBM-2	Exp.	IBM-2	Exp.	IBM-2	Exp.	IBM-2
$2_1 \rightarrow 2_2$		8.98×10^{-3}		1.52×10^{-4}		1.28×10^{-4}		7.44×10^{-3}
$2_1 \rightarrow 2_3$		8.14×10^{-2}		6.31×10^{-4}		3.28×10^{-4}		1.08×10^{-4}
$2_2 \rightarrow 2_3$		3.85×10^{-3}		3.05×10^{-6}		1.28×10^{-5}		2.35×10^{-5}
$2_2 \rightarrow 2_4$		2.96×10^{-5}		2.18×10^{-4}		9.62×10^{-8}		8.52×10^{-8}
$3_1 \rightarrow 2_1$		2.09×10^{-6}		1.52×10^{-4}		6.99×10^{-7}		2.78×10^{-7}
$3_1 \rightarrow 2_2$		9.66×10^{-4}		6.31×10^{-3}	1.48×10^{-2}	1.21×10^{-4}		4.93×10^{-7}
$4_1 \rightarrow 3_1$	1.05×10^{-2}	6.99×10^{-3}		3.05×10^{-6}		4.04×10^{-7}		2.09×10^{-6}
$5_1 \rightarrow 4_1$		1.21×10^{-3}		2.18×10^{-4}		1.85×10^{-5}		9.66×10^{-4}
$5_1 \rightarrow 4_2$		4.04×10^{-2}		1.15×10^{-5}		3.84×10^{-7}		6.99×10^{-7}
Isotopes	^{176}Yb				^{178}Yb			
	B(M1) (e^2b^2)		δ(E2/M1)		B(M1) (e^2b^2)		δ(E2/M1)	
$J_i^+ \rightarrow J_f^+$	Exp.	IBM-2	Exp.	IBM-2	Exp.	IBM-2	Exp.	IBM-2
$2_1 \rightarrow 2_2$		1.09×10^{-4}		1.43×10^{-5}		1.15×10^{-5}		1.36×10^{-5}
$2_1 \rightarrow 2_3$		2.96×10^{-3}		4.23×10^{-5}		3.46×10^{-6}		5.06×10^{-5}
$4_1 \rightarrow 2_1$	1.29×10^{-3}	2.52×10^{-3}		1.21×10^{-6}		9.29×10^{-6}		6.54×10^{-4}
$2_2 \rightarrow 2_4$		1.67×10^{-4}		2.09×10^{-6}		3.39×10^{-6}		1.69×10^{-6}
$2_4 \rightarrow 0_1$		3.93×10^{-3}		9.66×10^{-4}		3.27×10^{-5}		1.58×10^{-5}
$3_1 \rightarrow 2_1$		3.84×10^{-7}		6.99×10^{-7}		2.09×10^{-6}		6.99×10^{-7}
$3_1 \rightarrow 2_2$		1.23×10^{-7}		3.17×10^{-5}		9.66×10^{-4}		1.23×10^{-4}
$4_1 \rightarrow 3_1$		1.76×10^{-8}		4.04×10^{-7}		6.99×10^{-7}		4.04×10^{-7}
$5_1 \rightarrow 4_1$		2.59×10^{-5}		1.15×10^{-5}		1.21×10^{-4}		1.15×10^{-5}
$5_1 \rightarrow 4_2$		1.15×10^{-5}		3.84×10^{-7}		4.04×10^{-7}		3.84×10^{-7}

3.1.6 Electric Monopole Transition B(E0) and $X(E0/E2)$ Ratios

The deformation parameters for protons and neutrons are used to calculate monopole transition matrix elements for $^{160\text{-}178}$Yb isotopes that have been estimated using Equations (2.82) to (2.84). In addition to the available experimental data, the monopole transition matrix element and mixing ratio have been calculated using Equation (2.88) and listed in Table (3.8).

The ratio X(E0/E2) shows the strength of the competition between E0 and E2, where it is noted that the IBM-2 calculated values are not entirely consistent with the experimental values available, and the reason belongs to the strength of the transition between E2 and E0, as well as the fact that the difficulty of defining unified parameters for ($\tilde{\beta}_\nu$, $\tilde{\beta}_\pi$) gave the theoretical values in (IBM-2) that are closer to the available experimental data. Besides the fact that the experimental values available are also very few. The deformation parameters for protons and neutrons used to calculate monopole transition matrix elements ρ(E0) for $^{160\text{-}178}$Yb isotopes are ($\tilde{\beta}_\nu$ = +0.039 fm^2 , $\tilde{\beta}_\pi$ = -0.055 fm^2). Table (3.8) shows the electric monopole transition matrix and X(E0/E2) for $^{160\text{-}178}$Yb isotopes.

Table (3.8) Electric monopole transition and X(E0/E2) for $^{160\text{-}178}$Yb isotopes.

Isotopes	^{160}Yb				^{162}Yb			
	B(E0) (e^2b^2)		X(E0/E2)		B(E0) (e^2b^2)		X(E0/E2)	
$J_i^+ \rightarrow J_f^+$	Exp.	IBM-2	Exp.	IBM-2	Exp.	IBM-2	Exp.	IBM-2
$2_1 \rightarrow 2_2$		1.08×10^{-4}		1.73		6.54×10^{-4}		3.64
$2_1 \rightarrow 2_3$		1.27×10^{-3}		1.03		6.67×10^{-2}		8.10
$2_2 \rightarrow 2_3$		3.64×10^{-4}		2.34		6.55×10^{-4}		1.75
$2_2 \rightarrow 2_4$		1.82×10^{-2}		8.65		1.07×10^{-2}		4.69
$3_1 \rightarrow 2_1$		2.25×10^{-2}		9.34		3.59×10^{-2}		7.15
$3_1 \rightarrow 2_2$		8.05×10^{-2}		2.27		3.02×10^{-3}		4.66

$4_1 \rightarrow 3_1$		4.73×10^{-2}		8.86		3.46×10^{-2}		4.58
$5_1 \rightarrow 4_1$		4.61×10^{-3}		1.99		6.35×10^{-3}		6.82
$5_1 \rightarrow 4_2$		6.79×10^{-3}		7.66		3.59×10^{-2}		6.69
Isotopes	**^{164}Yb**				**^{166}Yb**			
	B(E0) (e^2b^2)		**X(E0/E2)**		**B(E0) (e^2b^2)**		**X(E0/E2)**	
$J_i^+ \rightarrow J_f^+$	**Exp.**	**IBM-2**	**Exp.**	**IBM-2**	**Exp.**	**IBM-2**	**Exp.**	**IBM-2**
$2_1 \rightarrow 2_2$		1.62×10^{-2}		5.34		3.52×10^{-4}		8.33
$2_1 \rightarrow 2_3$		1.93×10^{-2}		2.86		8.33×10^{-4}		5.01
$2_2 \rightarrow 2_3$		2.04×10^{-2}		3.24		7.59×10^{-3}		1.03
$2_2 \rightarrow 2_4$		5.09×10^{-2}		2.88	4.76×10^{-2}	4.02×10^{-3}		0.92
$3_1 \rightarrow 2_1$		2.34×10^{-2}		6.67		6.48×10^{-3}		1.52
$3_1 \rightarrow 2_2$		7.15×10^{-2}		1.58		1.65×10^{-2}		6.31
$4_1 \rightarrow 3_1$	9.41×10^{-2}	4.63×10^{-2}		3.58		4.08×10^{-2}		3.05
$5_1 \rightarrow 4_1$		4.51×10^{-3}		1.898		1.781×0^{-3}		0.218
$5_1 \rightarrow 4_2$		6.69×10^{-3}		1.78		2.58×10^{-3}		8.84
Isotopes	**^{168}Yb**				**^{170}Yb**			
	B(E0) (e^2b^2)		**X(E0/E2)**		**B(E0) (e^2b^2)**		**X(E0/E2)**	
$J_i^+ \rightarrow J_f^+$	**Exp.**	**IBM-2**	**Exp.**	**IBM-2**	**Exp.**	**IBM-2**	**Exp.**	**IBM-2**
$2_1 \rightarrow 2_2$		4.25×10^{-2}		8.54		3.59×10^{-2}		6.67
$2_1 \rightarrow 2_3$		4.34×10^{-2}		3.52		3.02×10^{-3}		1.58
$2_2 \rightarrow 2_3$		1.62×10^{-2}		1.67		3.46×10^{-2}		3.58
$2_2 \rightarrow 2_4$		5.37×10^{-3}		6.12		6.33×10^{-3}		1.89
$3_1 \rightarrow 2_1$		2.69×10^{-2}		3.58		1.52×10^{-4}		3.59
$3_1 \rightarrow 2_2$		8.12×10^{-2}		3.59		6.31×10^{-3}		3.02
$4_1 \rightarrow 3_1$	1.08×10^{-2}	3.79×10^{-2}		3.02		3.05×10^{-2}		3.46
$5_1 \rightarrow 4_1$		4.21×10^{-3}		3.46		2.18×10^{-4}		6.38
$5_1 \rightarrow 4_2$		6.79×10^{-3}		6.37		8.82×10^{-4}		8.34
Isotopes	**^{172}Yb**				**^{174}Yb**			
$J_i^+ \rightarrow J_f^+$	**B(E0) (e^2b^2)**		**X(E0/E2)**		**B(E0) (e^2b^2)**		**X(E0/E2)**	
	Exp.	**IBM-2**	**Exp.**	**IBM-2**	**Exp.**	**IBM-2**	**Exp.**	**IBM-2**
$2_1 \rightarrow 2_2$		8.98×10^{-2}		1.08×10^{-3}		1.28×10^{-3}		7.44
$2_1 \rightarrow 2_3$		8.14×10^{-3}		5.76×10^{-3}		3.28×10^{-3}		3.47

$2_2 \rightarrow 2_3$		3.85×10^{-2}		3.05×10^{-2}		1.26×10^{-3}		2.35
$2_2 \rightarrow 2_4$		2.96×10^{-3}		4.35×10^{-4}		9.61×10^{-5}		8.52
$3_1 \rightarrow 2_1$		2.09×10^{-2}		5.23×10^{-4}		6.99×10^{-4}		2.78
$3_1 \rightarrow 2_2$		9.66×10^{-4}		6.43×10^{-3}		2.19×10^{-7}		4.93
$4_1 \rightarrow 3_1$		6.99×10^{-4}		3.05×10^{-2}		4.04×10^{-4}		2.09
$5_1 \rightarrow 4_1$		9.11×10^{-7}		7.34×10^{-2}		1.85×10^{-3}		9.66
$5_1 \rightarrow 4_2$		4.04×10^{-4}		1.15×10^{-3}		3.84×10^{-4}		6.99
Isotopes	**^{176}Yb**				**^{178}Yb**			
	B(E0) (e^2b^2)		**X(E0/E2)**		**B(E0) (e^2b^2)**		**X(E0/E2)**	
$J_i^+ \rightarrow J_f^+$	**Exp.**	**IBM-2**	**Exp.**	**IBM-2**	**Exp.**	**IBM-2**	**Exp.**	**IBM-2**
$2_1 \rightarrow 2_2$		1.09×10^{-2}		1.43		1.15×10^{-2}		1.36
$2_1 \rightarrow 2_3$		2.96×10^{-2}		4.23		3.46×10^{-2}		5.06
$4_1 \rightarrow 2_1$		2.52×10^{-2}		1.07		9.29×10^{-2}		6.56
$2_2 \rightarrow 2_4$		1.67×10^{-2}		2.09	4.56×10^{-2}	3.39×10^{-2}		1.69
$2_4 \rightarrow 0_1$		3.93×10^{-3}		9.66		3.27×10^{-3}		4.67
$3_1 \rightarrow 2_1$		3.84×10^{-4}		6.99		2.09×10^{-2}		6.99
$3_1 \rightarrow 2_2$		1.23×10^{-4}		3.23		9.66×10^{-4}		1.23
$4_1 \rightarrow 3_1$		1.76×10^{-5}		4.04		6.99×10^{-4}		4.04
$5_1 \rightarrow 4_1$		2.59×10^{-3}		1.15		2.08×10^{-3}		1.15
$5_1 \rightarrow 4_2$		1.15×10^{-3}		3.84		4.04×10^{-4}		3.84

3.1.7 Potential Energy Surface (PES)

The surface of the potential energy as a function with contour diagrams for isotopes that have been calculated from Equation (2.58) with computer code is represented in Figures (3.17) to (3.26).

The parameters used in the program to calculate the potential energy surface are shown in Table (3.9).

Table (3.9) Potential energy surface parameters for $^{160\text{-}178}$Yb isotopes.

Isotops	N	ES	ED	A_1	A_2	A_3	A_4
$^{160}_{70}Yb_{90}$	10	-0.223	0.086	0.004	0.021	-0.178	0
$^{162}_{70}Yb_{92}$	11	-0.150	0.071	0.003	0.021	-0.12	0
$^{164}_{70}Yb_{94}$	12	-0.241	0.014	0.011	0.014	-0.193	0
$^{166}_{70}Yb_{96}$	13	-0.100	0.038	0.002	0.019	-0.08	0

$^{168}_{70}Yb_{98}$	14	-0.077	0.036	0.001	0.021	-0.062	0
$^{170}_{70}Yb_{100}$	15	0.195	0.095	0.009	0.014	-0.156	0
$^{172}_{70}Yb_{102}$	16	-0.071	0.03	0.002	0.003	-0.057	0
$^{174}_{70}Yb_{104}$	17	-0.068	0.03	0.002	0.002	-0.027	0
$^{176}_{70}Yb_{106}$	16*	-0.071	0.038	0.003	0.003	-0.057	0
$^{178}_{70}Yb_{108}$	15*	-0.072	0.037	0.003	0.003	-0.057	0

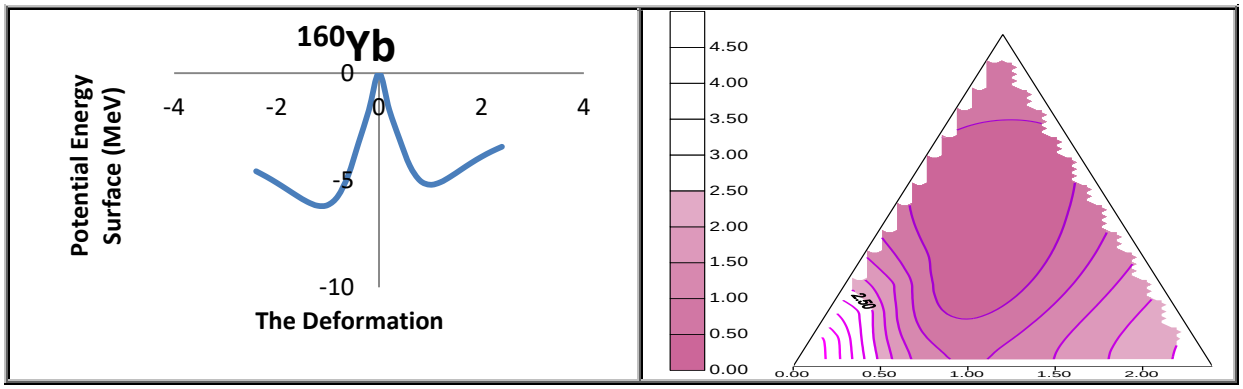

Figure (3.17) Potential energy surface with the deformation for ^{160}Yb.

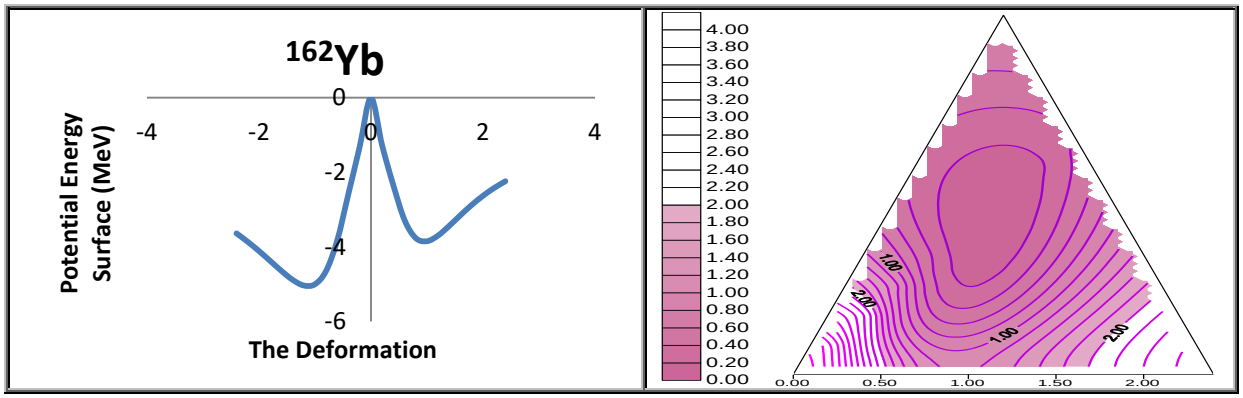

Figure (3.18) Potential energy surface with the deformation for ^{162}Yb.

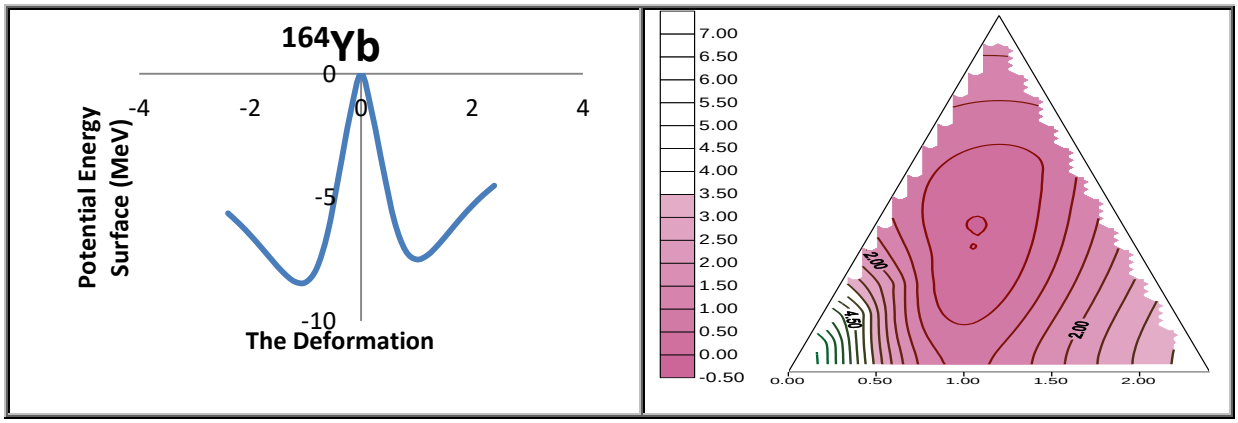

Figure (3.19) Potential energy surface with the deformation for ^{164}Yb.

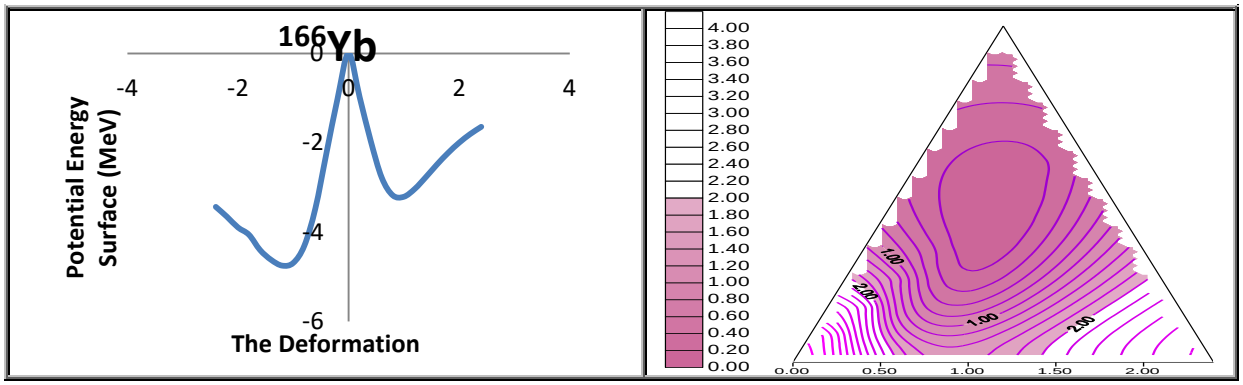

Figure (3.20) Potential energy surface with the deformation for ^{166}Yb.

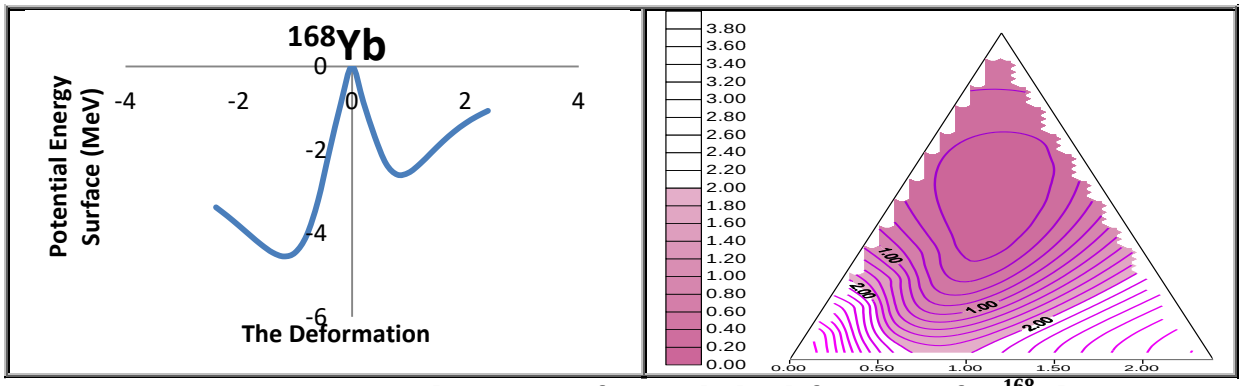

Figure (3.21) Potential energy surface with the deformation for ^{168}Yb.

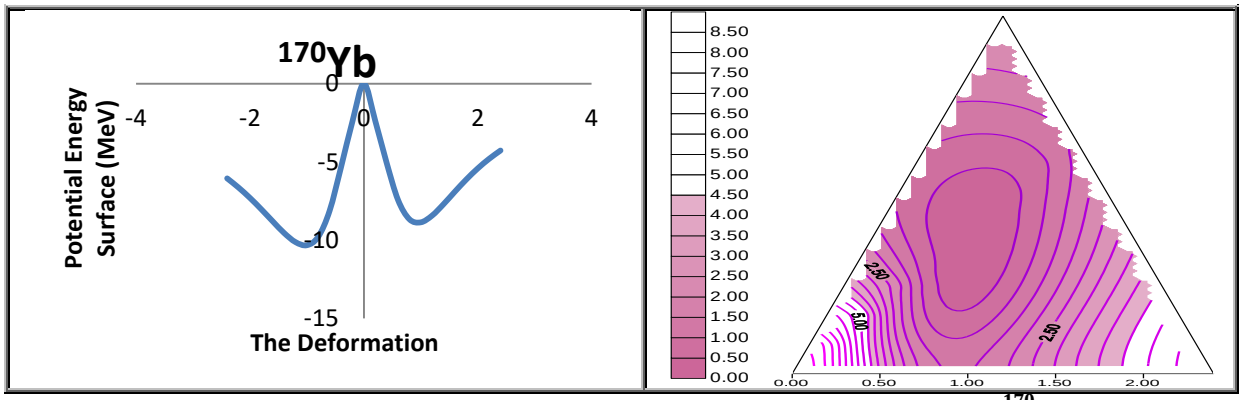

Figure (3.22) Potential energy surface with the deformation for ^{170}Yb.

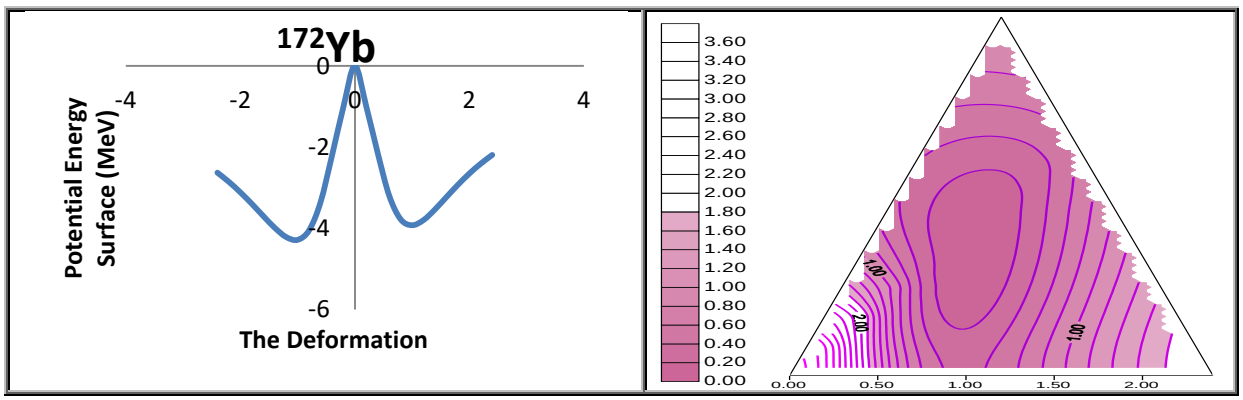

Figure (3.23) Potential energy surface with the deformation for ^{172}Yb.

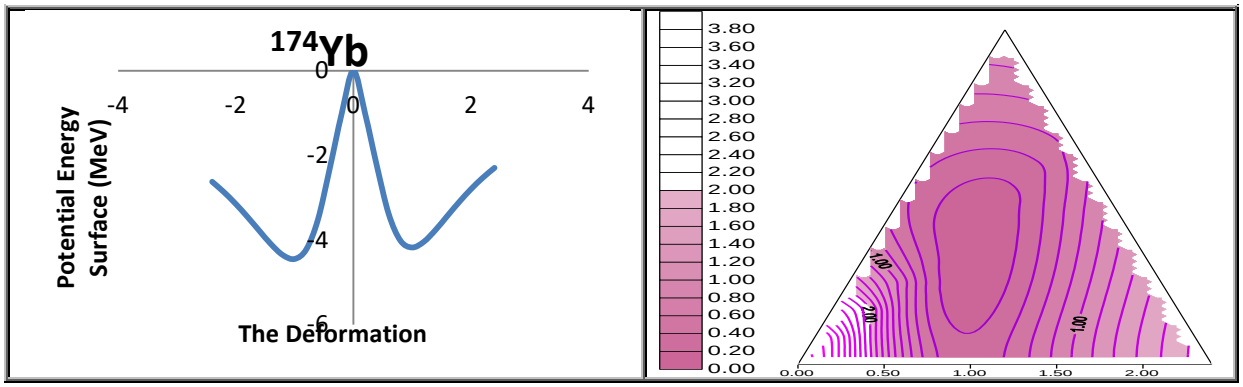

Figure (3.24) Potential energy surface with the deformation for ^{174}Yb.

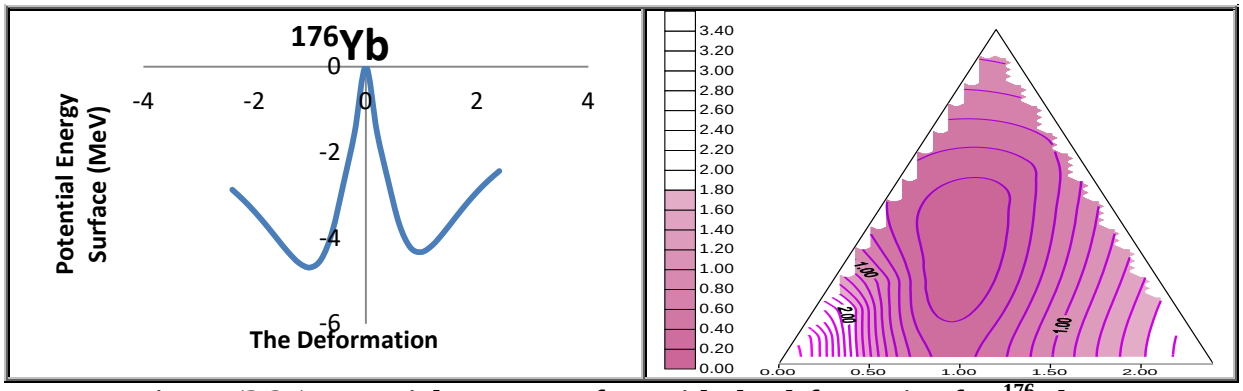

Figure (3.25) Potential energy surface with the deformation for ^{176}Yb.

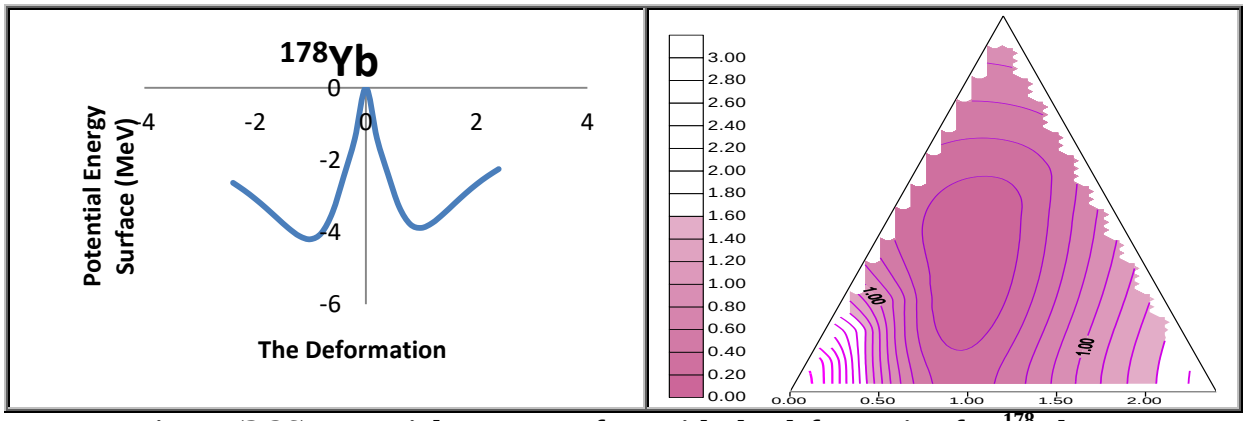

Figure (3.26) Potential energy surface with the deformation for ^{178}Yb.

3.1.8 Mixed Symmetry States (MSS)

Studying the effect of Majorana parameters ($\zeta_{1,3}$, ζ_2) on the calculated excitation energy level for $^{160\text{-}178}$Yb isotopes, the value of $\zeta_{1,3}$ vary between (0.12-0.16) and fixed the ζ_2 on (0.08) for all isotopes then vary this value between (0.05-0.1) around the best-fitted data. It is found that the energy values for the states $(2_3^+, 2_4^+, 2_5^+, 3_1^+, 5_1^+)$ are responded rapidly to the changes of the ζ_2 parameters in some isotopes only and therefore these states verify the first

property of the Mixed symmetry state (MSS). Figure (3.27) explain the energy variation of these states as a function of the Majorana parameter ζ_2.

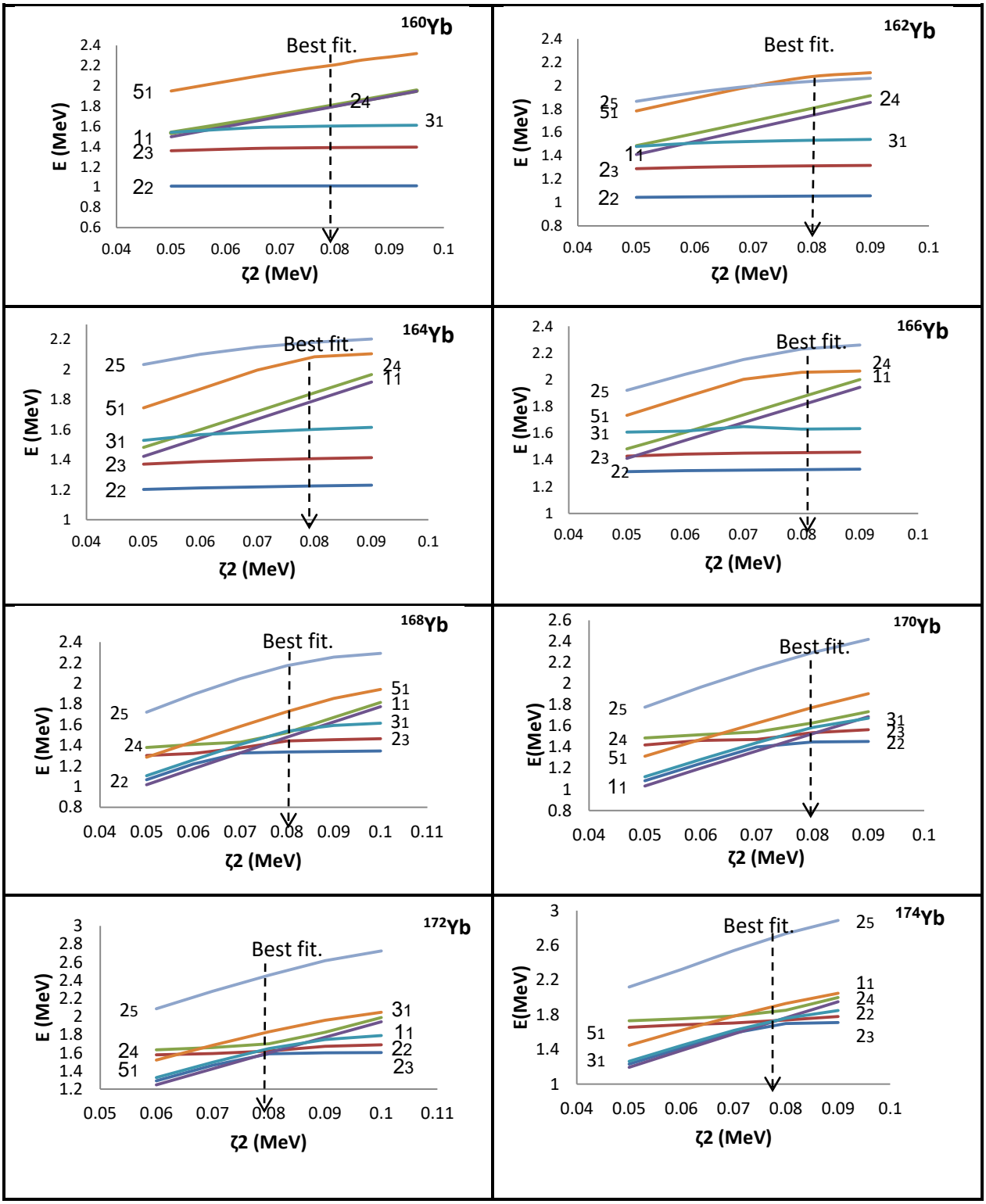

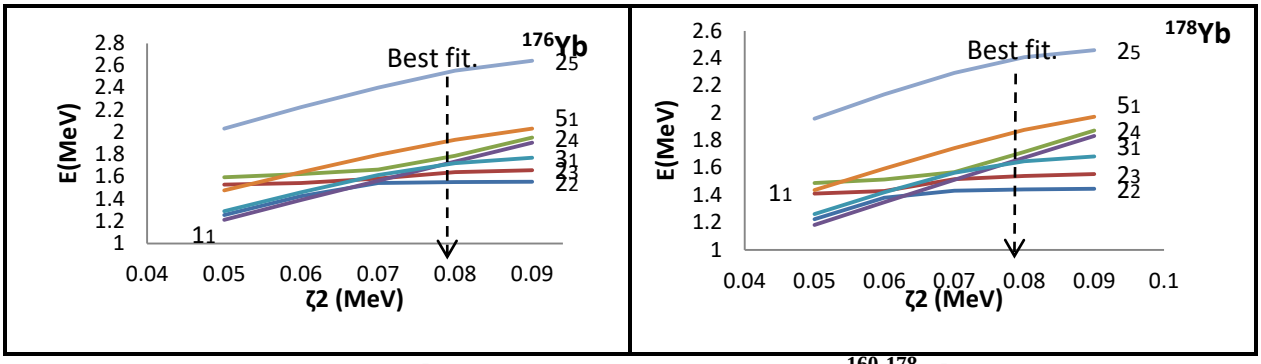

Figure (3.27) Mixed symmetry states in even-even $^{160\text{-}178}$Yb isotopes.

3.2 Hafnium Isotopes (Hf)

Hafnium is a chemical element with the symbol Hf and atomic number 72. A lustrous, silvery gray, tetravalent transition metal, Hafnium chemically resembles zirconium and is found in many zirconium minerals. Hafnium is named after Hafnium, the Latin name for Copenhagen, where it was discovered. This shiny metal that resists corrosion and can be drawn into wires is a good absorber of neutrons and is used to make control rods, such as those found in nuclear submarines. It also has a very high melting point and because of this is used in plasma welding torches. Hafnium is also used in vacuum tubes as a getter, a material that combines with and removes trace gases from vacuum tubes. Hafnium has been used as an alloying agent in iron, titanium, niobium and other metals [107].

The $^{166\text{-}180}$Hf isotopes (under studying), have Z=72 and the number of proton bosons is =5 while, neutron bosons range from 6-11. These isotopes are located in the deformed region in the dynamical symmetry O(6)-SU(3) (deformed nuclei).

3.2.1 Energy Level Calculations

The software package IBM computer code for neutron proton boson (NPBOS) code for IBM-2 have been used to calculate energy levels for $^{166\text{-}180}$Hf by estimating a set of parameters described in the Hamiltonian operator as it is

shown in Equations (2.2) and (2.50) parameters estimated for the low- lying calculations of the excited energy levels for Hafnium isotopes are given in Tables (3.10) and (3.11), the symbol (*) refers to hole boson, these parameters represented in Figures (3.28) and (3.29).

Table (3.10) Parameters used in the IBM-1 Hamiltonian for even-even $^{166\text{-}180}$Hf isotopes (in MeV).

Isotops	N	Ɛ	a_0	a_1	a_2	a_3	a_4	χ
$^{166}_{72}Hf_{94}$	11	0	0.0114	0.0184	-0.0165	0	0	-0.068
$^{168}_{72}Hf_{96}$	12	0	0.0116	0.0164	-0.0142	0	0	-1.17
$^{170}_{72}Hf_{98}$	13	0	0.0126	0.0132	-0.0123	0	0	-0.28
$^{172}_{72}Hf_{100}$	14	0	0.0112	0.0119	-0.0114	0	0	-0.112
$^{174}_{72}Hf_{102}$	15	0	0.0113	0.0106	-0.0115	0	0	-0.062
$^{176}_{72}Hf_{104}$	16	0	0.011	0.0098	-0.0112	0	0	-0.032
$^{178}_{72}Hf_{106}$	15*	0	0.0111	0.0108	-0.0114	0	0	-0.066
$^{180}_{72}Hf_{108}$	14*	0	0.0112	0.011	-0.0117	0	0	-0.073

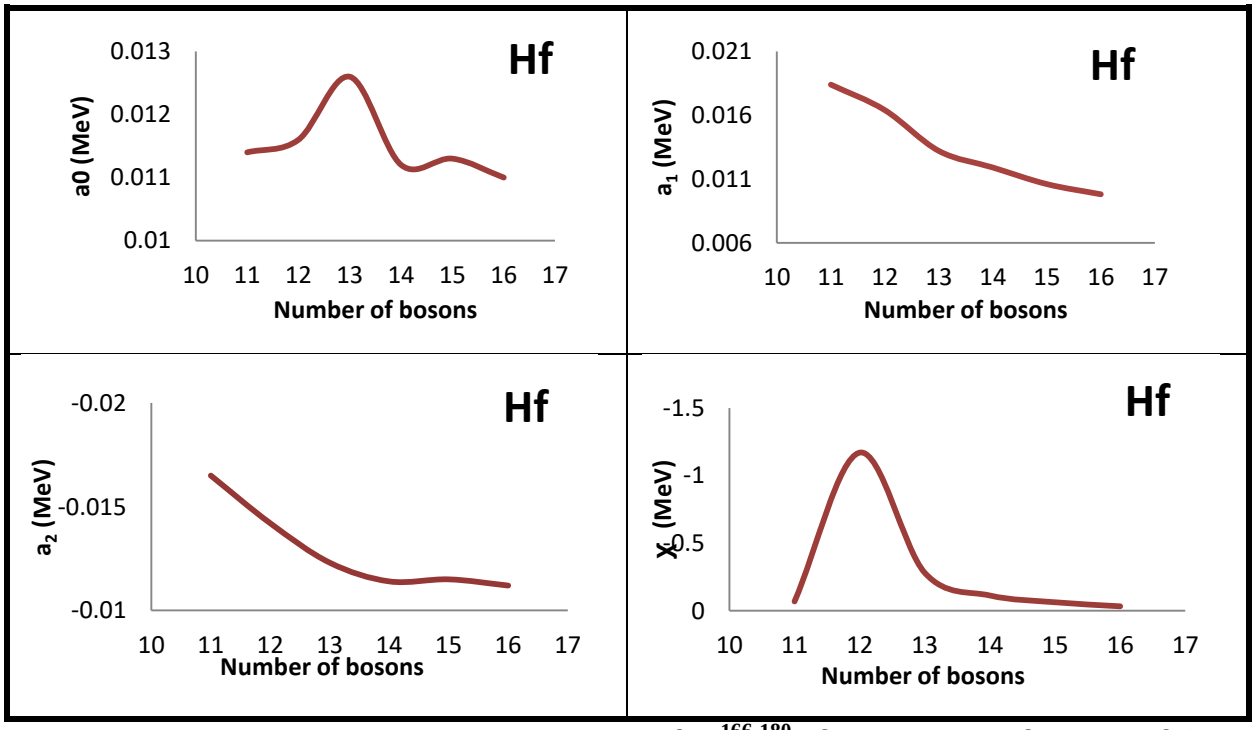

Figure (3.28) IBM-1 parameters (χ, a_0, a_1, a_2) for $^{166\text{-}180}$Hf isotopes as a function of the number of bosons.

Table (3.11) Parameters used in the IBM-2 Hamiltonian for even– even $^{166-180}$Hf isotopes (in MeV) except χ_ν and χ_π without units, N_π=5.

Isotops	N_υ	Ɛ	Ƙ	X_υ	X_π	$\zeta_{1=3}$	ζ_2	C^L_υ			C^L_π		
$^{166}_{72}Hf_{94}$	6	0.47	-0.054	-1.21	-1.2	0.18	0.07	-0.16	0.22	0.24	0.22	0.16	0.058
$^{168}_{72}Hf_{96}$	7	0.43	-0.056	-1.21	-1.2	0.16	0.07	-0.15	0.21	0.23	0.21	0.14	0.026
$^{170}_{72}Hf_{98}$	8	0.39	-0.058	-1.211	-1.2	0.16	0.07	-0.15	0.18	0.21	0.20	0.13	0.004
$^{172}_{72}Hf_{100}$	9	0.38	-0.056	-1.212	-1.2	0.16	0.07	-0.16	0.17	0.18	0.2	0.11	0.008
$^{174}_{72}Hf_{102}$	10	0.35	-0.052	-1.213	-1.2	0.15	0.07	-0.18	0.18	0.17	0.17	0.08	0.0003
$^{176}_{72}Hf_{104}$	11	0.34	-0.05	-1.213	-1.2	0.14	0.07	-0.18	0.19	0.16	0.16	0.07	0.0002
$^{178}_{72}Hf_{106}$	10*	0.36	-0.048	-1.214	-1.2	0.16	0.07	-0.18	0.21	0.17	0.17	0.12	0.0005
$^{180}_{72}Hf_{108}$	9*	0.36	-0.056	-1.214	-1.2	0.16	0.07	-0.18	0.29	0.17	0.17	0.12	0.003

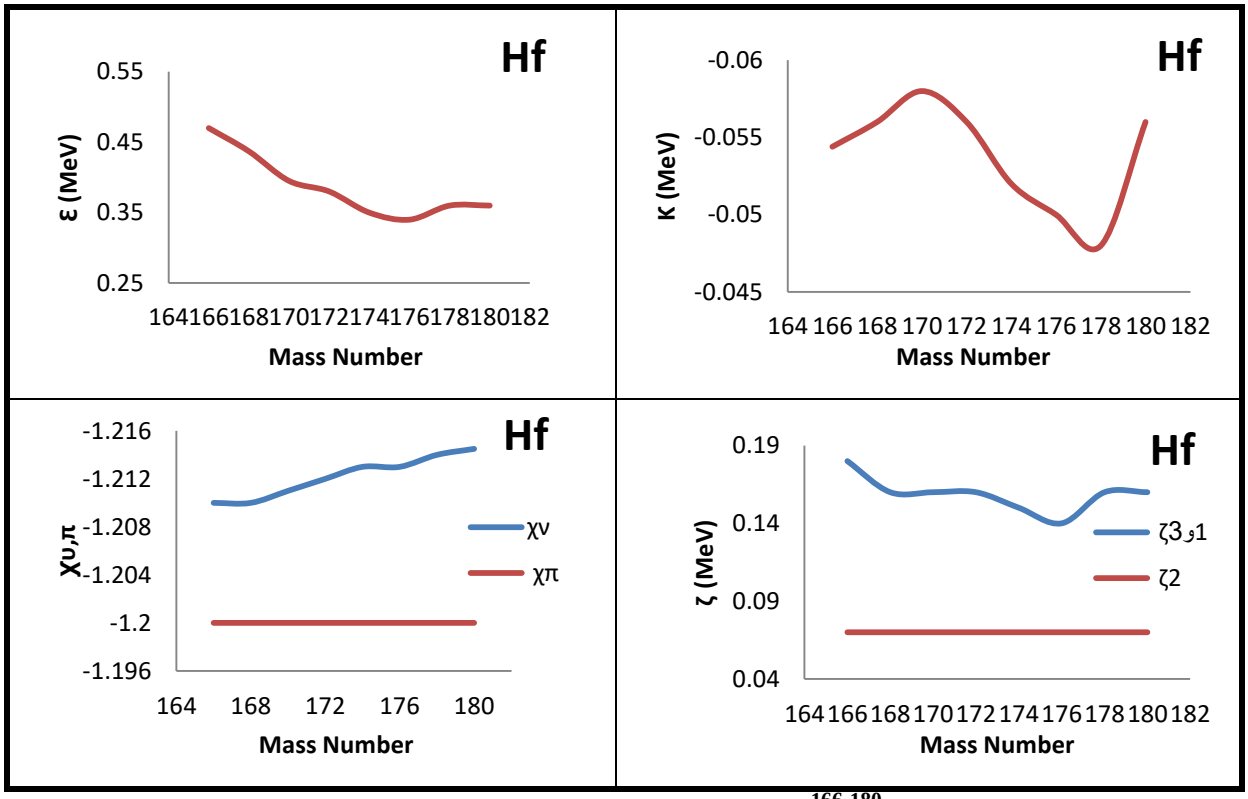

Figure (3.29) IBM-2 parameters (ε, κ, χ_π, χ_ν, ζ_2, $\zeta_{1,3}$) for $^{166-180}$Hf isotopes as a function of the mass number.

The calculated energy levels by IBM-1 and IBM-2 compared with the experimental data [97-104] for $^{166-180}$Hf isotopes have been shown in Figures from (3.30) to (3.37).

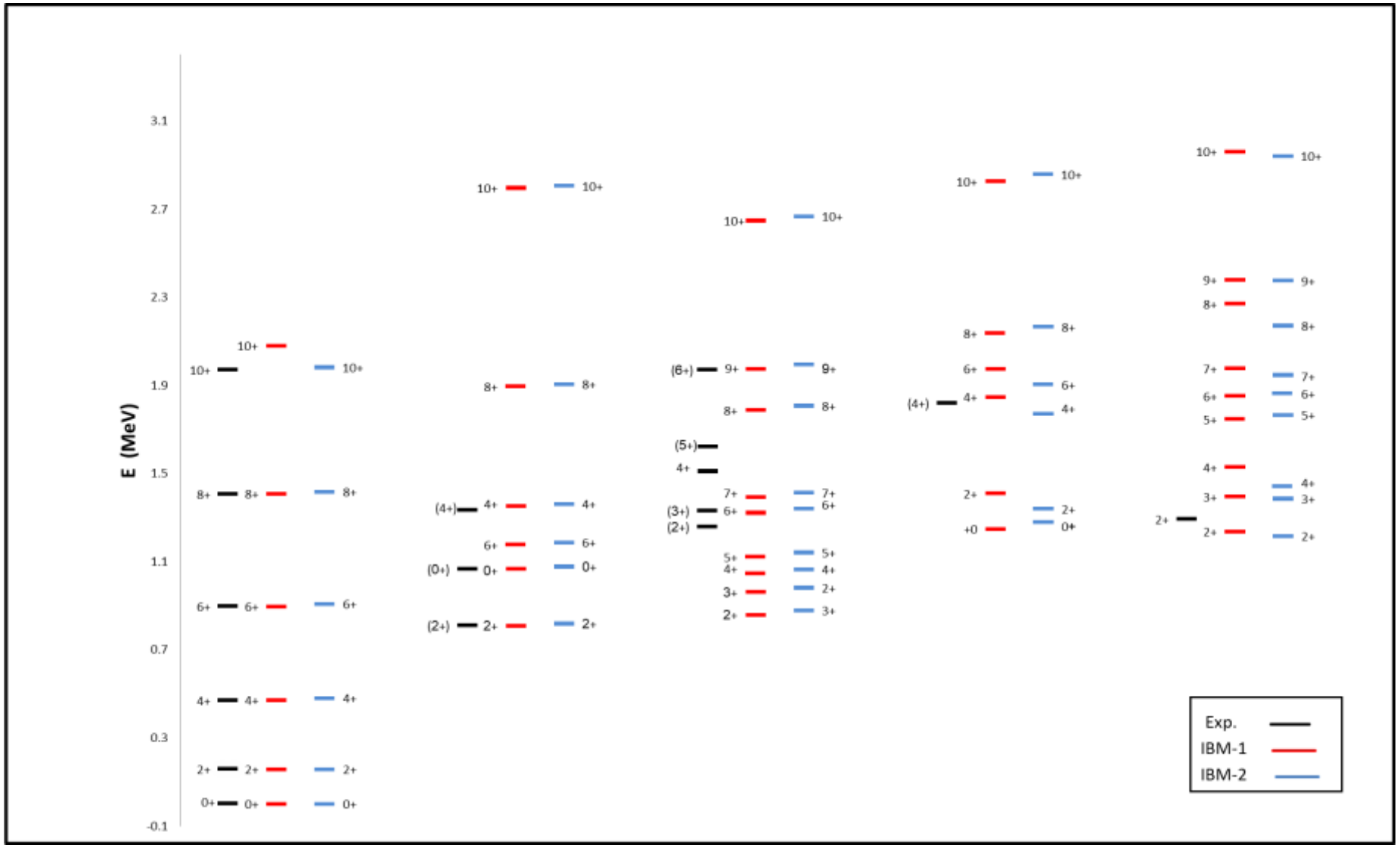

Figure (3.30) Energy levels for ^{166}Hf.

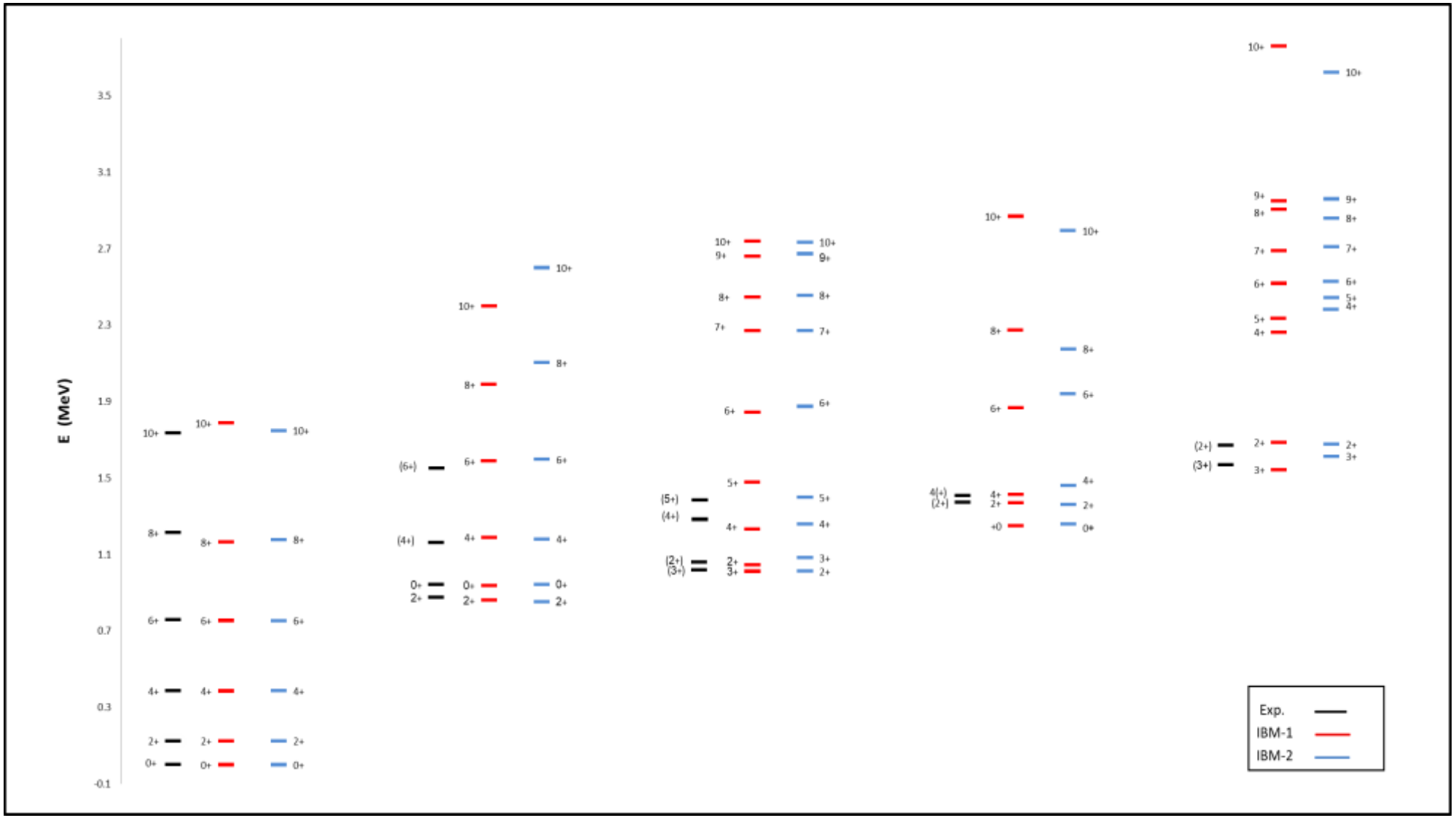

Figure (3.31) Energy levels for ^{168}Hf.

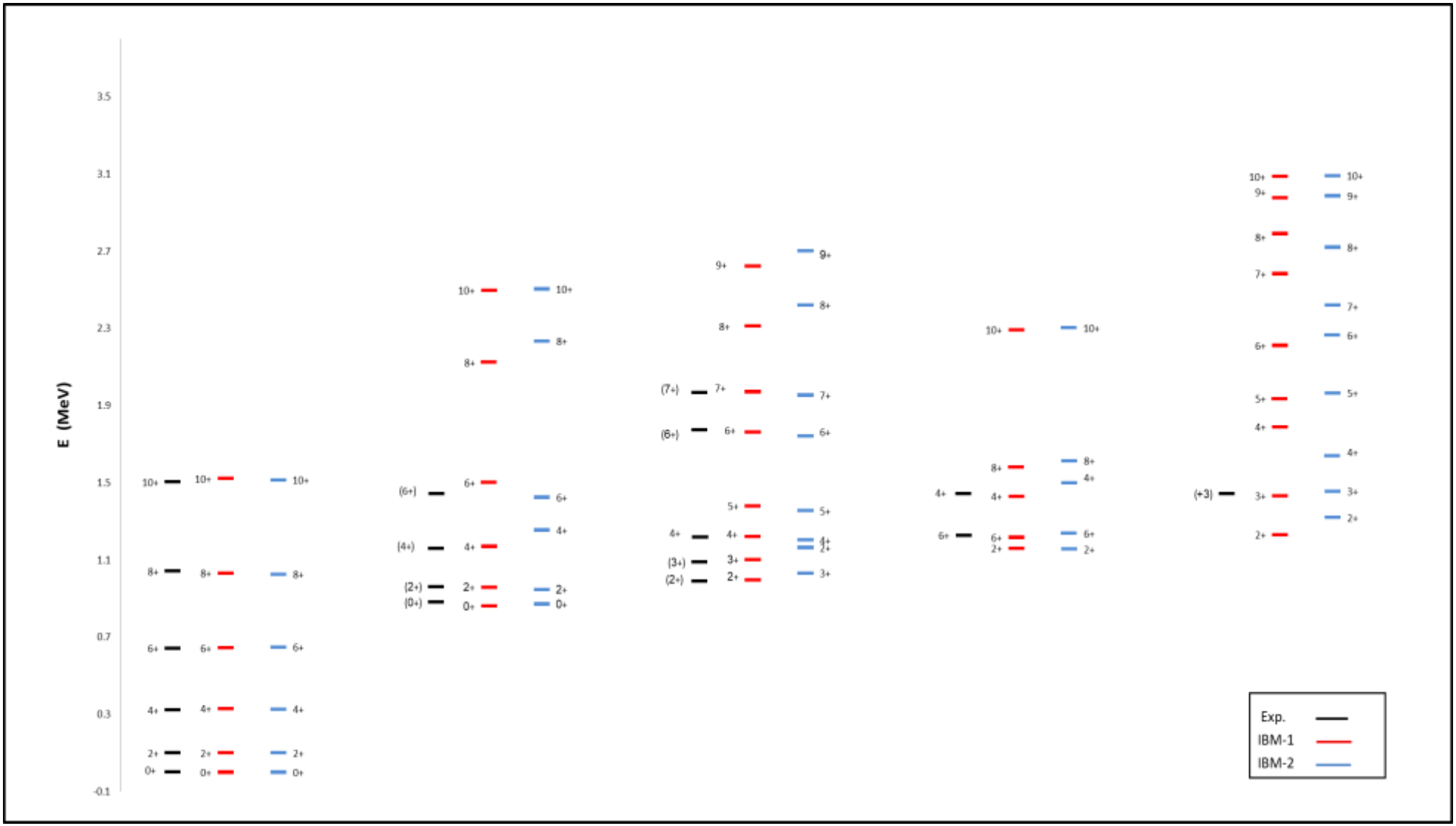

Figure (3.32) Energy levels for ^{170}Hf.

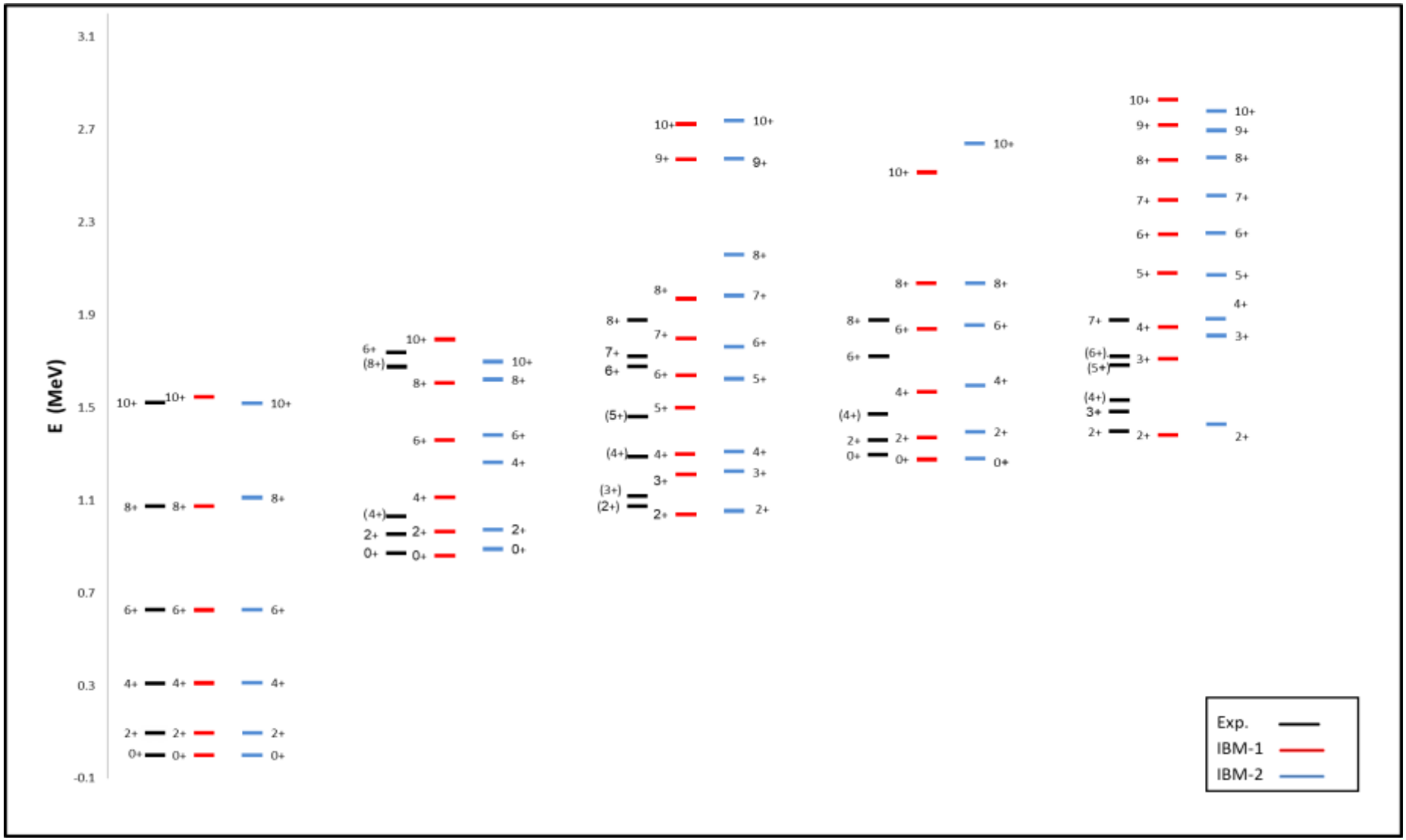

Figure (3.33) Energy levels for ^{172}Hf.

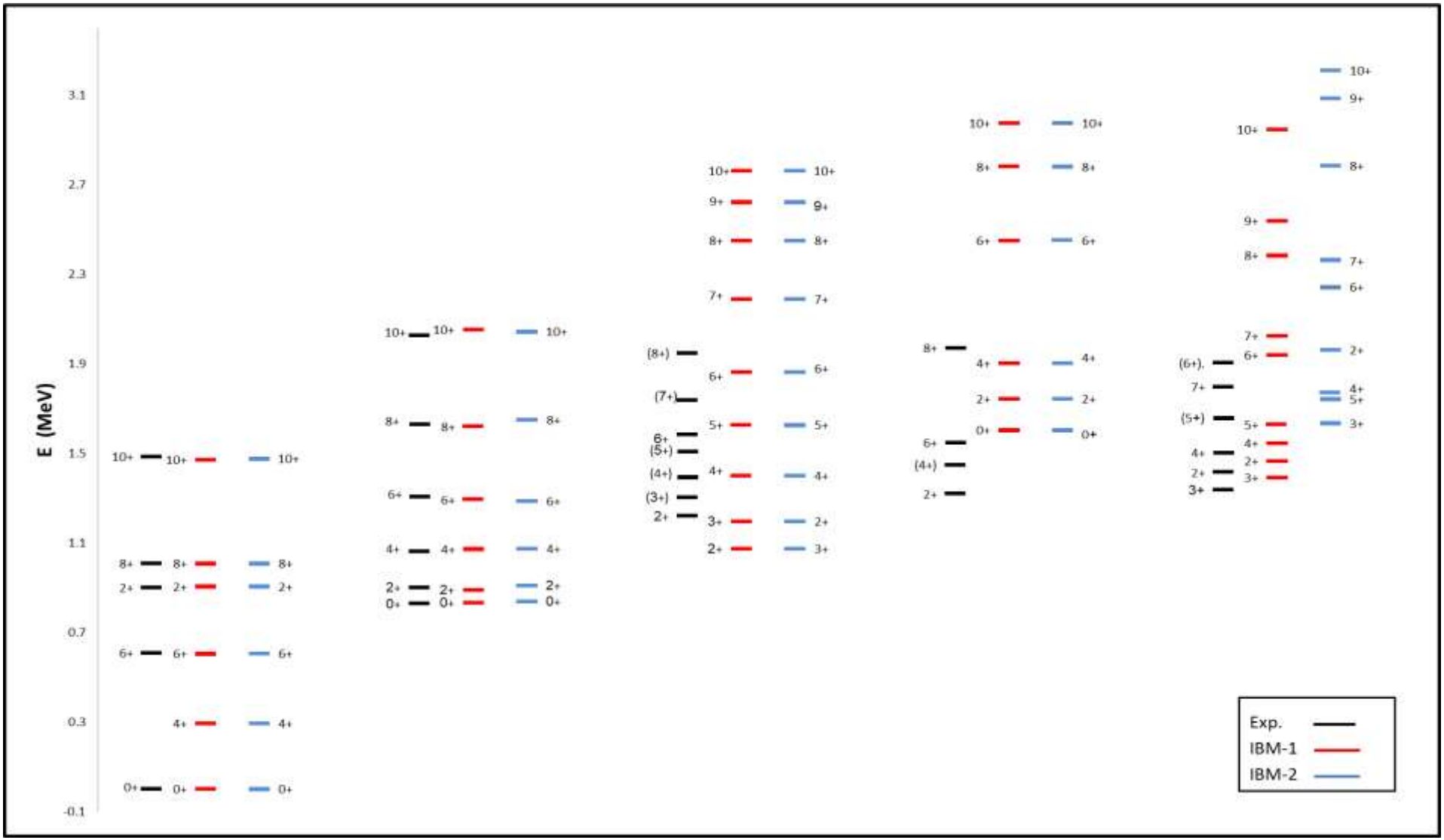

Figure (3.34) Energy levels for ^{174}Hf.

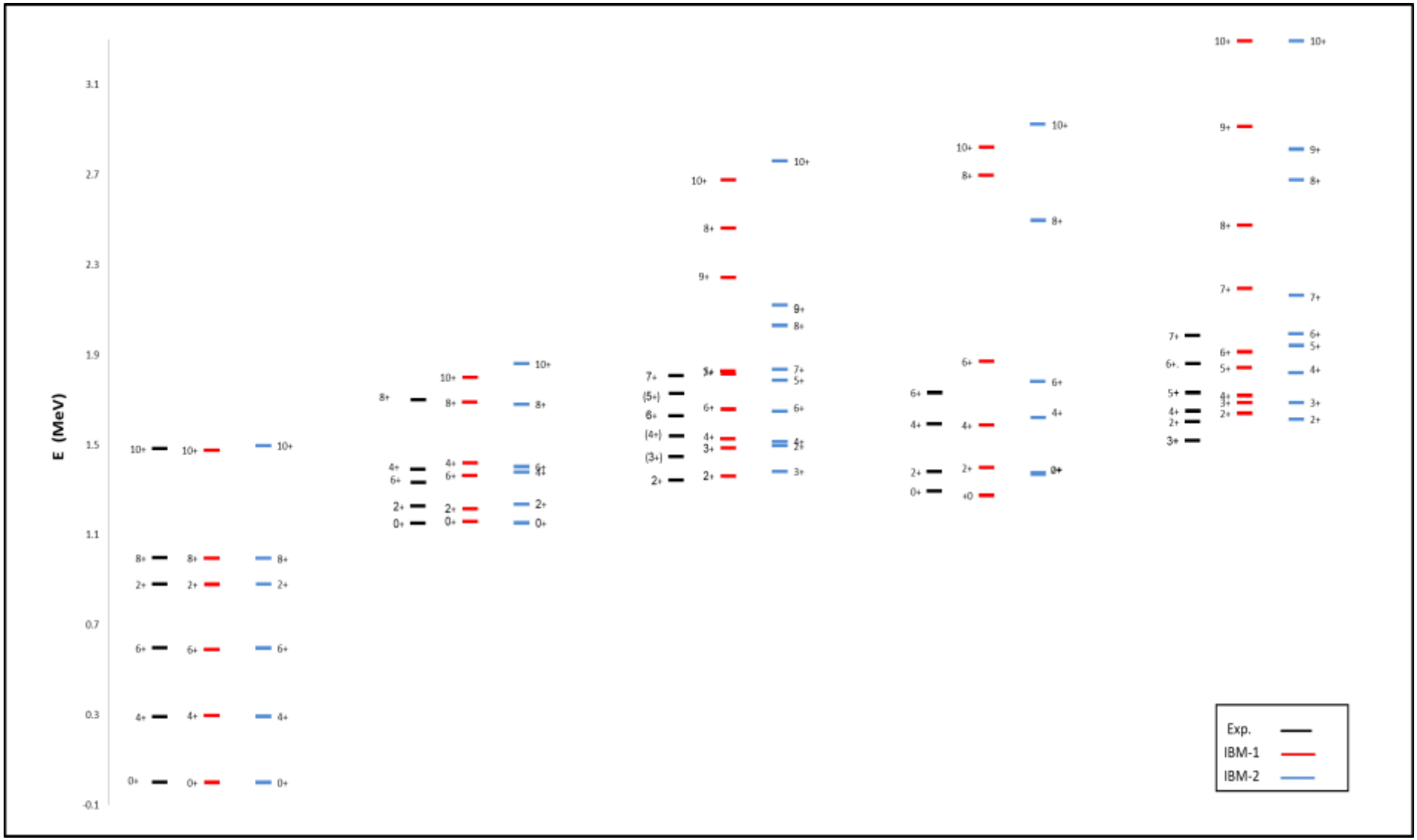

Figure (3.35) Energy levels for ^{176}Hf.

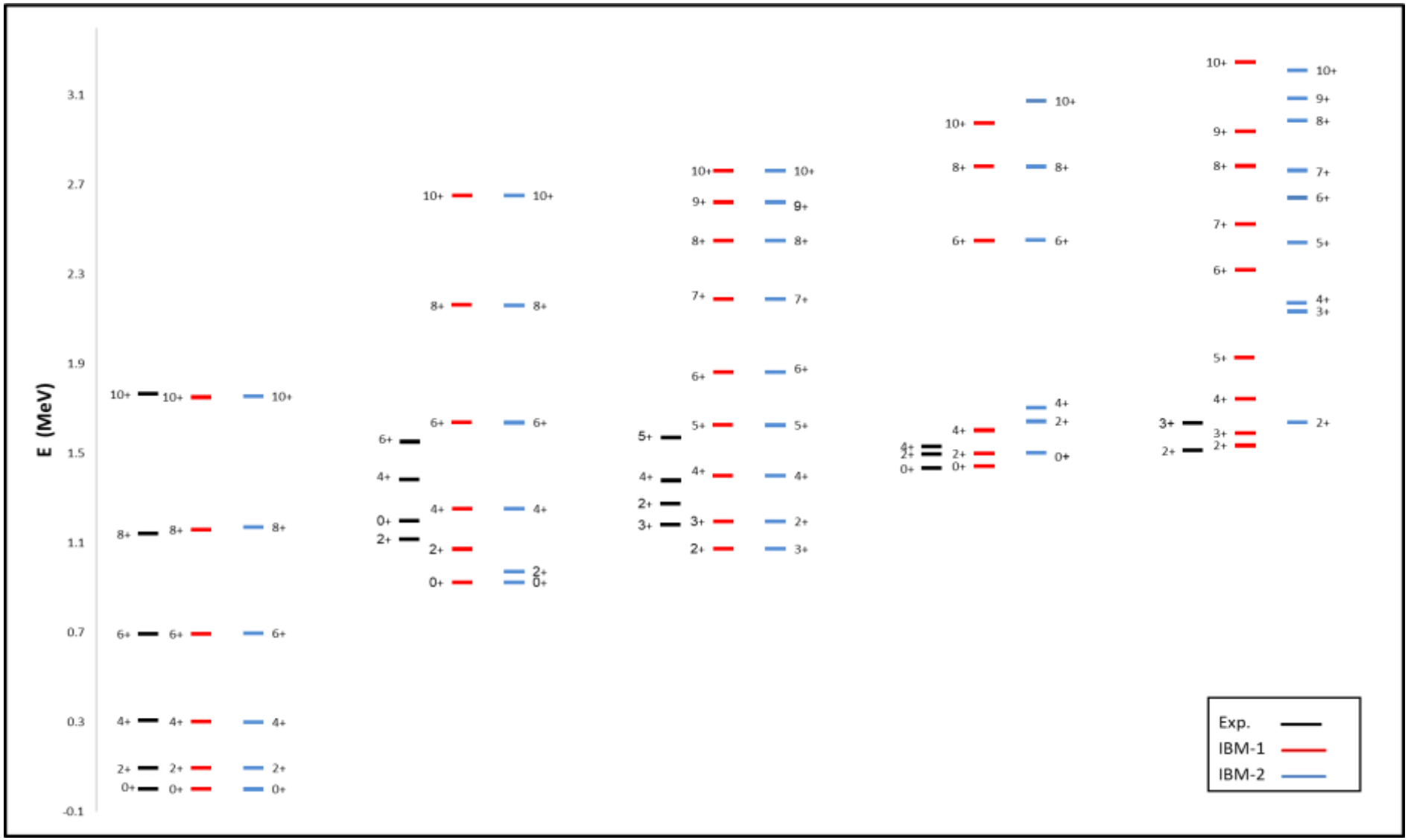

Figure (3.36) Energy levels for ^{178}Hf.

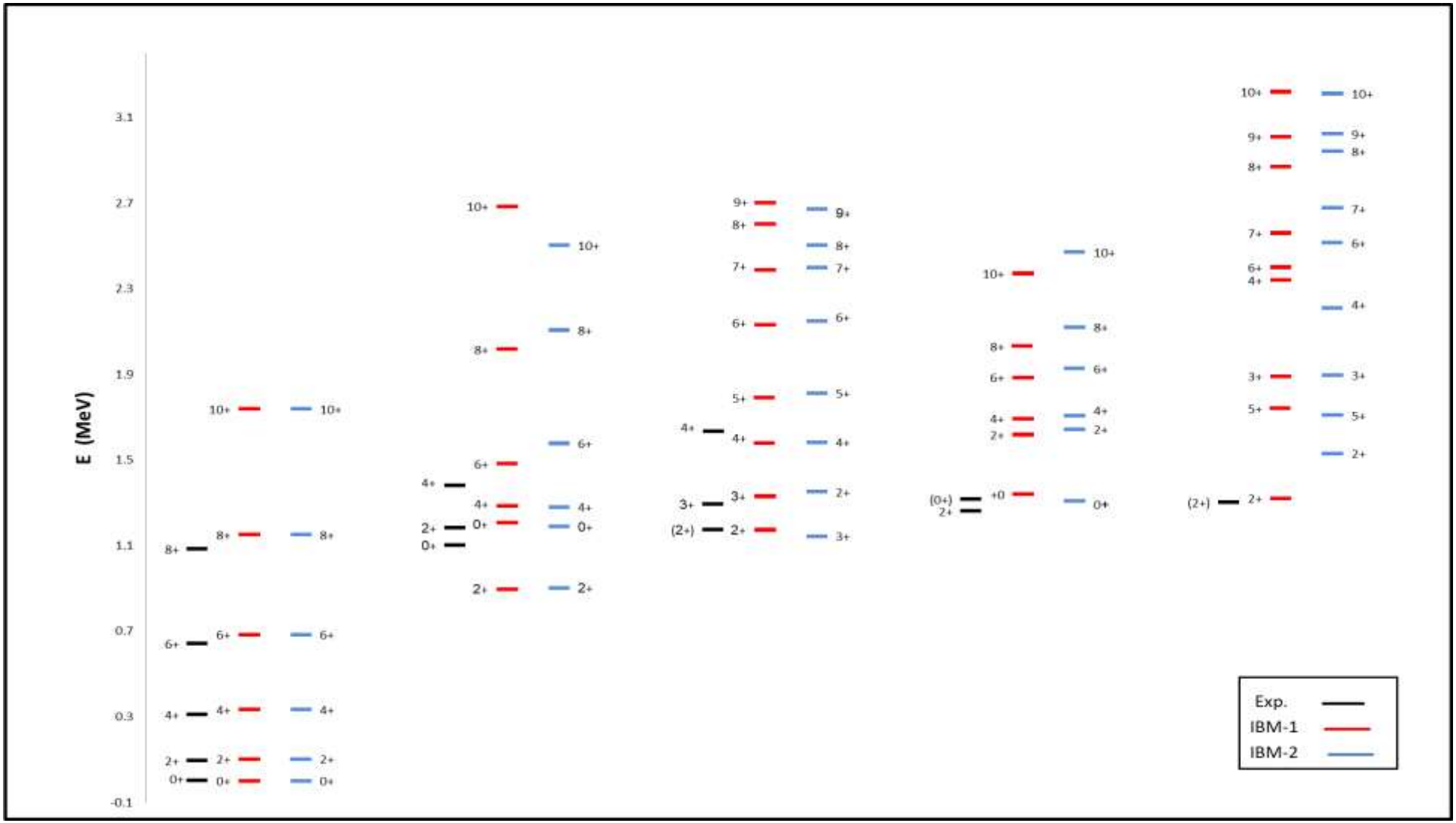

Figure (3.37) Energy levels for ^{180}Hf.

3.2.2. Energy Ratios

Calculating the energy ratios is one of the tests that are performed for each isotope to find out its position in the Casten triangle by comparing it with the ideal ratios in Table (2.4). This calculation of dynamic symmetries by IBM-1, IBM-2 and experimental energy levels and after a comparison with the standard values for the energy ratios of ($E0_2^+/E2_1^+$, $E4_1^+/E2_1^+$, $E6_1^+/E2_1^+$ and $E8_2^+/E2_1^+$) ratios for all studied isotopes have been indicated in Figures (3.38) to (3.41). This leads to guess the nearest dynamic symmetries corresponding to the characteristics one of the dynamic symmetries or may possess transitional features between two or more symmetries so from studying Table (3.12), it is found that the calculated energy ratios in the rotational region SU(3) for all Hafnium isotopes except ^{160}Hf isotope which in transitional region O(6)→ SU(3).

Table (3.12) Energy ratios for $^{166\text{-}180}$Hf isotopes.

Isotopes	Energy ratios											
	$E0_2^+/E2_1^+$			$E4_1^+/E2_1^+$			$E6_1^+/E2_1^+$			$E8_1^+/E2_1^+$		
	Exp. [97-104]	IBM-1	IBM-2	Exp. [97-104]	IBM-1	IBM-2	Exp. [97-104]	IBM-1	IBM-2	Exp. [97-104]	IBM-1	IBM-2
$^{166}_{72}Hf_{94}$	6.73	10.24	4.04	2.96	2.98	2.91	5.65	5.67	5.66	8.86	8.90	9.23
$^{168}_{72}Hf_{96}$	7.59	7.62	5.81	3.10	3.09	3.11	6.10	6.05	6.26	9.78	9.79	10.09
$^{170}_{72}Hf_{98}$	8.73	8.76	8.53	3.19	3.25	3.25	6.37	6.41	6.71	10.35	10.04	11.35
$^{172}_{72}Hf_{100}$	9.16	9.15	9.38	3.24	3.26	3.28	6.59	6.56	6.79	10.89	10.88	11.51
$^{174}_{72}Hf_{102}$	9.10	9.15	9.79	3.26	3.31	3.30	6.68	6.71	6.84	11.09	11.14	11.60
$^{176}_{72}Hf_{104}$	13.02	13.11	10.08	3.28	3.31	3.31	6.75	6.78	6.85	11.29	11.31	11.60
$^{178}_{72}Hf_{106}$	12.89	12.87	8.32	3.29	3.25	3.23	6.78	6.78	6.63	11.36	11.35	11.15
$^{180}_{72}Hf_{108}$	11.80	11.84	9.70	3.30	3.32	3.25	6.86	6.93	6.69	11.61	11.60	11.28

There is a good agreement between experimental data and the IBM-1 and IIBM-2 results appear clearly in the Table and Figures below.

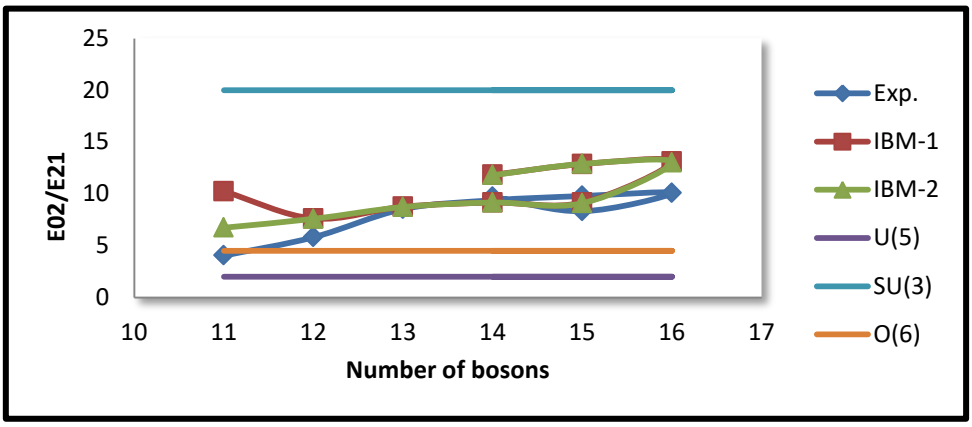

Figure (3.38) The experimental [105-112], theoretical and standard energy ratios ($E0_2^+/E2_1^+$), as a function of bosons numbers for even-even $^{166\text{-}180}$Hf isotopes.

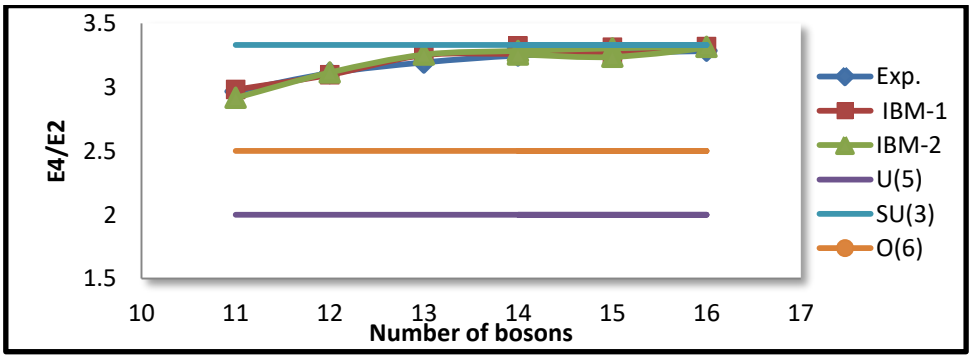

Figure (3.39) The experimental [97-104], theoretical and standard energy ratios ($E4_1^+/E2_1^+$), as a function of bosons numbers for even-even $^{166\text{-}180}$Hf isotopes.

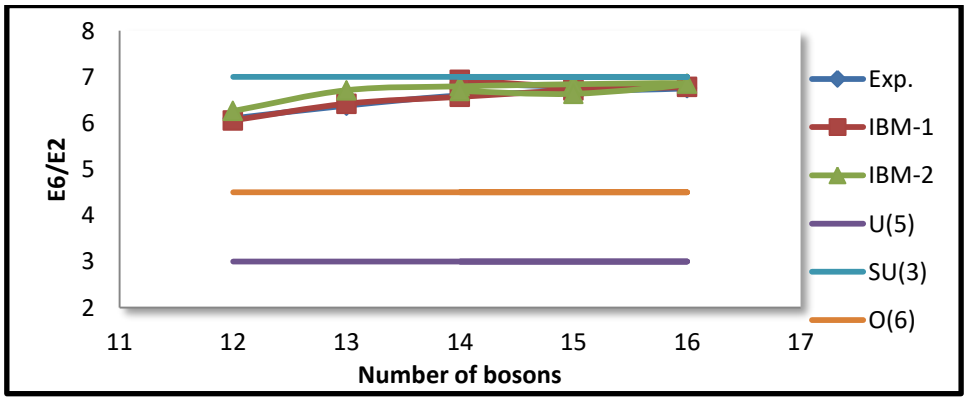

Figure (3.40) The experimental [97-104], theoretical and standard energy ratios ($E6_1^+/E2_1^+$), as a function of bosons numbers for even-even $^{166\text{-}180}$Hf isotopes.

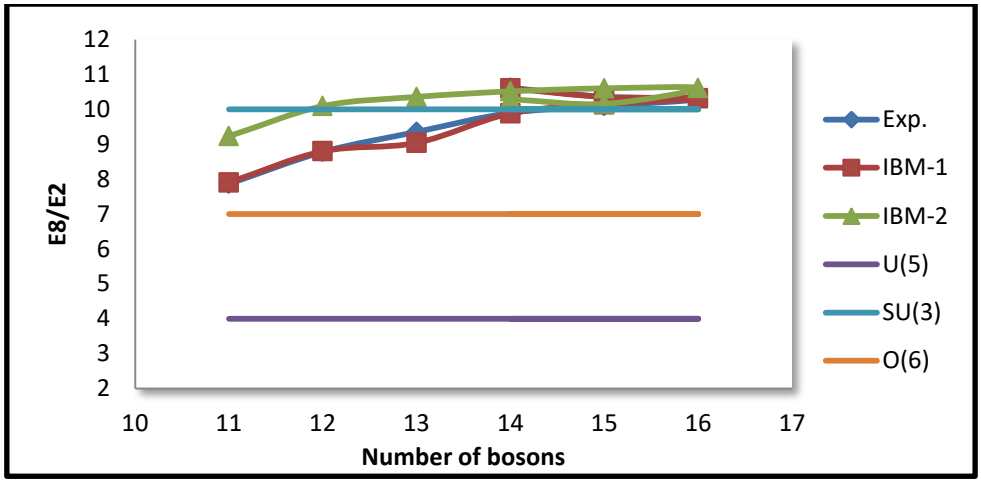

Figure (3.41) The experimental [97-104], theoretical and standard energy ratios ($E8_1^+/E2_1^+$), as a function of bosons numbers for even-even $^{166-180}$Hf isotopes.

3.2.3. Reduced Electric Quadruple Transitions Probability and Quadruple Momentum

The reduced electric quadrupole transition probability B(E2) is considered as one of the most important properties of the nuclear structure, it can be found in the type of the dynamic symmetries for the nuclei through some transitions that occur between the energy levels for these nuclei.

In IBM-1 the reduced electric transition probability values for $^{166-180}$Hf isotopes can be calculated by calculating the values of effective charge e_b= E2SD and β_2=E2DD from Equations (2.29) and by using the experimental value of $B(E2;2_1^+ \rightarrow 0_1^+)$ [97-104], these values are presented in Table (3.13). In IBM-2 effective charge for neutron (e_ν) and for proton (e_π) must be calculated by using Equations (2.72) to find the reduced electric transition probability. In this work, it found that the neutron's effective charge e_ν = 0.28(eb) and the proton's effective charge e_π = 0.035 (eb). The effective charges depend on the

total bosons number N_ρ and the ratios between N_ν/N_π, these parameters are free and can take any value to fit the experimental data.

Table (3.13) The coefficients (E2SD, E2DD) for $^{166\text{-}180}$Hf.

Isotopes	Number of bosons	$B(E2;2_1^+ \to 0_1^+)$ e^2b^2 [97-104]	E2SD(eb)	E2DD(eb)
$^{166}_{72}Hf_{94}$	11	0.692	0.141	-0.417
$^{168}_{72}Hf_{96}$	12	0.857	0.100	-0.295
$^{170}_{72}Hf_{98}$	13	1.001	0.1137	-0.336
$^{172}_{72}Hf_{100}$	14	0.876	0.1065	-0.3152
$^{174}_{72}Hf_{102}$	15	0.96	0.113	-0.336
$^{176}_{72}Hf_{104}$	16	1.054	0.125	-0.371
$^{178}_{72}Hf_{106}$	15*	0.964	0.112	-0.3314
$^{180}_{72}Hf_{108}$	14*	0.93	0.118	-0.349

Table (3.14) shows a comparison between B(E2) calculated by IBM-1, IBM-2 and experimental data. The values are acceptable in comparison and they have a good systematic.

Table (3.14) B(E2) values for $^{166\text{-}180}$Hf isotopes .

B(E2) (e^2b^2)									
Isotopes	^{166}Hf			^{168}Hf			^{170}Hf		
$J_i^+ \to J_f^+$	Exp. [97]	IBM-1	IBM-2	Exp. [98]	IBM-1	IBM-2	Exp. [99]	IBM-1	IBM-2
$2_1 \to 0_1$	0.692	0.693	0.691	0.857	0.856	0.854	1.001	1.006	0.998
$2_1 \to 0_2$	-----	0.127	0.057	-----	0.021	0.034	-----	0.018	
$2_1 \to 2_2$	-----	0.062	0.141	-----	0.033	0.018	-----	0.020	
$2_1 \to 2_3$	-----	0.032	0.004	-----	0.026	0.038	-----	0.023	
$4_1 \to 2_1$	1.095	1.095	1.049	1.344	1.166	0.012	1.471	1.349	
$2_2 \to 2_3$	-----	0.374	0.542	-----	0.005	1.362	-----	0.043	
$2_2 \to 2_4$	-----	0.003	0.007	-----	0.011	0.585	-----	0.002	
$2_4 \to 0_1$	-----	0.022	0.039	-----	0.0001	0.001	-----	0.001	
$4_3 \to 2_1$	-----	0.007	0.021	-----	0.001	0.022	-----	0.001	0.010
$4_3 \to 2_3$	-----	0.047	0.066	-----	0.952	0.036	-----	0.008	0.009

$4_2 \rightarrow 2_2$	-----	0.073	0.576	-----	0.330	0.712	-----	0.317	0.926
$6_1 \rightarrow 4_1$	1.198	1.198	1.185	1.570	-----	1.322	1.712	-----	1.469
$8_1 \rightarrow 6_1$	1.518	1.518	1.221	1.928	-----	1.344	1.925	-----	1.471
$Q_{2_1^+}$ (eb)	-----	2.712	1.95	-----	2.526	1.098	-----	2.785	1.564
B(E2) (e^2b^2)									
Isotopes	**^{172}Hf**			**^{174}Hf**			**^{176}Hf**		
$J_i^+ \rightarrow J_f^+$	**Exp. [100]**	**IBM-1**	**IBM-2**	**Exp. [101]**	**IBM-1**	**IBM-2**	**Exp. [102]**	**IBM-1**	**IBM-2**
$2_1 \rightarrow 0_1$	0.876	0.876	0.883	0.96	0.964	1.003	1.054	1.058	1.059
$2_1 \rightarrow 0_2$	-----	0.043	0.005	-----	0.102	0.012	----	0.203	0.011
$2_1 \rightarrow 2_2$	-----	0.020	0.027	-----	0.008	0.022	----	0.123	0.020
$2_1 \rightarrow 2_3$	-----	0.191	0.014	-----	0.048	0.016	----	0.046	0.017
$4_1 \rightarrow 2_1$	-----	1.172	1.436	-----	1.304	1.506	----	1.443	1.554
$2_2 \rightarrow 2_3$	-----	0.191	0.377	-----	0.378	0.260	----	0.645	0.224
$2_2 \rightarrow 2_4$	-----	0.001	0.001	-----	0.002	0.001	----	0.005	0.001
$2_4 \rightarrow 0_1$	-----	0.004	0.030	-----	0.004	0.030	----	0.003	0.034
$4_3 \rightarrow 2_1$	-----	0.001	0.091	-----	0.007	0.001	----	0.045	----
$4_3 \rightarrow 2_3$	-----	0.022	0.007	-----	0.041	0.006	----	0.062	0.006
$4_2 \rightarrow 2_2$	-----	0.005	1.042	-----	0.131	1.122	0.950	0.153	1.170
$6_1 \rightarrow 4_1$	-----	-----	1.549	-----	-----	1.622	----	-----	1.675
$8_1 \rightarrow 6_1$	-----	-----	1.564	-----	-----	1.638	----	-----	1.699
$Q_{2_1^+}$ (eb)	-----	2.685	1.42	-----	2.951	1.445	-----	3.271	1.564
B(E2) (e^2b^2)									
Isotopes	**^{178}Hf**			**^{180}Hf**					
$J_i^+ \rightarrow J_f^+$	**Exp. [103]**	**IBM-1**	**IBM-2**	**Exp. [104]**	**IBM-1**	**IBM-2**			
$2_1 \rightarrow 0_1$	0.964	0.964	1.002	0.930	0.935	0.915			
$2_1 \rightarrow 0_2$	-----	0.094	0.018	----	0.094	0.014			
$2_1 \rightarrow 2_2$	-----	0.005	0.036	----	0.006	0.030			
$2_1 \rightarrow 2_3$	-----	0.047	0.018	----	0.046	0.019			
$4_1 \rightarrow 2_1$	-----	1.301	1.429	1.389	1.258	1.437			
$2_2 \rightarrow 2_3$	-----	0.356	0.471	----	0.346	0.391			
$2_2 \rightarrow 2_4$	-----	0.002	0.001	----	0.002	0.001			
$2_4 \rightarrow 0_1$	-----	0.004	0.028	----	0.004	0.026			

$4_3 \rightarrow 2_1$	-----	0.006	0.002	----	0.006	0.021	
$4_3 \rightarrow 2_3$	-----	0.039	0.010	----	0.040	0.011	
$4_2 \rightarrow 2_2$	-----	0.136	1.019	----	0.124	1.008	
$6_1 \rightarrow 4_1$	-----	-----	1.549	1.323	-----	1.547	
$8_1 \rightarrow 6_1$	-----	-----	1.572	1.480	-----	1.554	
$Q_{2_1^+}$ (eb)	-----	2.929	1.420	-----	2.902	1.445	

3.2.4 Branching Ratio

One of the important properties which can be calculated is the branching ratios, through which one can identify the position of the nuclei studied in the Casten triangle, and hence to identify the dynamic symmetry for the nuclei by using the Equations (2.24)-(2.26), (2.38- 2.40) and (2.52)-(2.54). Table (3.15) shows the branching ratios for all studied Hafnium isotopes.

Table (3.15) Branching ratios for $^{166\text{-}180}$Hf isotopes.

Isotopes	**Branching ratios**								
	R			**R′**			**R″**		
	Exp. [97-104]	**IBM-1**	**IBM-2**	**Exp.**	**IBM-1**	**IBM-2**	**Exp.**	**IBM-1**	**IBM-2**
$^{166}_{72}Hf_{94}$	1.57	1.33	1.518	-----	0.016	0.204	-----	0.036	0.016
$^{168}_{72}Hf_{96}$	1.58	1.36	1.405	-----	0.096	0.097	-----	0.024	0.0079
$^{170}_{72}Hf_{98}$	1.44	1.43	1.364	-----	0.072	0.038	-----	0.0037	0.0036
$^{172}_{72}Hf_{100}$	1.424	1.33	1.626	-----	0.028	0.030	-----	0.0037	0.0011
$^{174}_{72}Hf_{102}$	1.421	1.35	1.501	-----	0.0005	0.021	-----	0.0212	0.0023
$^{176}_{72}Hf_{104}$	1.586	1.36	1.467	-----	0.047	0.018	-----	0.038	0.0020
$^{178}_{72}Hf_{106}$	1.589	1.35	1.426	-----	0.0016	0.035	-----	0.019	0.0035
$^{180}_{72}Hf_{108}$	1.49	1.344	1.570	-----	0.0019	0.032	-----	0.020	0.0030

Where observed that there is an acceptable agreement between theoretical calculation and available experimental values due to the strength of B(E2) values for each transition, which reflects the extent of deformation of these isotopes, which in turn affects on the position of energy levels and finally affects on the B(E2) values and branching ratios between them.

3.2.5 Reduced Transitions Probability for Magnetic Dipole and Mixing Ratio

In order to calculate B(M1) transition probability, one should estimate the effective g −factors for proton g_π and neutron g_ν by Equations (2.20). In Hafnium isotopes the g- factor values are g_π= 0.417 (μ_N) and g_ν= 0.418 (μ_N). Equations (2.19) were used to calculate the B(M1) transition probabilities as it is shown in Table (3.16). The calculated values for B(M1) are acceptable to some extent as compared with the available experiments values, where some of B(M1) values are small compared to the values of the quadrupole transition probabilities because the wavelength of the gamma ray transitions is greater than it is in the magnetic transitions according to Equation (3.1), this Equation shows that the B(M1)transition probability is less than B(E2) transition probability and our results confirm this. The calculation values for these isotopes and mixing ratio δ(E2/M1) have been compared with the available experiments data as shown in Table (3.16).

Table (3.16) The B(M1) transition and mixing ratio for $^{166\text{-}180}$Hf isotopes.

Isotopes	^{166}Hf				^{168}Hf			
	B(M1) (e^2b^2)		δ(E2/M1)		B(M1) (e^2b^2)		δ(E2/M1)	
$J_i^+ \rightarrow J_f^+$	Exp. [97]	IBM-2	Exp.	IBM-2	Exp. [98]	IBM-2	Exp.	IBM-2
$2_1 \rightarrow 2_2$	1.21×10^{-7}	3.27×10^{-9}		1.81×10^{-8}		7.53×10^{-9}		5.43×10^{-8}
$2_1 \rightarrow 2_3$	1.06×10^{-7}	1.11×10^{-8}		1.39×10^{-6}		8.77×10^{-9}		5.51×10^{-7}
$4_1 \rightarrow 2_1$		1.66×10^{-8}		1.52×10^{-7}		1.24×10^{-7}		2.34×10^{-2}

$2_2 \rightarrow 2_3$		1.22×10^{-5}		7.23×10^{-4}		8.14×10^{-6}		7.15×10^{-2}
$2_2 \rightarrow 2_4$		1.95×10^{-4}		2.49×10^{-5}		4.81×10^{-5}		4.63×10^{-2}
$3_1 \rightarrow 2_1$		1.38×10^{-4}		2.34×10^{-2}		1.66×10^{-4}		1.66×10^{-2}
$3_1 \rightarrow 2_2$	3.21×10^{-3}	2.29×10^{-3}		7.15×10^{-2}		1.22×10^{-4}		1.52×10^{-2}
$4_1 \rightarrow 3_1$		1.01×10^{-5}		4.63×10^{-2}		1.95×10^{-6}		1.95×10^{-3}
$5_1 \rightarrow 4_1$		5.02×10^{-4}		4.51×10^{-3}		1.38×10^{-7}		1.38×10^{-3}
$5_1 \rightarrow 4_2$		5.34×10^{-5}		6.69×10^{-3}	5.24×10^{-2}	2.29×10^{-2}		2.29×10^{-2}
Isotopse	**^{170}Hf**				**^{172}Hf**			
	B(M1) (e^2b^2)		**δ(E2/M1)**		**B(M1) (e^2b^2)**		**δ(E2/M1)**	
$J_i^+ \rightarrow J_f^+$	**Exp. [99]**	**IBM-2**	**Exp.**	**IBM-2**	**Exp. [100]**	**IBM-2**	**Exp.**	**IBM-2**
$2_1 \rightarrow 2_2$		3.11×10^{-8}		3.84×10^{-4}		1.55×10^{-3}		1.91×10^{-2}
$2_1 \rightarrow 2_3$		6.16×10^{-9}		1.23×10^{-3}	1.12×10^{-2}	4.27×10^{-4}		6.31×10^{-2}
$4_1 \rightarrow 2_1$	9.51×10^{-3}	2.93×10^{-8}		5.03×10^{-4}		3.68×10^{-5}		1.95×10^{-3}
$2_2 \rightarrow 2_3$		1.66×10^{-8}		1.76×10^{-4}		5.33×10^{-5}		1.88×10^{-3}
$2_2 \rightarrow 2_4$		1.25×10^{-7}		2.59×10^{-3}		1.68×10^{-4}		2.89×10^{-2}
$3_1 \rightarrow 2_1$		1.95×10^{-8}		3.93×10^{-3}		4.37×10^{-4}		1.61×10^{-3}
$3_1 \rightarrow 2_2$		1.38×10^{-9}		1.67×10^{-2}	2.34×10^{-2}	2.35×10^{-2}		4.37×10^{-4}
$4_1 \rightarrow 3_1$		2.29×10^{-9}		2.89×10^{-2}	5.65×10^{-2}	2.18×10^{-4}		2.35×10^{-2}
$5_1 \rightarrow 4_1$		1.01×10^{-7}		1.61×10^{-3}		2.15×10^{-2}		2.18×10^{-4}
$5_1 \rightarrow 4_2$		3.23×10^{-8}		4.13×10^{-4}		3.03×10^{-5}		2.15×10^{-2}
Isotopes	^{174}Hf				^{176}Hf			
	B(M1) (e^2b^2)		δ(E2/M1)		B(M1) (e^2b^2)		δ(E2/M1)	
$J_i^+ \rightarrow J_f^+$	Exp. [101]	IBM-2	Exp.	IBM-2	Exp. [102]	IBM-2	Exp.	IBM-2
$2_1 \rightarrow 2_2$		1.95×10^{-3}		2.45×10^{-7}		1.49×10^{-3}		1.64×10^{-7}
$2_1 \rightarrow 2_3$	1.22×10^{-3}	1.88×10^{-3}		2.09×10^{-8}		5.23×10^{-3}		4.71×10^{-8}
$2_2 \rightarrow 2_3$		2.89×10^{-4}		4.77×10^{-9}		1.65×10^{-4}		2.79×10^{-9}
$2_2 \rightarrow 2_4$	1.01×10^{-2}	1.61×10^{-3}		2.15×10^{-2}	1.34×10^{-3}	1.47×10^{-4}		4.36×10^{-4}
$3_1 \rightarrow 2_1$		4.32×10^{-3}		5.06×10^{-4}		4.33×10^{-4}		2.15×10^{-2}
$3_1 \rightarrow 2_2$		2.15×10^{-2}		4.37×10^{-4}		2.15×10^{-2}		2.78×10^{-4}
$4_1 \rightarrow 3_1$		2.78×10^{-4}		2.35×10^{-2}		2.78×10^{-4}		4.36×10^{-4}
$5_1 \rightarrow 4_1$		4.66×10^{-4}		2.18×10^{-4}		4.93×10^{-4}		2.15×10^{-2}
$5_1 \rightarrow 4_2$		4.94×10^{-4}		2.15×10^{-2}		2.09×10^{-2}		4.16×10^{-4}

Isotopes	^{178}Hf				^{180}Hf			
	B(M1) (e^2b^2)		δ(E2/M1)		B(M1) (e^2b^2)		δ(E2/M1)	
$J_i^+ \rightarrow J_f^+$	Exp. [103]	IBM-2	Exp.	IBM-2	Exp. [104]	IBM-2	Exp.	IBM-2
$2_1 \rightarrow 2_2$		2.15×10^{-2}		4.36×10^{-4}		2.33×10^{-2}		2.11×10^{-2}
$2_1 \rightarrow 2_3$		2.55×10^{-8}		2.15×10^{-2}		4.89×10^{-8}		6.28×10^{-7}
$4_1 \rightarrow 2_1$		1.96×10^{-2}		2.78×10^{-4}		5.03×10^{-9}		7.54×10^{-8}
$2_2 \rightarrow 2_3$	3.23×10^{-3}	4.36×10^{-4}		4.54×10^{-4}		2.15×10^{-2}		3.15×10^{-2}
$2_2 \rightarrow 2_4$		2.15×10^{-2}		2.78×10^{-2}		6.16×10^{-9}		8.66×10^{-9}
$3_1 \rightarrow 2_1$		2.78×10^{-4}		2.38×10^{-4}		1.42×10^{-7}		2.22×10^{-2}
$3_1 \rightarrow 2_2$		4.93×10^{-4}		2.78×10^{-4}		4.36×10^{-4}		2.78×10^{-4}
$4_1 \rightarrow 3_1$		2.09×10^{-2}		4.54×10^{-4}		2.15×10^{-2}		4.54×10^{-4}
$5_1 \rightarrow 4_1$		4.36×10^{-4}		2.78×10^{-2}		2.78×10^{-4}		2.78×10^{-2}
$5_1 \rightarrow 4_2$		2.15×10^{-2}		2.78×10^{-4}		4.93×10^{-4}		2.15×10^{-2}
$4_1 \rightarrow 3_1$		2.78×10^{-4}		4.54×10^{-4}	3.45×10^{-2}	2.09×10^{-2}		2.78×10^{-4}
$5_1 \rightarrow 4_1$		6.36×10^{-4}		2.78×10^{-2}		4.36×10^{-4}		4.93×10^{-4}
$5_1 \rightarrow 4_2$		4.46×10^{-4}		2.36×10^{-4}		4.36×10^{-4}		2.09×10^{-2}

3.2.6 Electric Monopole Transition B(E0) and $X(E0/E2)$ Ratios

The deformation parameters for protons and neutrons are used to calculate monopole transition matrix elements for $^{166\text{-}180}$Hf isotopes that have been estimated using Equations (2.67) to (2.69). In addition to the available experimental data, the monopole transition matrix element and mixing ratio have been calculated using Equations (2.65) and (2.71) listed in Table (3.17)

The ratio X(E0/E2) shows the strength of the competition between E0 and E2, where it is noted that the IBM-2 calculated values are not entirely consistent with the experimental values available, and the reason belongs to the strength of the transition between E2 and E0, as well as the fact that the difficulty of defining unified parameters for ($\tilde{\beta}_\nu$, $\tilde{\beta}_\pi$) give us the theoretical

values in (IBM-2) that are closer to the available experimental data. The deformation parameters for protons and neutrons used to calculate monopole transition matrix elements ρ(E0) for $^{166\text{-}180}$Hf isotopes are ($\tilde{\beta}_{\nu}$= 0.0079 fm^2, $\tilde{\beta}_{\pi}$ = -0.00543 fm^2). Table (3.17) shows the electric monopole transition matrix and X(E0/E2) for $^{166\text{-}180}$Hf isotopes.

Table (3.17) Electric monopole transition and X(E0/E2) for $^{166\text{-}180}$Hf isotopes.

Isotopes	**^{166}Hf**				**^{168}Hf**			
	B(E0) (e^2b^2)		**X(E0/E2)**		**B(E0) (e^2b^2)**		**X(E0/E2)**	
$J_i^+ \rightarrow J_f^+$	**Exp.**	**IBM-2**	**Exp.**	**IBM-2**	**Exp.**	**IBM-2**	**Exp.**	**IBM-2**
$2_1 \rightarrow 2_2$		3.27×10^{-9}		1.81×10^{-5}		7.53×10^{-9}		5.43×10^{-5}
$2_1 \rightarrow 2_3$		1.11×10^{-5}		1.39×10^{-2}		8.77×10^{-9}		5.51×10^{-4}
$2_2 \rightarrow 2_3$		4.65×10^{-9}		7.23×10^{-9}		8.14×10^{-9}		7.86×10^{-9}
$2_2 \rightarrow 2_4$		1.32×10^{-5}		2.49×10^{-3}		4.08×10^{-5}		1.79×10^{-4}
$3_1 \rightarrow 2_1$		2.78×10^{-4}		1.23×10^{-4}		2.09×10^{-2}		1.85×10^{-3}
$3_1 \rightarrow 2_2$		4.93×10^{-4}		1.15×10^{-3}		9.66×10^{-4}		3.15×10^{-3}
$4_1 \rightarrow 3_1$		2.09×10^{-2}		1.15×10^{-3}		6.99×10^{-4}		1.77×10^{-4}
$5_1 \rightarrow 4_1$		9.66×10^{-4}		1.68×10^{-4}		1.21×10^{-3}		3.24×10^{-4}
$5_1 \rightarrow 4_2$		6.99×10^{-4}		3.84×10^{-4}		4.04×10^{-4}		1.23×10^{-4}
Isotopes	**^{170}Hf**				**^{172}Hf**			
	B(E0) (e^2b^2)		**X(E0/E2)**		**B(E0) (e^2b^2)**		**X(E0/E2)**	
$J_i^+ \rightarrow J_f^+$	**Exp. [99]**	**IBM-2**	**Exp.**	**IBM-2**	**Exp.**	**IBM-2**	**Exp.**	**IBM-2**
$2_1 \rightarrow 2_2$		3.11×10^{-5}		3.84×10^{-4}		1.55×10^{-5}		1.91×10^{-4}
$2_1 \rightarrow 2_3$	5.96×10^{-5}	6.16×10^{-7}		1.23×10^{-4}		4.27×10^{-2}		6.31×10^{3}
$2_2 \rightarrow 2_3$		1.66×10^{-5}		1.76×10^{-5}		5.33×10^{-9}		7.05×10^{-9}
$2_2 \rightarrow 2_4$		1.72×10^{-4}		2.59×10^{-3}		1.68×10^{-4}		6.52×10^{-7}
$3_1 \rightarrow 2_1$		2.09×10^{-2}		6.99×10^{-4}		3.84×10^{-4}		6.99×10^{-4}
$3_1 \rightarrow 2_2$		9.66×10^{-4}		6.04×10^{-5}		1.23×10^{-4}		5.24×10^{-4}
$4_1 \rightarrow 3_1$		6.99×10^{-4}		4.04×10^{-4}		1.76×10^{-5}		4.04×10^{-4}
$5_1 \rightarrow 4_1$		9.01×10^{-2}		1.15×10^{-3}		2.59×10^{-3}		1.15×10^{-3}
$5_1 \rightarrow 4_2$		4.04×10^{-4}		3.84×10^{-4}		1.09×10^{-2}		3.84×10^{-4}

Isotopes	**^{174}Hf**				**^{176}Hf**			
	B(E0) (e^2b^2)		**X(E0/E2)**		**B(E0) (e^2b^2)**		**X(E0/E2)**	
$J_i^+ \rightarrow J_f^+$	**Exp.**	**IBM-2**	**Exp.**	**IBM-2**	**Exp.**	**IBM-2**	**Exp.**	**IBM-2**
$2_1 \rightarrow 2_2$		1.95×10^{-5}		2.45×10^{-4}		1.49×10^{-5}		1.64×10^{-4}
$2_1 \rightarrow 2_3$		1.88×10^{-9}		2.09×10^{-5}		5.23×10^{-9}		4.71×10^{-5}
$2_2 \rightarrow 2_3$		2.89×10^{-9}		4.77×10^{-9}		1.65×10^{-9}		2.79×10^{-9}
$2_2 \rightarrow 2_4$		1.61×10^{-4}		5.74×10^{-6}		1.47×10^{-4}		5.24×10^{-7}
$3_1 \rightarrow 2_1$		6.19×10^{-4}		2.78×10^{-4}		2.09×10^{-2}		6.99×10^{-4}
$3_1 \rightarrow 2_2$		5.84×10^{-5}		4.93×10^{-4}		9.66×10^{-4}		2.24×10^{-7}
$4_1 \rightarrow 3_1$		4.84×10^{-4}		2.09×10^{-2}		6.79×10^{-4}		4.04×10^{-4}
$5_1 \rightarrow 4_1$		1.03×10^{-3}		9.66×10^{-4}		5.24×10^{-5}		1.15×10^{-3}
$5_1 \rightarrow 4_2$		3.72×10^{-4}		6.99×10^{-4}		4.04×10^{-4}		3.84×10^{-4}
Isotopes	**^{178}Hf**				**^{180}Hf**			
	B(E0) (e^2b^2)		**X(E0/E2)**		**B(E0) (e^2b^2)**		**X(E0/E2)**	
$J_i^+ \rightarrow J_f^+$	**Exp. [103]**	**IBM-2**	**Exp. [103]**	**IBM-2**	**Exp.**	**IBM-2**	**Exp.**	**IBM-2**
$2_1 \rightarrow 2_2$		1.23×10^{-4}		4.93×10^{-4}		1.45×10^{-4}		2.23×10^{-4}
$2_1 \rightarrow 2_3$		2.55×10^{-5}		2.22×10^{-4}		4.89×10^{-5}		6.11×10^{-4}
$4_1 \rightarrow 2_1$		1.69×10^{-4}		2.03×10^{-5}		5.03×10^{-6}		7.54×10^{-5}
$2_2 \rightarrow 2_4$		8.64×10^{-6}		8.62×10^{-6}		6.16×10^{-6}		8.66×10^{-4}
$3_1 \rightarrow 2_1$	1.76×10^{-3}	2.09×10^{-2}		2.09×10^{-2}		1.54×10^{-4}		5.24×10^{-5}
$3_1 \rightarrow 2_2$		9.66×10^{-4}		9.66×10^{-4}		2.09×10^{-2}		3.39×10^{-2}
$4_1 \rightarrow 3_1$		6.95×10^{-4}		6.99×10^{-4}		1.6910^{-4}		3.24×10^{-3}
$5_1 \rightarrow 4_1$		5.33×10^{-7}		5.24×10^{-4}		6.79×10^{-4}		6.54×10^{-4}
$5_1 \rightarrow 4_2$		4.04×10^{-4}		4.54×10^{-4}		3.24×10^{-4}		5.14×10^{-5}

3.2.7 Potential Energy Surface (PES)

The surface of the potential energy as a function with contour diagrams for isotopes that have been calculated from Equation (2.42) with computer code is represented in Figures (3.42) to (3.49).

The parameters used in the program to calculate the potential energy surface are shown in Table (3.18).

Table (3.18) Potential energy surface parameters for $^{166\text{-}180}$Hf isotopes.

Isotops	N	ES	ED	A_1	A_2	A_3	A_4
$^{166}_{72}Hf_{94}$	11	-0.082	0.094	0.003	0.002	-0.066	0
$^{168}_{72}Hf_{96}$	12	-0.071	0.065	0.003	0.036	-0.057	0
$^{170}_{72}Hf_{98}$	13	-0.061	0.066	0.003	0.007	-0.049	0
$^{172}_{72}Hf_{100}$	14	0.057	0.06	0.003	0.003	-0.046	0
$^{174}_{72}Hf_{102}$	15	-0.058	0.052	0.003	0.002	-0046	0
$^{176}_{72}Hf_{104}$	16	-0.056	0.048	0.003	0.001	-0.045	0
$^{178}_{72}Hf_{106}$	15	-0.057	0.057	0.003	0.002	-0.046	0
$^{180}_{72}Hf_{108}$	14	-0.058	0.054	0.003	0.002	-0.047	0

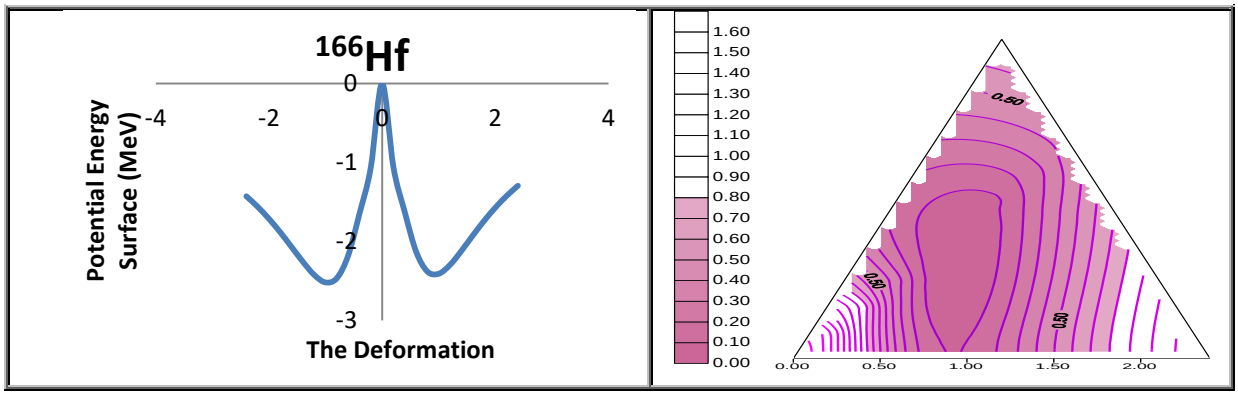

Figure (3.42) Potential energy surface with the deformation for ^{166}Hf.

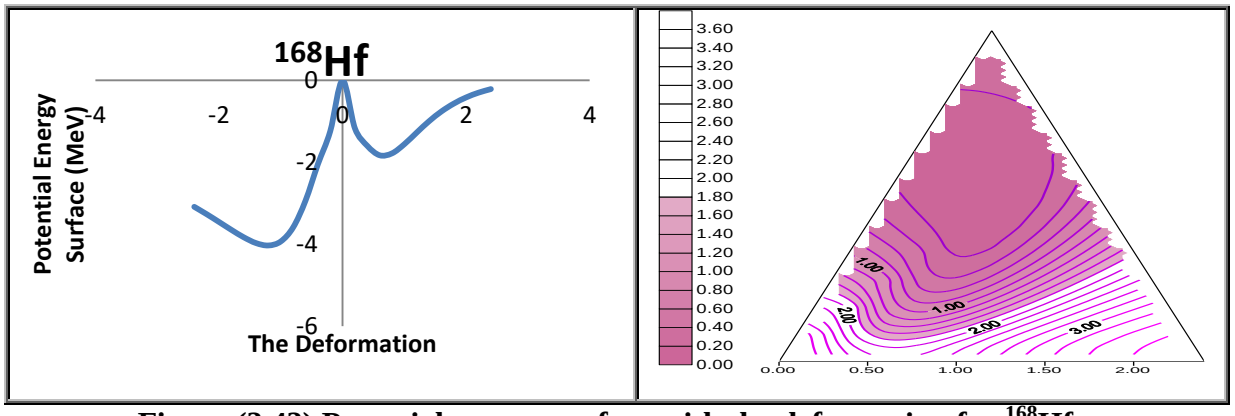

Figure (3.43) Potential energy surface with the deformation for ^{168}Hf.

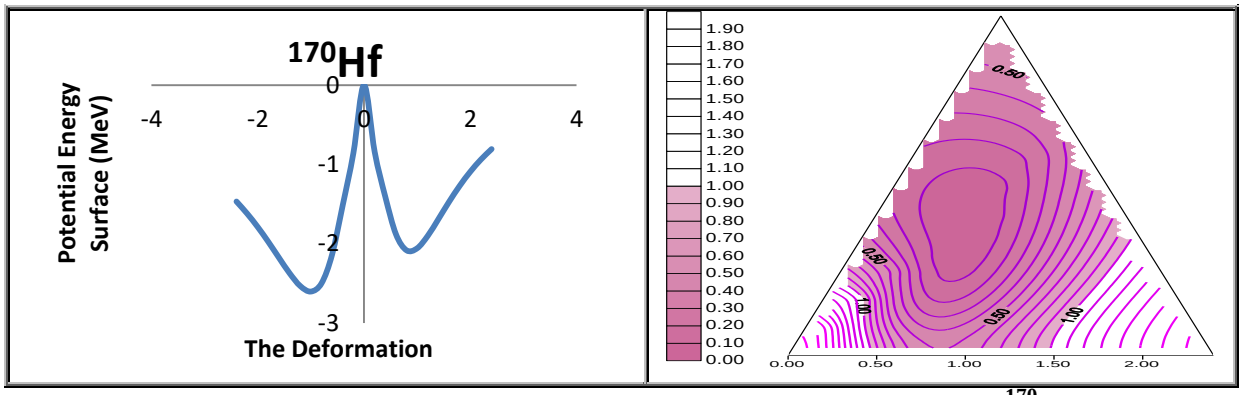

Figure (3.44) Potential energy surface with the deformation for ^{170}Hf.

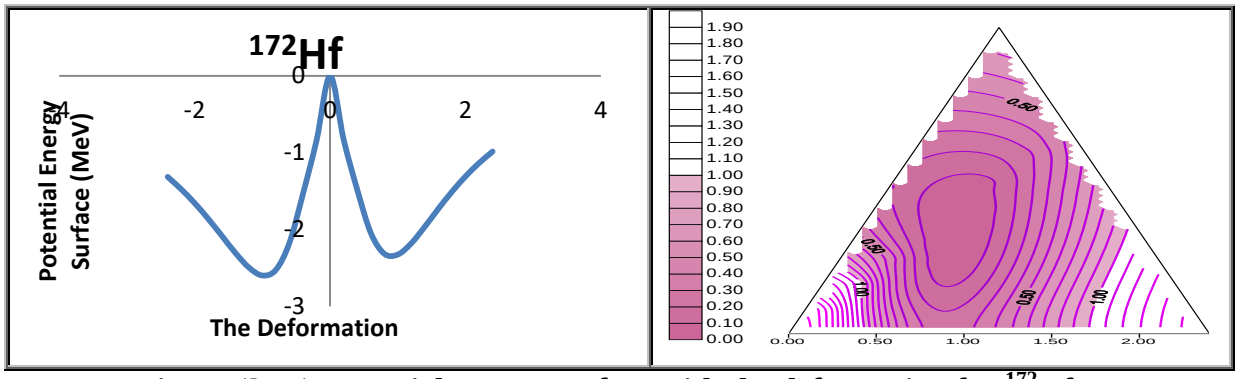

Figure (3.45) Potential energy surface with the deformation for ^{172}Hf.

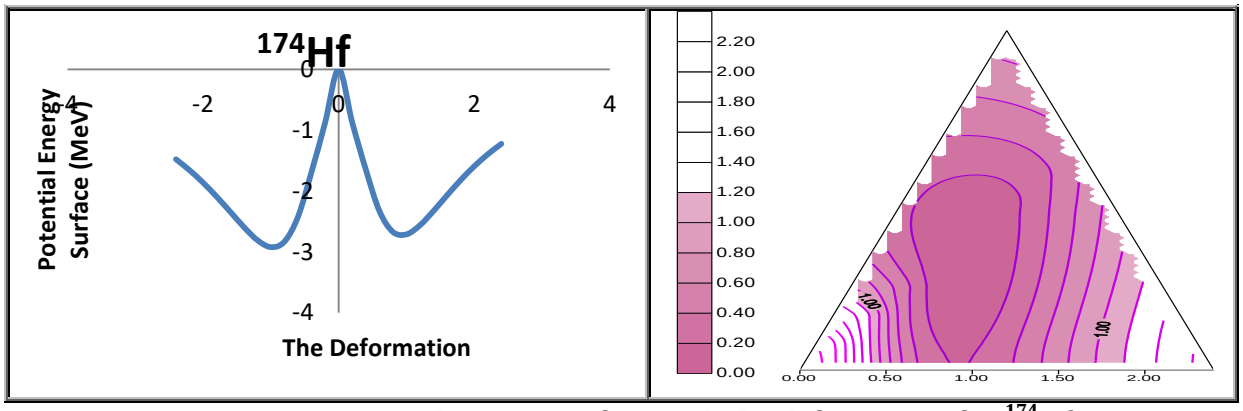

Figure (3.46) Potential energy surface with the deformation for ^{174}Hf.

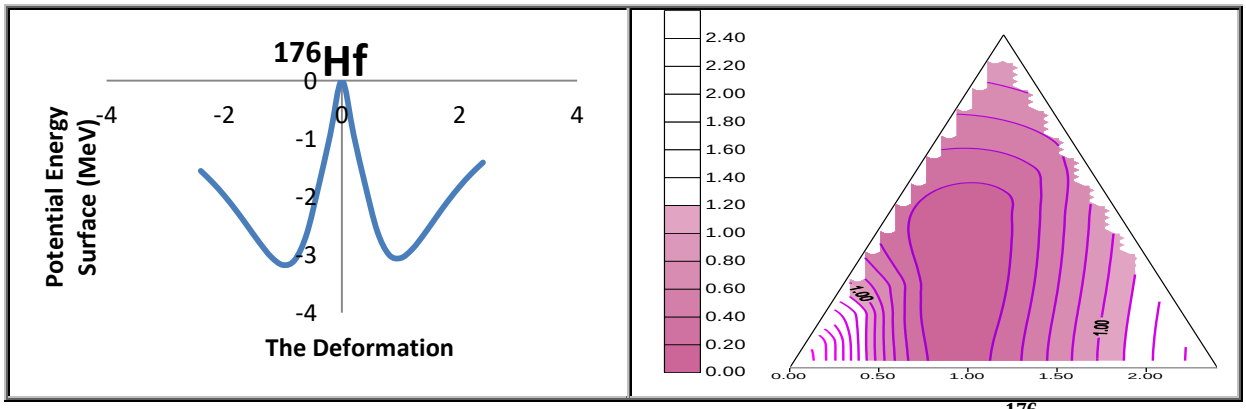

Figure (3.47) Potential energy surface with the deformation for ^{176}Hf.

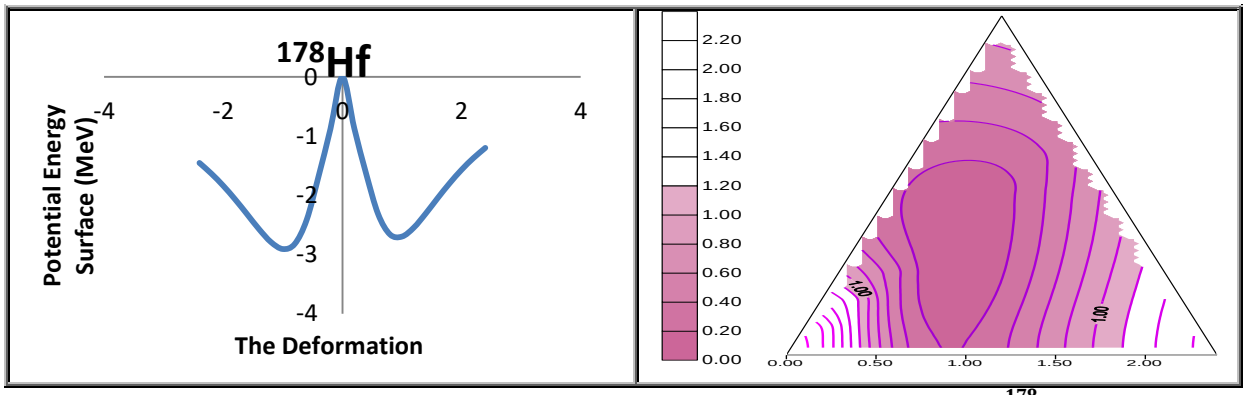

Figure (3.48) Potential energy surface with the deformation for ^{178}Hf.

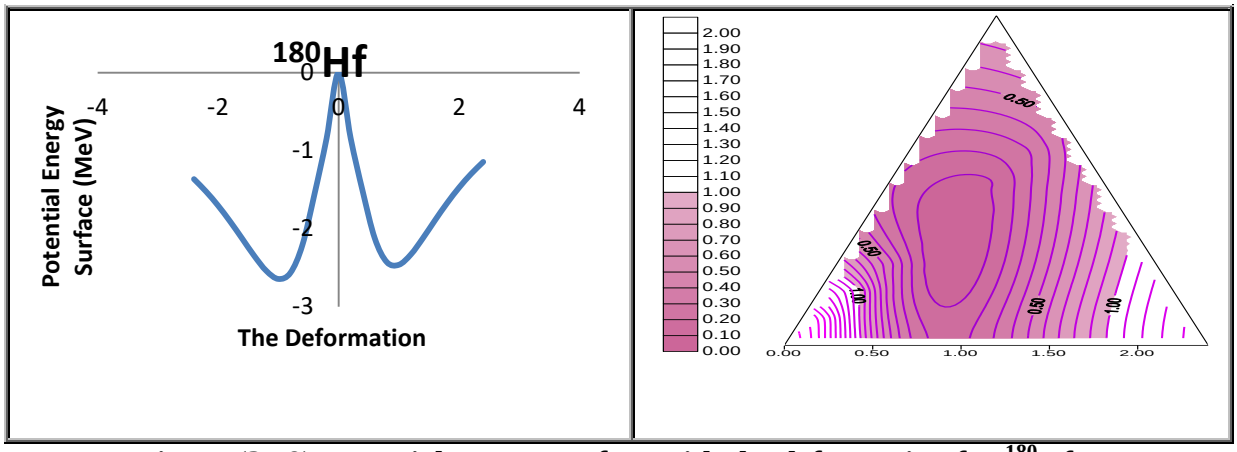

Figure (3.49) Potential energy surface with the deformation for ^{180}Hf.

3.2.8 Mixed Symmetry States (MSS)

The effect of Majorana parameters ($\zeta_{1,3}$, ζ_2) on the calculated excitation energy level for $^{166\text{-}180}$Hf isotopes studied, the value of $\zeta_{1,3}$ vary between (0.14-0.18) and the value of ζ_2 fixed on (0.07) for all isotopes then vary this value between (0.05-0.1) around the best-fitted data. It is found that the energy values for the states $(2_3^+, 2_4^+, 2_5^+, 3_1^+, 5_1^+)$ are responded rapidly to the changes of the ζ_2 parameters in some isotopes only and therefore these states verify the first property of the mixed symmetry state (MSS). Figure (3.50) describes the energy variation of these states as a function of the Majorana parameter ζ_2.

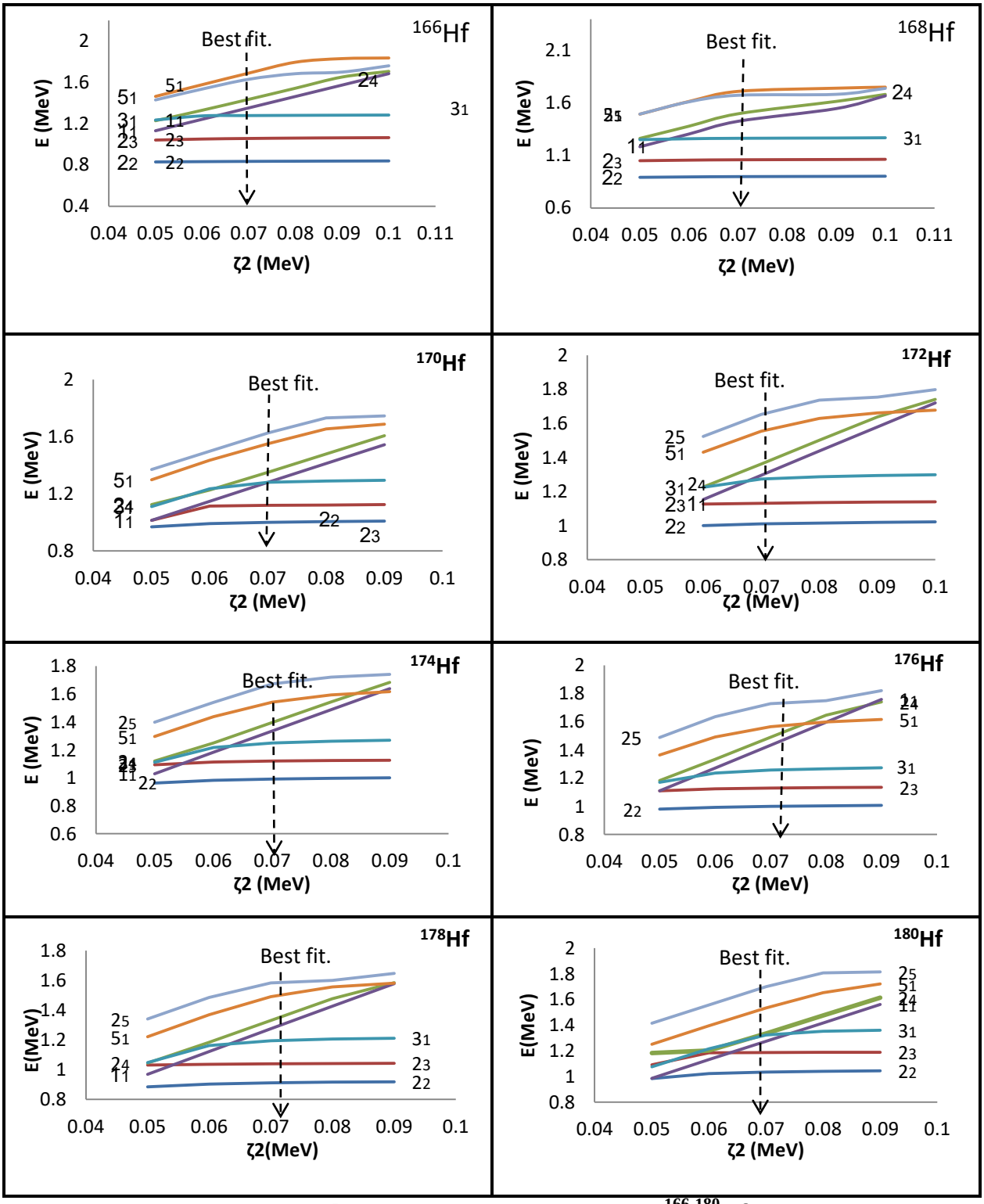

Figure (3.50) Mixed symmetry states in even-even $^{166-180}$Hf isotopes.

3.3 Tungsten Isotopes (W)

Tungsten or wolfram, is a chemical element with the symbol W and atomic number 74. Tungsten is a rare metal found naturally on Earth almost

exclusively as compounds with other elements. It was identified as a new element in 1781 and first isolated as a metal in 1783 [108].

The free element is remarkable for its robustness, especially the fact that it has the highest melting point of all the elements discovered except carbon (which sublimes at normal pressure), melting at 3422 °C (6192 °F; 3695 K). It also has the highest boiling point, at 5930 °C (10710 °F; 6200 K) [109]. Its density is 19.25 grams per cubic centimeter, comparable with that of uranium(19.1 grams per cubic centimeter) and gold (19.3 grams per cubic centimeter), and much higher (about 1.7 times) than that of lead(11.34 grams per cubic centimeter) [110]. Polycrystalline Tungsten is an intrinsically brittle and hard material making it difficult to work. However, pure single-crystalline Tungsten is more ductile and can be cut with a hard-steel hacksaw [111, 112].

Approximately half of the Tungsten is consumed for the production of hard materials (namely Tungsten carbide) with the remaining major use being in alloys and steels. Less than 10% is used in other chemical compounds [113]. Because of the high ductile-brittle transition temperature of Tungsten, its products are conventionally manufactured through powder metallurgy, spark plasma sintering, chemical vapor deposition, hot isostatic pressing, and thermoplastic routes. A more flexible manufacturing alternative is selective laser melting, which is a form of 3D printing and allows the creation of complex three-dimensional shapes [114].

Tungsten occurs in many alloys, which have numerous applications, including incandescent light bulb filaments, X-ray tubes, electrodes in gas Tungsten arc welding, super alloys, and radiation shielding. Tungsten's hardness and high density make it suitable for military applications in penetrating projectiles. Tungsten compounds are often used as industrial catalysts.

Tungsten is the only metal in the third transition series that is known to occur in biomolecules, being found in a few species of bacteria and archaea. However, Tungsten interferes with molybdenum and copper metabolism and is somewhat toxic to most forms of animal life [115, 116].

3.3.1 Energy Level Calculations

The software package IBM-1 computer code for neutron proton boson (NPBOS) code for IBM-2 have been used to calculate energy levels for $^{170\text{-}184}$W by estimating a set of parameters described in the Hamiltonian operator as it is shown in Equations (2.2) and (2.63) parameters estimated for the low- lying calculations of the excited energy levels for Tungsten isotopes are given in Tables (3.19) and (3.20), the symbol (*) refers to hole boson, these parameters represented in Figures (3.51) and (3.52).

Table (3.19) Parameters used in the IBM-1 Hamiltonian for even-even $^{170\text{-}184}$W isotopes (in MeV).

Isotops	N	Ɛ	a_0	a_1	a_2	a_3	a_4	x
$^{170}_{74}W_{96}$	11	0	0.0108	0.01558	-0.0276	0	0	-0.525
$^{172}_{74}W_{98}$	12	0	0.0102	0.01099	-0.0238	0	0	-1.097
$^{174}_{74}W_{100}$	13	0	0.018	0.0114	-0.0238	0	0	-1.269
$^{176}_{74}W_{102}$	14	0	0.022	0.0103	-0.0245	0	0	-1.255
$^{178}_{74}W_{104}$	15	0	0.098	0.0122	-0.0168	0	0	-0.849
$^{180}_{74}W_{106}$	14*	0	0.0162	0.0108	-0.0211	0	0	-0.508
$^{182}_{74}W_{108}$	13*	0	0.0146	0.0102	-0.0199	0	0	-0.268
$^{184}_{74}W_{110}$	12*	0	0.0158	0.01078	-0.0241	0	0	-1.2699

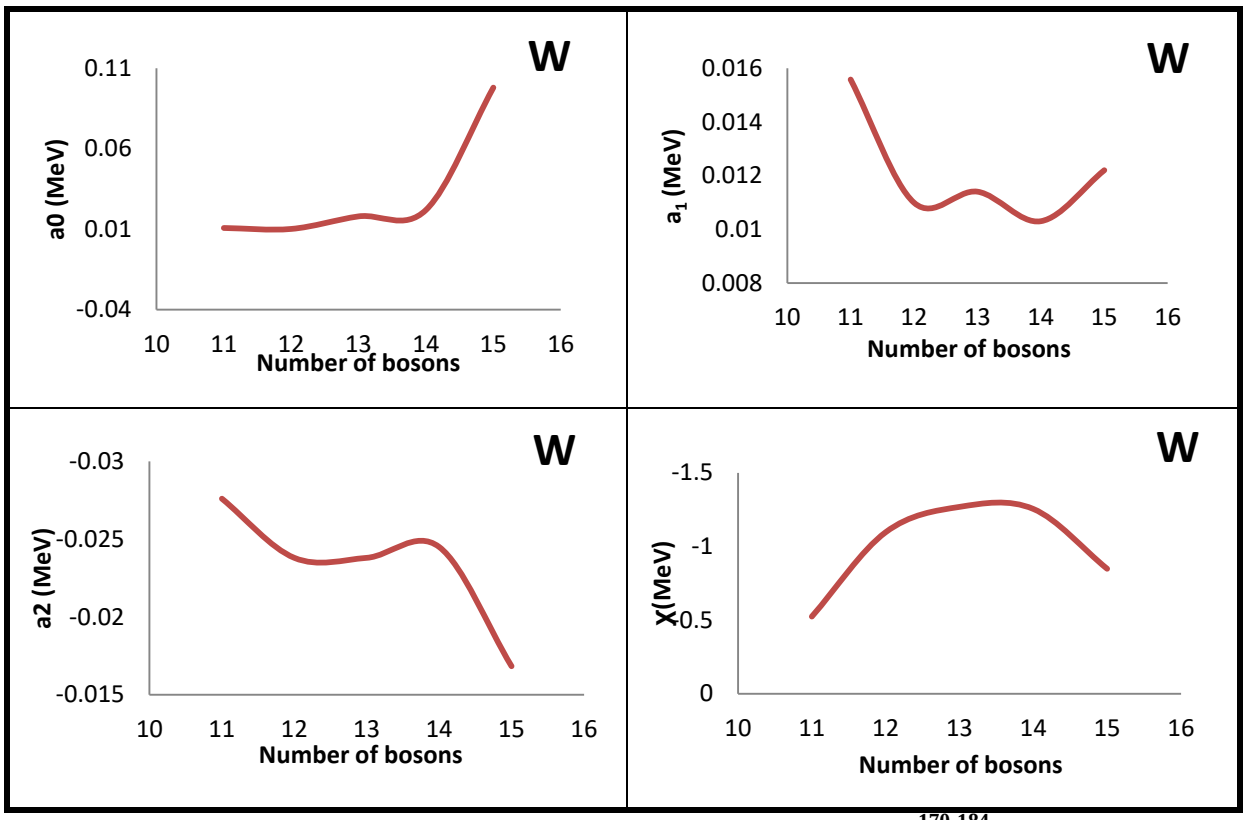

Figure (3.51) IBM-1 parameters (χ, a_0, a_1, a_2) for $^{170\text{-}184}$W isotopes as a function of the number of bosons.

Table (3.20) Parameters used in the IBM-2 Hamiltonian for even– even $^{170\text{-}184}$W isotopes (in MeV) except $\chi\nu$ and $\chi\pi$ without units, Nπ=4.

Isotops	N_υ	Ɛ	Ƙ	X_υ	X_π	$\zeta_{1=3}$	ζ_2	C^L_υ			C^L_π		
$^{170}_{74}W_{96}$	7	0.39	-0.064	-0.9018	-0.9	0.11	0.1	-0.34	0.24	0.15	1.8	0.37	0.36
$^{172}_{74}W_{98}$	8	0.31	-0.061	-0.9021	-0.9	0.11	0.1	-0.32	0.25	0.14	1.4	0.37	0.21
$^{174}_{74}W_{100}$	9	0.28	-0.063	-0.902	-0.9	0.12	0.1	-0.33	0.26	0.13	1.3	0.34	0.18
$^{176}_{74}W_{102}$	10	0.27	-0.064	-0.9021	-0.9	0.13	0.1	-0.32	0.27	0.12	1.2	0.315	0.145
$^{178}_{74}W_{104}$	11	0.23	-0.066	-0.9023	-0.9	0.13	0.1	-0.24	0.23	0.16	1.6	0.37	0.24
$^{180}_{74}W_{106}$	10*	0.228	-0.064	-0.9023	-0.9	0.15	0.1	-0.24	0.25	0.16	1.62	0.35	0.23
$^{182}_{74}W_{108}$	9*	0.225	-0.065	-0.9026	-0.9	0.14	0.1	-0.24	0.24	0.16	1.6	0.34	0.22
$^{184}_{74}W_{110}$	8*	0.242	-0.068	-0.902	-0.9	0.14	0.1	-0.27	0.26	0.21	1.8	0.36	0.24

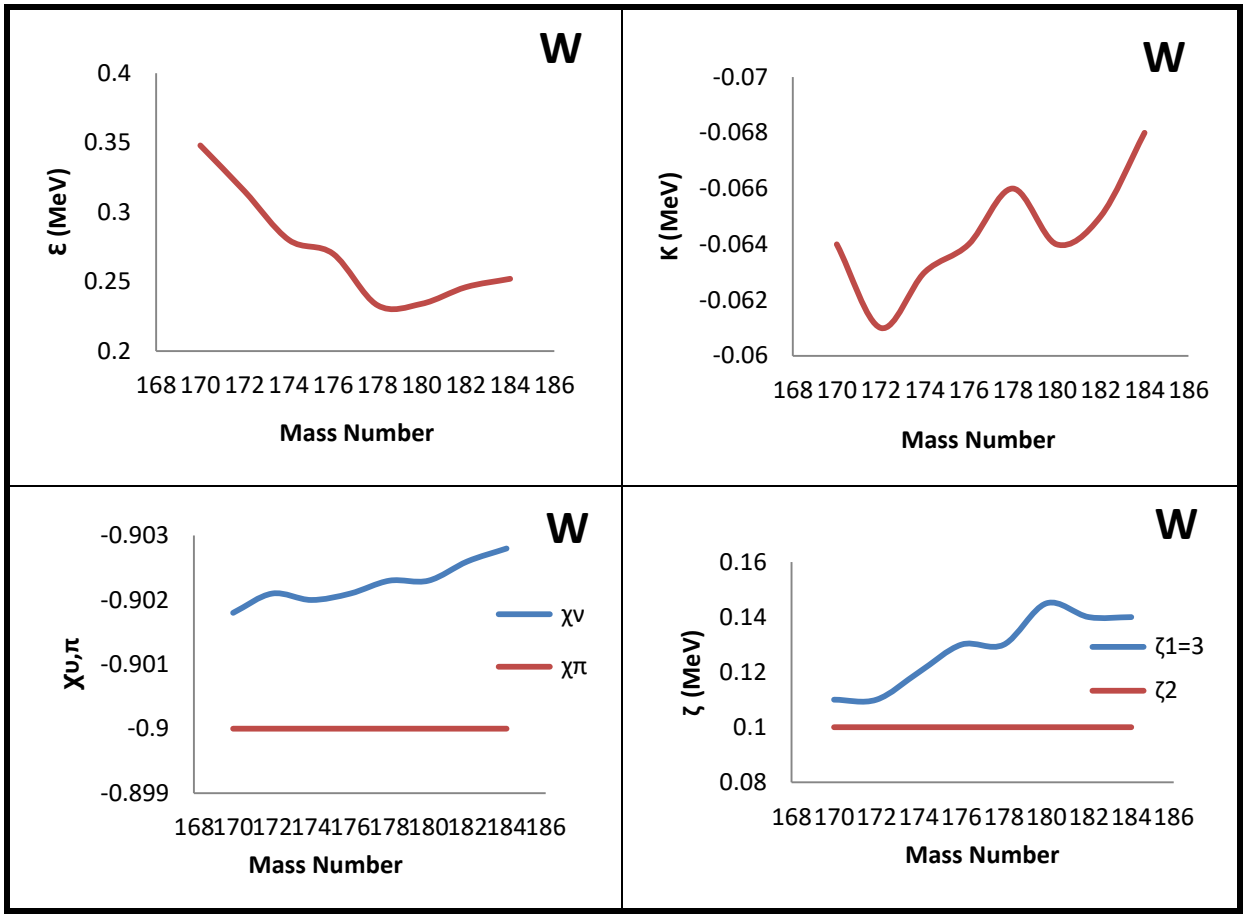

Figure (3.52) IBM-2 parameters (ε, κ, χ_π, χ_ν, ζ_2, $\zeta_{1,3}$) for $^{170\text{-}184}$W isotopes as a function of the mass number.

The calculated energy levels by IBM-1 and IBM-2 compared with the experimental data [99-106] for $^{170\text{-}184}$W isotopes have been shown in Figures from (3.53) to (3.60).

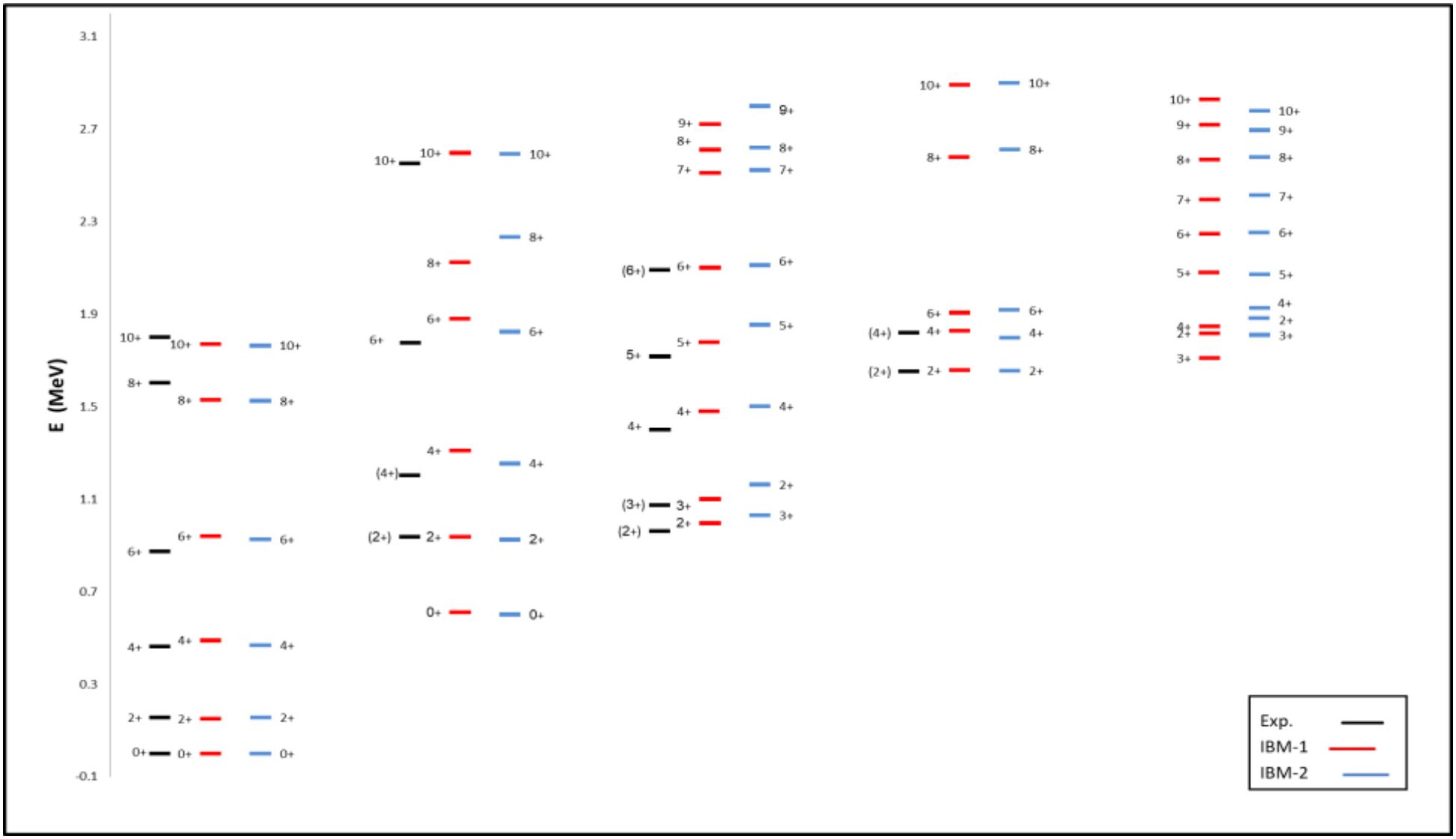

Figure (3.53) Energy levels for ^{170}W.

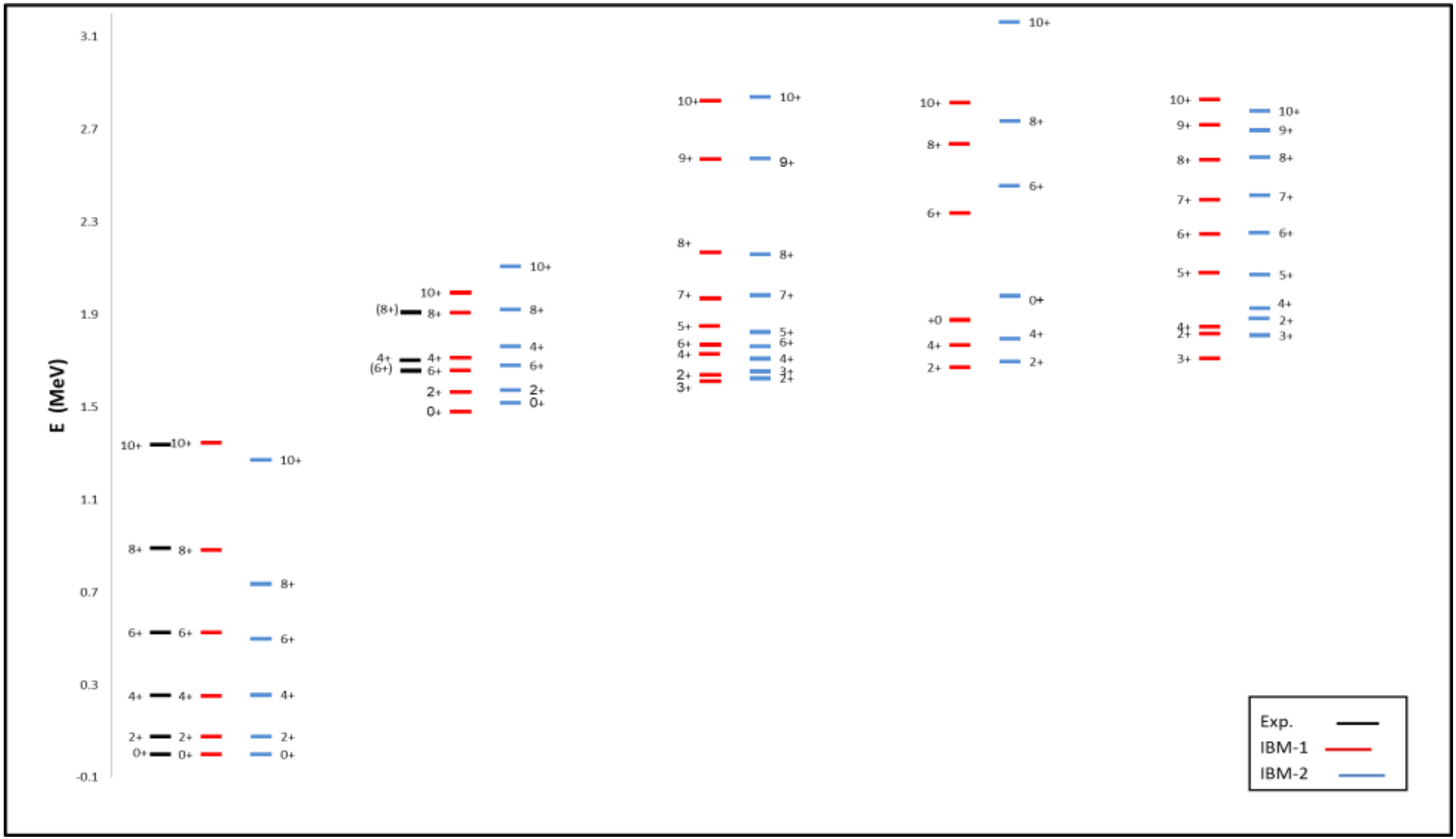

Figure (3.54) Energy levels for ^{172}W.

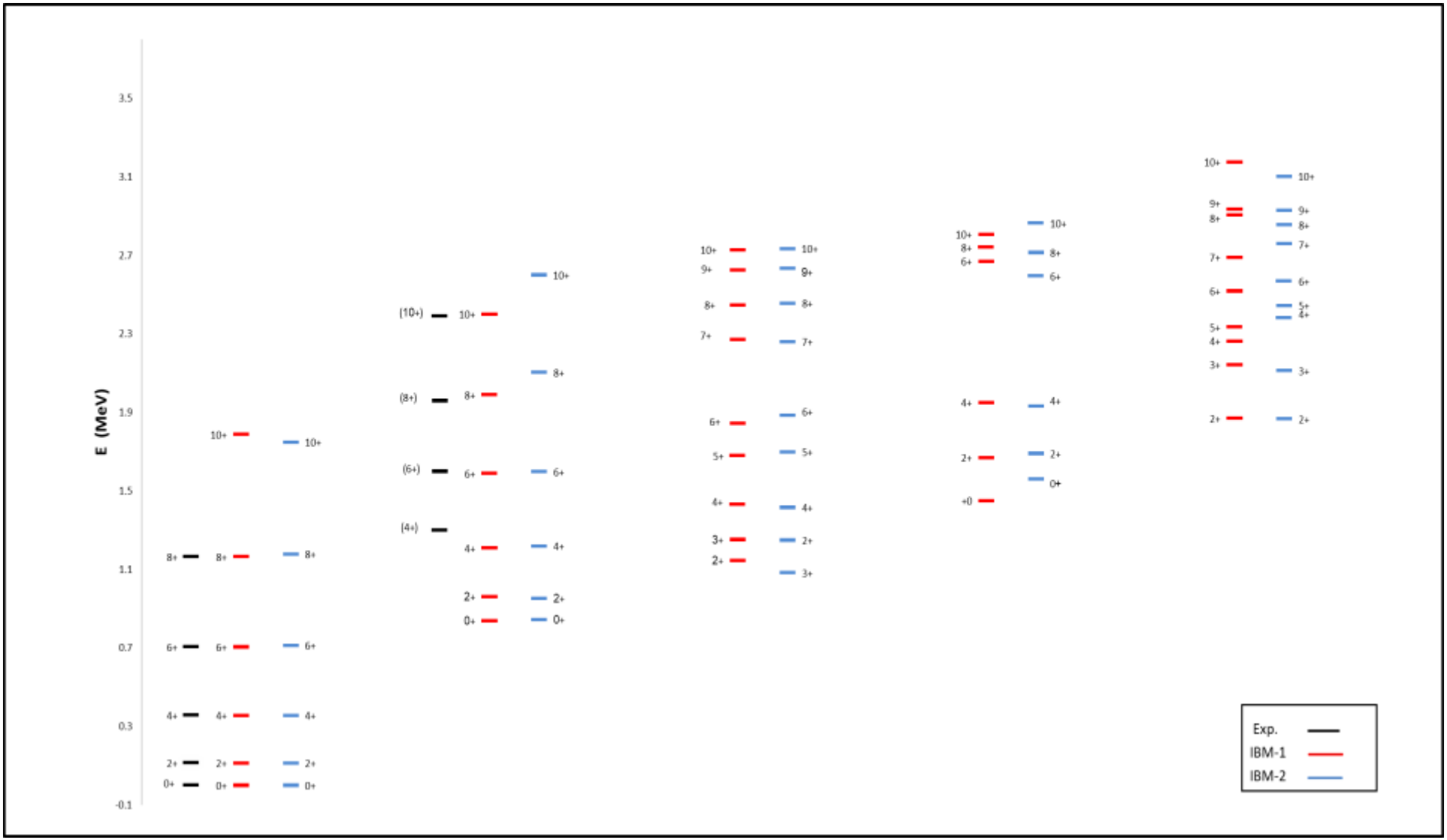

Figure (3.55) Energy levels for ^{174}W.

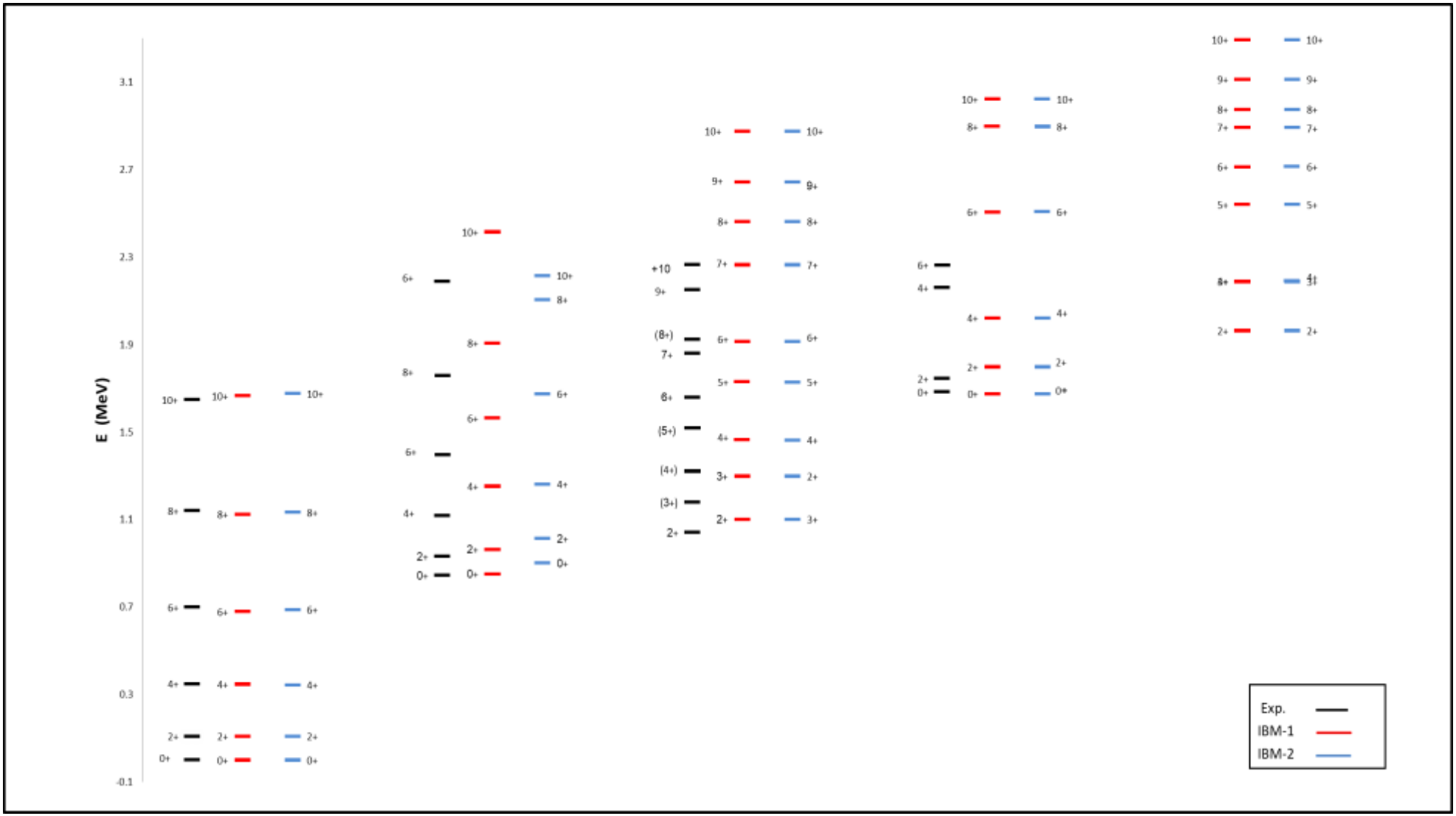

Figure (3.56) Energy levels for ^{176}W.

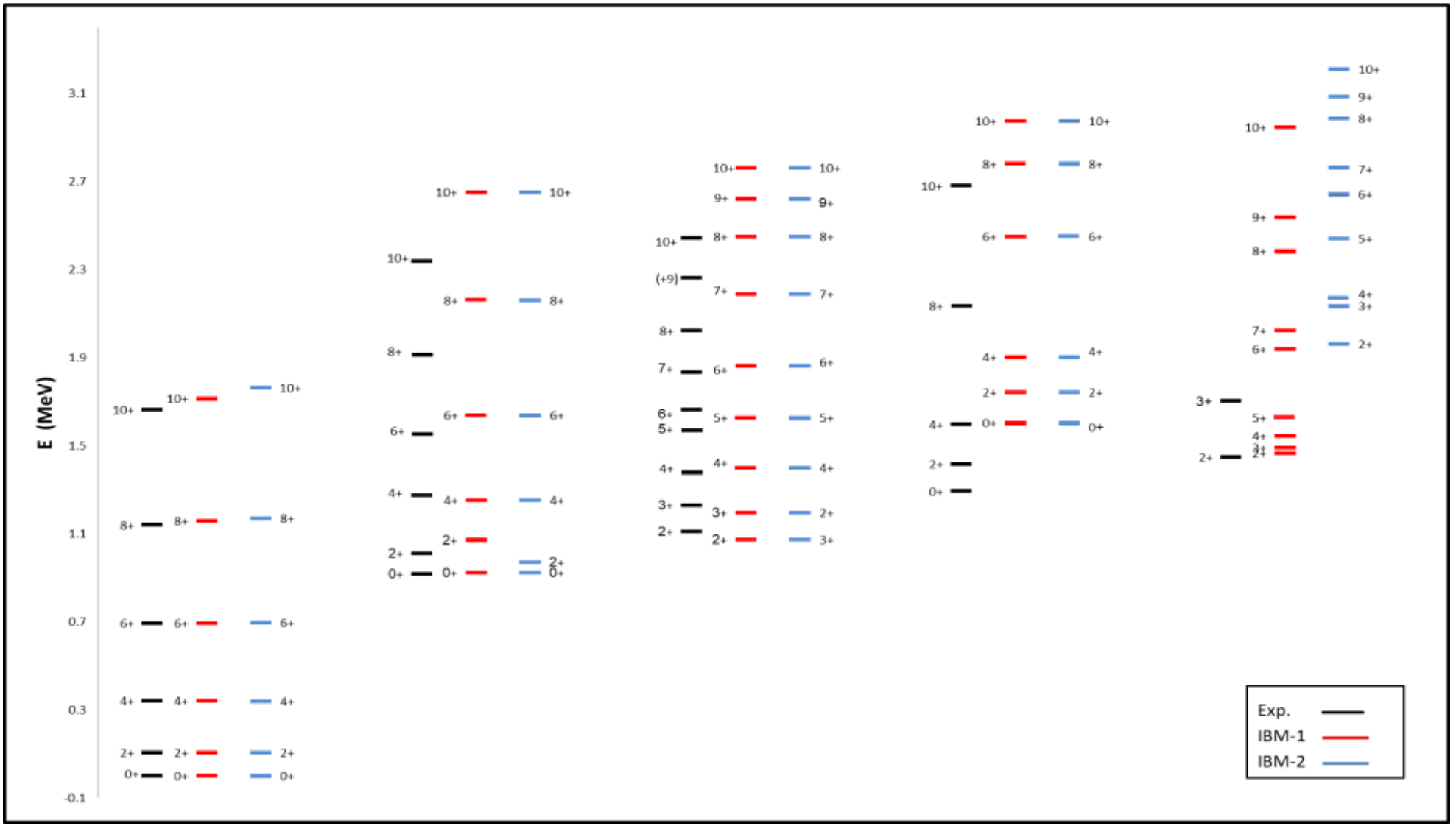

Figure (3.57) Energy levels for ^{178}W.

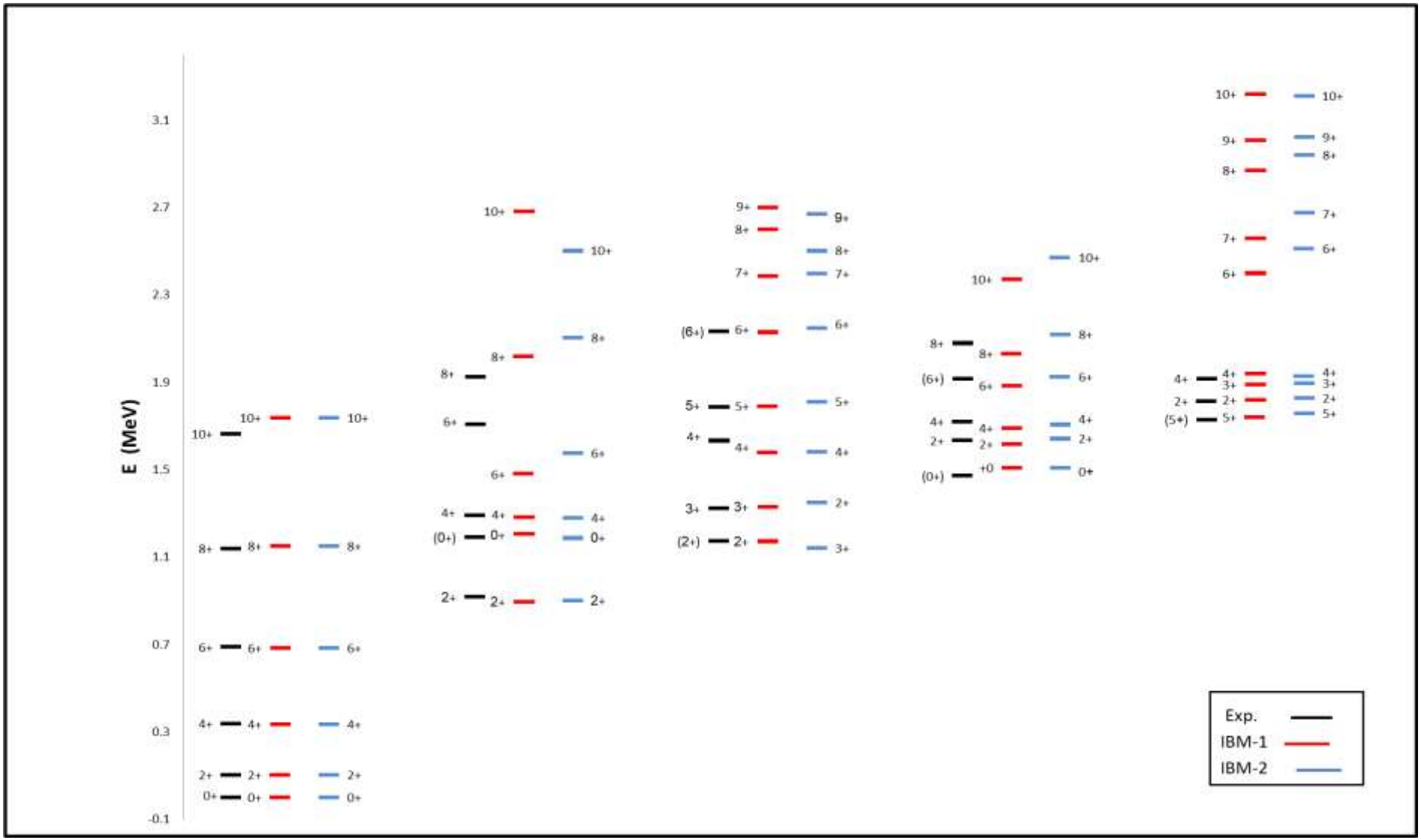

Figure (3.58) Energy levels for ^{180}W.

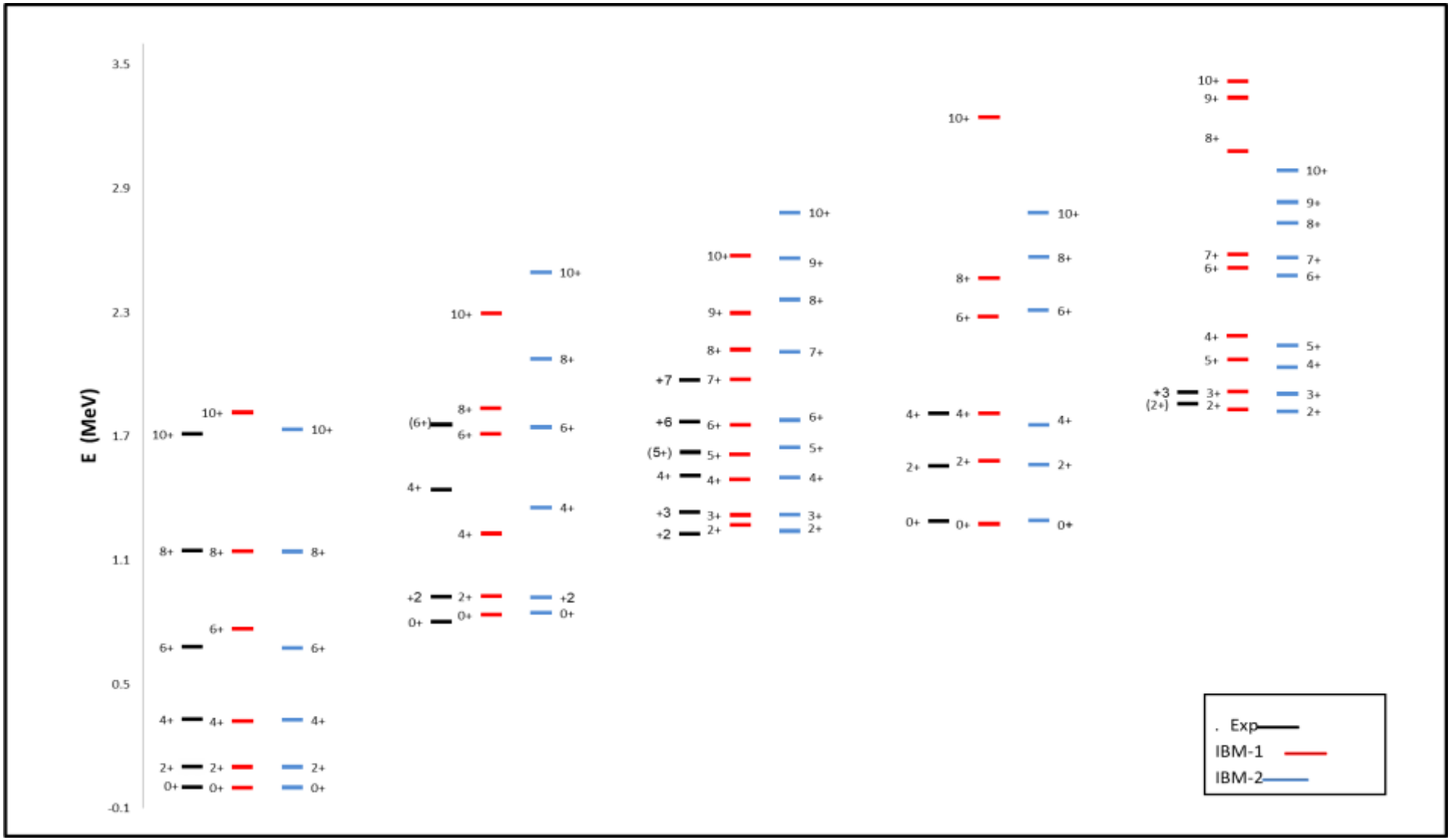

Figure (3.59) Energy levels for ^{182}W.

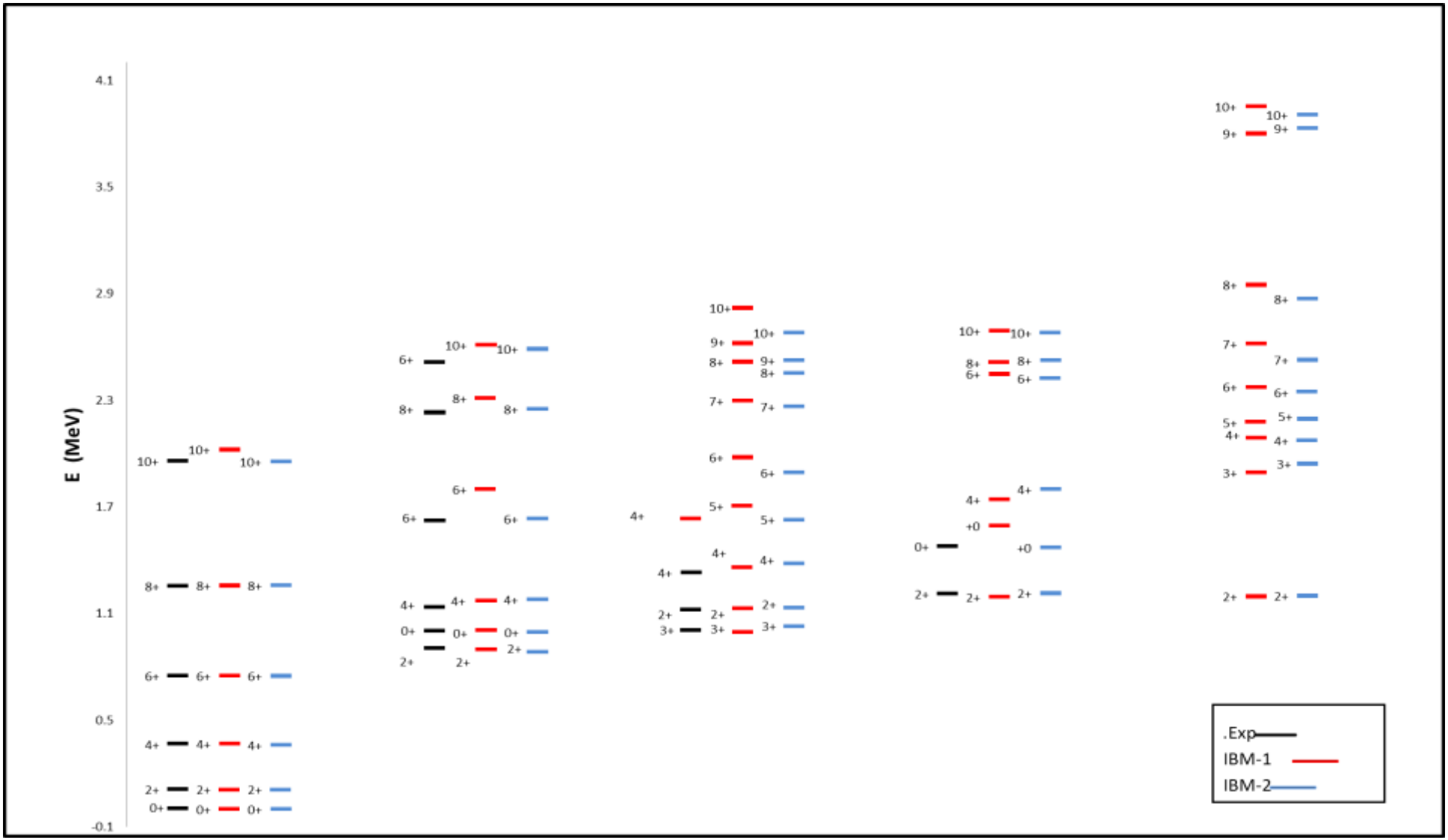

Figure (3.60) Energy levels for ^{184}W.

3.3.2. Energy Ratios

Calculating the energy ratios is one of the tests that are performed for each isotope to find out its position in the Casten triangle by comparing it with the ideal ratios in Table (2.1).

This calculation of dynamic symmetries by IBM-1, IBM-2 and experimental energy levels and after a comparison with the standard values for the energy ratios of ($E0_2^+/E2_1^+$, $E4_1^+/E2_1^+$, $E6_1^+/E2_1^+$ and $E8_2^+/E2_1^+$) ratios for all studied isotopes have been indicated in Figures (3.61) to (3.64). This leads to guessing the nearest dynamic symmetries corresponding to the characteristics of one of the dynamic symmetries or may possess transitional features between two or more symmetries so from studying Table (3.21), it is found that the calculated energy ratios in the rotational region SU(3) for all Tungsten isotopes except ^{170}W isotope which in transitional region O(6)→ SU(3). There is a good agreement between experimental data and the IBM-1 and IIBM-2 results appear clearly in the Table and Figures below.

Table (3.21) Energy ratios for $^{170\text{-}184}$W isotopes.

Isotopes	Energy ratios											
	$E0_2^+/E2_1^+$			$E4_1^+/E2_1^+$			$E6_1^+/E2_1^+$			$E8_1^+/E2_1^+$		
	Exp. [99-106]	IBM-1	IBM-2	Exp. [99-106]	IBM-1	IBM-2	Exp. [99-106]	IBM-1	IBM-2	Exp. [99-106]	IBM-1	IBM-2
$^{170}_{74}W_{96}$	___	4.14	6.25	2.95	3.32	3.00	5.58	6.96	5.93	8.69	11.90	9.76
$^{172}_{74}W_{98}$	___	9.25	7.43	3.06	3.34	3.07	5.90	7.03	6.12	9.30	12.07	10.11
$^{174}_{74}W_{100}$	___	15.30	8.27	3.15	3.33	3.13	6.24	7.01	6.28	10.07	12.05	10.38
$^{176}_{74}W_{102}$	7.80	8.12	8.78	3.21	3.33	3.15	6.45	7.01	6.31	10.52	12.05	10.41
$^{178}_{74}W_{104}$	9.49	9.49	8.3	3.23	3.33	3.23	6.55	7.01	6.62	10.77	12.02	11.12
$^{180}_{74}W_{106}$	13.33	12.15	8.37	3.25	3.33	3.21	6.64	7.00	6.58	10.99	12.00	11.08
$^{182}_{74}W_{108}$	11.35	8.37	7.65	3.29	3.31	3.24	6.79	6.90	6.69	11.43	11.75	11.32
$^{184}_{74}W_{110}$	9.02	15.00	7.62	3.27	3.33	3.26	6.72	7.01	6.77	11.25	12.05	11.56

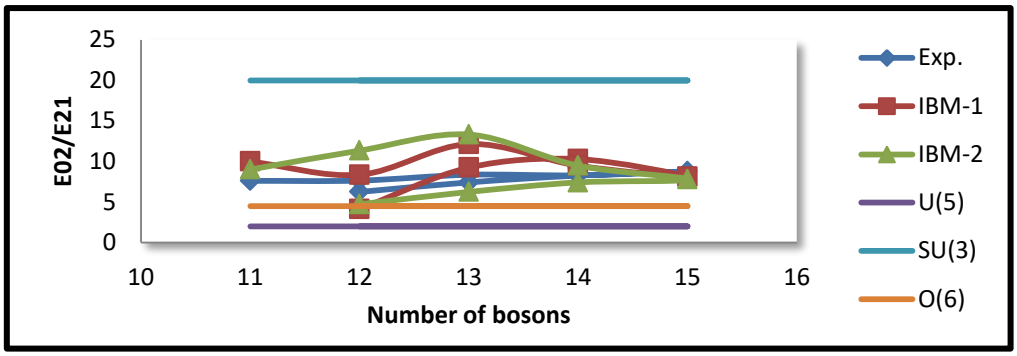

Figure (3.61) The experimental [99-106], theoretical and standard energy ratios ($E0_2^+/E2_1^+$), as a function of bosons numbers for even-even $^{170-184}$W isotopes.

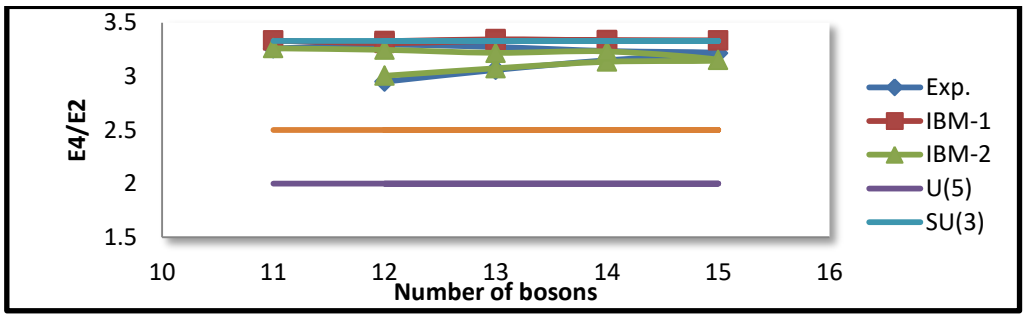

Figure (3.62) The experimental [99-106], theoretical and standard energy ratios ($E4_1^+/E2_1^+$), as a function of bosons numbers for even-even $^{170-184}$W isotopes.

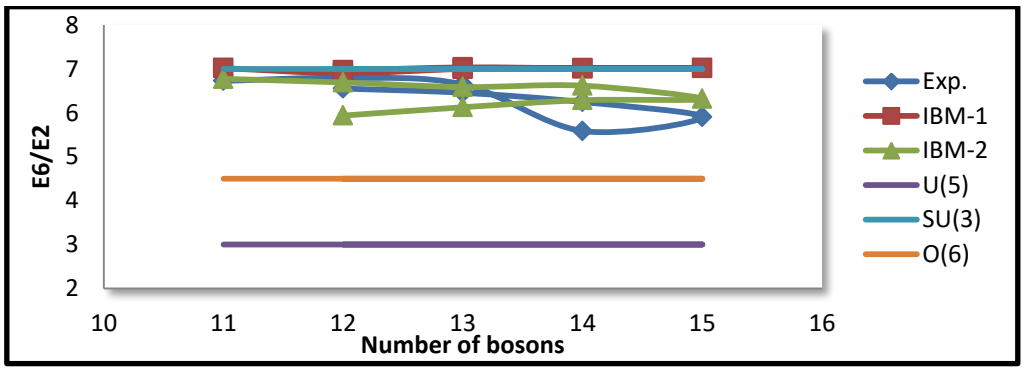

Figure (3.63) The experimental [99-106], theoretical and standard energy ratios ($E6_1^+/E2_1^+$), as a function of bosons numbers for even-even $^{170-184}$W isotopes.

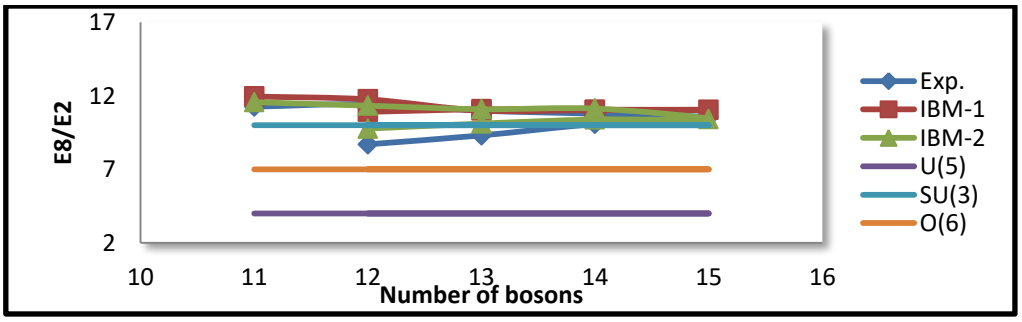

Figure (3.64) The experimental [99-106], theoretical and standard energy ratios ($E8_1^+/E2_1^+$), as a function of bosons numbers for even-even $^{170-184}$W isotopes.

Where observed that there is an acceptable agreement between theoretical calculation and available experimental values due to the strength of B(E2) values for each transition, which reflects the extent of deformation of these isotopes, which in turn affects the position of energy levels and finally affects on the B(E2) values and branching ratios between them.

3.3.3. Reduced Electric Quadruple Transitions Probability and Quadruple Momentum

The reduced electric quadrupole transition probability B(E2) is considered one of the most important properties of the nuclear structure, it can be found in the type of the dynamic symmetries for the nuclei through some transitions that occur between the energy levels for these nuclei.

In IBM-1 the reduced electric transition probability values for $^{170\text{-}184}$W isotopes can be calculated by calculating the values of effective charge e_b= E2SD and β_2 =E2DD from Equations (2.29) by using the experimental value of $B(E2;2_1^+ \rightarrow 0_1^+)$ [99-106], these values are put into a Table (3.22).

In IBM-2 effective charge for neutron (e_ν) and for proton (e_π) must be calculated by using Equations (2.72) to find the reduced electric transition probability. In this work, it found that the neutron's effective charge e_ν = 0.397(eb) and the proton's effective charge e_π = 0.012 (eb). The effective charges depend on the total bosons number N_ρ and the ratios between N_ν/N_π, these parameters are free and can take any value to fit the experimental data.

Table (3.22) The coefficients (E2SD, E2DD) for $^{170\text{-}184}$W.

Isotopes	Number of bosons	$B(E2;2_1^+ \to 0_1^+)$ e^2b^2 [99-106]	E2SD(eb)	E2DD(eb)
$^{170}_{74}W_{96}$	11	0.712	0.1076	-0.3184
$^{172}_{74}W_{98}$	12	1.17	0.1176	-0.348
$^{174}_{74}W_{100}$	13	0.684	0.08069	-0.238
$^{176}_{74}W_{102}$	14	0.808	0.082	-0.244
$^{178}_{74}W_{104}$	15	0.828	0.682	-0.242
$^{180}_{74}W_{106}$	14*	0.828	0.0914	-0.270
$^{182}_{74}W_{108}$	13*	0.835	0.104	-0.308
$^{184}_{74}W_{110}$	12*	0.68	0.087	-0.257

Table (3.23) shows a comparison between B(E2) calculated by IBM-1, IBM-2 and experimental data. The values are acceptable in comparison and they have a good systematic.

Table (3.23) B(E2) values for $^{170\text{-}184}$W isotopes .

B(E2) (e^2b^2)									
Isotopes	^{170}W			^{172}W			^{174}W		
$J_i^+ \to J_f^+$	Exp. [99]	IBM-1	IBM-2	Exp. [100]	IBM-1	IBM-2	Exp. [101]	IBM-1	IBM-2
$2_1 \to 0_1$	0.712	0.710	0.713	1.170	1.178	1.180	0.684	0.685	0.679
$2_1 \to 0_2$	----	0.026	0.017	----	0.031	0.012	----	0.014	0.008
$2_1 \to 2_2$	----	0.021	0.153	----	0.045	0.103	----	0.024	0.061
$2_1 \to 2_3$	----	0.034	0.008	----	0.038	0.011	----	0.017	0.024
$4_1 \to 2_1$	1.002	0.947	1.021	1.393	1.603	1.138	1.357	0.911	1.217
$2_2 \to 2_3$	----	0.003	0.391	----	0.005	0.645	----	0.004	0.934
$2_2 \to 2_4$	----	0.012	0.013	----	0.016	0.018	----	0.037	0.034
$2_4 \to 0_1$	----	0.001	0.001	----	0.004	0.044	----	0.0001	----
$4_3 \to 2_1$	----	0.002	0.331	----	0.002	0.004	----	0.001	0.002
$4_3 \to 2_3$	----	0.562	0.291	----	1.303	0.019	----	0.760	0.014
$4_2 \to 2_2$	----	0.222	0.540	----	0.452	0.631	----	0.269	0.820
$6_1 \to 4_1$	1.058	-----	1.124	1.478	-----	1.236	2.367	-----	1.316
$8_1 \to 6_1$	1.063	-----	1.159	1.649	-----	1.261	1.386	-----	1.336
$Q_{2_1^+}$ (eb)	0.951	2.339	0.905		2.966	1.068		2.220	1.176

B(E2) (e^2b^2)									
Isotopes	^{176}**W**			^{178}**W**			^{180}**W**		
$J_i^+ \rightarrow J_f^+$	**Exp. [102]**	**IBM-1**	**IBM-2**	**Exp. [103]**	**IBM-1**	**IBM-2**	**Exp. [104]**	**IBM-1**	**IBM-2**
$2_1 \rightarrow 0_1$	0.808	0.809	0.817	0.828	0.826	0.852	0.680	0.666	0.683
$2_1 \rightarrow 0_2$	-----	0.015	0.006	-----	0.019	0.082	-----	0.019	0.007
$2_1 \rightarrow 2_2$	-----	0.027	0.042	-----	0.022	0.067	-----	0.019	0.081
$2_1 \rightarrow 2_3$	-----	0.020	0.030	-----	0.025	0.001	-----	0.025	----
$4_1 \rightarrow 2_1$	-----	1.113	1.262	-----	1.151	1.204	-----	1.123	1.171
$2_2 \rightarrow 2_3$	-----	0.004	0.896	-----	0.001	0.377	-----	0.001	0.301
$2_2 \rightarrow 2_4$	-----	0.046	0.043	-----	0.052	----	-----	0.012	0.001
$2_4 \rightarrow 0_1$	-----	0.0001	----	-----	0.0001	----	-----	0.001	----
$4_3 \rightarrow 2_1$	-----	0.001	0.001	-----	0.002	0.007	-----	0.003	0.009
$4_3 \rightarrow 2_3$	-----	0.942	0.012	-----	0.970	0.013	-----	0.735	0.014
$4_2 \rightarrow 2_2$	-----	0.338	0.934	-----	0.350	0.531	-----	0.315	0.512
$6_1 \rightarrow 4_1$	-----	-----	1.364	-----	-----	1.299	-----	-----	1.262
$8_1 \rightarrow 6_1$	-----	-----	1.386	-----	-----	1.319	-----	-----	1.279
$Q_{2_1^+}$ (eb)	-----	2.443	1.232	-----	2.490	1.204	-----	2.491	1.143

B(E2) (e^2b^2)						
Isotopes	^{182}**W**			^{184}**W**		
$J_i^+ \rightarrow J_f^+$	**Exp. [105]**	**IBM-1**	**IBM-2**	**Exp. [106]**	**IBM-1**	**IBM-2**
$2_1 \rightarrow 0_1$	0.834	0.834	0.758	0.68	0.666	0.704
$2_1 \rightarrow 0_2$	----	0.018	0.008	----	0.015	0.010
$2_1 \rightarrow 2_2$	----	0.015	0.083	----	0.027	0.101
$2_1 \rightarrow 2_3$	----	0.022	----	----	0.019	----
$4_1 \rightarrow 2_1$	1.201	1.117	1.163	1.032	0.909	1.118
$2_2 \rightarrow 2_3$	0.041	0.048	0.261	----	0.005	0.174
$2_2 \rightarrow 2_4$	----	0.002	0.001	----	0.006	0.001
$2_4 \rightarrow 0_1$	----	0.002	0.001	----	0.0003	0.002
$4_3 \rightarrow 2_1$	----	0.0002	0.011	----	0.001	0.017
$4_3 \rightarrow 2_3$	----	0.009	0.013	----	0.745	0.014
$4_2 \rightarrow 2_2$	----	0.251	0.503	----	0.260	0.485
$6_1 \rightarrow 4_1$	1.232	-----	1.249	1.126	-----	1.200
$8_1 \rightarrow 6_1$	1.281	-----	1.259	1.151	-----	1.209
$Q_{2_1^+}$ (eb)		2.543	1.139	1.393	2.227	1.077

3.3.4. Branching Ratio

One of the important properties which can be calculated is the branching ratios, through which one can identify the position of the nuclei studied in the Casten triangle, and hence identify the dynamic symmetry for the nuclei by using the Equations (2.24)-(2.26), (2.38- 2.40) and (2.53).

Table (3.24) shows the branching ratios for all studied Tungsten isotopes. Where observed that there is an acceptable agreement between theoretical calculation and available experimental values due to the strength of B(E2) values for each transition, which reflects the extent of deformation of these isotopes, which in turn affects the position of energy levels and finally affects on the B(E2) values and branching ratios between them.

Table (3.24) Branching ratios for $^{170\text{-}184}$W isotopes.

Isotopes	Branching ratios								
	R			R′			R″		
	Exp. [99-106]	IBM-1	IBM-2	Exp.	IBM-1	IBM-2	Exp.	IBM-1	IBM-2
$^{170}_{74}W_{96}$	1.44	1.33	1.431	-----	0.095	0.214	-----	0.0074	0.0047
$^{172}_{74}W_{98}$	1.43	1.36	1.169	-----	0.096	0.087	-----	0.0052	0.0020
$^{174}_{74}W_{100}$	1.47	1.37	1.792	-----	0.089	0.089	-----	0.0042	0.0023
$^{176}_{74}W_{102}$	-----	1.37	1.544	-----	0.082	0.51	-----	0.0039	0.0014
$^{178}_{74}W_{104}$	-----	1.37	1.413	-----	0.073	0.078	-----	0.0048	0.0192
$^{180}_{74}W_{106}$	1.412	1.36	1.714	-----	0.075	0.118	-----	0.0047	0.0020
$^{182}_{74}W_{108}$	1.44	1.34	1.534	-----	0.069	0.109	-----	0.0044	0.0021
$^{184}_{74}W_{110}$	1.38	1.36	1.588	-----	0.097	0.014	-----	0.0046	0.0028

3.3.5 Reduced Transitions Probability for Magnetic Dipole and Mixing Ratio

In order to calculate B(M1) transition probability, one should estimate the effective g −factors for proton g_π and neutron g_ν by Equations (2.78). In Tungsten isotopes the g- factor values are g_π= 0.382 (μ_N) and g_ν= 0.397 (μ_N). Equations (2.79) were used to calculate the B(M1) transition probabilities as it is shown in Table (3.25). The calculated values for B(M1) are acceptable to some extent as compared with the available experiments values, where some of the B(M1) values are small compared to the values of the quadrupole transition probabilities because the wavelength of the gamma ray transitions is greater than it is in the magnetic transitions according to Equation (3.1), this Equation shows that the B(M1)transition probability is less than B(E2) transition probability and our results confirm this. The calculation values for these isotopes and mixing ratio δ(E2/M1) have been compared with the available experiments data as shown in Table (3.25).

Table (3.25) The B(M1) transition and mixing ratio for $^{170\text{-}184}$W isotopes.

Isotopes	^{170}W				^{172}W			
	B(M1) (e^2b^2)		δ(E2/M1)		B(M1) (e^2b^2)		δ(E2/M1)	
$J_i^+ \rightarrow J_f^+$	Exp. [99]	IBM-2	Exp. [99]	IBM-2	Exp. [100]	IBM-2	Exp.	IBM-2
$2_1 \rightarrow 2_2$		2.36×10^{-3}		3.19×10^{-7}		3.97×10^{-4}		6.08×10^{-7}
$2_1 \rightarrow 2_3$		5.23×10^{-3}		4.68×10^{-7}		5.17×10^{-3}		1.72×10^{-6}
$2_2 \rightarrow 2_3$		5.23×10^{-2}		4.36×10^{-7}	9.56×10^{-2}	7.89×10^{-3}		3.46×10^{-7}
$2_2 \rightarrow 2_4$		4.71×10^{-2}		2.15×10^{-6}		2.26×10^{-2}		3.55×10^{-6}
$3_1 \rightarrow 2_1$		2.36×10^{-7}		2.36×10^{-7}		3.23×10^{-3}		3.23×10^{-7}
$3_1 \rightarrow 2_2$		5.73×10^{-4}		4.23×10^{-9}		2.36×10^{-5}		2.36×10^{-7}
$4_1 \rightarrow 3_1$		5.53×10^{-5}		3.23×10^{-7}		5.23×10^{-3}		5.13×10^{-9}
$5_1 \rightarrow 4_1$	2.23×10^{-2}	4.67×10^{-4}		4.91×10^{-8}		5.23×10^{-2}		5.26×10^{-7}
$5_1 \rightarrow 4_2$		3.23×10^{-3}		3.93×10^{-7}		4.51×10^{-3}		4.62×10^{-8}

Isotopes	^{174}W				^{176}W			
	B(M1) (e^2b^2)		δ(E2/M1)		B(M1) (e^2b^2)		δ(E2/M1)	
$J_i^+ \rightarrow J_f^+$	Exp. [101]	IBM-2	Exp.	IBM-2	Exp. [102]	IBM-2	Exp.	IBM-2
$2_1 \rightarrow 2_2$		3.83×10^{-7}		4.03×10^{-7}		3.42×10^{-2}		2.23×10^{-7}
$2_1 \rightarrow 2_3$		5.38×10^{-7}		1.03×10^{-6}		5.08×10^{-3}		1.91×10^{-6}
$4_1 \rightarrow 2_1$		9.62×10^{-8}		5.97×10^{-9}	7.89×10^{-4}	6.67×10^{-3}		2.47×10^{-7}
$2_2 \rightarrow 2_4$		1.02×10^{-6}		2.61×10^{-7}		8.84×10^{-4}		2.01×10^{-7}
$2_4 \rightarrow 0_1$		4.65×10^{-7}		2.49×10^{-6}		5.69×10^{-3}		1.96×10^{-6}
$3_1 \rightarrow 2_1$	3.45×10^{-6}	3.19×10^{-7}		1.78×10^{-6}		3.08×10^{-2}		1.32×10^{-6}
$3_1 \rightarrow 2_2$		4.58×10^{-7}		3.46×10^{-7}		4.68×10^{-2}		3.26×10^{-7}
$4_1 \rightarrow 3_1$		4.38×10^{-7}		3.55×10^{-6}		4.36×10^{-4}		3.75×10^{-6}
$5_1 \rightarrow 4_1$		2.25×10^{-6}		3.93×10^{-7}		2.05×10^{-5}		3.23×10^{-7}
$5_1 \rightarrow 4_2$		2.61×10^{-7}		2.22×10^{-7}		2.72×10^{-2}		2.36×10^{-7}
Isotopes	^{178}W				^{180}W			
	B(M1) (e^2b^2)		δ(E2/M1)		B(M1) (e^2b^2)		δ(E2/M1)	
$J_i^+ \rightarrow J_f^+$	Exp. [103]	IBM-2	Exp.	IBM-2	Exp. [104]	IBM-2	Exp.	IBM-2
$2_1 \rightarrow 2_2$		3.59×10^{-7}		6.13×10^{-7}		3.71×10^{-7}		6.99×10^{-7}
$2_1 \rightarrow 2_3$		8.37×10^{-8}		6.38×10^{-5}		2.26×10^{-7}		6.14×10^{-7}
$2_2 \rightarrow 2_3$	1.78×10^{-6}	5.38×10^{-7}		3.51×10^{-7}		4.24×10^{-7}		4.04×10^{-7}
$2_2 \rightarrow 2_4$		1.54×10^{-8}		6.54×10^{-4}		8.37×10^{-8}		1.15×10^{-5}
$3_1 \rightarrow 2_1$		4.87×10^{-7}		6.67×10^{-2}		4.93×10^{-7}		5.44×10^{-7}
$3_1 \rightarrow 2_2$		6.54×10^{-4}		6.55×10^{-4}		6.24×10^{-4}		2.79×10^{-5}
$4_1 \rightarrow 3_1$		6.31×10^{-2}		1.07×10^{-2}		6.67×10^{-2}		3.71×10^{-7}
$5_1 \rightarrow 4_1$		6.49×10^{-4}		3.59×10^{-2}	5.87×10^{-4}	6.65×10^{-4}		2.26×10^{-7}
$5_1 \rightarrow 4_2$		1.37×10^{-2}		3.41×10^{-7}		1.05×10^{-2}		3.51×10^{-7}
Isotopes	^{182}W				^{184}W			
	B(M1) (e^2b^2)		δ(E2/M1)		B(M1) (e^2b^2)		δ(E2/M1)	
$J_i^+ \rightarrow J_f^+$	Exp. [105]	IBM-2	Exp.	IBM-2	Exp.	IBM-2	Exp.	IBM-2
$2_1 \rightarrow 2_2$	6.78×10^{-6}	3.35×10^{-7}		7.86×10^{-7}		2.46×10^{-7}		6.51×10^{-7}
$2_1 \rightarrow 2_3$		5.08×10^{-7}		6.67×10^{-2}		1.27×10^{-6}		2.52×10^{-2}
$2_2 \rightarrow 2_3$		4.16×10^{-7}		5.44×10^{-7}		2.78×10^{-7}		6.58×10^{-7}
$2_2 \rightarrow 2_4$		1.54×10^{-7}		2.79×10^{-5}		4.93×10^{-7}		1.83×10^{-2}
$3_1 \rightarrow 2_1$		4.24×10^{-7}		3.71×10^{-7}		6.54×10^{-4}		3.71×10^{-7}
$3_1 \rightarrow 2_2$		8.37×10^{-8}		2.26×10^{-7}		6.67×10^{-2}		2.26×10^{-7}
$4_1 \rightarrow 3_1$		4.93×10^{-7}		4.24×10^{-7}		6.55×10^{-4}		4.24×10^{-7}
$5_1 \rightarrow 4_1$		6.24×10^{-4}		8.37×10^{-8}		1.07×10^{-2}		8.37×10^{-8}
$5_1 \rightarrow 4_2$		6.67×10^{-2}		6.67×10^{-2}		3.59×10^{-2}		6.32×10^{-4}

3.3.6 Electric Monopole Transition B(E0) and $X(E0/E2)$ Ratios

The deformation parameters for protons and neutrons are used to calculate monopole transition matrix elements for $^{170\text{-}184}$W isotopes that have been estimated using Equations (2.67) to (2.69). In addition to the available experimental data, the monopole transition matrix element and mixing ratio have been calculated using Equations (2.65) and (2.71) listed in Table (3.26).

The ratio X(E0/E2) shows the strength of the competition between E0 and E2, where it is noted that the IBM-2 calculated values are not entirely consistent with the experimental values available, and the reason belongs to the strength of the transition between E2 and E0, as well as the fact that the difficulty of defining unified parameters for ($\tilde{\beta}_v$, $\tilde{\beta}_\pi$) give us the theoretical values in (IBM-2) that are closer to the available experimental data. Besides the fact that the experimental values available are also very few. The deformation parameters for protons and neutrons used to calculate monopole transition matrix elements ρ(E0) for $^{170\text{-}184}$W isotopes are ($\tilde{\beta}_v$ = -0.00251 fm^2, $\tilde{\beta}_\pi$ = -0.0674 fm^2). Table (3.26) shows the electric monopole transition matrix and X(E0/E2) for $^{170\text{-}184}$W isotopes.

Table (3.26) Electric monopole transition and X(E0/E2) for $^{170\text{-}184}$W isotopes.

Isotopes	^{170}W				^{172}W			
	B(E0)e^2b^2		X(E0/E2)		B(E0) (e^2b^2)		X(E0/E2)	
$J_i^+ \rightarrow J_f^+$	Exp. [99]	IBM-2	Exp. [99]	IBM-2	Exp. [100]	IBM-2	Exp. [100]	IBM-2
$2_1 \rightarrow 2_2$		2.36×10^{-4}		3.19×10^{-4}		3.97×10^{-4}		6.08×10^{-4}
$2_1 \rightarrow 2_3$		5.23×10^{-9}		4.68×10^{-4}		5.17×10^{-5}		1.82×10^{-2}
$2_2 \rightarrow 2_3$		5.23×10^{-4}		4.36×10^{-4}		7.89×10^{-4}		3.46×10^{-4}
$2_2 \rightarrow 2_4$		2.09×10^{-2}		2.15×10^{-2}		2.26×10^{-4}		3.55×10^{-2}
$3_1 \rightarrow 2_1$		9.66×10^{-4}		2.78×10^{-4}		2.09×10^{-2}		2.09×10^{-2}

$3_1 \rightarrow 2_2$		6.99×10^{-4}		4.93×10^{-4}		4.04×10^{-6}		4.34×10^{6}
$4_1 \rightarrow 3_1$		5.33×10^{-7}		2.09×10^{-2}		6.99×10^{-4}		6.99×10^{-4}
$5_1 \rightarrow 4_1$		4.04×10^{-4}		9.66×10^{-4}		6.14×10^{-7}		4.04×10^{-4}
$5_1 \rightarrow 4_2$		6.99×10^{-4}		4.89×10^{-4}		4.04×10^{-4}		4.87×10^{-4}
Isotopes	**^{174}W**				**^{176}W**			
	B(E0) (e^2b^2)		**X(E0/E2)**		**B(E0) (e^2b^2)**		**X(E0/E2)**	
$J_i^+ \rightarrow J_f^+$	**Exp.**	**IBM-2**	**Exp.**	**IBM-2**	**Exp.**	**IBM-2**	**Exp.**	**IBM-2**
$2_1 \rightarrow 2_2$		2.39×10^{-4}		2.88×10^{-3}		2.12×10^{-3}		3.09×10^{-3}
$2_1 \rightarrow 2_3$		5.38×10^{-4}		1.03×10^{-2}		5.08×10^{-4}		1.71×10^{-2}
$4_1 \rightarrow 2_1$		9.63×10^{-7}		5.97×10^{-9}		6.67×10^{-5}		2.47×10^{-4}
$2_2 \rightarrow 2_4$		1.02×10^{-2}		2.61×10^{-4}		8.84×10^{-4}		2.01×10^{-4}
$2_4 \rightarrow 0_1$		4.65×10^{-4}		2.49×10^{-2}		5.69×10^{-4}		1.96×10^{-2}
$3_1 \rightarrow 2_1$		4.36×10^{-4}		2.09×10^{-2}		2.09×10^{-2}		2.78×10^{-4}
$3_1 \rightarrow 2_2$		2.15×10^{-2}		9.66×10^{-4}		9.66×10^{-4}		4.93×10^{-4}
$4_1 \rightarrow 3_1$		2.78×10^{-4}		6.99×10^{-4}		6.99×10^{-4}		2.09×10^{-2}
$5_1 \rightarrow 4_1$		4.93×10^{-4}		4.74×10^{-7}		3.04×10^{-7}		9.66×10^{-4}
$5_1 \rightarrow 4_2$		8.84×10^{-4}		4.04×10^{-4}		4.04×10^{-4}		6.99×10^{-4}
Isotopes	**^{178}W**				**^{180}W**			
	B(E0) (e^2b^2)		**X(E0/E2)**		**B(E0) (e^2b^2)**		**X(E0/E2)**	
$J_i^+ \rightarrow J_f^+$	**Exp.**	**IBM-2**	**Exp.**	**IBM-2**	**Exp.**	**IBM-2**	**Exp.**	**IBM-2**
$2_1 \rightarrow 2_2$		3.59×10^{-4}		6.13×10^{-4}		3.71×10^{-4}		6.99×10^{-4}
$2_1 \rightarrow 2_3$		8.37×10^{-5}		6.38×10^{-3}		2.26×10^{-4}		4.04×10^{-7}
$2_2 \rightarrow 2_3$		5.38×10^{-4}		3.51×10^{-4}		4.24×10^{-4}		4.04×10^{-4}
$2_2 \rightarrow 2_4$		1.54×10^{-5}		2.09×10^{-2}		8.37×10^{-5}		1.15×10^{-3}
$3_1 \rightarrow 2_1$		2.78×10^{-4}		9.66×10^{-4}		4.93×10^{-4}		3.84×10^{-4}
$3_1 \rightarrow 2_2$		4.93×10^{-4}		6.99×10^{-4}		4.93×10^{-4}		1.23×10^{-4}
$4_1 \rightarrow 3_1$		2.09×10^{-2}		4.34×10^{-5}		2.09×10^{-2}		1.76×10^{-5}
$5_1 \rightarrow 4_1$		9.66×10^{-4}		4.04×10^{-4}		6.04×10^{-3}		2.59×10^{-3}
$5_1 \rightarrow 4_2$		6.99×10^{-4}		4.93×10^{-4}		1.23×10^{-4}		4.04×10^{-5}
Isotopes	**^{182}W**				**^{184}W**			
	B(E0) (e^2b^2)		**X(E0/E2)**		**B(E0) (e^2b^2)**		**X(E0/E2)**	
$J_i^+ \rightarrow J_f^+$	**Exp.**	**IBM-2**	**Exp.**	**IBM-2**	**Exp.**	**IBM-2**	**Exp.**	**IBM-2**
$2_1 \rightarrow 2_2$		3.35×10^{-4}		7.86×10^{-4}		2.46×10^{-4}		6.51×10^{-4}
$2_1 \rightarrow 2_3$		5.08×10^{-4}		6.28×10^{-4}		1.27×10^{-2}		6.33×10^{-4}
$2_2 \rightarrow 2_3$		4.31×10^{-4}		5.44×10^{-4}		2.78×10^{-4}		6.58×10^{-4}

$2_2 \rightarrow 2_4$		1.54×10^{-4}		2.79×10^{-3}		4.93×10^{-4}		5.88×10^{-4}
$3_1 \rightarrow 2_1$		3.84×10^{-4}		2.78×10^{-4}		2.09×10^{-2}		2.09×10^{-2}
$3_1 \rightarrow 2_2$		1.23×10^{-4}		4.93×10^{-4}		9.66×10^{-4}		9.66×10^{-4}
$4_1 \rightarrow 3_1$		1.76×10^{-5}		2.09×10^{-2}		6.99×10^{-4}		6.99×10^{-4}
$5_1 \rightarrow 4_1$		2.59×10^{-3}		9.66×10^{-4}		5.58×10^{-4}		3.58×10^{-4}
$5_1 \rightarrow 4_2$		4.93×10^{-4}		6.99×10^{-4}		4.04×10^{-4}		4.04×10^{-4}

3.3.7 Potential Energy Surface (PES)

The surface of the potential energy as a function with contour diagrams for isotopes that have been calculated from Equation (2.42) with computer code is represented in Figures (3.65) to (3.72). The parameters used in the program to calculate the potential energy surface are shown in Table (3.27).

Table (3.27) Potential energy surface parameters for $^{170\text{-}184}$W isotopes.

Isotops	N	ES	ED	A_1	A_2	A_3	A_4
$^{170}_{74}W_{96}$	11	-0.138	0.058	0.001	0.031	-0.11	0
$^{172}_{74}W_{98}$	12	-0.119	0.013	0.006	0.056	-0.095	0
$^{174}_{74}W_{100}$	13	-0.119	0.006	0.006	0.065	-0.095	0
$^{176}_{74}W_{102}$	14	-0.054	0.061	0.002	0.029	-0.043	0
$^{178}_{74}W_{104}$	15	-0.065	0.059	0.002	0.024	-0.052	0
$^{180}_{74}W_{106}$	14*	-0.106	0.038	0.002	0.023	-0.085	0
$^{182}_{74}W_{108}$	13*	-0.1	0.04	0.003	0.011	-0.08	0
$^{184}_{74}W_{110}$	12*	-0.12	0.002	0.007	0.065	-0.095	0

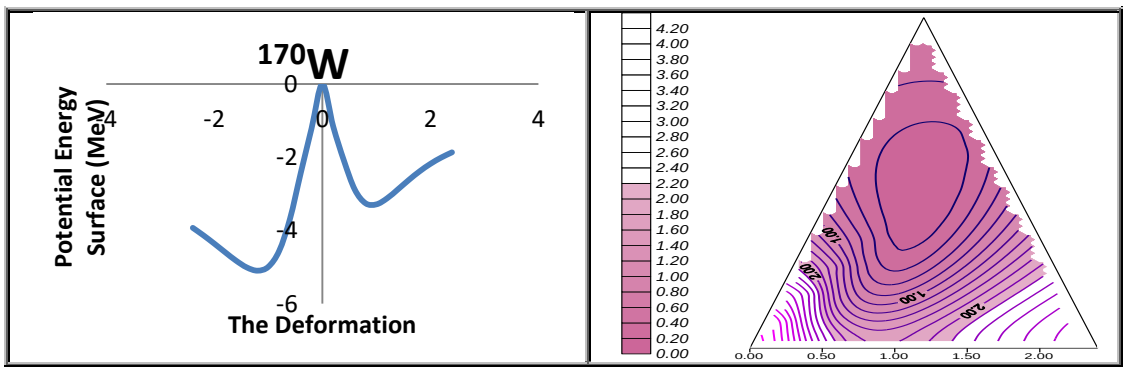

Figure (3.65) Potential energy surface with the deformation for ^{170}W.

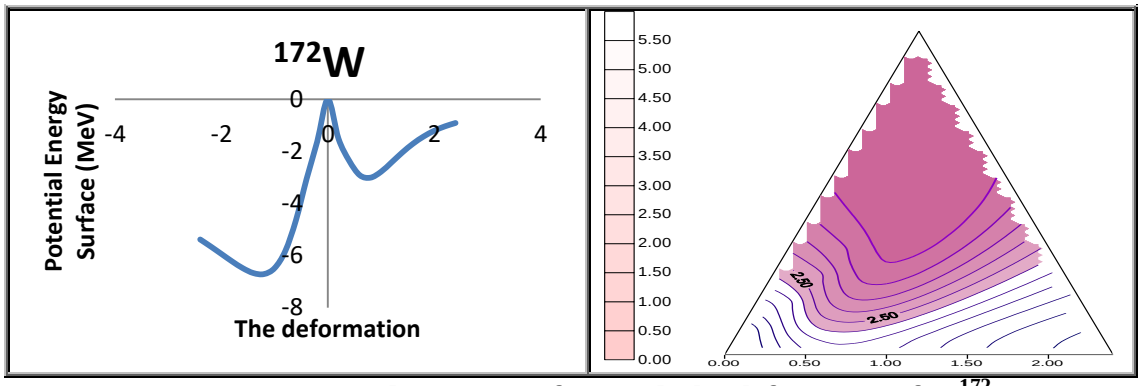

Figure (3.66) Potential energy surface with the deformation for ^{172}W.

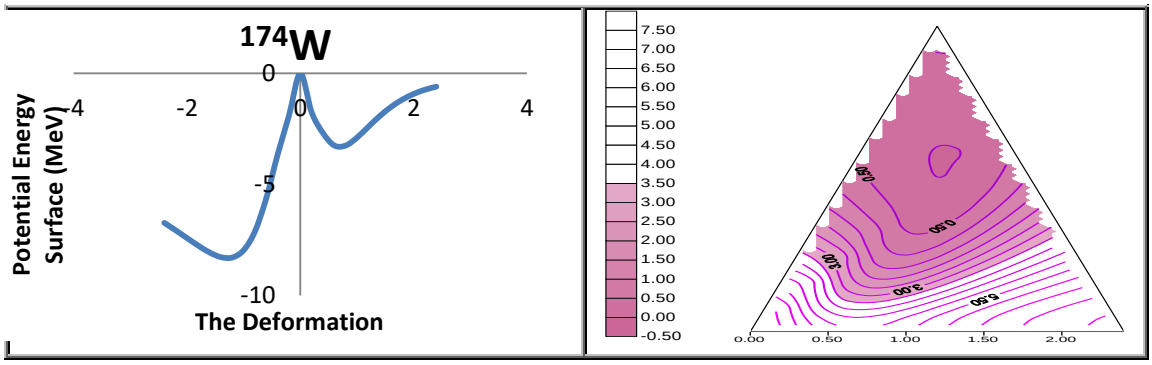

Figure(3.67) Potential energy surface with the deformation for ^{174}W.

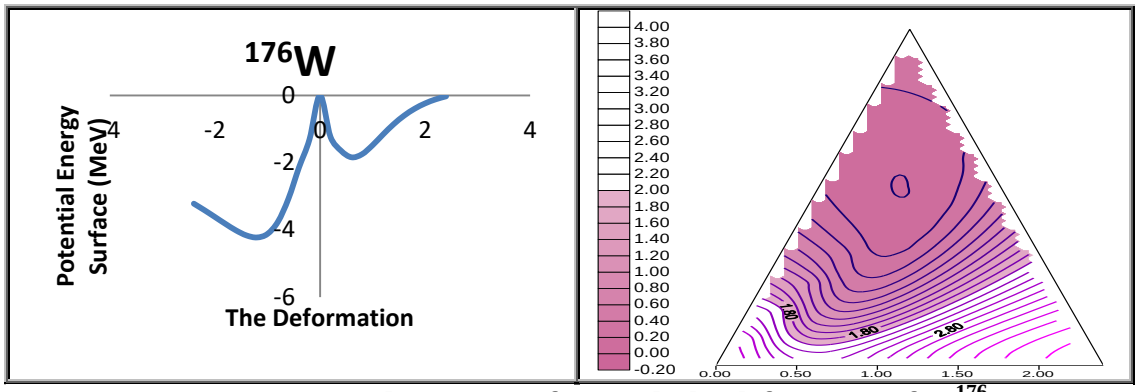

Figure(3.68) Potential energy surface with the deformation for ^{176}W.

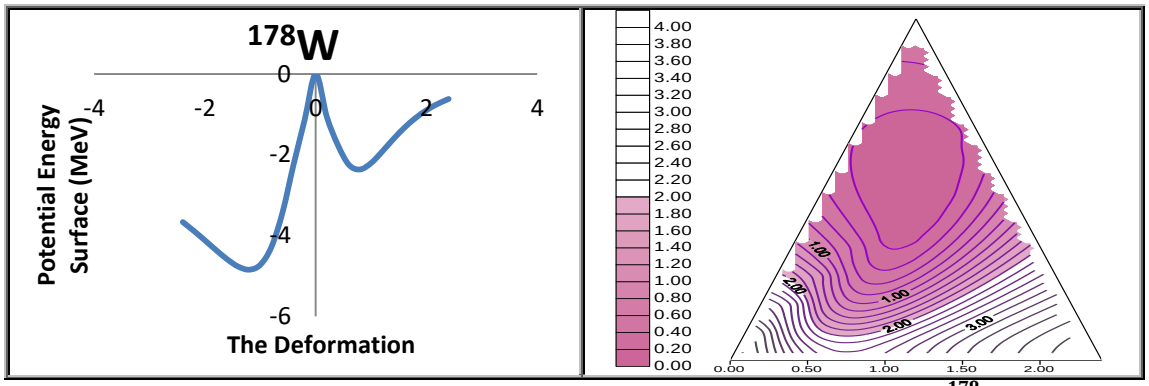

Figure (3.69) Potential energy surface with the deformation for ^{178}W.

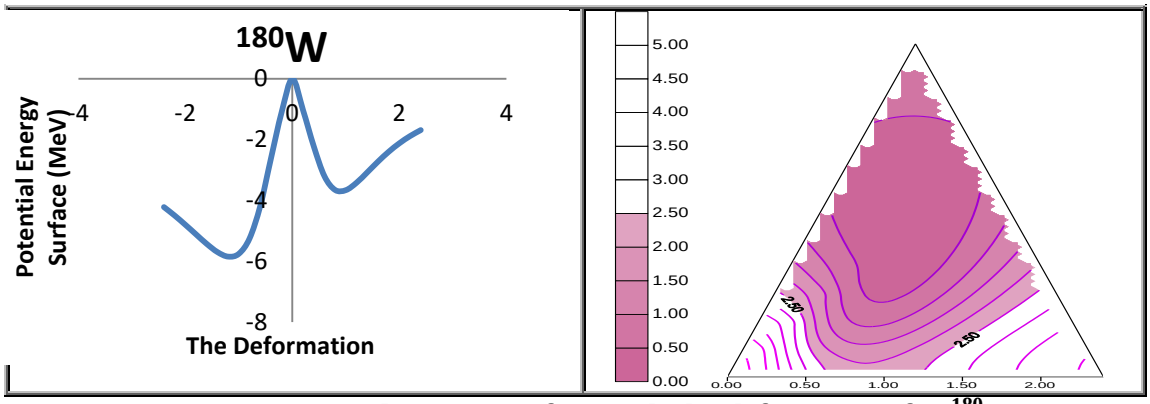

Figure (3.70) Potential energy surface with the deformation for ^{180}W.

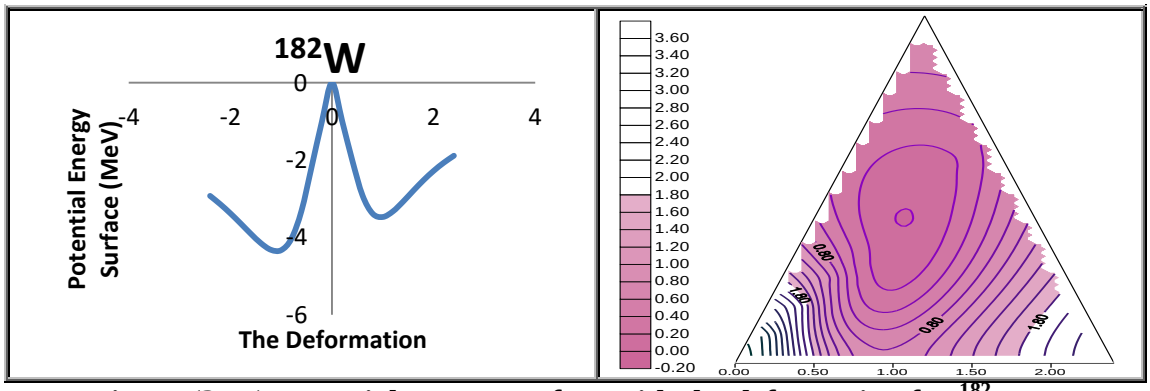

Figure (3.71) Potential energy surface with the deformation for ^{182}W.

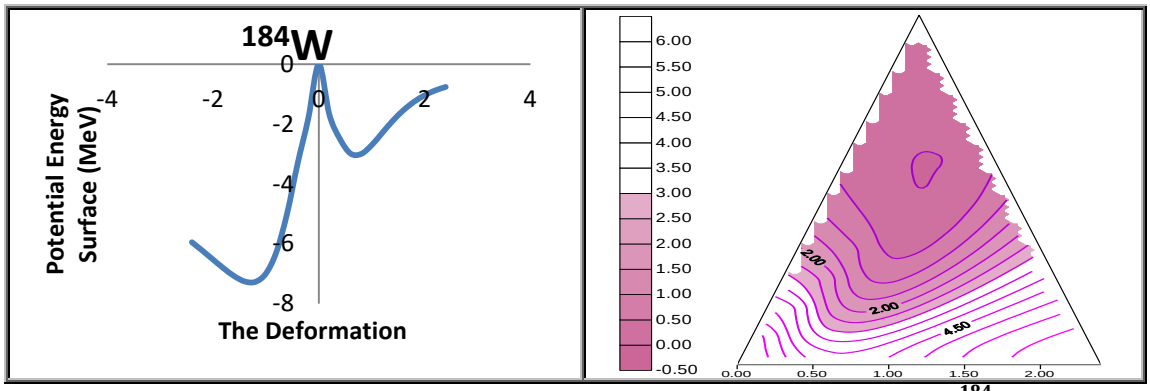

Figure (3.72) Potential energy surface with the deformation for ^{184}W.

3.3.8 Mixed Symmetry States (MSS)

Studying the effect of Majorana parameters ($\zeta_{1,3}$, ζ_2) on the calculated excitation energy level for $^{170\text{-}184}$W isotopes, the value of $\zeta_{1,3}$ vary between (0.11-0.15) and fixed the ζ_2 on (0.1) for all isotopes then vary this value between (0.08-0.12) around the best-fitted data. It is found that the energy values for the states $(2_3^+, 2_4^+, 2_5^+, 3_1^+, 5_1^+)$ are

responded rapidly to the changes of the ζ_2 parameters in some isotopes only and therefore these states verify the first property of the mixed symmetry state (MSS). Figure (3.73) explain the energy variation of these states as a function of the Majorana parameter ζ_2.

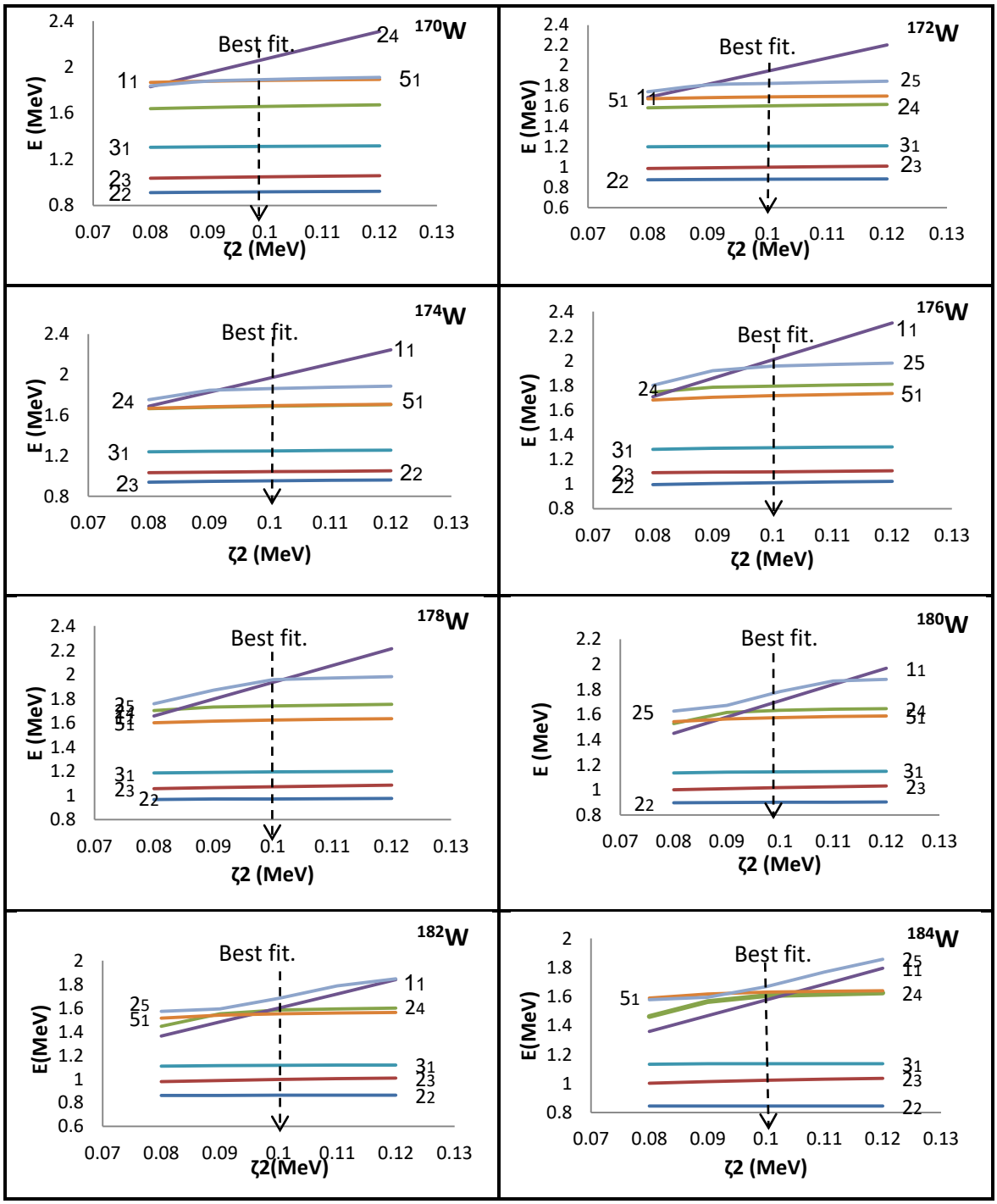

Figure (3.73) Mixed symmetry states in even-even $^{170\text{-}184}$W isotopes.

Chapter Four

Discussion and Conclusions

In this research, the nuclear structure of a series of (even-even) isotopes Yb, Hf, and W was studied. This study included calculating the energy levels, the ratios between these levels, the probability of reducing electric transitions B(E2), branching ratios, electric quadrupole momentums, magnetic and zero transitions, mixing ratios and the energy of surface potential of the mentioned isotopes.

The software package IBM computer code for IBM-1 and NPBOS program was used to determine the parameters of the Hamiltonian operator

4.1. Ytterbium Isotopes Discussion

For the purpose of studying the properties of any nucleus, it is necessary to determine the behavior of this nucleus in order to be able to choose the specific parameters of the Hamilton function for it. The type of dynamic symmetry was found based on several tests of finding theoretical values using the program of interacting bosons in its first and second versions and comparing them with practical values. The following is an explanation of each of these tests for each series of isotopes under study which begins with testing the energy levels, as the energy spectra of any nucleus are arranged in bundles starting with the ground band (G band), which takes the sequence (0_1^+, 2_1^+, 4_1^+, 6_1^+, 8_1^+……..) and the other excited band is the β-band which takes the sequence (0_2^+, 2_2^+, 4_2^+, 6_2^+, 8_2^+……..) The third band is the gamma band (γ band) which takes the sequence (2_3^+, 3_1^+, 4_3^+, 5_1^+, 6_3^+, 7_1^+……..). The general arrangement for these bands is (G-band, β-band, γ-band). If this arrangement occurs, the spectrum of the nucleus is either vibratory SU(5) or rotational SU(3), but

if the arrangement of the bands is (G-band, ɤ-band, β-band) i.e. the angular momentum2_3^+ appears before 0_2^+, a break occurs in the order, so the limitation is O(6).

4.1.1. Energy Levelse for $^{160\text{-}178}$Yb Isotopes Discution

For calculating the energy levels, the Hamiltonian operators that used were given in Table (3.1) and Table (3.2) these parameters were plotted in Figures (3.1) and (3.2) for $^{160\text{-}178}$Yb isotopes by noticing the change of parameters as a function of the change in the number of bosons in Figure (3.1), it was found that their behavior is non-linear, which indicates the irregularity of the nuclear phase, meaning that the nuclear phase is in a state of change, which means that these isotopes belong to the rotational shape or SU(3) so that it applies to Figure (3.2) where the parameters in IBM-2 are a function of mass number which change with randomly except χ_π and ζ_2 it remains constant and did not change because the number of protons bosons in series of isotopes does not change.

The values of the coefficients used in calculating these levels, which are shown in Table (3.1), it is noted that the value of the coefficient (EPS) does not appear for all isotopes, and (P.P), (L.L), (Q.Q) are dominant over the rest of the coefficients as it shows the dominance of the duplication reaction, the electric quadrupole interaction and the angular momentum interaction respectively. This is due to the limitation to which these isotopes belong.

As for the coefficient (CHI), it was found that its value increases with the increasing in the mass number due to the increasing in the distortion of these isotopes with the increase in the number of bosons and their approach to the rotational limitation SU(3).

Figure (3.1) shows what has been clarified about the relationship between these parameters and the number of bosons for the studied isotopes, where it is noted that the relationship between them is non-

linear, and this confirms a phase transition that occurs from one isotope to another and the appearance of the distorted region, and it is clear from this that these isotopes increase in distortion with the increase in the mass number and the number of bosons, and Figure (3.2) shows the relationship between the parameters used in the second version of the interactive boson program as functions of the mass number, and it shows a disorderly relationship and also indicates that there is a phase transition for the nuclides. It is noticed in all the isotopes of Ytterbium (under study) whome energy levels have been studied that all of them decreased in value of the level (2_1^+) by increasing the number of bosons, and this is clarified in Figures (3.3) to (3.12) that compare the practical and theoretical energy levels of the studied isotopes. It was noticed the clear drop in energy when moving from the isotope ^{160}Yb to the isotope^{174}Yb and then it goes back to increasing at the isotope ^{176}Yb and the isotope ^{178}Yb, where the number of bosons is a result of the holes and not the particles.

The values of energy levels in the current study according to energy bands (G, β, γ-bands) compared to the practically available values are shown in Figures (3.3) to (3.12), and they indicate the emergence of new energy levels in addition to the confirmation of the rotation and similarity in some energy levels that were not practically confirmed, it was concluded from those tables that there is a good match between the calculated values and the practical values, and this match appears clearly in the low energy levels, while we find that there is a difference between the practical and theoretical values calculated in the high energy levels and it was concluded that the IBM-1 model succeeds in explaining the low levels more than the other levels because of the approximations of this model, and the most important reasons is the lack of distinction between the proton bosons and the neutron bosons. In addition, the upper

bands with high spin pair with the rotational bands in the ground plane compressing the successive levels as this cause the intersection of these bands with each other. The isotopes of even-even Ytterbium ($^{160\text{-}178}$Yb) consist of (70) protons and (90-108) neutrons. It was noted that the number of protons is closer to the shell 82 than to the shell 50, so the number of proton bosons is calculated from the number of holes all the way to the closed crust (82), so the number of bosons of protons equals (6), and the number of particles neutrons' bosons (4-11) for $^{160\text{-}174}$Yb isotopes, and (10,9) for holes for the two isotopes $^{176\text{-}178}$Yb, we notice that it changes from the closest to the shell with the magic number 82 to the shell 126, so the number of the neutron bosons is calculated from the number of particles, so the number of the total number of bosons will be equal to (10-17) bosons for the isotopes $^{160\text{-}174}$Yb, respectively, as for the two isotopes $^{176\text{-}178}$Yb, the number of total bosons was calculated from the number of holes and their number was (16,15).

In the higher spin levels, the nucleus is more distorted due to the compression of the successive levels with each other. From the above-mentioned figures, it can be concluded that the beta band (β-band) is wider than the gamma band (γ-band). It is found this in isotopes that are close to the determination of SU(3), while the gamma band appears in excess for the isotopes that belong to the transition region SU(3). The calculation of dynamic symmetries by IBM-1, IBM-2 and experimental energy levels and after a comparison with the standard values for the energy ratios of ($E0_2^+/E2_1^+, E4_1^+/E2_1^+, E6_1^+/E2_1^+$ and $E8_1^+/E2_1^+$). The ratio between two levels for $^{160\text{-}178}$Yb isotopes has been plotted in Figures (3.13) to (3.16) for all isotopes in transitional region O(6)→ SU(3), that is clear in these Figures there is a good agreement between experimental data and the IBM-1 and IBM-2 results appear clearly in Table (3.3), these results are drawn in Figures (3.13) to (3.16), it is clear that these

isotopes transition between SU(3) to O(6) limit except ^{170}Yb tend to O(6), but Figure (3.13) clarifies and prove that these isotopes in the aforesaid limit because it belongs to U(5) limit.

4.1.2. The Reduced Electric Transition Probability Calculation for $^{160\text{-}178}$Yb Isotopes

The values of the parameters (E2SD) and (E2DD) were chosen in accordance with the transitional state of the isotopes between the limitation SU(3) and O(6) and with the rotational limitation of SU(3) for the isotopes so as to give the best match between the calculated B(E2) values and the practical values available.

In IBM-1 the reduced electric transition probability values for $^{160\text{-}178}$Yb isotopes are calculated by calculating the values of effective charge e_b = E2SD and β_2 =E2DD from Equations as mentioned in detail in chapter three by using the experimental value of $B(E2;2_1^+ \rightarrow 0_1^+)$, these values are putting into Table (3.4). In IBM-2 effective charge for neutron (e_ν) and for proton (e_π) was also calculated to find the reduced electric transition probability, it found that the neutron's effective charge e_ν = 0.214(eb) and the proton's effective charge e_π = 0.052 (eb). The effective charges depend on the total bosons number N_ρ and the ratios between N_ν/N_π, these parameters are free and can take any value to fit the experimental data, observing to Table (3.4), it is conclude that the value of B(E2:$2^+_1 \rightarrow 0^+_1$) increases with increasing mass number (that is, by increasing the number of neutrons) and this is due to the approach of the number of neutrons to the closed crust (126) and an increase in the number of bosons, and this increase corresponds to the rotational limitation properties.

Table (3.5) shows a comparison between B(E2) calculated by IBM-1, IBM-2 and experimental data. The values are acceptable in comparison and they have a good systematic.

The study of the rates of reduced electrical transitions B(E2) (which is one of the most important properties of the nuclear structure) showed the rotational property and the transitional nature between it and the unstable gamma of these nuclei through the decay of level $0_1^+$to level 2_1^+. It can also be seen that the IBM-1 and IBM-2 models were able to explain that the transitions in a single band are strong because of the selection rules such as the transitions ($2_1^+ \rightarrow 0_1^+$), ($2_2^+ \rightarrow 2_3^+$) and($4_1^+ \rightarrow 2_1^+$) but the transitions between different bands are very weak such as($2_1^+ \rightarrow 0_2^+$), ($2_1^+ \rightarrow 2_2^+$) and($4_3^+ \rightarrow 2_1^+$) this was shown by IBM-1 while some transitions did not appear in IBM-2 because they are forbidden such as($2_2^+ \rightarrow 0_1^+$), ($4_1^+ \rightarrow 2_2^+$) and ($3_1^+ \rightarrow 2_1^+$).

It should be noted here the importance of using branching ratios in knowing the distortion of the nuclei, including the ratios shown in Table (3.6). When the value of this ratio decreases, the distortion of the nucleus increases, and when this value is close to zero, the nucleus becomes too close to limitation SU(3). We observe that these values are close to zero, and by comparing them with the ideal values, we find that these isotopes belong to the rotational limitation SU(3), and this proves the validity of the previous statement.

When comparing the branching ratios (R, R', R'') for the isotopes under study with the typical values for each determination, we find that there is a good match between them, as shown in Table (3.6). In addition, it is concluded that $^{160\text{-}178}$Yb isotopes belong to the aforementioned limitations, as with an increasing mass number, it was found a decrease in the value of (R) and the previous isotopes tend to move toward the limitation SU(3).

The theoretical and the available practical electric quadrupole momentum values, showed a good convergence, and in light of these values it concluded that the first and second nuclei of the sequence (^{160}Yb) and (^{162}Yb) have the lowest momentum value and suffer less distortion than the rest of the isotopes because they are located in the transition region O(6)-SU(3). While the value of the momentum begins to increase relatively quickly when moving to the third nucleus, and therefore it has a distortion due to the nature of the transition region O(6)-SU(3) to which this nucleus belongs.

As for the remaining nuclei ($^{164\text{-}178}$Yb), it is found that they suffer from permanent distortions, due to the large value of the electric quadrupole momentum and their belonging to the rotational limitation SU(3).

4.1.3. Magnetic Transitions Probability Calculation for $^{160\text{-}178}$Yb Isotopes

In order to calculate B(M1) transition probability, one should estimate the effective $g-$factors for proton g_π and neutron g_ν by Equations (2.20). In Ytterbium isotopes the g- factor values are g_π= 0.422 (μ_N) and g_ν= 0.477 (μ_N). Equations (2.19) were used to calculate the B(M1) transition probabilities as it is shown in Table (3.7). The calculated values for B(M1) are acceptable to some extent as compared with the available experiments values, where some of the B(M1) values are small compared to the values of the quadrupole transition probabilities because the wavelength of the gamma ray transitions is greater than it is in the magnetic transitions according to Equation (3.1).

The calculation values for these isotopes and mixing ratio δ(E2/M1) have been compared with the available experiments data as shown in Table (3.7).

4.1.4. The Electric Monopole Transition Calculation for $^{160\text{-}178}$Yb Isotopes

Table (3.8) shows the electric monopole transition matrix and X(E0/E2) for $^{160\text{-}178}$Yb isotopes. The deformation parameters for protons and neutrons used to calculate monopole transition matrix elements ρ(E0) for $^{160\text{-}178}$Yb isotopes are ($\tilde{\beta}_v$ = +0.039 fm^2 , $\tilde{\beta}_\pi$ = -0.055 fm^2

The ratio X(E0⁄E2) shows the strength of the competition between E0 and E2, where it is noted that the IBM-2 calculated values are not entirely consistent with the experimental values available, and the reason belongs to the strength of the transition between E2 and E0, as well as the fact that the difficulty of defining unified parameters for ($\tilde{\beta}_v$, $\tilde{\beta}_\pi$) gave the theoretical values in (IBM-2) that are closer to the available experimental data. Besides the fact that the experimental values available are also very few.

4.1.5. The Surface Potential Energy for $^{160\text{-}178}$Yb Isotopes

The surface potential energy of the current isotopes can be studied through the known (β,γ) values and drawing the symmetrical diagrams of the axial symmetry angles as well as drawing the contour diagrams when ($\gamma=0^o$-60^o) shown in Figures (3.17) to (3.26) it becomes clear that the nuclei suffer from a large distortion by comparing these shapes with the ideal contour lines diagrams, as shown in Figure (2.5).

Table (3.9) represents the parameters of the "surfer program" which drew the contour shapes to show the extent of distortion in the nuclei of the isotopes under study.

The surface potential energy values that observed in these diagrams shown that these energies have variable values with (γ) and (β) values, which indicates the deviation of the nucleus shape from the spherical shape to the irregular distorted shape due to the increase in the number of

bosons and this confirms its belonging to the rotational limitation of SU(3).

The distortion can be described by a multipolar expansion, with the quadrupole distortion being the most significant deviation from the spherical shape. These quadrilaterals can have either axial symmetry, in which case one distinguishes the elongated (expanded) and flat shapes or the distortion can be without axial symmetry resulting in different elongations along the three axes of the system, referred to as the 'triaxial shape'.

4.1.6. Mixed Symmetry State for $^{160\text{-}178}$Yb Isotopes

The Majorana parameter effect on the calculated excitation energy level for $^{160\text{-}166}$Yb isotopes, has been investigated for isotopes and it varies around the best fitted. The ξ_2 allowed to vary with the $\xi_{1,3}$ at the best fit value. The lowest mixed state is $(1_1^+) and\ (2_4^+)$, the state staying conservative to its value in these isotopes denoting that these states may have a full symmetry. Other states $(5_1^+)$and (3_1^+) for ($^{168\text{-}178}$Yb) isotopes are slowly increased while no clear effect in isotopes as shown in figure (3.27). It cannot compare the calculated value of state with the experimental value due to data lack. The calculated energy of the scissor state respectively; this is close to the observed energy of the state of the other neighbored nuclei.

The state of mixing levels results from the interaction of the proton and neutron in terms of spin since if it is spinning in the same direction and it is positive, this leads to an increase in the level by increasing the Majorana factor, and this is what has appeared for all the isotopes, but if the spin of the proton is the opposite of spinning the neutron, it does not affect the levels, and if they have the same negative spin, the levels will decrease with the increase of Majorana factor.

4.2. $^{166-180}$Hf Isotopes Discussion

The isotopes of even-even Hafnium ($^{166-180}$Hf) consist of (72) protons and (94-108) neutrons. We note that the number of protons is closer to the shell 82 than to the shell 50, so the number of proton bosons is calculated from the number of holes all the way to the closed crust (82), so the number of bosons of protons equals (5), and the number of neutrons' bosons is equal (6-11), we notice that it changes from the closest to the shell with the magic number 82 to the shell 126, so the number of neutron bosons is calculated from the number of particles close to (82), so the total number of bosons will be equal to (11-16) for the isotopes $^{166-176}$Hf, respectively, as for two isotopes $^{178-180}$Hf, the number of neutron bosons is calculated from the number of holes and their number was (15,14), respectively.

4.2.1. Energy Levelse for $^{166-180}$Hf Isotopes Discussion

The parameters of the Hamiltonian operator, as listed in Tables (3.10) and (3.11), were plotted in Figures (3.28) and (3.29) for $^{166-180}$Hf isotopes by observing the change in parameters as a function of the number of bosons.

The values of the coefficients used in calculating these levels, it is noted that the value of the coefficient (EPS) does not appear for all isotopes, and (P.P), (L.L), (Q.Q) are dominant over the rest of the coefficients as it shows the dominance of the duplication reaction, the electric quadrupole interaction and the angular momentum interaction respectively. This is due to the limitation to which these isotopes belong.

As for the coefficient (CHI), we find that its value increases with the increase in the mass number due to the increase in the distortion of these isotopes with the increase in the number of bosons and their approach to the rotational limitation SU(3).

Figure (3.28) shows what has been clarified about the relationship between these parameters and the number of bosons for the studied isotopes, where it is noted that the relationship between them is non-linear, and this confirms a phase transition that occurs from one isotope to another and the appearance of the distorted region, and it is clear from this that these isotopes increase in distortion with the increase in the mass number and the number of bosons, and Figure (3.29) shows the relationship between the parameters used in the second version of the interactive boson program as functions of the mass number, and it shows a disorderly relationship and also indicates that there is a phase transition for the nuclides. It is noticed in all the isotopes of Hafnium whose energy levels have been studied that all of them decreased in value of the level (2_1^+) by increasing the number of bosons, and this is clarified in Figures (3.30) to (3.37) that compare the practical and theoretical energy levels of the studied isotopes. We notice the clear drop in energy when moving from the isotope ^{166}Hf to the isotope ^{176}Hf and then it goes back to increasing at the isotope ^{178}Hf and the isotope ^{180}Hf, where the number of bosons is a result of the holes and not the particles and experimental energy levels and after a comparison with the standard values for the energy ratios of ($E0_2^+/E2_1^+$, $E4_1^+/E2_1^+$, $E6_1^+/E2_1^+$ and $E8_1^+/E2_1^+$).

The ratio between two levels for Hafnium isotopes have been plotted in Figures (3.38) to (3.41) for all isotopes which in transitional region O(6)→ SU(3), that is clear in these Figures there is a good agreement between experimental data and the IBM-1 and IBM-2 results appear clearly in Table (3.12), these results are drew in Figures (3.37) to (3.41), it is clear that these isotopes transition between SU(3) to O(6) limit except ^{170}Hf tend to O(6), but Figure (3.38) clarifies and prove that the these isotopes in the aforesaid limit because it belongs to U(5) limit.

4.2.2. The Reduced Electric Transition Probability Calculation for $^{166-180}$Hf Isotopes

The values of the parameters (E2SD) and (E2DD) were chosen in accordance with the transitional state of the isotopes between the limitation SU(3) and O(6) and with the rotational limitation of SU(3) for the isotopes so as to give the best match between the calculated B(E2) values and the practical values available.

In IBM-1 the reduced electric transition probability values for $^{166-180}$Hf isotopes are calculated by calculating the values of effective charge e_b = E2SD and β_2 =E2DD from Equations as mentioned in detail in Chapter Three by using the experimental value of $B(E2;2_1^+ \rightarrow 0_1^+)$, these values are putting into Table (3.13). In IBM-2 effective charge for neutron (e_ν) and for proton (e_π) also calculated to find the reduced electric transition probability, it found that the neutron's effective charge e_ν = 0.28 (eb) and the proton's effective charge e_π = 0.035 (eb). The effective charges depend on the total bosons number N_ρ and the ratios between N_ν/N_π, these parameters are free and can take any value to fit the experimental data, observing Table (3.13), it is conclude that the value of B(E2:$2^+_1 \rightarrow 0^+_1$) increases with increasing mass number (that is, by increasing the number of neutrons) and this is due to the approach of the number of neutrons to the closed crust (82) and an increase in the number of bosons, and this increase corresponds to the rotational limitation properties.

Table (3.14) shows a comparison between B(E2) calculated by IBM-1, IBM-2 and experimental data. The values are acceptable in comparison and they have a good systematic.

The study of the rates of reduced electrical transitions B(E2) showed the rotational property and the transitional nature between it and the unstable gamma of these nuclei through the decay of level $0_1^+$to level 2_1^+. It can also be seen that the IBM-1 and IBM-2 models were able to explain that the transitions in a single band are strong because of the selection rules such as the transitions ($2_1^+ \rightarrow 0_1^+$), ($2_2^+ \rightarrow 2_3^+$) and ($4_1^+ \rightarrow 2_1^+$).

The values of energy levels in the current study according to energy bands (G, β, γ-bands) compared to the practically available values are shown in Figures (3.30) to (3.37), and they indicate the emergence of new energy levels in addition to the confirmation of the rotation and similarity in some energy levels that were not practically confirmed, and we conclude from those tables that there is a good match between the calculated values and the practical values, and this match appears clearly in the low energy levels, while we find that there is a difference between the practical and theoretical values calculated in the high energy levels and we conclude that the IBM-1 model succeeds in explaining the low levels more than the other levels because of the approximations of this model, and the most important reasons are the lack of distinction between the proton bosons and the neutron bosons. In addition, the upper bands with high spin pair with the rotational bands in the ground plane compressing the successive levels as this cause the intersection of these.

4.2.3. Magnetic Transitions Probability Calculation for $^{166\text{-}180}$Hf Isotopes

In order to calculate B(M1) transition probability, one should estimate the effective $g-$factors for proton g_π and neutron g_ν by Equations (2.20). In $^{166\text{-}180}$Hf isotopes the g- factor values are g_π= 0.417 (μ_N) and g_ν= 0.418 (μ_N). Equations (2.19) were used to calculate the B(M1) transition probabilities as it is shown in Table (3.16). The

calculated values for B(M1) are acceptable to some extent as compared with the available experiments values, where some of the B(M1) values are small compared to the values of the quadrupole transition probabilities because the wavelength of the gamma ray transitions is greater than it is in the magnetic transitions according to Equation (3.1), this Equation shows that the B(M1)transition probability is less than B(E2) transition probability and our results confirm this. The calculation values for these isotopes and mixing ratio δ(E2/M1) have been compared with the available experiments data as shown in Table (3.16).

4.2.4. The Electric Monopole Transition Calculation for $^{166\text{-}180}$Hf Isotopes

The ratio X(E0⁄E2) shows the strength of the competition between E0 and E2, where it is noted that the IBM-2 calculated values are not entirely consistent with the experimental values available, and the reason belongs to the strength of the transition between E2 and E0, as well as the fact that the difficulty of defining unified parameters for ($\tilde{\beta}_v$, $\tilde{\beta}_\pi$) give us the theoretical values in (IBM-2) that are closer to the available experimental data. The deformation parameters for protons and neutrons used to calculate monopole transition matrix elements ρ(E0) for $^{166\text{-}180}$Hf isotopes are ($\tilde{\beta}_v$= 0.0079 fm^2, $\tilde{\beta}_\pi$ = -0.00543 fm^2). Table (3.17) shows the electric monopole transition matrix and X(E0/E2) for $^{166\text{-}180}$Hf isotopes.

4.2.5. The Surface Potential Energy for $^{166\text{-}180}$Hf

Table (3.18) represents the parameters of the "surfer program" which drew the contour shapes to show the extent of distortion in the nuclei of the isotopes under study. The quadrupole is computed through programs as it has a value greater than zero.

When studying the surface potential energy of the current isotopes through the known (β,γ) values and drawing the symmetrical diagrams of

the axial symmetry angles as well as drawing the contour diagrams when ($\gamma=0^{o}$-60^{o}) shown in Figures (3.42) to (3.49) it becomes clear that the nuclei suffer from a large distortion by comparing these shapes with the ideal contour lines diagrams, as shown in Figure (2.5).

The surface potential energy values that we observe in the contour diagrams of the isotopes under study show that these energies have variable values with (γ) and (β) values, which indicates the deviation of the nucleus shape from the spherical shape to the irregular distorted shape due to the increase in the number of bosons and this confirms its belonging to the rotational limitation of SU(3).

The distortion can be described by a multipolar expansion, with the quadrupole distortion being the most significant deviation from the spherical shape. These quadrilaterals can have either axial symmetry, in which case one distinguishes the elongated (expanded) and flat shapes or the distortion can be without axial symmetry resulting in different elongations along the three axes of the system, referred to as the 'triaxial shape'.

4.2.6. Mixed Symmetry State for $^{166\text{-}180}$Hf Isotopes

The Majorana parameter effect on the calculated excitation energy level for ($^{166\text{-}180}$Hf) isotopes, has been investigated for isotopes and it varies around the best fitted. The ξ_2 allowed to vary with the $\xi_{1,3}$ at the best fit value. The lowest mixed state is $(1_1^+) and\ (2_4^+)$, the state staying conservative to its value in these isotopes denoting that these states may have a full symmetry. Other states (3_1^+) for ($^{174\text{-}180}$Hf) isotopes are slowly increased while no clear effected in isotopes as shown in figure (3.50). It cannot compare the calculated value of state with the experimental value due to data lack. The calculated energy of the scissor state respectively; this is close to the observed energy of the state of the other neighbored nuclei.

The state of mixing levels results from the interaction of the proton and neutron in terms of spin since if it is spinning in the same direction and it is positive, this leads to an increase in the level by increasing the Majorana factor, and this is what has appeared for all the isotopes, but if the spin of the proton is the opposite of spinning the neutron, it does not affect the levels, and if they have the same negative spin, the levels will decrease with the increase of Majorana factor.

4.3. $^{170\text{-}184}$W Isotopes Discussion

The parameters of the Hamiltonian operator, as listed in Tables (3.19) and (3.20), were plotted in Figures (3.51) and (3.52) for $^{170\text{-}184}$W isotopes by observing the change in parameters as a function of the number of bosons ,The values of the coefficients used in calculating these levels, it is noted that the value of the coefficient (EPS) does not appear for all isotopes, and (P.P), (L.L), (Q.Q) are dominant over the rest of the coefficients as it shows the dominance of the duplication reaction, the electric quadrupole interaction and the angular momentum interaction respectively. This is due to the limitation to which these isotopes belong.

As for the coefficient (CHI), we find that its value increases with the increase in the mass number due to the increase in the distortion of these isotopes with the increase in the number of bosons and their approach to the rotational limitation SU(3).

Figure (3.51) shows what has been clarified about the relationship between these parameters and the number of bosons for the studied isotopes, where it is noted that the relationship between them is non-linear, and this confirms a phase transition that occurs from one isotope to another and the appearance of the distorted region, and it is clear from this that these isotopes increase in distortion with the increase in the mass number and the number of bosons, and Figure (3.52) shows the

relationship between the parameters used in the second version of the interactive boson program as functions of the mass number, and it shows a disorderly relationship and also indicates that there is a phase transition for the nuclides.

4.3.1. Energy Levels for $^{170\text{-}184}$W Isotopes Discussion

It is noticed in all the isotopes of Tungsten (under study) which energy levels have been studied that all of them decreased in value of the level (2_1^+) by increasing the number of bosons, and this is clarified in Figures (3.53) to (3.60) that compare the practical and theoretical energy levels of the studied isotopes. We notice the clear drop in energy when moving from the isotope ^{170}W to the isotope^{178}W and then it goes back to increasing at the isotopes($^{180\text{-}184}$W), where the number of bosons is a result of the holes and not the particles.

The values of energy levels in the current study according to energy bands (G, β, γ-bands) compared to the practically available values are shown in Figures (3.53) to (3.60), and they indicate the emergence of new energy levels in addition to the confirmation of the rotation and similarity in some energy levels that were not practically confirmed, and we conclude from those tables that there is a good match between the calculated values and the practical values, and this match appears clearly in the low energy levels, while we find that there is a difference between the practical and theoretical values calculated in the high energy levels and we conclude that the IBM-1 model succeeds in explaining the low levels more than the other levels because of the approximations of this model, and the most important reasons are the lack of distinction between the proton bosons and the neutron bosons. In addition, the upper bands with high spin pair with the rotational bands in the ground plane compressing the successive levels as this cause the intersection of these bands with each other. The isotopes of even-even Tungsten ($^{170\text{-}184}$W)

consist of (74) protons and (96-110) neutrons. We note that the number of protons is closer to the shell 82 than to the shell 50, so the number of proton bosons is calculated from the number of holes all the way to the closed crust (82), so the number of bosons of protons equals (4), and the number of neutrons' bosons is equal to (7-11) for $^{170\text{-}178}$W isotopes and for the three isotopes $^{180\text{-}184}$W, the number of neutron bosons was calculated from the number of holes and their number was (10-8), we notice that it changes from the closest to the shell with the magic number 82 to the shell 126, so the number of neutron bosons is calculated from the number of particles close to (82), so the total number of bosons will be equal to (11-15) bosons for the isotopes $^{180\text{-}184}$W, respectively, as for the three isotopes $^{180\text{-}184}$W, the number of neutron bosons was calculated from the number of holes and their number was (14-12).

In the higher spin levels, the nucleus is more distorted due to the compression of the successive levels with each other. From the above-mentioned figures, it can be concluded that the beta band (β-band) is wider than the gamma band (γ-band). It is found in isotopes that are close to the determination of SU(3), while the gamma band appears in excess for the isotopes that belong to the transition region SU(3)-O(6).

The calculation of dynamic symmetries by IBM-1, IBM-2 and experimental energy levels and after a comparison with the standard values for the energy ratios of ($E0_2^+/E2_1^+, E4_1^+/E2_1^+, E6_1^+/E2_1^+$ and $E8_1^+/E2_1^+$). The ratio between two levels for Tungsten isotopes has been plotted in Figures (3.61) to (3.64) for all isotopes in transitional region O(6)→ SU(3), that is clear in these Figures there is a good agreement between experimental data and the IBM-1 and IBM-2 results appear clearly in Table (3.21), these results are drawn in Figures (3.61) to (3.64), it is clear that these isotopes transition between SU(3) to O(6)

limit except ^{170}W tend to O(6), but Figure (3.61) clarifies and prove that these isotopes in the aforesaid limit because it belongs to U(5) limit.

4.3.2. The Reduced Electric Transition Probability Calculation for $^{170\text{-}184}$W Isotopes

The values of the parameters (E2SD) and (E2DD) were chosen in accordance with the transitional state of the isotopes between the limitation SU(3) and O(6) and with the rotational limitation of SU(3) for the isotopes so as to give the best match between the calculated B(E2) values and the practical values available.

In IBM-1 the reduced electric transition probability values for $^{170\text{-}184}$W isotopes are calculated by calculating the values of effective charge e_b = E2SD and β_2 =E2DD from Equations as mentioned in detail in Chapter Three by using the experimental value of $B(E2;2_1^+ \rightarrow 0_1^+)$, these values are putting into Table (3.22). In IBM-2 effective charge for neutron (e_ν) and for proton (e_π) also calculated to find the reduced electric transition probability, it found that the neutron's effective charge e_ν = 0.397 (eb) and the proton's effective charge e_π = 0.012 (eb). The effective charges depend on the total bosons number N_ρ and the ratios between N_ν/N_π, these parameters are free and can take any value to fit the experimental data, observing to Table (3.22), it is concluded that the value of B(E2:$2^+_1 \rightarrow 0^+_1$) increases with increasing mass number (that is, by increasing the number of neutrons) and this is due to the approach of the number of neutrons to the closed crust (82) and an increase in the number of bosons, and this increase corresponds to the rotational limitation properties.

Table (3.23) shows a comparison between B(E2) calculated by IBM-1, IBM-2 and experimental data. The values are acceptable in comparison and they have a good systematic.

The study of the rates of reduced electrical transitions B(E2) showed the rotational property and the transitional nature between it and the unstable gamma of these nuclei through the decay from level $0_1^+$to level 2_1^+. It can also be seen that the IBM-1 and IBM-2 models were able to explain that the transitions in a single band are strong because of the selection rules such as the transitions ($2_1^+ \rightarrow 0_1^+$), ($2_2^+ \rightarrow 2_3^+$) and ($4_1^+ \rightarrow 2_1^+$) but the transitions between different bands are very weak such as ($2_1^+ \rightarrow 0_2^+$), ($2_1^+ \rightarrow 2_2^+$) and($4_3^+ \rightarrow 2_1^+$) this was shown by IBM-1 while some transitions did not appear in IBM-2 because they are forbidden such as($2_2^+ \rightarrow 0_1^+$), ($4_1^+ \rightarrow 2_2^+$) and ($3_1^+ \rightarrow 2_1^+$).

It should be noted here the importance of using branching ratios in knowing the distortion of the nuclei, including the ratios shown in Table (3.24). When the value of this ratio decreases, the distortion of the nucleus increases, and when this value is close to zero, the nucleus becomes too close to limitation SU(3). It was observed that these values are close to zero, and by comparing them with the ideal values, it's found that these isotopes belong to the rotational limitation SU(3), and this proves the validity of the previous statement.

When comparing the branching ratios (R, R', R'') for the isotopes under study with the typical values for each determination, we find that there is a good match between them, as shown in Table (3.24). In addition, it is concluded that Tungsten isotopes belong to the aforementioned limitations, as with an increasing mass number, we find a decrease in the value of (R) and the previous isotopes tend to move toward the limitation SU(3).

The theoretical and the available practical electric quadrupole momentum values showed a good convergence, and in light of these values, we conclude that the first to fifth nuclei of the sequence ($^{170\text{-}178}$W) have a higher momentum value and suffer more distortion than the rest of the isotopes because they are located in the transition region SU(3). While the value of the momentum begins to decrease relatively quickly when moving to the fifth nucleus, and therefore it has a distortion due to the nature of the transition region SU(3) to which this nucleus belongs.

As for the remaining nuclei ($^{180\text{-}184}$W), it is found that they suffer from permanent distortions, due to the large value of the electric quadrupole momentum and their belonging to the rotational limitation SU(3).

4.3.3. Magnetic Transitions Probability Calculation for $^{170\text{-}184}$W Isotopes

In order to calculate B(M1) transition probability, one should estimate the effective $g-$factors for proton g_π and neutron g_ν by Equations (2.25). In Tungsten isotopes the g- factor values are g_π= 0.382 (μ_N) and g_ν= 0.397 (μ_N). Equations (2.19) were used to calculate the B(M1) transition probabilities as it is shown in Table (3.25). The calculated values for B(M1) are acceptable to some extent as compared with the available experiments values, where some of the B(M1) values are small compared to the values of the quadrupole transition probabilities because the wavelength of the gamma ray transitions is greater than it is in the magnetic transitions according to Equation(3.1), this Equation shows that the B(M1) transition probability is less than B(E2) transition probability and our results confirm this. The calculation values for these isotopes and mixing ratio δ(E2/M1) have been compared with the available experiments data as shown in Table (3.25).

4.3.4. The Electric Monopole Transition Calculation for $^{170-184}$W Isotopes

The ratio X(E0⁄E2) shows the strength of the competition between E0 and E2, where it is noted that the IBM-2 calculated values are not entirely consistent with the experimental values available, and the reason belongs to the strength of the transition between E2 and E0, as well as the fact that the difficulty of defining unified parameters for ($\tilde{\beta}_v$, $\tilde{\beta}_\pi$), give us the theoretical values in (IBM-2) that are closer to the available experimental data. Besides the fact that the experimental values available are also very few. The deformation parameters for protons and neutrons used to calculate monopole transition matrix elements ρ(E0) for $^{170-184}$W isotopes are ($\tilde{\beta}_v$= -0.00251 fm^2, $\tilde{\beta}_\pi$= -0.0674 fm^2). Table (3.26) shows the electric monopole transition matrix and X(E0/E2) for $^{170-184}$W isotopes.

4.3.5. The Surface Potential Energy for $^{170-184}$W

The surface potential energy of the current isotopes can be studied through the known (β,γ) values and drawing the symmetrical diagrams of the axial symmetry angles as well as drawing the contour diagrams when (γ=0^o-60^o) shown in Figures (3.65) to (3.72) it becomes clear that the nuclei suffer from a large distortion by comparing these shapes with the ideal contour lines diagrams, as shown in Figure (2.5).

The surface potential energy values that observed in the contour diagrams of the isotopes under study show that these energies have variable values with (γ) and (β) values, which indicates the deviation of the nucleus shape from the spherical shape to the irregular distorted shape due to the increase in the number of bosons and this confirms its belonging to the rotational limitation of SU(3). Table (3.27) represents the parameters of the "surfer program" which drew the contour shapes to show the extent of distortion in the nuclei of the isotopes under study.

The quadrupole is computed through programs as it has a value greater than zero.

4.3.6. Mixed Symmetry State for $^{170\text{-}184}$W Isotopes

The Majorana parameter effect on the calculated excitation energy level for ($^{170\text{-}184}$W) isotopes, has been investigated for isotopes and it varies around the best fitted. The ξ_2 allowed to vary with the $\xi_{1,3}$ at the best fit value. The lowest mixed state is (1_1^+), the state staying conservative to its value in these isotopes denoting that these states may have a full symmetry. Other states (2_4^+) (5_1^+) for ($^{182\text{-}184}$W) isotopes are slowly increased while no clear effected in isotopes as shown in Figure (3.73). It cannot compare the calculated value of the state with the experimental value due to data lack. The calculated energy of the scissor state respectively; this is close to the observed energy of the state of the other neighbored nuclei.

The state of mixing levels results from the interaction of the proton and neutron in terms of spin since if it is spinning in the same direction and it is positive, this leads to an increase in the level by increasing the Majorana factor, and this is what has appeared for all the isotopes, but if the spin of the proton is the opposite of spinning the neutron, it does not affect the levels, and if they have the same negative spin, the levels will decrease with the increase of Majorana factor.

4.4. The Comparison

After the results obtained, the series of isotopes of the three studied elements can be compared to find out the relationship between their properties and what are the different or common properties between them.

The properties can be divided according to isotopes, isotopes, and isobars, as follows:

4.4.1. Isotopes

Each of the three studied series consists of a group of isotopes where the isotopes differ in terms of mass number and therefore differ in the number of neutrons for each element. gaps.

With regard to the energy ratios, it increases significantly for each isotope for isotopes with the number of bosons calculated from the particles, while it decreases for the bosons of the gaps and for all three series, and the reason for this is due to the high spin of these bosons.

The electrical transition potential between the first excited state and the stable state studies the shape and limits of isotopes. The probability of electrical transitions increases significantly with the increase in the number of bosons towards the neutron magic number 82 and 126 for Yb, Hf, and W respectively. This is the case because getting close to the magic numbers and reaching the stability nuclei causes a few photons to travel between levels.

It can be seen that the branching ratios of all the studied isotopes and each of the series are of close proportions and close to the standard ratios calculated for the rotational determination, especially (R), while the value of (R′) and (R″) approach zero, which confirms that all isotopes are in the same region.

The magnetic transition potential is a measure of the plane that has a mixed state of symmetry between the wave function of protons and neutrons. The magnetic transition is considered in our study, which increases with the increase in the number of bosons.

Reducing or increasing the mixing ratio does not directly depend on the number of bosons or access to the closed shell, but rather on the value of the electric and magnetic transitions. There is some decrease in this ratio near the gap bosons of electric and magnetic transitions.

The ratio between the zero-transition force and the corresponding electric transmission in this study is a result of the interaction strength between the proton and the neutron, which is provoked by the external electromagnetic field of the nucleus. This percentage decreases with the decrease in the number of bosons for all studied isotopes.

The surface potential energy shows the voltage distribution on the surface of the core. From the relationship between the distortion and the voltage surface energy, we can understand how the potential is distributed and to what extent. The large difference between the number of protons and the number of neutrons makes these isotopes have access to energy that causes disturbances in the nucleus.

From all of the above, it is clear that all the studied isotopes are located in the transition region between the rotational boundary and the unstable gamma, but it tends greatly to the rotational boundary of most of the isotopes.

4.4.2. Isobars

Since the selected isotopes are isotopes of adjacent (even atomic number) elements, so many isobars (five groups) appeared, namely, (^{170}Yb, ^{170}Hf, ^{170}W), (^{172}Yb, ^{172}Hf, ^{172}W), (^{174}Yb, ^{174}Hf, ^{174}W), (^{176}Yb, ^{176}Hf, ^{176}W), (^{178}Yb, ^{178}Hf, ^{178}W), It was observed that the energy levels of each group of isobars increased with the increase in the atomic number of the elements and their energy ratios.

The probability of electrical transitions decreases significantly as the number of neutrons increases for each state because approaching the magic numbers and reaching the stability nuclei results in the transmission of a few photons between the levels.

The magnetic transition potential is a measure of the plane that has a mixed state of symmetry between the wave function of protons and

neutrons. The magnetic transition is considered in our study, which increases with the increase in the number of neutron bosons.

4.4.3. Isotones

Low excited energy levels are proportional to the energy of bosons (ε), especially for the case2_1^+, where the studied nuclei can be divided into groups of isotopes with the same neutron numbers (Yb_{100}, Hf_{100},W_{100}), (Yb_{102}, Hf_{102},W_{102}), (Yb_{104}, Hf_{104}, W_{104}), (Yb_{106}, Hf_{106}, W_{106}). A slight difference was observed between the energy of the bosons of the nuclei, which have the same Nν bosons of the neutrons. This difference is due to the effect of the proton wave function, which is highly dependent on the number of proton bosons, for Ytterbium, Hafnium and Tungsten nuclei, respectively. The other reason is that the increase in the number of neutrons of bosons around the middle shell leads to an increase in the number of wave function states that describe the motion of these bosons, and this affects the energy bosons. This was observed when nuclei with higher values of energy values for the proton bosons, as in nuclei containing Nν=(9, 10, 11, 9*, 10*)

The probability of electrical transitions decreases significantly as the number of protons increases for each state because approaching the magic numbers and reaching the stability nuclei results in the transfer of a few photons between the levels. The transition of descending values B (E2) between two states 2_1^+ and 0_2^+, was adopted to study the shape of the electrical quadrupole transition probabilities to the existence of the experimental values available for this transition in addition to obtaining the best fit with the results of IBM-1 and IBM-2 for this transition. The reason for this is that the states 2_1^+, and 0_1^+, converge the closer to the

state 2_1^+, from the middle of the shell. This leads to a higher number of transmission of photons and as a result will increase the values of B(E2).

The possibility of magnetic transition increases with the increase in the number of proton bosons and this is due to the strong correlation between this transition and the states of mixed symmetry (MSS), where the nuclei with large values of B (M1) have large mixing states between the wave function of protons and the wave function of neutrons, and this is what was observed in the studied nuclei.

Finally, the similarity between all isotopes, isobars and isotons is the form of deformation occurring in the nuclei, where the potential energy shows the distribution of potential on the surface of the nucleus. From the relationship between the deformation and the surface potential energy, we can understand how the potential is distributed and to what extent. These numbers are shown in Figures (3.26)-(3.17) for Ytterbium and (3.42)-(3.49) for Hafnium (Figures (3.65)-(3.72) for degeneration, showing that there is a lot of deformation and the nucleus is close to the prolate shape. The figures represent an obvious distortion when approaching a closed neutron envelope. The large difference between the number of protons and the number of neutrons makes these isotopes have access to energy that causes disturbances in the nucleus.

4.5. Conclusions

By studying the nuclear structure of the chain of isotopes under study, several conclusions were reached as follows:

1. The agreement between the results of the two models is very clear through the convergence of these results with the experimental results, especially for low excitation energy levels.
2. Both models are more effective when the number of bosons increases.

3. The energy levels which resultant from the models decrease with the decreasing of boson number. The kind of bosons (hole or particle) affect the properties of the isotopes.

4. The branching ratios of the electric transitions are a good exam to know the limit of the isotope and emphasis it.

5. The calculations of *B(M1)* and *B(E2)* values show a good match with the existing experimental results. However, there is some difference between them, due to the effect of the deformation of these isotopes nuclei.

6. Magnetic transition probability and mixing ratio explain which levels have a symmetry state (full or mix) according which level change with ξ_2.

7. The calculated mixing ratios δ(E2/M1) give acceptable values as compared with the available experimental data which are high in some transitions and low in others depending on the strength of the transition for *B(E2)* and *B(M1)*.

8. X(E0/E2) this ratio depends on the monopole and electric transitions probability. This provides extra evidence for the shape of these nuclei.

9. Potential energy surfaces are giving us a good perception to get the shape of the nuclei from the contour lines. The symmetric figures explain the kind of symmetry in the nuclei. We can confirm that the predictions for the limits of our isotopes, which determined are correct.

4.6. Future Work

1. Using three dimension drawing for the potential energy surface to give a clear image of the deformation in the nuclei.

2. Using a comfortable developed language to use the model of interacting bosons in such as Matlab or any advanced system that is compatible with the work of the new operating systems.

3. When studying any series of isotopes, divergent numbers of mass numbers must be studied to see the extent of the change in properties, since there does not seem to be a clear distinction of properties in nearby numbers.

4. Study the nuclear structure and electromagnetic transitions using IBM-3 and IBM-4.

5. Further research on the use of the interaction boson model (1 and 2) for many isotopes with medium atomic numbers, and isotopes with medium mass numbers.

References

[1] Hady, H. N., (2020). A Theoretical Description of some Even-Even Isotopes $^{156\text{-}178}$Yb, $^{124\text{-}140}$Ba and $^{72\text{-}80}$Se using IBM Model, Ph.D. thesis, University of Babylon.

[2] Meyerhof, W. E., and Meyerhof, W. E. (1967). Elements of nuclear physics (174). New York: McGraw-Hill. 2nd Ed.

[3] Burcham, W. E. (1979). Elements of nuclear physics.

[4] National Research Council. (2012). Assuring a future US-based nuclear and radiochemistry expertise. National Academies Press.

[5] Arnikar, H. J. (1995). Essentials of nuclear chemistry (1653). New Age International.

[6] Cottingham, W. N., Greenwood, D. A., and Greenwood, D. A. (2001). An introduction to nuclear physics. Cambridge University Press.

[7] Pfeifer, W. (2003). An introduction to the interacting boson model of the atomic nucleus. arXiv.

[8] Semat, H. (2012). Introduction to atomic and nuclear physics. Springer Science and Business Media.

[9] Heyde, K., and Barrett, B. R. (1999). Basic Ideas and Concepts in Nuclear Physics: An Introductory Approach. Physics Today, 52(12), 60.

[10] Langanke, K., Maruhn, J. A., and Koonin, S. E. (Eds.). (1991). Computational nuclear physics. Springer.

[11] Davidson, J. P. (1968). Collective models of the nucleus.

[12] Ginocchio, J. N., and Kirson, M. W. (1980). Relationship between the Bohr collective Hamiltonian and the interacting-boson model. Physical Review Letters, 44(26), 1744.

[13] Zelevinsky, V., and Horoi, M. (2019). Nuclear level density, thermalization, chaos, and collectivity. Progress in Particle and Nuclear Physics, 105, 180-213.

[14] Singh, Y. P. (2021). Basic Concepts in Nuclear and Particle Physics. Amazon.

[15] Rowe, D. J., and Wood, J. L. (2010). Fundamentals of nuclear models: foundational models. World Scientific.

[16] McClure, D. S. (1949). Selection Rules for Singlet-Triplet Perturbations in Polyatomic Molecules. The Journal of Chemical Physics, 17(7), 665-666.

[17] Cottingham, W. N., Greenwood, D. A., and Greenwood, D. A. (2001). An introduction to nuclear physics. Cambridge University Press.

[18] Hawthorne, F. C. (Ed.). (2018). Spectroscopic methods in mineralogy and geology (18). Walter de Gruyter GmbH and Co KG.

[19] Zamfir, V. N., and Casten, R. F., (2003). Phase/shape transitions in nuclei. Proceedings of the Romanian Academy, Series A, 4(2), 9.

[20] Subber, A. R., (2005). Nuclear structure of low-lying states of Gd 152 in framework of the interacting boson model. University of Aden Journal of Natural and Applied Sciences, 8(1), 171-176.

[21] Rath, A. K., Walker, P. M., Praharaj, C. R., and Xu, F. R. (2006). K= 6+ Isomers in Hf, yb and W Nuclei. International Journal of Modern Physics E, 15(07), 1653-1663.

[22] Sarriguren, P., Rodríguez-Guzmán, R., and Robledo, L. M. (2008). Shape transitions in neutron-rich Yb, Hf, W, Os, and Pt isotopes within a Skyrme Hartree-Fock+ BCS approach. Physical Review C, 77(6), 064322.

[23] Robledo, L. M., Rodríguez-Guzmán, R., and Sarriguren, P. (2009). Role of triaxiality in the ground-state shape of neutron-rich Yb, Hf, W, Os and Pt isotopes. Journal of Physics G: Nuclear and Particle Physics, 36(11), 115104.

[24] Usmanov, P. N., Okhunov, A. A., Salikhbaev, U. S., and Vdovin, A. I. (2010). Analysis of electromagnetic transitions in nuclei 176, 178Hf. Physics of particles and Nuclei Letters, 7(3), 185-191.

[25] Nomura, K., Otsuka, T., Rodríguez-Guzmán, R., Robledo, L. M., and Sarriguren, P. (2011). Collective structural evolution in neutron-rich Yb, Hf, W, Os, and Pt isotopes. Physical Review C, 84(5), 054316.

[26] Sharrad, F. I., Abdullah, H. Y., Al-Dahan, N., Mohammed-Ali, A. A., Okhunov, A. A., and Kassim, H. A. (2012). Shape transition and collective excitations in neutron–rich $^{170\text{-}178}$Yb Nuclei. Rom. J. Phys, 57(9-10), 1346-1355.

[27] AL-Ammeer, M. A. and Hussein, M. A. (2013). Study Even-Even 188,190 W Isotopes In The Framework Of The Interacting Boson Model (IBM-). Journal of University of Babylon, 21(3).

[28] Okhunov, A. A., Turaeva, G. I., Kassim, H. A., Khandaker, M. U., and Rosli, N. B. (2015). Analysis of the energy spectra of ground

states of deformed nuclei in the rare-earth region. Chinese Physics C, 39(4), 044101.

[29] Mahapatro, S., Lahiri, C., Kumar, B., Mishra, R. N., and Patra, S. K. (2016). Nuclear structure and decay properties of even–even nuclei in Z= 7 0− 8 0 drip-line region. International Journal of Modern Physics E, 25(09), 1650062.

[30] Al-Jubbori, M. A., Al-Mtiuty, K. A., Saeed, K. I., and Sharrad, F. I. (2017). Properties of even $^{168-178}$Hf isotopes using IBM-1 and SEF. Chinese Physics C, 41(8), 084103.

[31] Kassim, H. H., Mohammed-Ali, A. A., Al-Jubbori, M. A., Sharrad, F. I., Ahmed, A. S., and Hossain, I. (2018). Calculation of some of the nuclear properties of even-even $^{172\text{-}176}$Hf isotopes using IBM-1. Journal of the National Science Foundation of Sri Lanka, 46(1).

[32] Al-Jubbori, M. A., Kassim, H. H., Abd-Aljbar, A. A., Abdullah, H. Y., Hossain, I., Ahmed, I. M., and Sharrad, F. I. (2020). Nuclear structure of the even–even rare-earth Er–Os nuclei for N= 102. Indian Journal of Physics, 94(3), 379-390.

[33] Hady, H. N., and Muttalb, M. K. (2021). Investigation of transition symmetry shapes of 160-168Yb nuclei using IBM. Iraqi Journal of Science, 1135-1143.

[34] Al-Jubbori, M. A., Kassim, H. H., Raheem, E. M., Ahmed, I. M., Khodair, Z. T., Sharrad, F. I., and Hossain, I. (2022). Nuclear Structure of Rare-Earth ^{172}Er, ^{174}Yb, ^{176}Hf, ^{178}W, ^{180}Os Nuclei. Ukrainian Journal of Physics, 67(2), 127-127.

[35] Zyriliou, A., Mertzimekis, T. J., Chalil, A., Vasileiou, P., Mavrommatis, E., Bonatsos, D., and Minkov, N. (2022). A study of

some aspects of the nuclear structure in the even–even Yb isotopes. The European Physical Journal Plus, 137(3), 352.

[36] Morrison, I., and Smith, R. (1980). The interacting boson approximation and the spectroscopy of the even cadmium and tin isotopes. Nuclear Physics A, 350(1-2), 89-108.

[37] Pan, F., Wang, T., Huo, Y. S., and Draayer, J. P. (2008). Quantum phase transitions in the consistent-Q Hamiltonian of the interacting boson model. Journal of Physics G: Nuclear and Particle Physics, 35(12), 125105.

[38] Al-Khudair, F. H. (2018). Investigation of isospin excited and mixed-symmetry states in even–even N= Z nuclei. International Journal of Modern Physics E, 27(08), 1850065.

[39] Elliott, J. P. (1985). The interacting boson model of nuclear structure. Reports on Progress in Physics, 48(2), 171.

[40] Abood, S. N., Hamida, M. B. B., and Najim, L. A. (2015). Structure Evolution in Odd-Even Eu-155 Nucleus within IBFM-2. American Journal of Modern Energy, 1(1), 17-24.

[41] Hossaina, I., Kassimb, H. H., Sharradb, F. I., and Ahmeda, A. S. Nuclear structure of yrast bands of 180Hf, 182W, and 184Os nuclei by means of interacting boson model-1. Science Asia, 42, 22-27.

[42] Hussain, W. N., Hossain, I., and Sharrad, F. I. (2019). Electromagnetic Transitions with Related Quantities for 80Se and 82Kr Nuclei. In Journal of Physics: Conference Series 1279(1), p. 012027). IOP Publishing.

[43] Jaber G. A., (2020). Nuclear Structure for Some Even-Even (Kr, Xe, Hg) Nuclei Using IBM1-2. Ph.D. thesis, University of Babylon.

[44] Pálffy, A., Evers, J., and Keitel, C. H. (2008). Electric-dipole-forbidden nuclear transitions driven by super-intense laser fields. Physical Review C, 77(4), 044602.

[45] Oss, S. (2009). Algebraic models in molecular spectroscopy. Advances in chemical physics: new methods in computational quantum mechanics/S. Oss, 455-469.

[46] Obiad, R. M. (2020). Study Mixed Symmetry States of Deformed Even-Even Nuclei Using Interacting Boson Model (IBM-2). Ph.D. thesis, University of Babylon.

[47] Al Qadiry, O. A. (2007). Nuclear Structure calculations of some even a (even-even) and odd A Nuclei using IBM-1 and IBFM-1 (Ph. D Thesis, Baghdad university).

[48] Aboud, S. N. (1990). An application of interacting boson model in nuclear (M. Sc. Thesis, Basra University).

[49] Khalaf, A. M., and Awwad, T. M. (2013). A theoretical description of U(5)-SU(3) nuclear shape transitions in the interacting boson model. Progress in Physics, 1, 7-11.

[50] Sharrad, F. I. (2017). Determination of the 108-112Pd isotopes identity using interacting boson model, 18(4), 313-318.

[51] Isacher, P. V., and Cheen, J. O. (1981). J. Phys. Rev. C, l(24), 689.

[52] Casten, R. F. (2001). Evolution of structure in exotic nuclei. Physics of Atomic Nuclei, 64(6), 1001-1004.

[53] Al-Khudair, F., Subber, A., and Ashwaq, F. (2014). Bands structure and electromagnetic transitions of O (6) nucleus ^{128}Xe. J, Basrah Researches Sciences, 40(1), 49-60.

[54] Mosbah, D. S., Evans, J. A., and Hamilton, W. D. (1994). An IBA-2 calculation of E2/M1 multipole mixing ratios of transitions in ^{182,184,186} W. Journal of Physics G: Nuclear and Particle Physics, 20(5), 787.

[55] Turkan, N., and Maras, I. (2007). Microscopic interacting boson model calculations for even-even $^{128–138}$Ce nuclei. Pramana, 68(5), 769-778.

[56] Yazar, H. R., and Uluer, I. (2004). E2/M1 Multipole Mixing Ratios of Transitions in Erbium Isotopes. Turkish Journal of Physics, 28(2), 89-94.

[57] Al-Khudair, F. H., Subber, A. R., and Jaafer, A. F. (2014). Shape Transition and Triaxial Interaction Effect in the Structure of $^{152–166}$Dy Isotopes. Communications in Theoretical Physics, 62(6), 847.

[58] Hamilton, W. D. (1990). The identification of mixed-symmetry states. Journal of Physics G: Nuclear and Particle Physics, 16(5), 745.

[59] Brown, B. A. (2005). Lecture notes in nuclear structure physics. National Super Conducting Cyclotron Laboratory, 11.

[60] Iachello, F., and Arima, A. (1987). The interacting boson model Cambridge Uni. Press, Cambridge.

[61] Siciliano, M., Valiente-Dobón, J. J., Goasduff, A., Rodríguez, T. R., Bazzacco, D., Benzoni, G., and Testov, D. (2021). Lifetime measurements in the even-even $^{102–108}$ Cd isotopes. Physical Review C, 104(3), 034320.

[62] Barrett, B. R., Kuyucak, S., Navrátil, P., and Van Isacker, P. (1999). Is there a proton-neutron interacting boson model rule for M1 properties. Physical Review C, 60(3), 037302.

[63] Navratil, P., Barrett, B. R., and Dobeš, J. (1996). M1 properties of Tungsten isotopes in the interacting boson model-2. Physical Review C, 53(6), 2794.

[64] Al-Sadi, M. A. K. H., Kadhim, Q. S., and Yasi, S. H. A. Z. (2019). Mixed symmetry states for $_{70}$Zn, $_{72}$Ge, $_{74}$Se, $_{76}$Kr isotones by using IBM-2. In Journal of Physics: Conference Series, IOP Publishing.1234(1), 12034.

[65] Epelbaum, E., Hammer, H. W., and Meibner, U. G. (2009). Modern theory of nuclear forces. Reviews of Modern Physics, 81(4), 1773.

[66] Chiang, H. C., Hsieh, S. T., Yen, M. K., and Han, C. S. (1985). IBA calculations on the even-even Pt isotopes. Nuclear Physics A, 435(1), 54-66.

[67] Girit, C., Hamilton, W. D., and Kalfas, C. A. (1983). Multipole mixing ratios of transitions in 154Gd. Journal of Physics G: Nuclear Physics, 9(7), 797.

[68] Krane, K. S. (1980). E2, M1 multipole mixing ratios: Supplement and corrections through December 1979. Atomic Data and Nuclear Data Tables, 25(1), 29-89.

[69] Obaid, R. M., and Al Shreefi, M. A. (2019). Study the proton-neutron mixed symmetry states in some deformed Gadolinium nuclei. In AIP Conference Proceedings, 2144(1), 30013. AIP Publishing LLC.

[70] Aldushchenkov, A. V., and Voinova, N. A. (1973). E0 transitions in atomic nuclei. Atomic Data and Nuclear Data Tables, 11(4), 299-325.

[71] Kibedi, T., and Spear, R. H. (2005). Electric monopole transitions between 0+ states for nuclei throughout the periodic table. Atomic Data and Nuclear Data Tables, 89(1), 77-100.

[72] Bijker, R., Dieperink, A. E. L., Scholten, O., and Spanhoff, R. (1980). Description of the Pt and Os isotopes in the interacting boson model. Nuclear Physics A, 344(2), 207-232.

[73] García-Ramos, J. E., Arias, J. M., Barea, J., and Frank, A. (2003). Phase transitions and critical points in the rare-earth region. Physical Review C, 68(2), 024307.

[74] Subber, A.R., (2005). Monopole Transitions in Deformed Nuclei of Hf Isotopes. Journal of Basrah Researches (Sciences), 31(3).

[75] Subber, A. R., and Al-Khudaie, F. H., (2012). Delta (E2/M1) and X (E0/E2) mixing ratios in^{134} Ba by means of IBM-2. Turkish Journal of Physics, 36(3), 368-376.

[76] Giannatiempo, A., Nannini, A., Perego, A., and Sona, P. (1987). Electric monopole transitions in Te 122. Physical Review C, 36(6), 2528.

[77] Matsuzaki, M., and Ueno, T. (2016). Quadrupole and monopole transition properties of 0+ 2 in Gd isotopes. Progress of Theoretical and Experimental Physics, 2016(4), 04303.

[78] Najam, L. A., Mohaisen, A. J., and Abood, S. N. (2021). Electric Monopole Transitions in Nd Nuclei within IBM-2. Egyptian Journal of Physics, 49(1), 89-100.

[79] Turkan, N., and Inci, I. (2007). IBM-2 calculations of some even–even neodymium nuclei. Physica Scripta, 75(4), 515.

[80] Al-Rahmani, A. A. M. (2010). neutron interacting boson model (IBM-2). Baghdad Science Journal, 7, 1.

[81] İnan, S., Türkan, N., and Maraş, İ. (2012). The Investigation of ^{130,132} Te by IBM-2. Mathematical and Computational Applications, 17(1), 48-55.

[82] Muttaleb, M. K., (2021). Transitions probabilities B (E2), B (M1) and B (E0) in ^{130}Ba isotope. In Journal of Physics: Conference Series, IOP Publishing, 1897(1), 12063.

[83] Al-Sadi, M. A. K. H., Alnasraui, A. H. F., and Altbtbiey, D. A., (2020). Mixed Symmetry States for even-even $^{218-224}$ Ra Isotopes by using (IBM-2). In Journal of Physics: Conference Series, IOP Publishing, 1664(1), 12140.

[84] Al–Sadi, M. A. K., Al Shareefi, M. A., and Subber, A. R. H. (2015). δ (E2/M1) and X (E0/E2) Ratios for $^{192-202}$ Pt Isotopes by Using the Proton and Neutron Interacting Boson Model (IBM-2). International Journal of Physics, 3(3), 119-124.

[85] Reşit, H., and Uluer, I. (2005). A correspondence between IBA-1 and IBA-2 models and electromagnetic transitions in the decay of some erbium isotopes. Pramana, 65(3), 393-402.

[86] Yazar, H. R. (2005). Using the microscopic background of the IBA-2 model electromagnetic transitions in the decay of some gadolinium isotopes. Journal of the Korean Physical Society, 47(4), 592.

[87] Brown, B. A. (2005). Lecture notes in nuclear structure physics. National Super Conducting Cyclotron Laboratory, 11.

[88] Beck, T., Beller, J., Pietralla, N., Bhike, M., Birkhan, J., Derya, V., and Zweidinger, M. (2017). E2 decay strength of the M1 scissors mode of ^{156}Gd and its first excited rotational state. Physical Review Letters, 118(21), 212502.

[89] Daniel, T. (2017). Nuclear structure studies of low-lying states in 194Os using fast-timing coincidence gamma-ray spectroscopy. University of Surrey (United Kingdom).

[90] Kadhim, M. A. (2015). Nuclear Structure of Even-Even Os, Pt and Hg Isotopes By Using IBM-2 (Ph.D. thesis University of Babylon).

[91] Hammond, C. R. (2000). The elements. Handbook of chemistry and physics, 81.

[92] Ganjali, M. R., Gupta, V. K., Faridbod, F., and Norouzi, P. (2016). Lanthanides series determination by various analytical methods. Elsevier.

[93] Habashi, F. (2013). Extractive metallurgy of rare earths. Canadian metallurgical quarterly, 52(3), 224-233.

[94] Reich, C. W., (2005). Nuclear data sheets for A= 160. Nuclear Data Sheets, 105, 557.

[95] Reich, C. W., (2007). Nuclear data sheets for A= 162. Nuclear Data Sheets, 108,1807.

[96] Balraj, S. and Jun, C., (2018). Nuclear data sheets for A= 164. Nuclear Data Sheets, 147, 1.

[97] Baglin, C. M., (2008). Nuclear data sheets for A= 166. Nuclear Data Sheets, 109, 1103.

[98] Baglin, C. M., (2010). Nuclear data sheets for A= 168. Nuclear Data Sheets, 111, 1807.

[99] Baglin, C. M., Mccutchan, E. A., Basunia, S. (2018). Nuclear data sheets for A= 170. Nuclear Data Sheets, 153, 1.

[100] Balraj, S., (1995). Nuclear data sheets for A= 172. Nuclear Data Sheets, 75,199.

[101] Browne, E., Junde, H., (1999). Nuclear data sheets for A= 174. Nuclear Data Sheets, 87, 15.

[102] Basunia, M. S., (2006). Nuclear data sheets for A= 176. Nuclear Data Sheets, 107, 791.

[103] Achterberg, E., Capurro ,O. A., Marti, G. V., (2009). Nuclear data sheets for A= 178. Nuclear Data Sheets, 110, 1473.

[104] Baglin, C. M., (2008). Nuclear data sheets for A= 180. Nuclear Data Sheets, 109, 1103.

[105] Baglin, C. M., (2010). Nuclear data sheets for A= 182. Nuclear Data Sheets, 111, 1807.

[106] Baglin, C. M., Mccutchan, E. A., Basunia, S. (2018). Nuclear data sheets for A= 184. Nuclear Data Sheets, 153, 1.

[107] Nielsen, R. H. (2000). Hafnium and Hafnium compounds. Kirk-Othmer Encyclopedia of Chemical Technology.

[108] Lassner, E., and Schubert, W. D. (1999). Tungsten: properties, chemistry, technology of the elements, alloys, and chemical compounds. Springer Science and Business Media.

[109] Zhang, Y., Evans, J. R., and Yang, S. (2011). Corrected values for boiling points and enthalpies of vaporization of elements in handbooks. Journal of Chemical and Engineering Data, 56(2), 328-337.

[110] Daintith, J. (Ed.). (2005). The facts on file dictionary of chemistry. Infobase Publishing.

[111] Gludovatz, B., Wurster, S., Weingärtner, T., Hoffmann, A., and Pippan, R. (2011). Influence of impurities on the fracture behaviour of Tungsten. Philosophical Magazine, 91(22), 3006-3020.

[112] Stwertka, A. (2002). A Guide to the Elements. Oxford University Press.

[113] Lassner, E., Schubert, W. D., Lüderitz, E., and Wolf, H. U. (2000). Tungsten, Tungsten alloys, and Tungsten compounds. Ullmann's Encyclopedia of Industrial Chemistry.

[114] Tan, C., Zhou, K., Ma, W., Attard, B., Zhang, P., and Kuang, T. (2018). Selective laser melting of high-performance pure Tungsten: parameter design, densification behavior and mechanical properties. Science and Technology of advanced MaTerialS, 19(1), 370-380.

[115] McMaster, J., and Enemark, J. H. (1998). The active sites of molybdenum-and Tungsten-containing enzymes. Current opinion in chemical biology, 2(2), 201-207.

[116] Hille, R. (2002). Molybdenum and Tungsten in biology. Trends in biochemical sciences, 27(7), 360-367.

الخلاصة

تمت دراسة التركيب النووي لسلسلة من النظائر الزوجية- الزوجية للإيتربيوم Yb ذات الاعداد الكتلية (١٦٠-١٧٨) ونظائر الهافنيومHf الزوجية الزوجية ذات الاعداد الكتلية (١٦٦-١٨٠) و نظائر التنغستن W ذات الاعداد الكتلية (١٧٠-١٨٤) نظريًا باستخدام هيكلية نموذج البوزونات المتفاعلة الأول IBM-1 ونموذج البوزونات المتفاعلة الثاني IMB-2 ، حيث تم دراسة مستويات الطاقة ، النسب بين هذه المستويات، التناظرات الديناميكية، احتمالية الانتقال المنخفضة للرباعي الكهربائي B(E2)، نسب التفرع، احتمالية الانتقالات المغناطيسية B(M1)، احتمالية الانتقالات الصفرية B(E0) ونسب الخلط δ (E2/M1) و X (E0/E2) بالتفصيل.

كذلك تم حساب طاقة جهد السطح لهذه السلاسل من النظائر ورسم مخططاتها الكنتورية باستخدام برنامج (surfer) ورسم المخططات البيانية لها، وتم تحليل النتائج ومناقشتها. كما تم أيضًا حساب حالات الخلط المتماثل (MSS) للمستويات.

لقد وجد أن جميع النظائر المدروسة تقع ضمن المنطقة الدورانية SU(3) ومنطقة جاما غير المستقرة O(6) والتي تقع على مثلث كاستن. تمت مقارنة النتائج بالنتائج العملية ووجد أن هناك تطابقًا جيدًا بينهما.

توضح طاقة سطح الجهد المحسوبة لسلاسل النظائر الثلاثة أن الشكل النووي حساس للغاية للتأثيرات الهيكلية ويمكن أن يتغير من النواة إلى النواة المجاورة لها بالإضافة إلى تغيرات الشكل مع عدد البروتونات أو النيوترونات.

جمهورية العراق
وزارة التعليم العالي والبحث العلمي
جامعة بابل
كلية العلوم
قسم الفيزياء

دراسة بعض خصائص التركيب النووي وطاقة الجهد للنوى الزوجية ـ الزوجية Yb ، Hf و W باستخدام هيكلية نموذج البوزونات المتفاعلة

اطروحة دكتوراه مقدمة إلى مجلس كلية العلوم - جامعة بابل كجزء من متطلبات نيل درجة الدكتوراه فلسفة في علوم الفيزياء

من قبل

سلار حسين ابراهيم محمد

بكالوريوس علوم فيزياء ٢٠٠٣

ماجستير علوم فيزياء ٢٠٠٧

بإشراف

أ.د.

محسن كاظم مطلب الجنابي

١٤٤٤هـ ٢٠٢٢ م